The Universe in Explosive Expansion

Samuel Sánchez López

Department of Physics

Faculty of Science and Technology

Lancaster University

A thesis submitted for the degree of

Doctor of Philosophy

June, 2024

Abstract

Cosmic inflation, a phase of accelerated expansion of the early Universe, not only solves the horizon and flatness problems of the Hot Big Bang but also provides the initial conditions for the density perturbations that source all structure in the Universe. 9 billion years later, the Universe started engaging in another bout of accelerated expansion, observed today, 13.8 billion years after the Big Bang. This thesis is mainly concerned with quintessential inflation, a framework that suggests that the same substance responsible for the period of primordial inflation, the inflaton field, is also responsible for the current accelerated expansion. By considering a simple and theoretically motivated setup in modified gravity, we manage to bring back to life two of the most popular inflationary models, chaotic and power-law inflation, hitherto discarded by the Planck data. We also achieve late-time inflation for fairly natural parameter values, with significantly less fine-tuning than in ΛCDM. Furthermore, we explore one specific limit of the modified gravity setup, characterised by a period of quartic kinetic domination of the inflaton, and its effects on the production of primordial gravitational waves by inflation. We find that during this period, which we call hyperkination, the peak in the density spectrum of gravitational waves corresponding to kination is truncated, thereby safely evading Big Bang Nucleosynthesis constraints. This allows us to bring the gravitational wave spectrum down to observable frequencies. If detected by future gravitational wave interferometers, it would provide valuable insight into the underlying theory. Lastly, mirroring the minimalist philosophy of quintessential inflation, we propose a toy model of unified early dark energy and quintessence, which raises the value of the Hubble constant inferred from the Planck data to values compatible with local measurements. It simultaneously explains the current accelerated expansion of the Universe, without significant additional fine-tuning than in ΛCDM.

Acknowledgements

First and foremost, I would like to thank my supervisor, Kostas. Your support was crucial for my growth during the last few years, both as a physicist and as a person. Thank you for believing in me.

I thank my parents, Antonio and Concha, for being there for me no matter what. If I ever become a parent I have you to look up to.

Special mention to all my friends, scattered across the globe. The list is long, but if you are reading this, you know who you are. I am incredibly grateful to have you in my life.

I would also like to thank my collaborators, Lucy Brissenden, Alexandros Karam, and Eemeli Tomberg. It was always a pleasure to work together. I would also like to thank my examiners, Arttu Rajantie and David Sloan, for attentively reading my thesis and for the insightful discussion during my viva.

Lastly, and most importantly, I thank Erica for being my companion through the whole thing.

I dedicate this thesis to my parents.

Declaration

I declare that the work presented in this thesis is, to the best of my knowledge and belief, original. The material has not been submitted, either in whole or in part, for a degree at this, or any other university. Chapters 1 through 3, containing introductory material, were written by myself by following many references, cited when appropriate. Chapters 4 through 7 are based on the original research articles [1, 2, 3, 4, 5, 6], written by myself in collaboration with Lucy Brissenden, Konstantinos Dimpoulos, Alexandros Karam, and Eemeli Tomberg. I participated in developing the idea behind Ref. [1], as well as performing all analytical and numerical calculations. In Refs. [2, 3] I performed all analytical and numerical calculations, either originally or as checks for my co-authors. In Ref. [5] I contributed to the writing and editing, including the production of the figures. I participated in developing the idea behind Ref. [4] and performed all analytical and numerical calculations, either originally or as checks for my co-authors. In Ref. [6], where I am the first author, I performed all analytical and numerical calculations, either originally or as checks for my co-authors. Chapter 8 contains a discussion and overview of the thesis as a whole, as well as of work in progress.

This thesis does not exceed the maximum permitted word length of 80,000 words including appendices and footnotes, but excluding the bibliography. A rough estimate of the word count is: 70500

Samuel Sánchez López

List of Publications

– K. Dimopoulos and **S. Sánchez López**, *Quintessential inflation in Palatini $f(R)$ gravity, Physical Review D* **103** (2021), no. 4 043533, [arXiv:2012.06831].

– K. Dimopoulos, A. Karam, **S. Sánchez López**, and E. Tomberg, *Modelling Quintessential Inflation in Palatini-Modified Gravity, Galaxies* **10** (2022), no. 2 57, [arXiv:2203.05424].

– K. Dimopoulos, A. Karam, **S. Sánchez López**, and E. Tomberg, *Palatini R^2 quintessential inflation, Journal of Cosmology and Astroparticle Physics* **10** (2022) 076, [arXiv:2206.14117].

– L. Brissenden, K. Dimopoulos and **S. Sánchez López**, *Non-ocillating early dark energy and quintessence from α-attractors, Astroparticle Physics* **157** (2024) 102925, [arXiv:2301.03572].

– K. Dimopoulos, L. Brissenden, and **S. Sánchez López**, *Explaining the Hubble tension and dark energy from α-attractors, Proceedings of Science* **CORFU2022** (2023) 247, [arXiv:2303.15523].

– **S. Sánchez López**, K. Dimopoulos, A. Karam, and E. Tomberg, *Observable gravitational waves from hyperkination in Palatini gravity and beyond, European Physical Journal C* **83** (2023), no. 12 1152, [arXiv:2305.01399].

Contents

List of Tables

List of Figures

Conventions

We use natural units with

$$c = \hbar = \kappa = 1, \tag{1}$$

and the reduced Planck mass

$$m_{\rm P} = \frac{1}{\sqrt{8\pi G}} \simeq 2.44 \times 10^{18}\,{\rm GeV}, \tag{2}$$

where G is Newton's gravitational constant. Notice the difference with $M_{\rm P} = 1/\sqrt{G}$, which can be sometimes found in the literature.

We use the "mostly plus" sign convention for the metric $(-,+,+,+)$. Repeated upper and lower indices are always summed over all their possible values. Greek indices take values $\mu, \nu = 0, 1, 2, 3$ while latin indices take values $i, j = 1, 2, 3$. Sometimes a boldface quantity represents a spatial vector, *e.g.*, $\mathbf{k} = k^i$.

Derivatives with respect to cosmic times are denoted by an overdot while derivatives with respect to conformal time are denoted by a prime

$$\dot{a} = \frac{{\rm d}a}{{\rm d}t}, \quad a' = \frac{{\rm d}a}{{\rm d}\eta}. \tag{3}$$

Our Fourier convention is

$$\mathcal{R}_{\mathbf{k}} = \int \frac{{\rm d}^3x}{(2\pi)^{3/2}} \mathcal{R}(\mathbf{x}) e^{-i\mathbf{k}\cdot\mathbf{x}} \quad \text{and} \quad \mathcal{R}(\mathbf{x}) = \int \frac{{\rm d}^3x}{(2\pi)^{3/2}} \mathcal{R}_{\mathbf{k}} e^{i\mathbf{k}\cdot\mathbf{x}} \tag{4}$$

Chapter 1

Introduction

Out of the cradle
onto dry land
here it is
standing:
atoms with consciousness;
matter with curiosity.

Stands at the sea,
wonders at wondering: I
a universe of atoms
an atom in the universe.

Richard P. Feynman

Cosmology is the study of the Universe as a whole. Although humans have wondered about the origin and structure of the Universe for millennia, cosmology as a rigorous science is only a few decades old. It wasn't until 1915 that Einstein discovered the appropriate language to describe the evolution of the Universe, the theory of general relativity. One hundred years ago, we did not know that the Universe is expanding or that there exist galaxies beyond our own. Just twenty-seven years ago we didn't know of the existence of dark energy, the main constituent

of the Universe at present.

During the current millennium, cosmology has experienced extraordinary developments. Perhaps most strikingly, we have measured the statistical properties of the Cosmic Microwave Background (CMB), light that was emitted when the Universe was about 370 000 years old and that has been travelling largely freely until the present day, and discovered the perturbations in the primordial universe that eventually grew into all the structure we observe today. The leading theory to explain such primordial perturbations, that of cosmic inflation, suggests that they have a quantum origin, stretched to cosmic scales just a billionth of a trillionth of a trillionth of a second after the Big Bang in a period of accelerated expansion. Another milestone was the discovery that after decelerating for 9 billion years, the Universe engaged in another bout of accelerated expansion, still ongoing at present, 13.8 billion years after the Big Bang. However, the nature of this dark energy, which accounts for around 70% of the contents of the present Universe, is still a mystery.

This thesis is mainly a study of inflation and dark energy. Since they are the only two (known) periods of accelerated expansion, we consider the natural possibility that they share a common origin, in what is called quintessential inflation. We also study the effect of including theoretically motivated modifications to the theory of general relativity, finding that it is helpful from a model-building perspective. Finally, we study other phenomenological aspects, such as the production of primordial gravitational waves (GWs) by inflation and the possibility of quintessential inflation aiding us in relaxing recent tensions between different cosmological datasets.

Chapter 2 provides a general introduction to the topics of FRW cosmology required for adequately following the subsequent chapters and aiming at making the text self-contained. We provide descriptions of the horizon and flatness problems, derive the spectrum of inflationary primordial perturbations, making contact with current observations of the CMB, and explain how the inflationary density can be transferred to the baryonic matter, during the process of reheating. Related to the

density of the Universe at present, we review the Hubble tension and explain the physics of dark energy, covering topics such as the cosmological constant problem and quintessence. We finish with quintessential inflation and its unique predictions. Chapter 3 also contains background material, namely an introduction to $f(R)$ gravity, both in the metric and Palatini formalisms. Since all subsequent chapters take place in the Palatini formalism, we explore in depth the main differences between the two.

Chapters 4 through 7 are based on the original research by the author, in collaboration with Lucy Brissenden, Konstantinos Dimopoulos, Alexandros Karam, and Eeemeli Tomberg. Chapter 4 showcases how modified gravity can help with model-building quintessential inflationary models. We consider a toy model, based on the original potential proposed by Peebles and Vilenkin, and analytically study the effect of adding a term proportional to the Ricci scalar squared to the gravitational action. We are able to rescue inflationary models otherwise discarded by the latest observational data of the CMB. More specifically, chaotic inflation with a mass term, arguably the simplest model of inflation, is brought back to life in the context of Palatini R^2 gravity. The dynamics of kination and quintessence are also studied, achieving successful dark energy with less fine-tuning than in ΛCDM. We finish by showing how the setup evades observational bounds.

Chapter 5 refines the philosophy of Chapter 4, by considering a better theoretically motivated potential and providing a more in-depth analysis. We consider a single-branch exponential potential and modify the gravitational action by including a non-minimal coupling between the field and gravity, expected from quantum field theory in curved spacetime, as well as the αR^2 term, where α is a non-perturbative coupling constant. We provide a thorough analysis, both analytically and numerically, throughout the history of the Universe, from inflation, through kination and reheating, until the present time. Again, we are able to resurrect the previously discarded exponential potential as a valid inflationary model and to achieve successful dark energy with less fine-tuning than in ΛCDM. We ensure this

is the case by performing a parameter scan of the model.

Chapter 6 takes the same setup in Palatini R^2 gravity and studies the production of GWs during the post-inflationary evolution of the Universe, in the limit where α is very large. We find a new period of cosmic evolution, prior to kination, which we name hyperkination. We calculate the density spectrum of GWs, both analytically and numerically, and find that it is flat for modes that re-enter the horizon during hyperkination. This truncates the infamous peak corresponding to kination, allowing us to bring the spectrum to frequencies accessible by future GW observations, such as LISA or ET. We perform a parameter scan of the model for all relevant GW observations, locating the parameter values required for detectability in each case and finding ample parameter space.

Chapter 7 does not follow the theme of the previous chapters in that it is not in the context of modified gravity. Rather, it proposes a simple toy model of unified early dark energy (EDE) and quintessence, in the context of α-attractors. EDE is one of the leading proposals to alleviate the Hubble tension, the discrepancy between the locally *measured* and cosmologically *inferred* values for the expansion rate today H_0. Were it to be discovered, one of the more pressing questions would be the unification with dark energy. We do so by means of a simple scalar field, originally frozen at an enhanced symmetry point, which briefly behaves as EDE before free-falling and re-freezing, to later behave as thawing quintessence. After providing some analytical estimates, we solve the dynamics numerically and perform a parameter scan at the background level, finding parameter values without additional fine-tuning than ΛCDM.

We conclude in Chapter 8, including an overview of the thesis as a whole in the context of the current state of the research field, as well as commenting on ideas for future work.

Chapter 2

Acceleration in a Dynamical Universe

The dynamics of the spacetime geometry and its matter content is governed by the action

$$S = S_{\rm EH} + S_{\rm m} = \frac{m_{\rm P}^2}{2}\int {\rm d}^4x\sqrt{-g}R + S_{\rm m}[g_{\mu\nu},\psi], \tag{2.1}$$

where the first term is the Einstein-Hilbert (EH) action, g is the determinant of the metric $g_{\mu\nu}$, $S_{\rm m}$ is the action for the matter fields, collectively denoted by ψ, such as the particles of the Standard Model (SM) and the inflaton, and R is the curvature scalar, defined as the contraction between the metric and the Ricci tensor $R_{\mu\nu}$, which, in turn can be written in terms of the connection $\Gamma^{\alpha}_{\mu\nu}$ as

$$R_{\mu\nu} = \partial_\lambda\Gamma^{\lambda}_{\mu\nu} - \partial_\nu\Gamma^{\lambda}_{\mu\lambda} + \Gamma^{\lambda}_{\lambda\rho}\Gamma^{\rho}_{\mu\nu} - \Gamma^{\rho}_{\mu\lambda}\Gamma^{\lambda}_{\nu\rho}. \tag{2.2}$$

Note that *a priori* the connection may be a gravitational field independent from the metric. This is so in the Palatini formalism [17, 18, 19]. Conversely, in the metric formalism, the only independent gravitational field is the metric. In this scenario, one usually assumes metric compatibility $\nabla_\alpha g_{\mu\nu} = 0$, where ∇_α is the covariant derivative. If one further assumes that the connection is torsionless $\Gamma^{\alpha}_{\mu\nu} = \Gamma^{\alpha}_{\nu\mu}$, it can then be shown that the connection takes the Levi-Civita form

$$\Gamma^{\alpha}_{\mu\nu} = \frac{1}{2}g^{\alpha\beta}\left(\partial_\mu g_{\beta\nu} + \partial_\nu g_{\beta\mu} - \partial_\beta g_{\mu\nu}\right). \tag{2.3}$$

Importantly, both formalisms agree for an EH action, but differ when more complicated functions of the Ricci scalar are considered. This is why it is important to specify the gravitational degrees of freedom before studying a specific inflationary model. In the present chapter, however, we limit ourselves to the EH action, so we postpone a discussion regarding the differences between the metric and Palatini formalisms, as well as details on modified gravity, to Chapter 3.

Extremising the action in Eq. (2.1) with respect to the metric we find the Einstein field equations

$$G_{\mu\nu} \equiv R_{\mu\nu} - \frac{1}{2} g_{\mu\nu} R = \frac{T_{\mu\nu}}{m_{\rm P}^2}. \tag{2.4}$$

The left-hand-side of this equation is a measure of the spacetime curvature, while the right-hand-side is a measure of the matter content, expressed through the energy-momentum tensor $T_{\mu\nu}$, which is defined as

$$T_{\mu\nu} = -\frac{2}{\sqrt{-g}} \frac{\delta S_{\rm m}}{\delta g^{\mu\nu}}. \tag{2.5}$$

In order to solve Eq. (2.4) we have to first specify the metric $g_{\mu\nu}$. Since the Universe (at cosmological scales) is homogeneous and isotropic to a very good approximation, we are led to the Friedmann-Robertson-Walker (FRW) metric

$$\mathrm{d}s^2 = g_{\mu\nu}\mathrm{d}x^\mu \mathrm{d}x^\nu = -\mathrm{d}t^2 + a^2(t)\left[\frac{\mathrm{d}r^2}{1-kr^2} + r^2(\mathrm{d}\theta^2 + \sin^2\theta \mathrm{d}\phi^2)\right], \tag{2.6}$$

where t is the cosmic time, and r, θ and ϕ are the radial and angular coordinates, respectively, of the spatial slices and k is the spatial curvature parameter. The latter can be chosen to be $k = 0$ for a flat space, $k > 0$ for a spherical space and $k < 0$ for a hyperbolic space. Note that the only dynamical degree of freedom is now the scale factor $a(t)$, which is a function of time only. It is standard practice to normalise it at the present time t_0 as $a(t_0) = 1$.

Homogeneity and isotropy also constrain the energy-momemtum to be that of a perfect fluid

$$T_{\mu\nu} = (\rho + p)u_\mu u_\nu + p g_{\mu\nu}, \tag{2.7}$$

where ρ and p are, respectively, the energy density and isotropic pressure of the fluid in the rest frame and u^μ is its comoving four-velocity. However, in order to solve the dynamics one extra relation between ρ and p, which may also depend on a, needs to be given. This is called the equation of state (EoS) and it reads

$$p = w\rho, \tag{2.8}$$

where w is the barotropic parameter.

The energy-momentum tensor should be conserved $\nabla_\mu T^{\mu\nu} = 0$ and the $\nu = 0$ equation gives the continuity equation

$$\dot{\rho} + 3\frac{\dot{a}}{a}\rho(1+w) = 0, \tag{2.9}$$

where an overdot represents a time derivative. For a constant w, this equation can be immediately integrated to obtain

$$\rho \propto a^{-3(1+w)}, \tag{2.10}$$

giving the usual scalings $\rho \propto a^{-3}$ for pressureless dust ($w = 0$), $\rho \propto a^{-4}$ for radiation ($w = 1/3$), and $\rho = $ const. for a cosmological constant ($w = -1$).

After plugging Eqs. (2.6)-(2.7) in the Einstein equation, its 00 component gives the first Friedmann equation

$$H^2 \equiv \left(\frac{\dot{a}}{a}\right)^2 = \frac{\rho}{3m_{\rm P}^2} - \frac{k}{a^2}, \tag{2.11}$$

where we have defined the Hubble parameter H. We can write the same equation in conformal time, which is defined as

$$\mathrm{d}\eta = \frac{\mathrm{d}t}{a}. \tag{2.12}$$

It reads

$$\mathcal{H}^2 = a^2\left(\frac{\rho}{3m_{\rm P}^2} - \frac{k}{a^2}\right), \tag{2.13}$$

where

$$\mathcal{H} \equiv \frac{a'}{a} = aH \tag{2.14}$$

is the Hubble parameter in conformal time and a prime denotes a derivative with respect to η.

The first Friedmann equation is often written in terms of the density parameters

$$\Omega_{\rm a} \equiv \frac{\rho_{\rm a}}{\rho_{\rm c}}, \tag{2.15}$$

where the subscript "a" stands for any component that contributes to the total energy density and $\rho_{\rm c}(t) = 3m_{\rm P}^2 H^2$ is the critical energy density. Indeed, taking into account the different scalings of the relevant components, the Friedmann equation can be rewritten as

$$H^2 = H_0^2 \left[\Omega_{\rm m,0} a^{-3} + \Omega_{\rm r,0} a^{-4} + \Omega_{\Lambda,0} + \Omega_{k,0} a^{-2}\right], \tag{2.16}$$

where the subscript "0" indicates that a quantity is evaluated at the present time t_0. For example, $\Omega_{k,0}$ is the density parameter of curvature, which reads

$$\Omega_k(t) = -\frac{k}{(aH)^2}, \tag{2.17}$$

evaluated at t_0.

Defining redshift as

$$z \equiv \frac{a(t_0)}{a(t)} - 1 = \frac{1}{a(t)} - 1, \tag{2.18}$$

where we have used the normalization $a(t_0) = 1$ at present, the Friedmann equation in terms of z reads

$$H^2 = H_0^2 \left[\Omega_{\rm m,0}(1+z)^3 + \Omega_{\rm r,0}(1+z)^4 + \Omega_{\Lambda,0} + \Omega_{k,0}(1+z)^2\right]. \tag{2.19}$$

Observations of the CMB temperature anisotropies suggest [8] that the contribution of the spatial curvature term to the total energy density of the universe is smaller than one part in a thousand $\Omega_{k,0} = 0.0007 \pm 0.0019\,(68\%\text{C.L.})$. From the Hot Big Bang until the present time, the comoving Hubble radius grows (see below), which means that $\Omega_k(t)$ also grows, *i.e.*, if $\Omega_{k,0}$ is so small at present, it had to be even smaller in the past. Thus, it is a very good approximation to take the Universe

as flat so that the second term in the r.h.s of Eq. (2.11) can be safely ignored and the FRW metric is simplified as

$$\mathrm{d}s^2 = a^2(t)\left[-\mathrm{d}\eta^2 + \delta_{ij}\mathrm{d}x^i\mathrm{d}x^j\right], \tag{2.20}$$

where we have used the definition of conformal time in Eq. (2.12).

The spatial components of the Einstein equations lead to the Raychaudhuri equation (also known as the second Friedmann equation)

$$\frac{\ddot{a}}{a} = -\frac{1}{6m_{\mathrm{P}}^2}(\rho + 3p), \tag{2.21}$$

which can also be obtained by taking a time derivative of the first Friedmann equation and combining it with the continuity equation. Note that Eq. (2.21) holds regardless of the spatial curvature parameter k. It is sometimes useful to combine this with the first Friedmann equation to obtain

$$\dot{H} = -\frac{1}{2m_{\mathrm{P}}^2}(\rho + p). \tag{2.22}$$

Conventional matter satisfies the Strong Energy Condition (SEC) $\rho + 3p \geq 0$. Thus, from Eq. (2.21) follows that $\ddot{a} < 0$. In this way, one would naively expect that the Universe expansion has been decelerating since its birth. We are in for a ride...

2.1 Inflation

Inflation is a hypothetical cosmological period, occurring at very early times, during which the Universe experiences accelerated expansion. It is prior to the hot Big Bang and it explains the observed high degree of homogeneity and spatial flatness. What is more, when treated quantum mechanically, it also provides the primordial perturbations that act as seeds for structure. We observe this today in the temperature anisotropies of the CMB and in the distribution of galaxies and galaxy clusters, also known as large scale structure (LSS).

The first ideas of inflation can be traced back to the early works of, *e.g.*, R. Brout *et al.* [20], D. Kazanas [21], K. Sato [22] and L. Z. Fang [23], while the first

model was proposed by A. A. Starobinsky [11] in 1980. The name *inflation* was coined by A. H. Guth some months after in Ref. [24], where it is also shown how inflation solves the horizon and flatness problems. Inflation was then developed into a full-fledged model by A. D. Linde [25] and A. Albrecht and P. J. Steinhardt [26] in 1981 and 1982, respectively. Since then, inflationary cosmology has become an extremely active area of research. Some excellent reviews can be found in Refs. [27, 28, 29, 30, 31, 32, 33, 34, 35].

2.1.1 Why inflation? The horizon and flatness problems

In order to explain the horizon problem, it is important to first understand the difference between the particle horizon d_h and the (comoving) Hubble radius $(aH)^{-1}$. The first is defined as the maximal comoving distance from which light can been received. In other words, the particle horizon determines the size of a causally connected patch of space. Since light follows null geodesics $\mathrm{d}s^2 = 0$, from Eq. (2.20) follows that the particle horizon is equal to the amount of conformal time

$$d_h = \eta - \eta_i = \int_{t_i}^{t} \frac{\mathrm{d}t'}{a(t')} = \int_{\ln a_i}^{\ln a} (aH)^{-1} \mathrm{d}\ln a. \tag{2.23}$$

In this equation $a_i \equiv a(t_i \equiv 0) = 0$ corresponds to the Big Bang singularity.

The comoving Hubble radius $(aH)^{-1}$ is the comoving distance that particles can travel in one expansion time. In other words, it is the maximal distance below which particles are causally connected at a given moment in time. Notice that if two particles are separated by a distance larger than the particle horizon they could have never been in causal contact, while if they are separated by a distance larger than the comoving Hubble radius they are not in causal contact at this specific moment in time. From the first Friedmann equation (with $a(t_0) = 1$) and Eq. (2.10) we have

$$(aH)^{-1} = H_0^{-1} a^{(1+3w)/2}. \tag{2.24}$$

Plugging this in Eq. (2.23) gives

$$d_h = \frac{2}{H_0(1+3w)} \left[a^{(1+3w)/2} - a_i^{(1+3w)/2} \right]. \tag{2.25}$$

Thus, for matter sources satisfying the SEC the comoving Hubble radius always grows and the integral in Eq. (2.23) is dominated by late time contributions giving $d_h \simeq (aH)^{-1}$. It also follows that the amount of conformal time between the Big Bang singularity and the emission of the CMB is much smaller than the conformal time between the singularity and today. In other words, most visible parts of the CMB had non-overlapping past lightcones at recombination, *i.e.*, when the CMB was emitted. However, not only the Universe today is homogeneous (at cosmological scales) to a very high degree of accuracy, but the tiny temperature anisotropies that are measured in the CMB are correlated over acausal distances. This is the horizon problem.

Before we continue with the discussion, let us emphasize that from now on we use the terms *horizon* and *comoving Hubble radius* interchangeably. If we ever need to refer to the particle horizon, we use its full name so that the distinction is clear. To make the discussion more quantitative, we can estimate how many casually disconnected patches there are in the sky. For our present purposes it is enough to consider a universe filled with matter and radiation only. Indeed, the inclusion of dark energy (see Sec. 2.2 for further details on dark energy) modifies the result only by $\sim 10\%$. From Eq. (2.16), the comoving Hubble radius then reads

$$(aH)^{-1} = \frac{1}{H_0\sqrt{\Omega_{\mathrm{m},0}}}\frac{a}{\sqrt{a+a_{\mathrm{eq}}}}, \tag{2.26}$$

where $a_{\mathrm{eq}} = \Omega_{\mathrm{m},0}/\Omega_{\mathrm{r},0} = 3388^{-1}$ [8] is the scale factor at the time of equality, *i.e.*, at the time at which the contributions from matter and radiation to the total energy density became equal. It is then straightforward to obain the particle horizon today

$$d_h(\eta_0) = \eta_0 = \frac{1}{H_0\sqrt{\Omega_{\mathrm{m},0}}}\int_0^1 \frac{\mathrm{d}a}{\sqrt{a+a_{\mathrm{eq}}}} \simeq \frac{2}{H_0\sqrt{\Omega_{\mathrm{m},0}}}, \tag{2.27}$$

where we have used that $a_0 = 1 \gg a_{\mathrm{eq}}$. Likewise, the particle horizon at recombination reads

$$d_h(\eta_{\mathrm{rec}}) = \eta_{\mathrm{rec}} = \frac{2}{H_0\sqrt{\Omega_{\mathrm{m},0}}}\left[\sqrt{a_{\mathrm{rec}}+a_{\mathrm{eq}}} - \sqrt{a_{\mathrm{eq}}}\right] \simeq 0.0176\eta_0, \tag{2.28}$$

where we have used that the scale factor at recombination is $a_{\rm rec} = 1091^{-1}$ [8]. Using the value of the Hubble parameter today $H_0 \simeq 70 {\rm km\,s^{-1}\,Mpc^{-1}} = 2 \times 10^{-4} {\rm Mpc}^{-1}$ and the fraction of matter today $\Omega_{\rm m,0} = 0.31$ [8] gives $\eta_{\rm rec} \simeq 314 {\rm Mpc}$, which should be compared with the distance from us to the last-scattering surface. The angle subtended by the horizon at recombination then reads

$$\theta = \frac{2\eta_{\rm rec}}{\eta_0 - \eta_{\rm rec}} = \frac{2 \times 0.0176}{1 - 0.0176} = 0.035\,{\rm rad} = 2.0^\circ. \tag{2.29}$$

Thus, at last scattering the Universe was composed of $\sim 10^5$ causally disconnected patches. We emphasize that the CMB temperature anisotropies over these 10^5 *a priori* causally disconnected patches are, in fact, correlated.

The flatness problem can also be explained in terms of the comoving Hubble radius. Indeed, from Eq. (2.17) we see that the density parameter of curvature is proportional to the comoving Hubble radius squared, so that for matter sources that satisfy the SEC it can only grow. Since its observed value today is $\Omega_{k,0} = 0.0007 \pm 0.0019\,(68\%{\rm C.L.})$ the initial conditions must have been highly fine-tuned. This can be easily quantified by combining Eqs. (2.17) and (2.26) to obtain

$$\Omega_k(t) = \frac{\Omega_{k,0}}{\Omega_{\rm m,0}} \frac{a^2}{a + a_{\rm eq}} \tag{2.30}$$

Evaluating this expression at matter-radiation equality ($a_{\rm eq} = 3388^{-1}$), at the time of Big Bang nucleosynthesis (BBN) ($a_{\rm BBN} \simeq 2.5 \times 10^{-9}$) and at the electroweak phase transition ($a_{\rm EW} \simeq 10^{-15}$) gives

$$\begin{aligned} |\Omega_k(t_{\rm eq})| &< 10^{-6}, \\ |\Omega_k(t_{\rm BBN})| &< 10^{-16}, \\ |\Omega_k(t_{\rm EW})| &< 10^{-29}. \end{aligned} \tag{2.31}$$

It is also instructive to study the evolution of the density parameter of curvature from the point of view of a dynamical system. Taking a derivative with respect to the number of e-folds $N \equiv \ln(a/a_i)$ of Eq. (2.17) and using the first and second Friedmann equations we obtain

$$\frac{{\rm d}\Omega_k}{{\rm d}N} = (1 + 3w)\Omega_k(1 - \Omega_k). \tag{2.32}$$

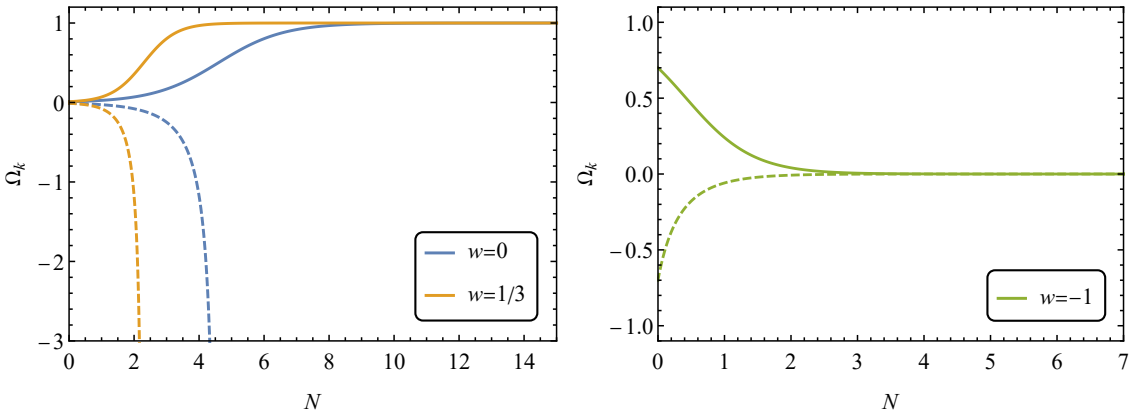

Figure 2.1: Left: Density parameter of curvature as a function of the elapsing number of e-folds $N \equiv \ln(a/a_i)$. Full lines have a positive initial condition $\Omega_k(N_i) = 0.01$ while dashed lines have a negative initial condition $\Omega_k(N_i) = -0.01$. Blue lines correspond to a matter-dominated universe while orange lines correspond to a radiation-dominated universe. Right: An analogous figure to the left panel, only now the universe is dominated by a cosmological constant. The initial condition for the full line is $\Omega_k(N_i) = 0.7$ while the initial condition for the dashed line is $\Omega_k(N_i) = -0.7$.

It is now clear that $\Omega_k = 0$ is an unstable fixed point for matter sources that satisfy the SEC. For any positive initial perturbation, the system evolves towards its second fixed point $\Omega_k = 1$, which is stable. In other words, $\Omega_k(N)$ grows until it becomes the dominant component of the Universe, making it an empty universe filled by a negative curvature component. Conversely, for small negative initial perturbations, the growth of $\Omega_k(N)$ accelerates and ends up diverging at the moment when the Hubble rate becomes zero, indicating a turn-around point of the scale factor. This corresponds to a $k > 0$ closed universe. We have numerically solved Eq. (2.32) and plotted the results in the left panel in Fig. 2.1. There it can be seen that the qualitative behaviour we have described for any source with $w \geq -1/3$ indeed is the same for both matter and radiation.

The solution to both the horizon and flatness problems seems now evident: a

shrinking comoving Hubble radius

$$\frac{\mathrm{d}}{\mathrm{d}t}(aH)^{-1} = -\frac{\ddot{a}}{\dot{a}^2} < 0, \tag{2.33}$$

where we have used that $aH = \dot{a}$. It is clear that the comoving Hubble radius decreases if and only if there is accelerated expansion, which is the usual definition of inflation. Equivalently, we can express the comoving Hubble radius in terms of the *first slow-roll parameter*

$$\epsilon_H \equiv -\frac{\dot{H}}{H^2} = 1 - \frac{\mathcal{H}'}{\mathcal{H}^2}, \tag{2.34}$$

since

$$\frac{\mathrm{d}}{\mathrm{d}t}(aH)^{-1} = -\frac{\dot{a}H + a\dot{H}}{(aH)^2} = -\frac{1}{a}(1-\epsilon). \tag{2.35}$$

Thus, accelerated expansion occurs if and only if

$$\epsilon_H < 1. \tag{2.36}$$

We emphasize that the three conditions $(aH)^{-1} < 1$, $\ddot{a} > 1$ and $\epsilon < 1$ are equivalent. More specifically, from the second Friedmann equation we can see that only matter sources with $w < -1/3$ lead to an accelerated expansion. With this, the second addend in the particle horizon in Eq. (2.25) diverges as

$$\lim_{a_i \to 0} \frac{2}{H_0(1+3w)} a_i^{(1+3w)/2} = -\infty \tag{2.37}$$

In other words, the initial singularity has been pushed to $\eta_i = -\infty$, while $\eta = 0$ corresponds to the end of inflation. In this way, there is now much more conformal time between the singularity and recombination, so that all the different CMB patches in the sky do have overlapping past lightcones. This is also why the perturbations in the CMB seem to be correlated over acausal distances. At sufficiently large negative conformal times all the fluctuations were inside the horizon. As the latter decreased in size, the fluctuations exited it. Then, after inflation, the comoving Hubble radius started growing, and the fluctuations progressively started re-entering it (see Fig. 2.2). Today, the particle horizon is much larger than the comoving Hubble radius.

In a similar way, in Eq. (2.32), if $w < -1/3$ then $\Omega_k = 0$ is an attractor. We show this in the right panel of Fig. 2.1 for the case of a cosmological constant. Therefore, whatever the initial curvature is, if inflation lasts long enough the value of Ω_k will be driven close enough to zero such that the subsequent post-inflationary evolution does not increase it above the observational bounds.

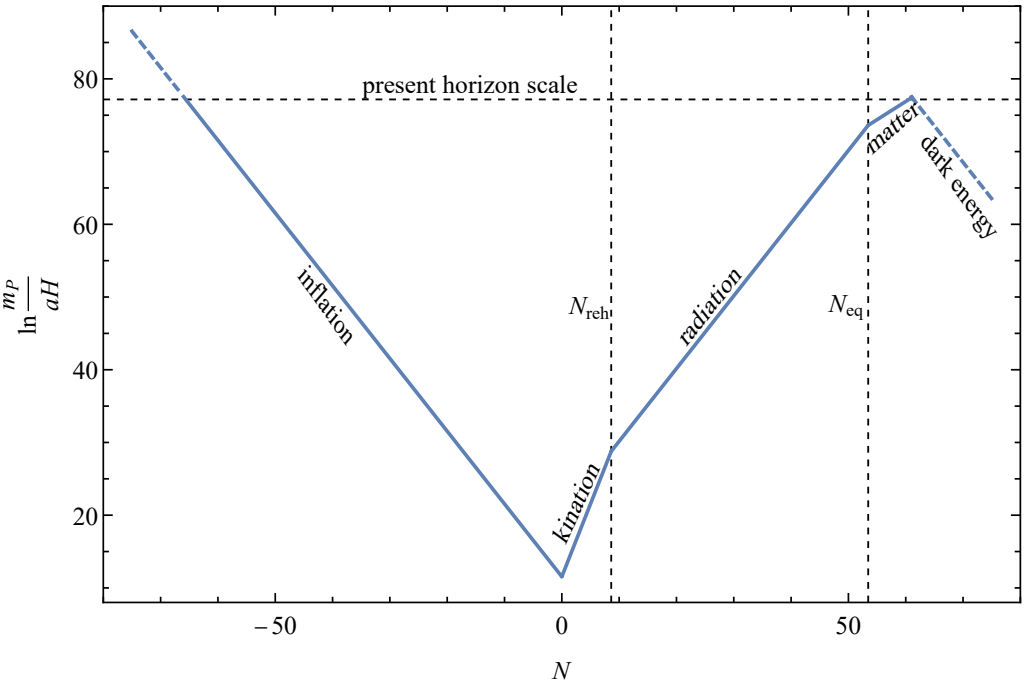

Figure 2.2: Comoving Hubble radius $(aH)^{-1}$ (in natural units) as a function of the number of e-folds $N = \ln a/a_i$, with the scale factor normalised at the end of inflation as $a_i = 1$. We have approximated the energy density of inflation as a constant, with a value of $\rho = 10^{-10} m_{\rm P}^4$ (GUT scale). The inclusion of the kination era increases the number of inflationary e-folds, as given by Eq. (2.45). $N_{\rm reh}$ signals the moment of reheating, the temperature of which has been set to $T_{\rm reh} = 10^{10}\,$GeV. The recent dark energy domination has initiated a new epoch of inflation.

We can estimate the minimum duration of the inflationary phase in order for it solve the horizon and flatness problems [36, 37]. To this end, we need to assume a specific post-inflationary expansion history of the Universe. Although for times between BBN and the present the details are well known, there is a lot

of uncertainty for times between the end of inflation and BBN. This is mainly because the period of reheating, *i.e.*, the period during which the inflationary energy density is transformed into the matter and radiation of the hot Big Bang, is highly model dependent. We parametrise our ignorance by assuming that the Universe is dominated by a perfect fluid with barotropic parameter w, so that the energy density scales as in Eq. (2.10). Furthermore, as we will see below, the spectrum of scalar perturbations is almost scale invariant, in support of a quasi-de Sitter expansion during inflation. Therefore, it is a good approximation to assume that the Hubble parameter is constant during this period.

As we mention above, the scales k that are re-entering the horizon today should have been inside the comoving Hubble radius during inflation. This means that $(a_0 H_0)^{-1} < (a_k H_k)^{-1}$, where $k = a_k H_k$. Notice that we are using the comoving Hubble radius rather than the particle horizon: inflation could have started many e-folds before the scale k left the horizon, but have no access to this information.

Comparing the scale k with the comoving Hubble radius today gives

$$\frac{k}{a_0 H_0} = \frac{a_k H_k}{a_0 H_0} = \frac{a_k}{a_{\rm end}} \frac{a_{\rm end}}{a_{\rm reh}} \frac{a_{\rm reh}}{a_{\rm eq}} \frac{H_{\rm end}}{H_{\rm eq}} \frac{a_{\rm eq} H_{\rm eq}}{a_0 H_0}, \tag{2.38}$$

where end stands for the end of inflation, reh for reheating, eq for matter-radiation equality, 0 for the present time and we have used that $H_k \simeq H_{\rm end}$, since $H \simeq$ cte during inflation. Remembering that during matter domination the Hubble parameter scales as $H \propto a^{-3/2}$, we have

$$\frac{a_{\rm eq} H_{\rm eq}}{a_0 H_0} = \left(\frac{a_0}{a_{\rm eq}} \right)^{1/2} = \sqrt{1 + z_{\rm eq}} \simeq 58, \tag{2.39}$$

where we have used $z_{\rm eq} = 3387$ [8] and ignored the negligible contribution from dark energy. The other factor can be rewritten as

$$\frac{a_{\rm end}}{a_{\rm reh}} \frac{a_{\rm reh}}{a_{\rm eq}} \frac{H_{\rm end}}{H_{\rm eq}} = \left(\frac{\rho_{\rm reh}}{\rho_{\rm end}} \right)^{\frac{1}{3(1+w)}} \frac{T_{\rm eq}}{T_{\rm reh}} \frac{V_{\rm end}^{1/2}}{\rho_{\rm eq}^{1/2}}, \tag{2.40}$$

where have used that between the end of inflation and reheating the density scales as $\rho \propto a^{-3(1+w)}$, $a \propto 1/T$ after reheating and the Friedmann equation $H \propto \sqrt{\rho}$.

This expression can be further simplified by taking into account that the energy density of radiation reads

$$\rho = \frac{\pi^2 g_*}{30} T^4, \tag{2.41}$$

where g_* is the relativistic number of effective degrees of freedom. The result reads

$$\frac{a_{\rm end}}{a_{\rm reh}} \frac{a_{\rm reh}}{a_{\rm eq}} \frac{H_{\rm end}}{H_{\rm eq}} = \left(\frac{\pi^2 g_*(T_{\rm reh})}{30} \right)^{\frac{1}{3(1+w)}} \left(\frac{T_{\rm reh}}{V_{\rm end}^{1/4}} \right)^{\frac{1-3w}{3(1+w)}} \sqrt{\frac{30}{\pi^2 g_*(T_{\rm eq})}} \frac{V_{\rm end}^{1/4}}{T_{\rm eq}}. \tag{2.42}$$

Using that $T_{\rm eq} \simeq 8.2 \times 10^{-10}\,{\rm GeV}$ [8], $g_*(T_{\rm eq}) = 3.36$ and $g_*(T_{\rm reh}) = 106.75$, we obtain that the number of e-folds reads

$$N = \ln \frac{a_{\rm end}}{a_k} = 61.77 + \frac{1}{3(1+w)} \ln (35.12) + \frac{1-3w}{3(1+w)} \ln \left(\frac{T_{\rm reh}}{V_{\rm end}^{1/4}} \right) + \ln \left(\frac{V_{\rm end}^{1/4}}{10^{16}{\rm GeV}} \right) \tag{2.43}$$

Of course, this expression could be refined, *e.g.*, by taking into account a more realistic inflationary quasi-de Sitter expansion so that $H_{\rm end} < H_k$ or by not neglecting the recent period of dark energy domination. However, for our present purposes Eq. (2.43) is accurate enough. For example, for GUT-scale inflation $V_{\rm end}^{1/4} \simeq 10^{16}\,{\rm GeV}$ followed by a period of perturbative reheating, for which $w = 0$ (see Sec. 2.1.5 for more details on reheating) with $T_{\rm reh} = 10^{10}\,{\rm GeV}$, the number of e-folds is $N \simeq 58$. Of course, the number of e-folds is lower the lower $T_{\rm reh}$ is. Nevertheless, the Universe has to be dominated by radiation by the time BBN commences, at a temperature of approximately 100 keV. Therefore, we have a hard bound on the minimum reheating temperature allowed

$$T_{\rm reh} > 0.1\,{\rm MeV}. \tag{2.44}$$

The number of e-folds with $T_{\rm reh} = 0.1\,{\rm MeV}$ and GUT-scale inflation is $N \simeq 50$. This the reason why in the literature the number of e-folds is typically taken to be between 50 and 60.

N could be significantly increased if inflation was followed by some non-conventional period of cosmic expansion. For example, during kination (see Sec. 2.2.5 for further details on kination and quintessential inflation) $w = 1$. If we change

the barotropic parameter of the Universe before reheating as $0 \to 1$, the prefactor of the third term in the right-hand-side of Eq. (2.43) changes as $1/3 \to -1/3$ (and as $1/3 \to 1/6$ in the second term, although this effect is subdominant). Therefore, the number of e-folds is increased by

$$\Delta N = -\frac{2}{3} \ln \left(\frac{T_{\rm reh}}{V_{\rm end}^{1/4}} \right). \tag{2.45}$$

Choosing again $T_{\rm reh} = 10^{10}\,\text{GeV}$ and GUT-scale inflation gives $\Delta N = 9$. In Fig. 2.2 we show the comoving Hubble radius as a functions of the number of e-folds in precisely this situation. It becomes visually obvious how the existence of the kination period increases the number of inflationary e-folds. As a final comment, note that the increase could be as much as $\Delta N = 30$, corresponding to $T_{\rm reh} = T_{\rm BBN}$, although this situation is obviously unrealistic.

In summary, inflation solves the horizon and flatness problems, provided it lasts long enough, *i.e.*, longer than the number of e-folds in Eq. (2.43). As we have seen, this happens when ϵ_H remains small for a sufficient amount of e-folds (around 60 according to our estimation). To this end, we define the *second slow-roll parameter*

$$\eta_H \equiv \frac{\mathrm{d} \ln \epsilon_H}{\mathrm{d}N} = \frac{\dot{\epsilon}_H}{H \epsilon_H}. \tag{2.46}$$

Inflation occurs when $\epsilon_H < 1$ and persists when $|\eta_H| < 1$, *i.e.*, when the fractional change of the first slow-roll parameter is small.

2.1.2 The physics of inflation: the background

The simplest way to achieve inflation is by introducing a scalar field $\phi = \phi(t, \mathbf{x})$, named the inflaton, with its dynamics governed by the action in Eq. (2.1) and the inflationary sector given by

$$S_\phi = \int \mathrm{d}^4x \sqrt{-g} \left[-\frac{1}{2} g^{\mu\nu} \partial_\mu \phi \partial_\nu \phi - V(\phi) \right], \tag{2.47}$$

where $V(\phi)$ is the potential energy density of the field. Using the definition in Eq. (2.5), the associated energy-momentum tensor reads

$$T^{(\phi)}_{\mu\nu} = \partial_\mu \phi \partial_\nu \phi - g_{\mu\nu} \left[\frac{1}{2} g^{\alpha\beta} \partial_\alpha \phi \partial_\beta \phi + V(\phi) \right], \tag{2.48}$$

while the equation of motion of the inflaton reads

$$\frac{\delta S_\phi}{\delta \phi} = 0 = \frac{1}{\sqrt{-g}} \partial_\mu \left(\sqrt{-g} g^{\mu\nu} \partial_\nu \phi \right) - V'(\phi), \tag{2.49}$$

where a prime in the potential represents a total derivative with respect to its argument. Plugging in the flat FRW metric gives the Klein-Gordon (KG) equation

$$\ddot{\phi} + 3H\dot{\phi} - \frac{1}{a^2} \delta^{ij} \partial_i \partial_j \phi + V' = 0. \tag{2.50}$$

At the background level, homogeneity and isotropy make the field a function of time only $\phi = \phi(t)$. Thus, the Laplacian term in the KG equation vanishes. Likewise, the energy density and pressure read can be read off from the energy-momentum tensor to be

$$\rho = \frac{1}{2}\dot{\phi}^2 + V, \tag{2.51}$$

$$p = \frac{1}{2}\dot{\phi}^2 - V. \tag{2.52}$$

The barotropic parameter of the field is defined as

$$w_\phi = \frac{p}{\rho} = \frac{\dot{\phi}^2/2 - V}{\dot{\phi}^2/2 + V}. \tag{2.53}$$

The dynamics of the system is then determined by

$$\ddot{\phi} + 3H\dot{\phi} + V' = 0, \tag{2.54}$$

and the Friedmann equations

$$H^2 = \frac{1}{3m_{\mathrm{P}}^2} \left(\frac{1}{2}\dot{\phi}^2 + V \right), \tag{2.55}$$

$$\frac{\ddot{a}}{a} = -\frac{1}{3m_{\mathrm{P}}^2} \left(\dot{\phi}^2 - V \right). \tag{2.56}$$

Note that the latter can be derived from the other two by taking a time derivative of the first Friedmann equation and combining it with the KG equation. From the second Friedmann equation it follows that accelerated expansion occurs when

$$V > \dot{\phi}^2. \tag{2.57}$$

It is instructive to obtain the same condition from the first slow-roll parameter. Plugging Eqs. (2.51)-(2.52) in Eq. (2.22) gives $\dot{H} = -\dot{\phi}^2/(2m_{\rm P}^2)$. Using this in Eq. (2.34) we have

$$\epsilon_H = \frac{\dot{\phi}^2}{2m_{\rm P}^2 H^2}. \tag{2.58}$$

Imposing $\epsilon_H < 1$ we recover Eq. (2.57).

We have just found that a scalar field can sustain inflation when it is the dominant contribution to the density of the Universe and its potential energy density is larger than (twice) its kinetic energy density. But inflation should also last long enough. At this point it is useful to define the dimensionless acceleration per Hubble time

$$\delta_H \equiv -\frac{\ddot{\phi}}{\dot{\phi}H} = 1 - \frac{\phi''}{\mathcal{H}\phi'}. \tag{2.59}$$

We can then obtain an expression for the second slow-roll parameter

$$\eta_H = \frac{\dot{\epsilon}_H}{\epsilon_H H} = -2\frac{\dot{H}}{H^2} + 2\frac{\ddot{\phi}}{H\dot{\phi}} = 2(\epsilon_H - \delta_H), \tag{2.60}$$

where we have used Eq. (2.58). As we explain below, *slow-roll inflation* is in very good agreement with observations. The *slow-roll* conditions read

$$\epsilon_H \ll 1 \quad \text{and} \quad |\eta_H| \ll 1. \tag{2.61}$$

From Eq. (2.60) we see that if $\{\epsilon_H, |\delta_H|\} \ll 1$ then the slow-roll conditions $\{\epsilon_H, |\eta_H|\} \ll 1$ are satisfied. In other words, if the speed of the inflaton in field space is small inflation takes place and if the acceleration of the inflaton is small inflation lasts for a long time.

So far all the presented results have been exact. However, the slow-roll conditions help simplify the equations of motion. Indeed, from $\delta_H \ll 1$ we can safely neglect the acceleration term in the KG equation, which now reads

$$3H\dot{\phi} + V' \simeq 0, \tag{2.62}$$

and from $\epsilon_H \ll 1$ we can neglect the kinetic energy term in the first Friedmann, which reduces to

$$H^2 \simeq \frac{V}{3m_{\rm P}^2}. \tag{2.63}$$

These approximated equations are first order ordinary differential equations and thus easier to solve than Eqs. (2.54)-(2.55). Of course, they are more accurate the smaller δ_H and ϵ_H are. Importantly, they can also be used to express the slow-roll parameters solely in terms of the potential. Indeed, plugging Eqs. (2.62) and (2.63) in Eq. (2.58) gives

$$\epsilon_H = \frac{\dot{\phi}^2}{2m_{\rm P}^2 H^2} \simeq \frac{m_{\rm P}^2}{2}\left(\frac{V'}{V}\right)^2. \tag{2.64}$$

It is now convenient to consider the combination

$$\delta_H + \epsilon_H \simeq \frac{V''}{3H^2} + \frac{\dot{H}}{H^2} - \frac{\dot{H}}{H^2} = m_{\rm P}^2\frac{V''}{V}, \tag{2.65}$$

where we have taken a time derivative of Eq. (2.62) and plugged it in the definition of δ_H in the first step and used Eq. (2.63) in the second step.

We are led to define the *potential* slow-roll parameters

$$\epsilon_V \equiv \frac{m_{\rm P}^2}{2}\left(\frac{V'}{V}\right)^2, \tag{2.66}$$

$$\eta_V \equiv m_{\rm P}^2\frac{V''}{V}, \tag{2.67}$$

which are related to the Hubble slow-roll parameters via

$$\epsilon_V \simeq \epsilon_H \quad \text{and} \quad \eta_V \simeq 2\epsilon_H - \frac{1}{2}\eta_H. \tag{2.68}$$

If $\{\epsilon_V, |\eta_V|\} \ll 1$ then $\{\epsilon_H, |\eta_H|\} \ll 1$ are satisfied. At this point it is important to emphasize that the potential slow-roll conditions $\{\epsilon_V, |\eta_V|\} \ll 1$ are a necessary condition for slow-roll inflation, but they are not a sufficient. Indeed, they determine the slope and curvature of the potential, but they have nothing to say about the velocity of the field in field space, which could initially be very large. However, if an inflationary solution exists, all inflationary trajectories in field space approach each other, even exponentially fast when in the linear regime [38, 39] This means that, if a potential has a large enough region with $\{\epsilon_V, |\eta_V|\} \ll 1$, unless the initial conditions of the inflaton are fine-tuned with very large velocity, the inflaton will always end up in a slow-roll trajectory. In other words, slow-roll inflation is an attractor.

The expression for the number of inflationary e-folds is also simplified by the slow-roll conditions. It is easy to show that it can be written as

$$N = \int_{t_*}^{t_{\rm end}} \mathrm{d}t\, H = \frac{1}{m_{\rm P}} \int_{\phi_{\rm end}}^{\phi_*} \frac{\mathrm{d}\phi}{\sqrt{2\epsilon_H}} \simeq \frac{1}{m_{\rm P}} \int_{\phi_{\rm end}}^{\phi_*} \frac{\mathrm{d}\phi}{\sqrt{2\epsilon_V}} = \frac{1}{m_{\rm P}^2} \int_{\phi_{\rm end}}^{\phi_*} \mathrm{d}\phi \frac{V}{V'}, \qquad (2.69)$$

where $\phi_{\rm end}$ is the field value at the end of inflation, determined by the condition $\epsilon_H(\phi_{\rm end}) = 1$ ($\epsilon_V(\phi_{\rm end}) = 1$ is a good approximation if slow-roll lasts until the end of inflation), and ϕ_* is the field value at which the cosmological scales that we observe today exited the horizon.

To gain some intuition regarding the dynamics of the inflaton it is useful to note that Eq. (2.54) resembles the equation of a particle moving in a potential V subject to friction $3H$ in field space, where the coordinate is ϕ. Slow-roll inflation takes place when the potential density is much larger than the kinetic energy. From Eq. (2.63), we see that the larger V is, the larger the H is. This means that we can picture the inflaton as ball rolling down a potential in which the friction is larger the higher in the potential it is. During slow-roll, the acceleration term in the KG equation can be neglected and the evolution of the inflaton is determined by a balance between the slope of the potential and the friction. Of course, the inflaton evolves in a way that tries to diminish its potential density, so at some point the friction decreases enough, its kinetic energy grows and slow-roll inflation ceases. Inflation lasting long enough is guaranteed by a small enough second slow-roll parameter. Indeed, if the second derivative of the potential is small, the slope does not change much, ensuring the inflaton stays in the region with large V for a long time.

2.1.3 The physics of inflation: from quantum to classical

So far our treatment has been at the background level, with all quantities being a function of cosmic time only. However, although the Universe is homogeneous and isotropic to a very high degree, it is not perfectly so, which means that the cosmological fields need to have some spatial dependence. The way this is usually described is via cosmological perturbation theory (see, *e.g.*, Ref. [40] or

Refs. [41, 42] for a review), where the metric and energy-momentum tensor are expanded as a perturbative series around the FRW solution. In this context, the inflaton perturbations $\delta\phi(\eta, \mathbf{x})$, after being quantized, act as the initial conditions for the subsequent hot Big Bang evolution. Indeed, the exponential expantion during inflation stretches the perturbations $\delta\phi(\eta, \mathbf{x})$ to super-Hubble scales $k \ll \mathcal{H}$, making them classical [43, 44, 45, 46, 47, 48]. Later, after the end of inflation, when the comoving Hubble radius starts increasing, they re-enter the causally connected patches and act as the seeds of structure. In this section we calculate the spectrum of these quantum fluctuations. Further details on cosmological perturbation theory can be found in Appendix A.1.

In cosmological perturbation theory, quantities are expanded as

$$\chi(\eta, \mathbf{x}) = \bar{\chi}(\eta) + \delta\chi(\eta, \mathbf{x}), \tag{2.70}$$

where $\chi(\eta, \mathbf{x})$ stands for any cosmological field. For example, the most general FRW metric perturbed to first order reads [49, 50]

$$\begin{aligned} \mathrm{d}s^2 &= (\bar{g}_{\mu\nu} + \delta g_{\mu\nu})\,\mathrm{d}x^\mu \mathrm{d}x^\nu \\ &= a^2(\eta)\left[-(1+2A)\mathrm{d}\eta^2 + 2B_i \mathrm{d}\eta \mathrm{d}x^i + (\delta_{ij} + 2E_{ij})\,\mathrm{d}x^i \mathrm{d}x^j\right], \end{aligned} \tag{2.71}$$

where the factors of 2 have been chosen for convenience. The perturbed energy-momentum tensor can be written as

$$T^0{}_0 = -(\bar{\rho} + \delta\rho), \tag{2.72}$$

$$T^i{}_0 = -(\bar{\rho} + \bar{p})v_i \equiv q_i, \tag{2.73}$$

$$T^i{}_j = (\bar{p} + \delta p)\delta^i_j + \Pi^i{}_j, \tag{2.74}$$

where v^i is the bulk velocity (notice it is a perturbation) and we have defined the momentum density q_i and anisotropic stress $\Pi^i{}_j$, which is traceless $\Pi^i{}_i = 0$. Since the spacetime dependent perturbations are much smaller than the homogeneous background, *i.e.*, $\delta\chi \ll \bar{\chi}$, the perturbed Einstein and continuity equations, $\delta G_{\mu\nu} = \delta T_{\mu\nu}/m_{\mathrm{P}}^2$ and $\nabla_\mu \delta T^{\mu\nu} = 0$, approximate well the full non-linear solution.

Another important property is that scalar, vector and tensor perturbations do not mix at linear order [32]. This allows us to treat them separately by using the scalar-vector-tensor (SVT) decomposition [51]. Importantly[1], at second order, scalar perturbations do, in fact, act as a source for tensor perturbations [70, 71, 72, 73] (see also Ref. [74] for a review). However, for our present purposes this is not relevant.

The first step is to identify the physical degrees of freedom. To do so it is important to realize that perturbations generally depend on our gauge choice. Indeed, perturbations are defined as the difference between tensors in the physical (perturbed) spacetime and a given background spacetime, $\delta\chi(\eta,\mathbf{x}) = \chi(\eta,\mathbf{x}) - \bar{\chi}(\eta)$. In other words, we are comparing tensors in two different manifolds, although for this comparison to be meaningful it should be made at the same point of a given manifold. This is the gauge problem [49]. Thus, a prescription identifying points in the perturbed spacetime with points in the background spacetimes needs to be given. This is called a gauge choice. A change in this correspondence (keeping the background coordinates fixed) is called a gauge transformation, which can be generally written as

$$x^\mu \mapsto \tilde{x}^\mu = x^\mu + \xi^\mu(t,\mathbf{x}). \tag{2.75}$$

In order to address the gauge problem there are two possible avenues. We can either construct gauge invariant quantities [49], *i.e.*, quantities that remain invariant under gauge transformations, or we can fix a specific gauge and keep track of all perturbations.

We now give a simple example to illustrate the gauge problem. Consider a homogeneous energy density $\bar{\rho}(\eta)$ and a change in time slicing $\eta \mapsto \tilde{\eta} = \eta + \xi^0(\eta,\mathbf{x})$. In terms of the new coordinates the density reads $\bar{\rho}(\eta) = \bar{\rho}(\tilde{\eta} - \xi^0) = \bar{\rho}(\tilde{\eta}) - \bar{\rho}'(\tilde{\eta})\xi^0$. We see that the energy density is no longer homogenous, having a perturbation

[1] Although the amplitude of the scalar perturbations is tiny at CMB scales, at small scales it may be enhanced, leading to the production of Primordial Black Holes (PBHs). In this way, the production of GWs would also be enhanced at such scales [52, 53, 54, 55, 56, 57, 58, 59, 60, 61, 62, 63, 64]. This has recently lead to a surge of interest [65, 66, 67, 68, 69] since the GW spectrum may inherit the small anisotropies found in the scalar spectrum.

given by $\delta\rho(\tilde{\eta},\mathbf{x}) = -\bar{\rho}'(\tilde{\eta})\xi^0(\tilde{\eta},\mathbf{x})$. Likewise, a physical perturbation can be hidden away by choosing an appropriate time slicing (of course, we would not actually get rid of the perturbation, as it would reappear in the metric).

A detailed analysis on how perturbations behave under gauge transformations can be found in Appendix A.1. With these transformation properties in hand, we are able to count the physical scalar degrees of freedom. During inflation there are five scalar perturbations: four coming from the metric, *i.e.*, A, B, C and E, and one from the inflaton, *i.e.*, $\delta\phi$. The freedom in choosing ξ and ξ^0 allows to set two perturbations to zero. Furthermore, the Einstein equations relate the perturbations to each other, acting as constraint equations. This allows to set another two perturbations to zero. We are left with one physical scalar degree of freedom.

We choose to parametrize the only scalar degree of freedom by one of the following two important gauge invariant quantities. The first one is the curvature perturbation on uniform density hypersurfaces [75]

$$\zeta = -C + \nabla^2 E + \mathcal{H}\frac{\delta\rho}{\bar{\rho}'}, \tag{2.76}$$

called this way since it reduces to the intrinsic curvature of spatial slices in the uniform density gauge ($\delta\rho = 0$). The second one is the comoving curvature perturbation

$$\mathcal{R} = -C + \nabla^2 E - \mathcal{H}(v + B), \tag{2.77}$$

where v is the scalar part in the SVT decomposition of the velocity v_i. It is called this way since it corresponds to the intrinsic curvature of spatial slices in the comoving gauge ($v = B = 0$). Both curvature perturbations are related via the linearized Einstein equations

$$-\zeta = \mathcal{R} + \left(\frac{k}{aH}\right)^2 \frac{2\bar{\rho}}{3(\bar{p}+\bar{\rho})}\Psi, \tag{2.78}$$

where $\Psi \equiv A + \mathcal{H}(B - E') + (B + E')'$ is one of the Bardeen potentials [49]. Thus, on super-horizon scales $k \ll aH$ both curvature perturbations are equal and can be used interchangeably. Furthermore, also on super-horizon scales, they are both

constant if the matter perturbations are adiabatic [76], *i.e.*, if

$$\delta p_{\rm en} \equiv \delta p - \frac{\dot{\bar{p}}}{\dot{\bar{\rho}}}\delta\rho = 0, \tag{2.79}$$

where we have defined the non-adiabatic or entropy perturbation $\delta p_{\rm en}$. Note that $\delta p_{\rm en}$ is gauge invariant. This critical feature makes them the best candidate to describe the scalar perturbations.

Let us work in the comoving gauge with

$$\delta\phi = E = 0, \tag{2.80}$$

and solve for B and C by using the Einstein equations. Thus, the perturbed metric reads (we do not consider vector perturbations as they decay exponentially during inflation)

$$\mathrm{d}s^2 = a^2(\eta)\left[-\mathrm{d}\eta^2 + (1-2\mathcal{R})\delta_{ij}\mathrm{d}x^i\mathrm{d}x^j\right], \tag{2.81}$$

where we have ignored the tensorial perturbations for now. Note that in this gauge the inflaton is unperturbed, and all scalar degrees of freedom are parametrized by the comoving curvature perturbation $\mathcal{R}(\eta,\mathbf{x})$. In order to obtain the equation of motion for the latter, we need to expand the action to second order in $\mathcal{R}$. This is a somewhat technical calculation that involves the ADM formalism [77] (see Ref. [78] for a more didactic presentation). The full derivation can be found in Ref. [79]. The result reads

$$S = \frac{1}{2}\int \mathrm{d}^4x\, a^3\frac{\dot{\phi}^2}{H^2}\left[\dot{\mathcal{R}}^2 - \frac{1}{a^2}\delta^{ij}\partial_i\mathcal{R}\partial_j\mathcal{R}\right] + \mathcal{O}(\mathcal{R}^3). \tag{2.82}$$

Introducing the Mukhanov-Sasaki variable[2] [80, 81]

$$v \equiv z\mathcal{R}, \tag{2.83}$$

where

$$z \equiv a\frac{\dot{\phi}}{H} = a\frac{\phi'}{\mathcal{H}} = a\sqrt{2\epsilon_H}m_{\rm P}, \tag{2.84}$$

[2]Note that the Mukhanov-Sasaki variable and the scalar part of the off-diagonal components of the perturbed energy-momentum tensor are both denoted by v. The difference between them is obvious by the context.

and switching to conformal time, Eq. (2.82) can be rewritten as

$$\begin{aligned} S &= \frac{1}{2}\int \mathrm{d}\eta \mathrm{d}^3x \left[(v')^2 - \delta^{ij}\partial_i v \partial_j v + \frac{z''}{z}v^2\right] \\ &= \frac{1}{2}\int \mathrm{d}\eta \mathrm{d}^3k \left[(v_{\mathbf{k}}')^2 - \left(k^2 - \frac{z''}{z}\right)v_{\mathbf{k}}^2\right], \end{aligned} \tag{2.85}$$

where we have switched to Fourier space in the second step by introducing

$$v(\eta, \mathbf{x}) = \int \frac{\mathrm{d}^3k}{(2\pi)^{3/2}} v_{\mathbf{k}}(\eta) e^{i\mathbf{k}\cdot\mathbf{x}}. \tag{2.86}$$

The conjugate momentum to the canonically normalised variable v reads

$$\pi(\eta, \mathbf{x}) = \frac{\delta S}{\delta(\partial_\eta v)} = v'(\eta, \mathbf{x}). \tag{2.87}$$

Extremising Eq. (2.85) gives the Mukhanov-Sasaki equation

$$v_k'' + \left(k^2 - \frac{z''}{z}\right)v_k = 0. \tag{2.88}$$

This is the equation for a harmonic oscillator with a time dependent frequency $\omega_k^2(\eta) = k^2 + z''/z$. Let us emphasize that all the couplings between the metric and the inflaton (to first order in perturbation theory) are contained in this simple equation. Also note that we have dropped the vector notation $\mathbf{k} \to k$, since Eq. (2.88) only depends on the modulus of the wavenumber. Finally, note that the time-dependent part of the frequency can be written in terms of the slow-roll parameters. Indeed, differentiating z twice in Eq. (2.84) with respect to conformal time we obtain

$$\frac{z''}{z} = 2\mathcal{H}^2\left[1 + \epsilon_H - \frac{3}{2}\delta_H + \left(\epsilon_H - \frac{\delta_H}{2}\right)(\epsilon_H - \delta_H) - \frac{\delta_H'}{2\mathcal{H}}\right]. \tag{2.89}$$

No approximations have been made, we have simply rewritten the time dependent part in terms of ϵ_H and δ_H.

Since inflation is a period of quasi-de Sitter expansion (see below), we can analyze the Mukhanov-Sasaki equation in the pure de Sitter limit in order to gain some intuition. During de Sitter, the scale factor reads $a(t) \propto e^{Ht}$, or, in conformal time,

$$a(\eta) = -\frac{1}{H\eta}, \tag{2.90}$$

where $\eta \in (-\infty, 0)$, with minus infinity corresponding to the initial Big Bang singularity at $t = 0$ and zero corresponding to the end of inflation. Note that it is not possible for inflation to be a period of pure de Sitter expansion, since inflation could have not ended. Using that the de Sitter limit corresponds to $\{\epsilon_H, \delta_H\} \to 0$ in Eq. (2.89), Eq. (2.88) now reads

$$v_k'' + \left(k^2 - \frac{2}{\eta^2}\right) v_k = 0. \tag{2.91}$$

We can immediately identify two different limits. For modes with wavelength much smaller than the comoving Hubble radius $k^{-1} \gg (aH)^{-1} = -\eta$, or $k|\eta| \gg 1$, the Mukhanov-Sasaki becomes the equation of a massless scalar field in Minkowski space

$$v_k'' + k^2 v_k = 0, \tag{2.92}$$

the solution of which is a superposition of plane waves

$$v_k = c_1 e^{-ik\eta} + c_2 e^{ik\eta}. \tag{2.93}$$

This makes sense, since modes deep inside the horizon do not feel the expansion of the Universe. In the opposite limit, we have

$$\frac{v_k''}{v_k} = \frac{z''}{z} = \frac{2}{\eta^2}, \tag{2.94}$$

which is solved by a superposition of growing and decaying modes

$$v_k = c_1 \eta^{-1} + c_2 \eta^2. \tag{2.95}$$

In the super-horizon limit $k|\eta| \ll 1$ this solution is dominated by the growing mode $v_k = c_1 \eta^{-1}$, which means that super-horizon perturbations are frozen. Indeed, using Eq. (2.83), we have

$$\lim_{k|\eta|\to 0} \mathcal{R}_{\mathbf{k}} = \lim_{k|\eta|\to 0} \frac{v_{\mathbf{k}}}{z} \propto \frac{\eta}{\eta} = \text{const}. \tag{2.96}$$

We conclude that $\mathcal{R}_{\mathbf{k}}$ is constant on super-horizon scales during de Sitter expansion. This gives a clear and intuitive picture of the evolution of the scalar perturbations during inflation. Indeed, at sufficiently early times, many e-folds before the end

of inflation, the scalar modes are insensitive to the expansion of the Universe and behave as plane waves. Then, as the comoving Hubble radius shrinks, the modes progressively exit the horizon and freeze.

However, from an analytical standpoint we can do much better. Let us now derive the general solutions to the Mukhanov-Sasaki equation for constant slow-roll parameters. We also work to first order in the slow-roll parameters. We start by noting that for constant ϵ_H we can directly integrate Eq. (2.34) to obtain

$$\mathcal{H} = -\frac{1}{(1-\epsilon_H)\eta}. \tag{2.97}$$

Plugging this in Eq. (2.89) we have

$$\frac{z''}{z} = \frac{1}{(1-\epsilon_H)^2\eta^2}\left(2+2\epsilon_H-3\delta_H\right) = \frac{2+6\epsilon_H-3\delta_H}{\eta^2}. \tag{2.98}$$

It is convenient to make one further redefinition, given by

$$\frac{z''}{z} \equiv \frac{\nu^2-1/4}{\eta^2}, \quad \text{where} \quad \nu = \frac{3}{2}+2\epsilon_H-\delta_H. \tag{2.99}$$

With this, and making the change of variables $x = -k\eta$, the Mukhanov-Sasaki equation can be rewritten as

$$x^2\frac{\mathrm{d}^2 v_k}{\mathrm{d}x^2} + \left(x^2-\nu^2+\frac{1}{4}\right)v_k = 0. \tag{2.100}$$

Finally, redefining the mode functions as $v_k = \sqrt{x}g$, we have

$$x^2\frac{\mathrm{d}^2 g}{\mathrm{d}x^2} + x\frac{\mathrm{d}g}{\mathrm{d}x} + (x^2-\nu^2)g = 0. \tag{2.101}$$

This is a Bessel equation, the most general solution to which is a linear combination of Hankel functions $g(x) = c_1 H_\nu^{(1)}(x) + c_2 H_\nu^{(2)}(x)$, where a Hankel function of the first kind is given by $H_\nu^{(1)} = J_\nu + iY_\nu$ and a Hankel function of the second kind is given by $H_\nu^{(2)} = (H_\nu^{(1)})^* = J_\nu - iY_\nu$. J_ν and Y_ν are Bessel functions of the first and second kind, respectively. Thus, the solution to the Mukhanov-Sasaki equation reads

$$v_k(\eta) = \sqrt{-k\eta}\left[c_1 H_\nu^{(1)}(-k\eta) + c_2 H_\nu^{(2)}(-k\eta)\right]. \tag{2.102}$$

To make further progress we need to quantize the theory. This is done in the standard way, by promoting the canonically normalised variable v and its conjugate momentum v' to quantum operators, *i.e.*, $v \to \hat{v}$ and $v' \to \hat{v}'$, and imposing the commutation relation

$$[\hat{v}(\eta, \mathbf{x}), \hat{v}'(\eta, \mathbf{y})] = i\delta^{(3)}(\mathbf{x} - \mathbf{y}). \tag{2.103}$$

Alternatively, we can promote the Fourier components of both fields to operators, *i.e.*, $v_{\mathbf{k}} \to \hat{v}_{\mathbf{k}}$ and $v'_{\mathbf{k}} \to \hat{v}'_{\mathbf{k}}$, according to the decomposition

$$\hat{v}_{\mathbf{k}}(\eta) = v_k(\eta)\hat{a}_{\mathbf{k}} + v_k^*\hat{a}^\dagger_{-\mathbf{k}}, \tag{2.104}$$

$$\hat{v}'_{\mathbf{k}}(\eta) = v'_k(\eta)\hat{a}_{\mathbf{k}} + (v')_k^*\hat{a}^\dagger_{-\mathbf{k}}, \tag{2.105}$$

where $\hat{a}_{\mathbf{k}}$ and $\hat{a}^\dagger_{\mathbf{k}}$ are annihilation and creating operators, respectively, and the mode functions $v_k(\eta)$ satisfy the classical equation of motion (2.88). Note that because of this the mode functions still only depend on the magnitude of the wavenumber, while the ladder operators define initial conditions which might depend on direction. The sign in the wavenumber of the creation operators in Eqs. (2.104)-(2.105) is negative since $\hat{v}$ and $\hat{v}'$ are Hermitian, *i.e.*, $\hat{v}^\dagger = \hat{v}$ and $(\hat{v}')^\dagger = \hat{v}'$. Indeed, using Eq. (2.86), this means that the Fourier components must satisfy $\hat{v}_{\mathbf{k}}(\eta)^\dagger = \hat{v}_{-\mathbf{k}}(\eta)$ (and likewise for the conjugate momentum).

The ladder operators $a_{\mathbf{k}}$ and $a^\dagger_{\mathbf{k}}$ satisfy the usual commutation relations

$$\left[\hat{a}_{\mathbf{k}}, \hat{a}^\dagger_{\mathbf{p}}\right] = \delta^3(\mathbf{k} - \mathbf{p}) \quad \text{and} \quad [\hat{a}_{\mathbf{k}}, \hat{a}_{\mathbf{p}}] = [\hat{a}^\dagger_{\mathbf{k}}, \hat{a}^\dagger_{\mathbf{p}}] = 0, \tag{2.106}$$

if and only if the Wronskian of the mode functions satisfies the following constraint

$$W[v_k, v_k^*] \equiv v_k(v'_k)^* - v'_k v_k^* = i. \tag{2.107}$$

This gives the first constraint on the integration constants c_1 and c_2 in Eq. (2.102). At this point it is useful to remember that the derivatives of the Hankel functions read

$$\frac{\mathrm{d}H_\nu^{(1,2)}(x)}{\mathrm{d}x} = \frac{\nu H_\nu^{(1,2)}(x)}{x} - H_{\nu+1}^{(1,2)}(x), \tag{2.108}$$

and that their Wronskian is given by

$$W[H_\nu^{(1)}(x), H_\nu^{(2)}(x)] = -\frac{4i}{\pi x}. \tag{2.109}$$

Plugging Eq. (2.102) in Eq. (2.107) then gives

$$|c_1|^2 - |c_2|^2 = \frac{\pi}{4k}. \tag{2.110}$$

The second constraint, necessary to completely fix the solutions from the second order ODE (2.88), comes from the choice of vacuum. We do this with the standard prescription [82], which we quickly review here. For an unambiguous choice of vacuum $|0\rangle$, the mode functions $v_k(\eta)$ need to be fixed. Indeed, changing $v_k(\eta)$ while keeping $\hat{v}$ fixed would change $a_{\mathbf{k}}$ and hence $|0\rangle$, defined via $a_{\mathbf{k}}|0\rangle = 0$. In Minkowski space the choice is straightforward: the mode functions $v_k(\eta)$ should be selected such that the expectation value of the Hamiltonian in the vacuum is minimized. However, this cannot be done for a general quasi-de Sitter spacetime, where the frequency $\omega_k^2(\eta) = k^2 - z''/z$ is time-dependent. Even if in principle we could select the mode functions that minimize the vacuum expectation value of the Hamiltonian instantaneously, at a given η_0, the mode functions satisfying this condition will generally be different at a later time, thereby changing the definition of $|0\rangle$. In order to find a solution we need to notice that at very early times, deep inside the horizon, all modes satisfy $k|\eta| \gg 1$. From Eq. (2.89) this means that

$$k^2 \gg \frac{z''}{z}\frac{1}{2 + 2\epsilon_H - 3\delta_H + (2\epsilon_H - \delta_H)(\epsilon_H - \delta_H) - \frac{\delta_H'}{\mathcal{H}}} > \frac{z''}{2z}. \tag{2.111}$$

Thus, in this limit, the Mukhanov-Sasaki equation takes again the form given in Eq. (2.92), *i.e.*, the equation of a massless scalar field in Minkowski space. Accordingly, we impose the initial condition[3]

$$\lim_{k\eta\to-\infty} v_k(\eta) = \frac{1}{\sqrt{2k}} e^{-ik\eta}. \tag{2.112}$$

[3]We remind the reader that the mode function satisfying Eq. (2.92) and which minimizes the vacuum expectation value of the Hamiltonian in Minkowski space reads $v_k(\eta) = e^{-ik\eta}/\sqrt{2k}$.

This condition defines a unique vacuum, called the Bunch-Davies vacuum, as well as a preferable set of modes. Remembering that the large argument limit of the Hankel functions is

$$\lim_{x\to\infty} H^{(2)}(x) = \sqrt{\frac{2}{\pi x}} e^{-i(x-\frac{1}{2}\nu\pi-\frac{1}{4}\pi)}, \tag{2.113}$$

we can impose the Bunch-Davies initial condition in Eq. (2.102). The result reads

$$\frac{1}{\sqrt{2k}} e^{-ik\eta} = \sqrt{\frac{2}{\pi}} \left[c_1 e^{-i(k\eta+\nu\pi/2+\pi/4)} + c_2 e^{i(k\eta+\nu\pi/2+\pi/4)} \right]. \tag{2.114}$$

From this, we find that $c_2 = 0$ and $c_1 = \sqrt{\pi/(4k)} e^{i(\nu\pi/2+\pi/4)}$, giving

$$v_k(\eta) = e^{i\frac{\pi}{4}(2\nu+1)} \sqrt{\frac{\pi}{4}} \sqrt{-\eta} H_\nu^{(1)}(-k\eta), \tag{2.115}$$

where ν is given by Eq. (2.99). Note that the condition (2.110) is also satisfied.

Now that the have the solution for the canonically normalised field, to first order in the slow-roll parameters, we only need $z(\eta)$ in order to find $\mathcal{R}$. From Eq. (2.84) we have

$$\frac{z'}{z} = \mathcal{H}\left(1 + \epsilon_H - \delta_H\right) = \frac{1}{\eta}\left(\frac{1}{2} - \nu\right), \tag{2.116}$$

where we used Eq. (2.97) and expanded to linear order in the slow-roll parameters in the second step. Integrating gives

$$z(\eta) = z_* \left(\frac{\eta}{\eta_*}\right)^{1/2-\nu}, \tag{2.117}$$

where η_* is an integration constant which can be conveniently associated with the time of horizon crossing of the perturbations, *i.e.*, $k_* = a_* H_*$ or $\eta_* = -k_*^{-1}$, where an asterisk denotes horizon crossing. Finally, the comoving curvature perturbation mode functions read

$$\mathcal{R}_k(\eta) = \frac{v_k(\eta)}{z(\eta)} = e^{i\pi(2\nu+1)/4} \sqrt{\frac{\pi}{4}} \frac{(-k_*)^{\nu-1/2}}{a_* \sqrt{2\epsilon_H^*} m_{\rm P}} \eta^\nu H_\nu^{(1)}(-k\eta), \tag{2.118}$$

where, again, quantities with an asterisk are evaluated at horizon crossing. Remembering that the small argument limit of the Hankel functions reads

$$\lim_{x\to 0} H_\nu^{(1)}(x) = -\frac{i}{\pi}\Gamma(\nu)\left(\frac{x}{2}\right)^{-\nu} + \frac{1}{\Gamma(1+\nu)}\left(\frac{x}{2}\right)^{\nu}, \tag{2.119}$$

we can now take the super-horizon limit $k\eta \to 0$ of the mode functions of the comoving curvature perturbation

$$\lim_{k|\eta|\to 0} \mathcal{R}_k(\eta) = e^{\pi(2\nu+1)/4} \frac{2^{\nu-1}}{\sqrt{\pi}} \Gamma(\nu) \frac{k_*^{-1/2}}{a_* \sqrt{2\epsilon_H^*} m_{\rm P}} \left(\frac{k}{k_*}\right)^{-\nu}. \tag{2.120}$$

We conclude that, as for the de Sitter case (*cf.* Eq. (2.96)), $\mathcal{R}_{\mathbf{k}}$ is constant on super-horizon scales during inflation. Furthermore, it can be shown [76, 83] that it is also constant on super-horizon scales after a general single-field slow-roll inflationary phase. This property together with the fact that the comoving curvature perturbation is gauge independent make it the ideal candidate to describe the scalar spectrum from inflation. Indeed, since it becomes constant at horizon crossing during inflation, and remains so until horizon re-entry at much later times, we can safely ignore all the complex high-energy processes of the early Universe and make a direct comparison between inflationary predictions and late-time observables, such as the temperature anisotropies in the CMB.

We now compute the spectrum of inflationary perturbations, which, to linear order, are fully determined by their 2-point correlation function. Indeed, we have seen (*cf.* Eq. (2.89)) that the fluctuations follow the equation of motion of a harmonic oscillator (with a time-dependent frequency). As we know, the wave function corresponding to the ground state of a harmonic oscillator is a Gaussian, and so we expect the initial inflationary perturbations to also follow a Gaussian distribution. Because of this, all odd N-point functions vanish, while all even N-point functions can be obtained from the 2-point function. Of course, it could be that contributions coming from higher order terms in perturbation theory play a role. The current observational constraints [84] for the leading order correction, or non-Gaussianity, are compatible with zero. Although this is a promising direction in order to learn about the microphysics of inflation, it is beyond the scope of the present work.

We are interested in the quantum statistics of the operator

$$\hat{\mathcal{R}}(\eta, \mathbf{x}) = \int \frac{\mathrm{d}^3 k}{(2\pi)^{3/2}} \left[\mathcal{R}_k(\eta) a_{\mathbf{k}} + \mathcal{R}_k^*(\eta) a_{-\mathbf{k}}^\dagger\right] e^{i\mathbf{k}\cdot\mathbf{x}}, \tag{2.121}$$

where the mode functions $\mathcal{R}_k(\eta)$ are given by Eq. (2.118). The expectation value of $\hat{\mathcal{R}}$ vanishes, *i.e.*, $\langle 0|\,\hat{\mathcal{R}}(\eta,\mathbf{x})\,|0\rangle = 0$, but its variance does not

$$\begin{aligned}\langle|\hat{\mathcal{R}}|^2\rangle &= \langle 0|\,\hat{\mathcal{R}}(\eta,0)\hat{\mathcal{R}}(\eta,0)\,|0\rangle = \int\frac{\mathrm{d}^3k}{(2\pi)^{3/2}}\frac{\mathrm{d}^3p}{(2\pi)^{3/2}}\mathcal{R}_k(\eta)\mathcal{R}_p^*(\eta)\,\langle 0|\,\hat{a}_{\mathbf{k}}\hat{a}^\dagger_{-\mathbf{p}}\,|0\rangle \\ &= \int\frac{\mathrm{d}^3k}{(2\pi)^3}|\mathcal{R}_k(\eta)|^2 = \int\mathrm{d}\ln k\frac{k^3}{2\pi^2}|\mathcal{R}_k(\eta)|^2 \equiv \int\mathrm{d}\ln k\Delta^2_{\mathcal{R}}(\eta,k), \quad (2.122)\end{aligned}$$

where we have used the definition of the vacuum in the second step, the commutation relations (2.106) in the third step and in the final step we have defined the dimensionless power spectrum

$$\Delta^2_{\mathcal{R}}(\eta,k) \equiv \frac{k^3}{2\pi^2}|\mathcal{R}_k(\eta)|^2. \quad (2.123)$$

The variance of the comoving curvature perturbation is completely determined by the modulus squared of the mode functions, which is often called the power spectrum

$$P_{\mathcal{R}}(\eta,k) \equiv |\mathcal{R}_k(\eta)|^2. \quad (2.124)$$

The information contained in the power spectrum and in the 2-point function of the perturbations is equivalent. Indeed, it is easy to see that the former is the Fourier transform of the latter.

From Eq. (2.118), the dimensionless power spectrum of the curvature perturbation reads

$$\Delta^2_{\mathcal{R}}(\eta,k) = \frac{k^3}{16\pi}\frac{(-k_*)^{2\nu-1}}{a_*^2\epsilon_H^* m_{\mathrm{P}}^2}\eta^{2\eta}\left|H_\nu^{(1)}(-k\eta)\right|^2. \quad (2.125)$$

In the super-horizon limit, using Eq. (2.120) and $a_* = k_*/H_*$, we have

$$\lim_{k|\eta|\to 0}\Delta^2_{\mathcal{R}}(\eta,k) = \frac{k^3 2^{2\nu-4}\Gamma(\nu)^2 H_*^2 k_*^{-3}}{\pi^3\epsilon_H^* m_{\mathrm{P}}^2}\left(\frac{k}{k_*}\right)^{-2\nu}. \quad (2.126)$$

Note that the time dependence has disappeared. Using that $2^{2\nu}\Gamma(\nu)^2/\pi^2 \simeq 2/\pi$ and $\nu = 3/2 + 2\epsilon_H^* - \delta_H^*$, we finally obtain

$$\Delta^2_{\mathcal{R}}(k) = \frac{H_*^2}{8\pi^2 m_{\mathrm{P}}^2\epsilon_H^*}\left(\frac{k}{k_*}\right)^{-4\epsilon_H^*+2\delta_H^*}. \quad (2.127)$$

We remind the reader that inflation can only occur when $\{\epsilon_H, |\delta_H|\} < 1$. Therefore, inflation generally predicts a weak scale dependence for the scalar perturbations.

With $\{\epsilon_H, |\delta_H|\} = 0$, corresponding to de Sitter, we would have perfect scale invariance. Deviations from de Sitter, needed for inflation to end, imply deviations from scale invariance in the scalar spectrum, which are usually parametrised via the scalar spectral index

$$n_s - 1 \equiv -4\epsilon_H^* + 2\delta_H^* = -2\epsilon_H^* - \eta_H^*, \tag{2.128}$$

where we have used Eq. (2.60) and the number one is featured due to historical reasons.

In summary, the power spectrum of the comoving curvature perturbation takes the form of a power law given by

$$\Delta^2_{\mathcal{R}}(k) = A_s \left(\frac{k}{k_*}\right)^{n_s - 1}, \tag{2.129}$$

where the amplitude and spectral index read

$$A_s = \frac{H_*^2}{8\pi^2 m_{\rm P}^2 \epsilon_H^*}, \tag{2.130}$$

$$n_s = 1 - 2\epsilon_H^* - \eta_H^*. \tag{2.131}$$

The latest observational constraints [8] for these two quantities, evaluated at the pivot scale $k_* = 0.05\,\mathrm{Mpc}^{-1}$, are

$$A_s = (2.099 \pm 0.101) \times 10^{-9}\,(68\%\text{C.L.}), \tag{2.132}$$

$$n_s = 0.9649 \pm 0.0042\,(68\%\text{C.L.}), \tag{2.133}$$

corresponding to zero or approximately zero tensors (see Figs. 2.4 and 2.5). We can relate these results to the shape of the potential by using the slow-roll approximation, in Eqs. (2.62)-(2.63), and relating the Hubble slow-roll parameters to the potential ones, via Eq. (2.68). The amplitude and the tilt of the power spectrum in the slow-roll approximation then read

$$A_s = \frac{V(\phi_*)}{24\pi^2 m_{\rm P}^4 \epsilon_V^*}, \tag{2.134}$$

$$n_s = 1 - 6\epsilon_V^* + 2\eta_V^*. \tag{2.135}$$

Observations around the pivot scale k_* probe the shape of the potential around the field value $\phi_* = \phi(t_*)$, where t_* is the time at which the scale k_* crossed the horizon $k_* = a_* H_*$. This time is usually given in terms of the remaining number of inflationary e-folds, given by Eq. (2.69), where $\phi_{\rm end}$ is determined via $\epsilon_V(\phi_{\rm end}) = 1$.

For completeness, we also mention here the scale-dependence of the tilt, defined as

$$\alpha_s = \frac{{\rm d}n_s}{{\rm d}\ln k}. \tag{2.136}$$

In the slow-roll approximation it reads

$$\alpha_s = 16\epsilon_V\eta_V - 24\epsilon_V^2 - 2\xi_V, \tag{2.137}$$

where we have defined the third potential slow-roll parameter

$$\xi_V = m_{\rm P}^4 \frac{V'V'''}{V^2}. \tag{2.138}$$

The latest observational constraint [10] is

$$\alpha_s = -0.0069 \pm 0.0069\,(68\%{\rm C.L.}). \tag{2.139}$$

Having dealt with the scalar perturbations, the treatment for their tensorial counterpart is straightforward. The perturbed metric reads

$${\rm d}s^2 = a^2(\eta)\left[-{\rm d}\eta^2 + (\delta_{ij} + h_{ij}){\rm d}x^i{\rm d}x^j\right], \tag{2.140}$$

where $\partial_i h^{ij} = h^i{}_i = 0$. The calculation of the action to second order in h_{ij} is simpler than for $\mathcal{R}$ (for a pedagogical review see, *e.g.*, Ref. [85]). We give a detailed calculation in Appendix A.2. The result reads

$$S = \frac{m_{\rm P}^2}{8}\int {\rm d}\eta {\rm d}^3x a^2\left[(h'_{ij})^2 - \partial_m h_{ij}\partial^m h^{ij}\right] \tag{2.141}$$

$$= \sum_{s=\oplus,\otimes}\frac{m_{\rm P}^2}{4}\int {\rm d}\eta {\rm d}^3k a^2\left[|h^{s\,\prime}_{\mathbf{k}}|^2 - k^2|h^s_{\mathbf{k}}|^2\right], \tag{2.142}$$

where s denotes the two GW polarisations $\oplus$ and $\otimes$, and we have switched to Fourier space in the second step by introducing

$$h_{ij}(\eta,\mathbf{x}) = \sum_{s=\oplus,\otimes}\int \frac{{\rm d}^3k}{(2\pi)^{3/2}}\,\epsilon^s_{ij}(k)h^s_{\mathbf{k}}(\eta)\,e^{i\mathbf{k}\cdot\mathbf{x}}, \tag{2.143}$$

where have defined a polarization tensor that satisfies $(\epsilon^s)^i{}_i = k^i\epsilon^s_{ij} = 0$ with the normalization $\delta^{im}\delta^{jn}\epsilon^s_{ij}(k)\epsilon^{s'}_{mn}(k) = 2\delta^{ss'}$. In this way, $\epsilon^s_{ij}h^s_{\mathbf{k}}(\eta)$ describes oscillations of a given polarization in directions perpendicular to the wave vector $\mathbf{k}$.

In an analogous way to the scalar perturbations, we introduce the canonically normalised variable

$$f^s_{\mathbf{k}} = \frac{m_{\rm P}}{\sqrt{2}}ah^s_{\mathbf{k}}, \tag{2.144}$$

so that the action becomes

$$S = \sum_{s=\oplus,\otimes}\frac{1}{2}\int \mathrm{d}\eta\mathrm{d}^3k\left[(f^{s\prime}_{\mathbf{k}})^2 - \left(k^2 - \frac{a''}{a}\right)(f^s_{\mathbf{k}})^2\right]. \tag{2.145}$$

This action is the sum of two copies, one for each polarization, of the same action as for the scalar perturbations (2.85), only with z''/z substituted by a''/a. Extremising it, we find that each polarization of the canonically normalised variable obeys the following equation

$$(f^s_k)'' + \left(k^2 - \frac{a''}{a}\right)f^s_k = 0. \tag{2.146}$$

Using Eq. (2.97), we find, to first order in the slow-roll parameters,

$$\frac{a''}{a} = \mathcal{H}' + \mathcal{H}^2 = \frac{1}{(1-\epsilon_H)\eta^2} + \frac{1}{(1-\epsilon_H)^2\eta^2} = \frac{2+3\epsilon_H}{\eta^2}. \tag{2.147}$$

Making again the redefinition

$$\frac{a''}{a} \equiv \frac{\mu^2 - 1/4}{\eta^2}, \quad \text{where} \quad \mu = \frac{3}{2} + \epsilon_H, \tag{2.148}$$

and following the same steps as for the scalar perturbations, we find that the solution to Eq. (2.146) reads

$$f^s_k(\eta) = \sqrt{-k\eta}\left[c_1H^{(1)}_\mu(-k\eta) + c_2H^{(2)}_\mu(-k\eta)\right]. \tag{2.149}$$

Quantization also proceeds in a similar way. We promote f^s and its conjugate momentum $f^{s\prime}$ to quantum operators as

$$f^s \;\to\; \hat{f}^s(\eta,\mathbf{x}) = \int\frac{\mathrm{d}^3k}{(2\pi)^{3/2}}\left[f^s_k(\eta)\hat{a}^s_{\mathbf{k}} + f^{s*}_k(\eta)\hat{a}^{s\dagger}_{-\mathbf{k}}\right]e^{i\mathbf{k}\cdot\mathbf{x}}, \tag{2.150}$$

$$f^{s\prime} \;\to\; \hat{f}^{s\prime}(\eta,\mathbf{x}) = \int\frac{\mathrm{d}^3k}{(2\pi)^{3/2}}\left[f^{s\prime}_k(\eta)\hat{a}^s_{\mathbf{k}} + f^{s*\prime}_k(\eta)\hat{a}^{s\dagger}_{-\mathbf{k}}\right]e^{i\mathbf{k}\cdot\mathbf{x}}. \tag{2.151}$$

and impose the commutation relation

$$\left[\hat{f}^s(\eta,\mathbf{x}),\hat{f}^{r\prime}(\eta,\mathbf{y})\right]=i\delta^{sr}\delta^{(3)}(\mathbf{x}-\mathbf{y}). \tag{2.152}$$

The ladder operators satisfy the commutation relations

$$\left[\hat{a}^s_{\mathbf{k}},\hat{a}^{r\dagger}_{\mathbf{p}}\right]=\delta^{sr}\delta^{(3)}(\mathbf{k}-\mathbf{p}) \quad \text{and} \quad [\hat{a}^s_{\mathbf{k}},\hat{a}^{r}{}_{\mathbf{p}}]=\left[\hat{a}^{s\,\dagger}_{\mathbf{k}},\hat{a}^{r\dagger}_{\mathbf{p}}\right]=0, \tag{2.153}$$

if and only if the Wronskian of the mode functions satisfies

$$W[f^s_k,f^{s*}_k]\equiv f^s_k(f^{s\prime}_k)^*-f^{s\prime}_k f^{s*}_k=i. \tag{2.154}$$

We again define the vacuum as the state annihilated by $a^s_{\mathbf{k}}$ when the mode functions satisfy the initial condition

$$\lim_{k\eta\to-\infty}f^s_k(\eta)=\frac{1}{\sqrt{2k}}e^{-ik\eta}. \tag{2.155}$$

Analogously to the scalar perturbations, we find that each polarization of the canonically normalised field is given by

$$f^s_k(\eta)=e^{i\frac{\pi}{4}(2\mu+1)}\sqrt{\frac{\pi}{4}}\sqrt{-\eta}H^{(1)}_\mu(-k\eta), \tag{2.156}$$

where μ is given by Eq. (2.148). Of course, the metric perturbations also freeze in the super-horizon limit. To show this, we first need to obtain the scale factor. By integrating Eq. (2.97), we have

$$a(\eta)=a_*\left(\frac{\eta}{\eta_*}\right)^{-1/(1-\epsilon_H)}\simeq a_*\left(\frac{\eta}{\eta_*}\right)^{-1-\epsilon_H}, \tag{2.157}$$

where, again, starred quantities correspond to horizon crossing $k_*=a_*H_*$. With this, we find

$$\lim_{k|\eta|\to0}h^s_k(\eta)=\frac{\sqrt{2}}{m_{\rm P}}\lim_{k|\eta|\to0}\frac{f^s_k(\eta)}{a(\eta)}=\frac{e^{i(1+\epsilon_H)/2}}{m_{\rm P}k^{3/2}}2^{\epsilon_H}\frac{\Gamma(\mu)}{\Gamma(3/2)}\frac{k_*}{a_*}\left(\frac{k}{k_*}\right)^{-\epsilon}, \tag{2.158}$$

where the time dependency has dropped out, as expected.

We are interested in the quantum statistics of the operator

$$\hat{h}_{ij}(\eta,\mathbf{x})=\sum_{s=\oplus,\otimes}\int\frac{\mathrm{d}^3k}{(2\pi)^{3/2}}\epsilon^s_{ij}(k)\frac{\sqrt{2}}{m_{\rm P}a}\left[f^s_k(\eta)\hat{a}^s_{\mathbf{k}}+f^{s*}_k(\eta)\hat{a}^{s\,\dagger}_{-\mathbf{k}}\right]e^{i\mathbf{k}\cdot\mathbf{x}}, \tag{2.159}$$

where the mode functions $f_k^s(\eta)$ are given by Eq. (2.156). The expectation value of $\hat{h}_{ij}$ vanishes, *i.e.*, $\langle 0|\,\hat{h}_{ij}(\eta,\mathbf{x})\,|0\rangle = 0$, but its variance does not

$$\begin{aligned}\langle|h_{\mu\nu}|^2\rangle &= \langle 0|\,h_{ij}(\eta,0)h^{ij}(\eta,0)\,|0\rangle \qquad (2.160)\\ &= \sum_{s,s'=\oplus,\otimes}\int\frac{\mathrm{d}^3k}{(2\pi)^{3/2}}\frac{\mathrm{d}^3p}{(2\pi)^{3/2}}\delta^{im}\delta^{jn}\epsilon_{ij}^s(k)\epsilon_{mn}^{s'}(p)\frac{2}{m_{\mathrm{P}}^2a^2}f_k^s(\eta)f_p^{s'*}(\eta)\,\langle 0|\,\hat{a}_{\mathbf{k}}^s\hat{a}_{-\mathbf{p}}^{s'\,\dagger}\,|0\rangle\\ &= \sum_{s=\oplus,\otimes}\int\frac{\mathrm{d}^3k}{(2\pi)^3}\frac{4}{m_{\mathrm{P}}^2a^2}|f_k^s(\eta)|^2 = \frac{8}{m_{\mathrm{P}}^2a^2}\int\mathrm{d}\ln k\frac{k^3}{2\pi^2}|f_k^s(\eta)|^2 = \int\mathrm{d}\ln k\Delta_h^2(\eta,k),\end{aligned}$$

where we have defined the dimensionless power spectrum of the metric perturbations $\Delta_h^2(\eta,k)$ in a completely analogous way to its scalar counterpart. Since the mode functions for both polarizations obey the same Eq. (2.146), their contributions in the integral are equal. This is where the extra factor of two comes from in the fourth step. Using Eq. (2.158), the super-horizon limit of the dimensionless power spectrum reads

$$\Delta_h^2(k) = \frac{2H_*^2}{\pi^2m_{\mathrm{P}}^2}\left(\frac{k}{k_*}\right)^{-2\epsilon_H^*}. \qquad (2.161)$$

In summary, we have found that tensor spectrum takes the form of a power law given by

$$\Delta_h^2(k) = A_t\left(\frac{k}{k_*}\right)^{n_t}, \qquad (2.162)$$

where the amplitude and the spectral index read

$$A_t = \frac{2H_*^2}{\pi^2m_{\mathrm{P}}^2} \qquad (2.163)$$

$$n_t = -2\epsilon_H^*. \qquad (2.164)$$

The observational constraints on the tensor perturbations are usually given in terms of the tensor-to-scalar ratio, defined as

$$r \equiv \frac{A_t}{A_s} = 16\epsilon_H^* = -8n_t. \qquad (2.165)$$

The latest observational constraint [9] for this quantity, evaluated at the pivot scale $k_* = 0.05\,\mathrm{Mpc}^{-1}$, is

$$r < 0.036\,(95\%\mathrm{C.L}). \qquad (2.166)$$

Note that since A_s has been measured, r quantifies both the amplitude and the tilt of the tensor perturbations. Furthermore, since $r > 0$, the spectrum is necessarily red-tilted, *i.e.*, $n_t < 0$, meaning that the perturbations are larger at smaller scales.

We can relate Eqs. (2.163) and (2.165) to the shape of the potential by using the slow-roll approximations. The result reads

$$A_t = \frac{2}{3\pi^2}\frac{V(\phi_*)}{m_{\rm P}^4}, \tag{2.167}$$

$$r = 16\epsilon_V^*. \tag{2.168}$$

Detection of a primordial stochastic background of GWs, possibly via the B-mode polarization of the CMB, is usually considered to be a smoking gun for inflation. It would also tell us about the energy scale of inflation (at times around horizon crossing). Indeed,

$$E_{\rm inf} \equiv \rho_{\rm inf}^{1/4} = (3m_{\rm P}^2 H_*^2)^{1/4} = 4\times 10^{-3}\left(\frac{r}{0.01}\right)^{1/4} m_{\rm P}, \tag{2.169}$$

where we have used Eqs. (2.163) and (2.165). Note that since $E_{\rm inf} \propto r^{1/4}$, we would need a change by a factor of 10^4 in r to achieve an order of magnitude variation in $E_{\rm inf}$. In order for tensor modes to be observable in the near future, with $r \simeq 0.01$, inflation should have occurred at around the GUT scale $E_{\rm inf} \simeq 10^{16}$GeV.

The tensor-to-scalar ratio is also related to the total field excursion, from the time of horizon crossing to the end of inflation. Using Eq. (2.58) with $\mathrm{d}N = H\mathrm{d}t$, we can write

$$r = \frac{8}{m_{\rm P}^2}\left(\frac{\mathrm{d}\phi}{\mathrm{d}N}\right)^2. \tag{2.170}$$

Integrating, we have

$$\frac{\Delta\phi}{m_{\rm P}} = \int_0^{N_*}\mathrm{d}N\sqrt{\frac{r}{8}} \simeq \sqrt{\frac{r_*}{0.01}}\int_0^{N_*}\frac{\mathrm{d}N}{60}\sqrt{\frac{r}{r_*}}, \tag{2.171}$$

where r_* is the tensor-to-scalar ratio at horizon crossing. Since r does not change much during slow-roll evolution, and remembering that $N_* \simeq 60$, we obtain the Lyth bound [86]

$$\frac{\Delta\phi}{m_{\rm P}} = \mathcal{O}(1)\times\sqrt{\frac{r_*}{0.01}}. \tag{2.172}$$

Large values for r are correlated with super-Planckian field excursions.

2.1.4 Contact with observations and inflationary model building

As we have explained in the previous section, inflation predicts an almost scale-invariant spectrum for the scalar and tensor perturbations. It also predicts a small deviation from perfect scale invariance coming from the broken time-translation symmetry required for inflation to end. This is parametrised in Eqs. (2.129) and (2.162) via the the spectral indices n_s and n_t. Although tensor modes have not been observed, from Eq. (2.164) follows that the tensor spectral index is necessarily negative (something that may be used to distinguish inflation from alternative theories of structure formation, such as string gas cosmology [87, 88]). This is *a priori* not necessarily the case for the scalar modes, since n_s depends on η_V (see Eq. (2.135)), which may be positive or negative. However, the latest observations [8] suggest that $n_s \simeq 0.97$. Using the fact that the bound on the tensor-to-scalar ratio (2.166) implies $\epsilon_V^* \simeq \epsilon_H^* = r/16 < 0.002$, we can conclude that concave potentials, with $\eta_V < 0$, are favoured. Even more, after the publication of the first round of results by Planck [89], in Ref. [90] a Bayesian study of many different models of single-field slow-roll inflation is carried out, arriving to the conclusion that plateau-like potentials are statistically favoured.

The power spectrum of both matter and radiation has been measured and it is clear that the results agree with the predictions from inflation, a great success in itself. However, "this is not what tingles our spines when we look at the data", as Dodelson says in Ref. [91]. Instead, it has to do with the peaks and troughs structure in the temperature power spectrum of the CMB (see left panel of Fig. 2.3), which can only arise if all Fourier modes of the perturbations that re-enter the horizon prior to recombination have the same phase. Inflation naturally provides a mechanism for this to happen.

In comoving coordinates, the Fourier modes of the scalar perturbations $\mathcal{R}_k$ progressively exit the horizon, and freeze when they do, as the comoving Hubble

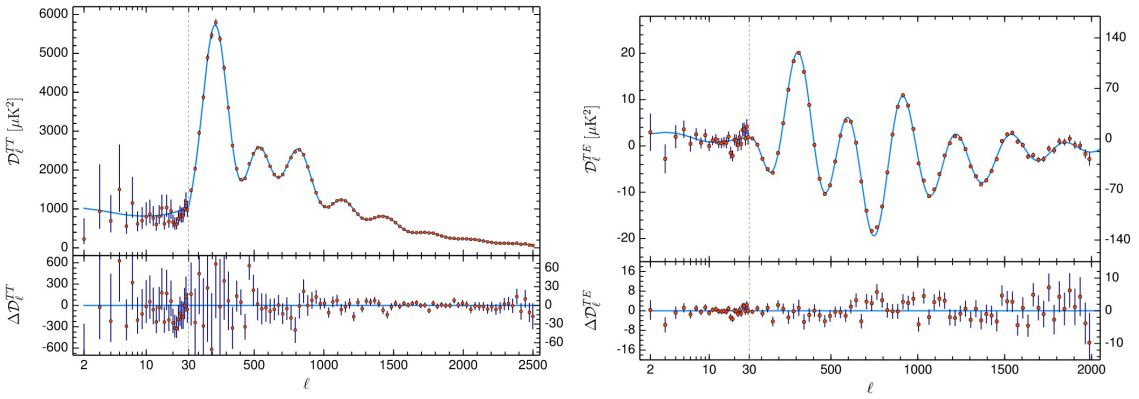

Figure 2.3: Temperature power spectrum (left) and TE power spectrum (right) of the CMB, from Planck 2018. Both are shown as a function of angular scale. The peaks and troughs structure in the left panel is a consequence of all Fourier modes re-entering the horizon having the same phase. The anticorrelation between temperature and polarization at $100 < l < 200$ in the right panel corresponds to scales that were outside the horizon at recombination. Since polarization is generated before recombination, creating such a signal without inflation would violate causality [7]. Figures taken from [8].

radius $(aH)^{-1}$ decreases in size. We emphasize that after they leave the horizon no causal physics can alter them. Then, at much later times, after inflation ends, they again enter the horizon and start oscillating. However, since they are frozen, they have very small $\mathcal{R}_k'$ when they do. Seeing $\mathcal{R}_k$ as a combination of sine and cosine solutions, inflation excites the cosine only, or, in other words, all modes have the same phase when they re-enter the horizon. As the horizon grows, modes with smaller k re-enter earlier and have a longer time to oscillate before recombination than those with larger k, which re-enter at later times. In this way, summing all modes that have undergone half an oscillation before recombination, having maximal amplitude at that moment, leads to the first peak in the power spectrum. Likewise, summing all modes that have undergone 3/4 of an oscillation, having null amplitude, leads to the first through of the power spectrum. And so on so forth.

It is important to emphasize that if the phases were random (and constant power

across different scales), we would not see peaks or troughs in the CMB power spectrum. Both the cosine and sine components of the Fourier modes would be excited and summing all modes would lead a flat spectrum. The structure that can be found in the left panel of Fig. 2.3 is a direct consequence of all modes that re-enter the horizon being coherent. However, even if inflation provides a natural mechanism for this coherence, one could still postulate another physical process to achieve this. Indeed, the peaks and troughs are all at $l > 200$, *i.e.*, at scales smaller than one degree, meaning that they were in causal contact at recombination.

The most important piece of evidence in favour of inflation comes from the cross correlation between temperature fluctuations and E-mode polarization of the CMB (see the right panel in Fig. 2.3). One can find a negative correlation at $100 < l < 200$, *i.e.*, at scales larger than one degree, which were not in causal contact at recombination. Since polarization is generated before recombination, via Compton scattering of the radiation field, creating such a signal without inflation would violate causality [7].

The peak structure in the temperature power spectrum of the CMB also reveals information about isocurvature perturbations [92]. In our discussion of single-field inflation there is only one scalar degree of freedom, which induces purely adiabatic initial conditions. However, for more general models of inflation (such as multi-field inflation) this is not necessarily the case. If isocurvature fluctuations were produced, they would imprint distinctive features in the CMB spectrum [93]. More specifically, adiabatic initial conditions generate cosine oscillation in the pre-recombination plasma, while isocurvature initial conditions generate a since oscillation [35]. This is incompatible with the peak structure of the temperature power spectrum of the CMB and isocurvature perturbations are highly constrained. For example, in the case that they are totally correlated with the adiabatic modes, the matter isocurvature is proportional to the curvature perturbation $S_{\rm m} = \sqrt{\alpha}\mathcal{R}$ [35]. The latest observational bound on the proportionally constant α is [10] $\alpha < 0.0003^{+0.0016}_{-0.0012}$ (95%C.L).

In summary, there is ample observational evidence that agrees with the most generic instance of the inflationary picture. The power spectrum of the primordial perturbations needs to be almost scale-invariant and all Fourier modes have to be coherent. Inflation provides a framework where these two qualities are naturally obtained. Furthermore, observations favor adiabatic initial conditions and small levels of non-Gaussianity. This makes sense if we are to believe the single-field slow-roll picture. Indeed, single-field models generate zero isocurvature modes. Furthermore, slow-roll typically happens in a flat region of the potential, so the self-interactions of the field are small. If this is the case, the linearised equation of motion, which takes the form of that of a harmonic oscillator, is a good approximation. But the wavefunction associated with the ground state of a harmonic oscillator is a Gaussian, so it is expected that the statistics of the initial perturbations also follow a Gaussian distribution.

Perhaps the aspect of this picture that is most lacking has to do with the microphysics of inflation, which is still a mystery. To improve our understanding in this respect, the detection of primordial tensor modes and non-Gaussianities are two very promising directions. The former because, if detected, will tell us about the energy scale of inflation. The latter because, even if small, non-Gaussianities are related to the inflaton self-interactions. In any case, at present there exists a plethora of models that agree with observations (see Figs. 2.4-2.5), something that has been a source of criticism (although many other models have been discarded thanks to ever-improving observations). Better or worse motivated, the strategy that is usually followed in inflationary model building is to calculate the inflationary observables n_s, A_s, r and α_s, evaluated at horizon crossing, in the slow-roll approximation, to then compare them with the observational data. In order to exemplify this procedure, we give here the specific examples of chaotic inflation [94] and power-law inflation [95].

We start with chaotic inflation. Let the potential be

$$V(\phi) = V_0 \left(\frac{\phi}{m_{\rm P}} \right)^n , \tag{2.173}$$

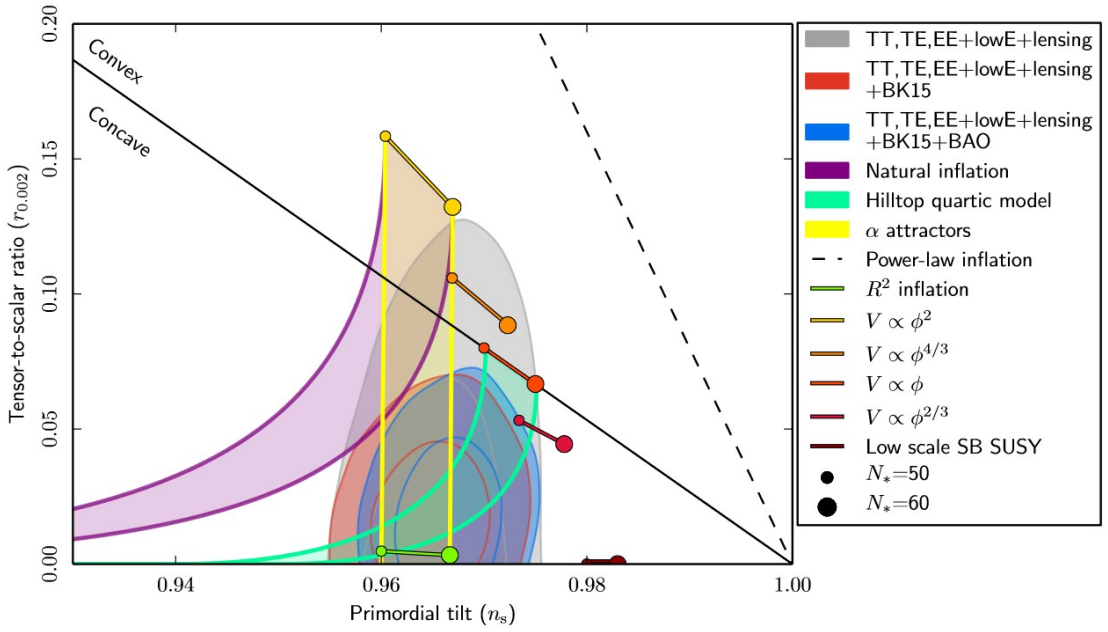

Figure 2.4: Marginalized joint 68% and 95% C.L. regions for n_s and r at $k = 0.002\,\mathrm{Mpc}^{-1}$ from Planck alone and in combination with BK15 or BK15+BAO data, compared to the theoretical predictions of a few inflationary models. $\alpha_s = 0$ is assumed. Note that this figure is dated, as the tensor-to-scalar ratio has been further constrained to $r < 0.036$ [9] since its publication (see Fig. 2.5). Figure taken from Ref. [10].

where V_0 is some constant density scale. Using Eqs. (2.66)-(2.67) we have

$$\epsilon_V = \frac{n^2}{2}\left(\frac{m_\mathrm{P}}{\phi}\right)^2, \quad \text{and} \quad \eta_V = n(n-1)\left(\frac{m_\mathrm{P}}{\phi}\right)^2. \tag{2.174}$$

Inflation ends when the condition $\epsilon_V(\phi_\mathrm{end}) = 1$ is met, which means that $\phi_\mathrm{end} = m_\mathrm{P} n/\sqrt{2}$. Plugging this and the first slow-roll parameter in Eq. (2.69) we obtain the field as a function of the number of e-folds

$$\phi(N) = \sqrt{2n}\, m_\mathrm{P} \sqrt{N + \frac{n}{4}}. \tag{2.175}$$

Combining this with Eq. (2.174), the inflationary observables in the slow-roll approximation read

$$n_s = 1 - \frac{n+2}{2\left(N + \frac{n}{4}\right)}, \tag{2.176}$$

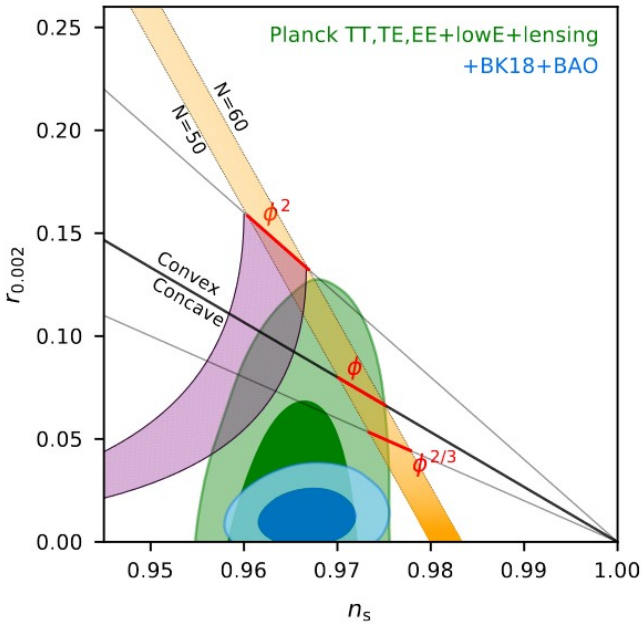

Figure 2.5: Constraints in the r-n_s plane for the Planck 2018 baseline analysis (green contours), and when also adding BICEP/Keck data (blue contours). The constraint on r is tightened to $r < 0.036$. The purple region corresponds to natural inflation. Figure taken from Ref. [9].

$$r = \frac{4n}{N + \frac{n}{4}}, \tag{2.177}$$

$$A_s = \frac{V_0}{m_{\rm P}^4 12\pi^2 n^2} \left[2n\left(N + \frac{n}{4}\right)\right]^{-n/2-1}. \tag{2.178}$$

The first two can be combined to give the consistency relation

$$r = \frac{8n}{n+2}(1 - n_s). \tag{2.179}$$

Using $n_s \simeq 0.965$ and $r < 0.036$ in this expression gives

$$n < 0.3. \tag{2.180}$$

However, plugging Eq. (2.180) in Eq. (2.176) with $n_s \simeq 0.965$ gives that the number of inflationary e-folds is $N < 32.8$, which is hard to achieve, unless the period of primordial inflation is followed by subsequent periods of thermal and fast-roll inflation [27]. In any case, the historically celebrated models with $n = 2$ and

$n = 4$ are observationally excluded. This can also be seen from Figs. 2.4-2.5, where the predictions for $n = 2/3, 1, 4/3, 2$ are represented. They all lie above the marginal value $r = 0.036$.

The potential for power-law inflation is given by

$$V(\phi) = V_0 e^{-\lambda\phi/m_{\rm P}}. \tag{2.181}$$

The KG equation for this potential has the following exact solution [27]

$$\phi(t) = -\frac{m_{\rm P}}{\lambda}\ln\left[\frac{2(6-\lambda^2)}{\lambda^4 V_0}\left(\frac{m_{\rm P}}{t}\right)^2\right]. \tag{2.182}$$

It follows that the Hubble parameter reads

$$H(t) = \frac{1}{m_{\rm P}\sqrt{3}}\sqrt{\frac{1}{2}\dot{\phi}^2 + V(\phi)} = \frac{2}{\lambda^2 t}. \tag{2.183}$$

Integrating this expression we obtain the scale factor

$$a(t) \propto t^{2/\lambda^2}, \tag{2.184}$$

which shows that for an exponential potential the inflationary expansion follows a power-law behaviour, rather than quasi-exponential. The Hubble slow-roll parameters can also be directly obtained from Eq. (2.183) as

$$\epsilon_H = -\frac{\dot{H}}{H^2} = \frac{\lambda^2}{2}, \quad \text{and} \quad \eta_H = \frac{\dot{\epsilon}_H}{\epsilon_H H} = 0. \tag{2.185}$$

This means that inflation occurs for

$$\epsilon_H < 1 \quad \Leftrightarrow \quad \lambda < \sqrt{2}. \tag{2.186}$$

The same condition for λ can be obtained from the barotropic parameter

$$w_\phi = \frac{\dot{\phi}^2/2 - V(\phi)}{\dot{\phi}^2/2 - V(\phi)} = \frac{\lambda^2}{3} - 1, \tag{2.187}$$

by imposing $w_\phi < -1/3$. However, since $\epsilon_H =$ const. inflation can never end, unless the model is augmented, *e.g.*, by adding another field with a hybrid mechanism [96].

Even then, the predictions of power-law inflation are in conflict with observations. Indeed, the scalar spectral index and the tensor-to-scalar ratio read

$$n_s = 1 - \lambda^2, \quad \text{and} \quad r = 8\lambda^2. \tag{2.188}$$

Using $n_s \simeq 0.965$ gives $\lambda \simeq 0.19$, which implies that $r \simeq 0.28$, clearly incompatible with the observational bound in Eq. (2.166).

In the original research in Chapter 4 we consider a quintessential inflation model with an inflationary sector governed by the potential in Eq. (2.173). By adding an R^2 term to the gravitational action, and working in the Palatini formalism, we are able to rescue chaotic inflation with $2 < n < 4$ by bringing it back within observational bounds. In the same spirit, in the original research in Chapter 5 we rescue the also discarded exponential potential, although the setup is slightly more complicated.

2.1.5 Reheating

In the discussion made so far we have ignored the elephant in the room: the Universe is filled with the particles of the SM, dark matter and dark energy. Even if the inflaton is responsible for the current acceleration of the Universe (an intriguing possibility that will be studied at length in this thesis), there still needs to be a mechanism that transforms the inflationary energy density into the matter we observe today[4]. Such a process is called reheating. In this section we start by quickly reviewing the canonical example of perturbative reheating to then comment on gravitational reheating [97]. Ricci reheating [98, 99] is discussed in Chapter 5. Although other mechanisms exist such that the inflaton is allowed to survive until the present, as instant preheating [100], we focus on these two since they are the ones used in the original research in Chapters 4 and 5. Reheating is generally highly

[4]An exception is quintessential inflation (or, more generally, non-oscillatory inflation), where the inflaton survives until the present day to account for dark energy observations. In this case, reheating needs to take place via other means (see Sec. 2.2.5)

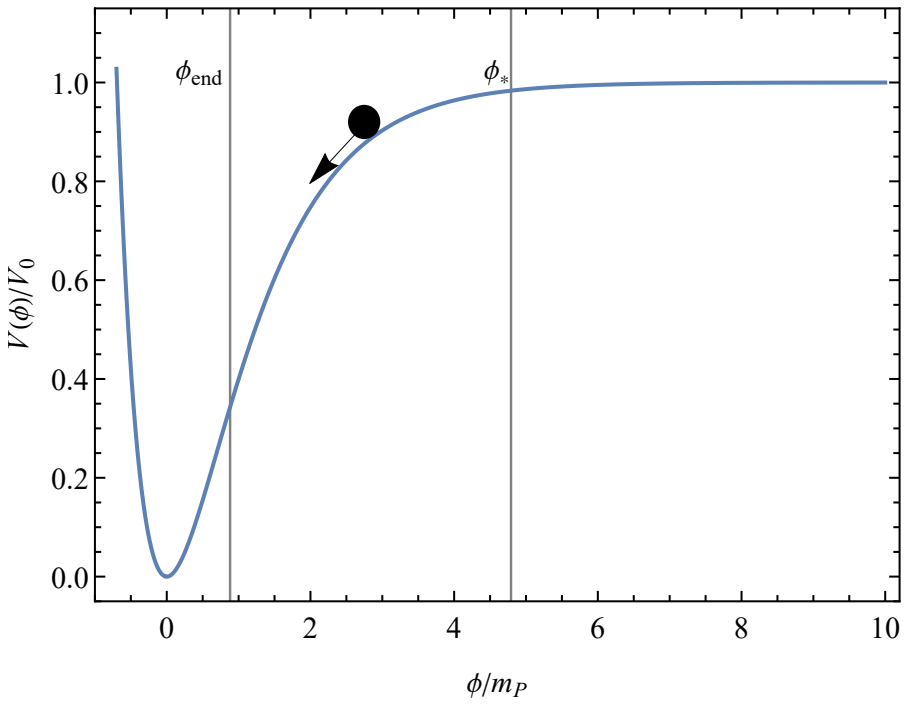

Figure 2.6: Field evolution in the Starobinsky potential [11]. The field values ϕ_* and $\phi_{\rm end}$ correspond to the perturbations observed in the CMB and to the end of inflation, respectively. After inflation ends the field oscillates around the minimum of the potential and pertubatively reheats the Universe.

model dependent and it is a very active area of research. An in depth analysis is beyond the scope of the present work. We refer the interested reader to Refs. [101, 102, 103, 104, 105] for reviews.

In the canonical scenario, as the field ϕ rolls along the potential, the latter becomes progressively steeper so that the kinetic energy of the field becomes more and more important. Inflation ends when the condition $\epsilon_H(\phi_{\rm end}) = 1$ is met and after that ϕ oscillates the around the minimum located at ϕ_0 (in Fig. (2.6) $\phi_0 = 0$), where $V(\phi_0) = 0$ (or else the Universe would engage in a new bout of inflation). Such a homogeneous oscillating field can be thought of as a collection of massive particles, *i.e.*, inflatons, with zero momenta (if $V'' = \text{const.} > 0$). If the Lagrangian of the inflaton has a coupling to another field[5], the collections of inflatons will decay

[5]Here we assume only one coupling for simplicity, but of course there could be many.

into this field, with decay rate Γ. The equation of motion of the inflaton then reads

$$\ddot{\phi} + (3H + \Gamma)\dot{\phi} + m^2\phi = 0, \tag{2.189}$$

where we have Taylor expanded the potential around its minimum $V'(\phi) \simeq V''(\phi_0)(\phi - \phi_0) \equiv m^2\phi$ and introduced the phenomenological term $\Gamma\dot{\phi}$. This is the equation of motion of a damped harmonic oscillator. Since over the timescale of a few oscillations, the Hubble parameter does not change much, we can use the ansatz

$$\phi \propto \exp\left\{\int \mathrm{d}t\, \lambda(t)\right\}, \tag{2.190}$$

leading to

$$\lambda(t) = \frac{-3H - \Gamma}{2} \pm im, \tag{2.191}$$

where we have taken into account that the regime of interest is that of an underdamped oscillator, with $(3H + \Gamma)^2 < 4m^2$. Thus, the solution can be written as

$$\phi(t) = \Phi(t)\sin(mt + c), \tag{2.192}$$

where

$$\Phi(t) \propto \exp\left\{-\frac{1}{2}\int \mathrm{d}t\, (3H(t) + \Gamma)\right\}, \tag{2.193}$$

and c is a constant phase determined by initial conditions. The kinetic and potential energy density of the field immediately follow

$$\rho_{\rm kin} = \frac{\dot{\phi}^2}{2} = \frac{1}{2}\left[\dot{\Phi}(t)\sin(mt + c) + \Phi(t)m\cos(mt + c)\right]^2, \tag{2.194}$$

$$V(\phi) = \frac{m^2\phi^2}{2} = \frac{1}{2}\Phi^2(t)m^2\sin^2(mt + c). \tag{2.195}$$

Noting that over one oscillation $\Phi(t)$ is basically constant, the averages per oscillation are also easily obtained

$$\overline{\rho_{\rm kin}} = \overline{V(\phi)} = \frac{1}{4}\Phi^2(t)m^2. \tag{2.196}$$

Furthermore, in this limit, the first term in the brackets in Eq. (2.194) can be neglected so that the total energy density reads

$$\rho_\phi = \frac{1}{2}\Phi^2(t)m^2 = 2\overline{\rho_{\rm kin}} = 2\overline{V(\phi)}. \tag{2.197}$$

This approximation is not as accurate over many oscillations, when the expansion of the Universe changes the Hubble factor appreciably. The continuity equation may now be obtained by noting

$$\dot{\rho}_\phi = \frac{\mathrm{d}}{\mathrm{d}t}\left(\frac{1}{2}\dot{\phi}^2 + V\right) = \dot{\phi}(\ddot{\phi} + V') = -\dot{\phi}^2(3H + \Gamma), \tag{2.198}$$

where we have used Eq. (2.189) in the last step. Using Eq. (2.197), on average $\dot{\phi}^2 = 2\overline{\rho_{\rm kin}} = \rho_\phi$, so that we finally obtain

$$\dot{\rho}_\phi + (3H + \Gamma)\rho_\phi = 0. \tag{2.199}$$

The solution to this equation reads

$$\rho_\phi = \rho_\phi^{\rm end}\left(\frac{a_{\rm end}}{a}\right)^3 e^{-\Gamma(t - t_{\rm end})}, \tag{2.200}$$

where we have assumed that Γ is constant and $t_{\rm end}$ is the time at which inflation ends. We can distinguish two different regimes. For $\Gamma \ll H$, $\rho_\phi \propto a^{-3}$. Thus, the energy density of an inflaton oscillating around a quadratic potential decreases as pressureless matter[6]. As time grows, the Hubble parameter $H(t) = 2/(3t)$ decreases and when $H \sim \Gamma$ the decay products grow faster than they can be diluted by the Universe expansion. Finally, when $\Gamma \gg H$, the Hubble friction term in Eq. (2.199) is negligible, the energy density of the inflaton decays exponentially fast $\rho_\phi \propto e^{-\Gamma t}$ and reheating is completed. As a side comment, it could be that $\Gamma \gtrsim H_{\rm end}$. This case is called prompt reheating and the duration of this period is negligible.

From the discussion above it is clear why the reheating epoch affects the number of inflationary e-folds and therefore the inflationary observables. Indeed, different reheating mechanisms lead to different expansion histories during this period. This of course changes the amount of elapsing e-folds from the end of inflation until the present time, which, in turn, changes the number of e-folds before the end of inflation

[6]In general, a field oscillating in a power-law potential $V \propto |\phi|^{2n}$ has a barotropic parameter given by $w_\phi = (n-1)/(n+1)$ [106]. The quadractic potential case, with $n = 1$, gives the expected matter-like barotropic parameter $w_\phi = 0$, while for a quartic potential, with $n = 2$, we have a radiation-like barotropic parameter $w_\phi = 1/3$.

at which the CMB scales left the horizon, in order to match the observations today (see Fig. 2.2).

As we have said, while $\Gamma < H$, the Universe is dominated by a coherently oscillating inflaton condensate, with a matter-like barotropic parameter $w = 0$. Then, when $\Gamma \sim H$ the inflaton particles start decaying efficiently, a process which is fast since at the end, when $\Gamma > H$ the energy density of the inflaton decays exponentially fast. Thus, it a fair approximation to say that reheating occurs when $\Gamma \simeq H_{\rm reh}$. Using the first Friedmann equation and Eq. (2.41) we find that the reheating temperature, defined as the temperature of the thermalised radiation bath at the moment when it becomes the dominant component of the Universe, reads

$$T_{\rm reh} = \left(\frac{90}{\pi^2 g_*}\right)^{1/4} \sqrt{m_{\rm P}\Gamma} \simeq \sqrt{m_{\rm P}\Gamma}, \tag{2.201}$$

where we have used that $g_* \lesssim 100$. The decay rate Γ may take different forms depending on the interaction terms in the Lagrangian. For example, a fermionic coupling of the form

$$\mathcal{L}_{\rm int} = -h\phi\bar{\psi}\psi, \tag{2.202}$$

where ψ is a generic fermionic field and h is a dimensionless coupling constant, leads to a decay rate given by [107]

$$\Gamma_{\phi\to\bar{\psi}\psi} = \frac{h^2 m}{8\pi}. \tag{2.203}$$

Considering GUT-scale inflation $V_{\rm end}^{1/4} \sim 10^{16}\,{\rm GeV}$, and noting that at the end of slow-roll inflation $1 = |\eta_{\rm end}| \Rightarrow m \equiv \sqrt{V''_{\rm end}} \simeq \sqrt{V_{\rm end}}/m_{\rm P}$ (where we have Taylor expanded around the minimum of the potential), we have that the reheating temperature is $T_{\rm reh} \sim h \times 10^{15}\,{\rm GeV}$.

Let us finish our discussion on perturbative reheating by mentioning that so far we have considered decays of individual inflaton particles into other fields. However, the inflaton condensate may act a coherent whole, leading to parametric resonance effects. This non-perturbative decay is called preheating [108] and results in explosive decay. In turn, if the decay particles decay fast enough, the mechanism

is called instant preheating [100]. If (instant) preheating, takes place it is usually much more efficient than perturbative reheating, so it is important to take it into account. However, if the inflaton is not significantly coupled to any other field in the Lagrangian, reheating proceeds via gravitational reheating [97], which does not require the existence of any extra dynamical degree of freedom other than the inflaton, or via Ricci reheating, which does.

Gravitational reheating can be heuristically understood by first noting that the cosmological horizon during accelerated expansion is an event horizon. Then, following a similar reasoning to the one that leads to the Hawking temperature of the black body radiation emitted by black holes [109], one finds that during de Sitter expansion a thermal bath of particles with temperature

$$T = \frac{H}{2\pi} \tag{2.204}$$

is generated. In the case of black holes, creation and annihilation of virtual pairs close to the event horizon can lead to one member of the pair to fall into the black hole. But be cause of this, annihilation is no longer possible, resulting in the other member of the pair becoming a real particle, escaping to infinity. The case of inflation is similar. Virtual pairs are pulled apart over to acausal distances by the accelerated expansion of the Universe, before they have a chance to annihilate. In other words, they become real particles. This process occurs everywhere and therefore all space is filled with Hawking radiation.

All non-conformally invariant light ($m < H$) fields gravitationally produce particles. Combining Eqs. (2.41) and (2.204), their energy density is [97]

$$\rho_{\rm gr} = q\frac{\pi^2 g_*}{30}\left(\frac{H}{2\pi}\right)^4 \simeq 10^{-2}H^4, \tag{2.205}$$

where we have introduced an efficiency factor $q \sim 1$ since the spectrum is not exactly thermal and $g_* \sim \mathcal{O}(100)$ is the effective non-conformally invariant relativistic degrees of freedom of the gravitationally produced particles.

In most cases, $\rho_{\rm gr}$ is negligible compared to the energy density of radiation generated via other reheating mechanisms. However, if the inflaton survives until

the present day and there are no other dynamical degrees of freedom, so that instant preheating or Ricci reheating cannot occur, it is the only viable mechanism for the generation of the Hot Big Bang radiation bath. In order for gravitational reheating to be efficient enough, so that GWs are not overproduced during kination enough to violate BBN bounds (see below), $g_* \gtrsim 300$ is required.

2.2 Dark Energy

Having dealt with the physics of the very early Universe, we now turn our attention to the present day. As is discussed in the introduction of this chapter, conventional matter satisfies the SEC and so decelerated expansion would be *a priori* expected. In order to have accelerated expansion, the energy density of the Universe needs to be dominated by a component with barotropic parameter $w < -1/3$ (see Eq. (2.21)). This is the case of inflation, a period of accelerated expansion at very early times that could be sourced by a scalar field with energy density dominated by its potential. However, after the end of inflation, with the horizon and flatness problems solved, as well as with the initial perturbations that seed all structure provided for, the expectation was that the Universe would have been decelerating until the present day. This is why the discovery [110, 111] that the Universe has recently started to accelerate again came in as a shock (although it solved the cosmic age problem).

The substance responsible for the acceleration of the Universe was called dark energy (DE), a term coined by Michael S. Turner [112], reflecting its mysterious nature. Although since its discovery many mechanisms have been proposed attempting to explain it (for a review see Ref. [113]), they all have to satisfy the most up-to-date constraints on the density parameter and barotropic parameter, which are [8]

$$\Omega_{\rm de} = 0.6889 \pm 0.0056\,(68\%\text{C.L.}), \tag{2.206}$$

$$w_{\rm de} = -1.028 \pm 0.031\,(68\%\text{C.L}). \tag{2.207}$$

Importantly, the constraint in Eq. (2.207) assumes that dark energy has been

constant throughout the history of the Universe. However, this need not be the case and deviations from this behaviour can be parametrized as a function of the scale factor as (with the normalization at present $a(t_0) = 1$)

$$w_{\rm de}(a) = w_0 + (a-1)\frac{\mathrm{d}w}{\mathrm{d}a}\Big|_0 \equiv w_0 + (1-a)w_a, \tag{2.208}$$

in what is called the Chevallier-Polarski-Linder (CPL) parametrization [114, 115] and we have defined $w_a \equiv \mathrm{d}w/\mathrm{d}a|_0$. Note that Eq. (2.208) is simply a Taylor expansion of $w(a)$ around the present time $a(t_0)$. Assuming this parametrization, the constraints now read [8]

$$w_0 = -0.957 \pm 0.080\,(68\%\text{C.L})\tag{2.209}$$

$$w_a = -0.29^{+0.32}_{-0.26}\,(68\%\text{C.L.}).\tag{2.210}$$

Note that w_a, also known as the running of the barotropic parameter, is compatible with zero. Future experiments, such as the recently launched EUCLID [116] may be able to resolve this uncertainty shedding light on the nature of dark energy. Finally, imposing the restriction $w_0 > -1$, as is the case for quintessence, leads to [8]

$$-1 < w_0 < -0.95\,(68\%\text{C.L.}).\tag{2.211}$$

The CMB temperature power spectrum also reveals information about the critical density today, and, thus, about the energy density of dark energy. Indeed, the Planck 2018 results [8] indicate that the Hubble parameter at present is (including BAO)

$$H_0 = 67.66 \pm 0.42\frac{\text{km}}{\text{s}\cdot\text{Mpc}} = (5.912 \pm 0.037)\times 10^{-61} m_{\rm P}\,(68\%\text{C.L.}),\tag{2.212}$$

where we have switched to natural units in the second step. This means that the critical density today is

$$\rho_{\rm c}^0 = 1.048\times 10^{-120} m_{\rm P}^4.\tag{2.213}$$

Combining this with Eq. (2.206) gives the energy density of dark energy today

$$\rho_{\rm de}^0 = 7.222\times 10^{-121} m_{\rm P}^4.\tag{2.214}$$

2.2.1 ΛCDM

The first solution one might think of when addressing the nature of dark energy is having it correspond to a positive cosmological constant (see [117, 118, 119, 120] for reviews). Indeed, there is the freedom of adding $\Lambda g_{\mu\nu}$, where Λ is a constant, to the Einstein equations. From the point of view of the action this amounts to writing

$$S = \frac{m_{\rm P}^2}{2}\int \mathrm{d}^4x\sqrt{-g}\,(R - 2\Lambda)\,. \tag{2.215}$$

This action is, in fact, the most general covariant one that can be written in terms of the metric and its first and second derivatives. Equivalently, the new term may be thought as a source in the energy momentum tensor given by $T_{\mu\nu} = -m_{\rm P}^2\Lambda g_{\mu\nu}$. Of course, its conservation $\nabla_\mu T^{\mu\nu} = 0$ is still satisfied. Since the energy density is constant, $\rho_\Lambda = m_{\rm P}^2\Lambda$, its continuity equation leads to

$$w_\Lambda = -1. \tag{2.216}$$

The modified Friedmann equations read[7]

$$H^2 = \frac{\rho}{3m_{\rm P}^2} + \frac{\Lambda}{3}, \tag{2.217}$$

$$\frac{\ddot{a}}{a} = -\frac{1}{6m_{\rm P}^2}(\rho + 3p) + \frac{\Lambda}{3}. \tag{2.218}$$

It is clear that the cosmological constant acts as a negative pressure $p_\Lambda = -m_{\rm P}^2\Lambda$ and therefore has a repulsive effect. As long as it is the dominant component of the Universe, the expansion will be accelerated.

[7]The cosmological constant was originally introduced by Einstein in order to obtain a static universe. Reinstating the spatial curvature term in Eq. (2.217), it is easy to see that a universe dominated by dust ($p = 0$), with energy density $\rho = 2m_{\rm P}^2\Lambda$ and curvature $k = \Lambda a^2$ is static. Furthermore, since $\rho > 0$, the cosmological constant is also positive, which means that the universe is closed $k > 0$. However, after the discovery that the Universe is, in fact, expanding [121], Einstein was forced to drop the cosmological constant term in what he called "my biggest blunder" (according to George Gamow [122]).

The assumption that dark energy, which accounts for about 69% of the energy budget of the Universe, is a cosmological constant, together with the density parameters of matter and radiation [8] at present

$$\Omega_{\rm m} = 0.3111 \pm 0.0056\,(68\%\text{C.L.}), \tag{2.219}$$

is called ΛCDM or the concordance model. From the totality of matter in the Universe, only 15.8% is baryonic, while the rest corresponds to cold dark matter (CDM). In other words, 95% of the total of the energy density of Universe corresponds to unknown substances!

2.2.2 The Cosmological Constant Problem

We have a measurement for the critical energy density, and we know what proportion of the Universe corresponds to dark energy, so we could claim the cosmological constant has been observed. Unfortunately, when one starts taking into account the different contributions from fundamental physics that could act as a cosmological constant, things do not go as planned. In this section we comment on these contributions and lay out what is known as the cosmological constant problem [123, 124].

Classically, there exist two contributions. The first one is of course the cosmological constant Λ that is allowed in the Einstein equations. However, there is no preferred choice for what its value might be. The second one has to do with the energy density of the different fields that exist in the Universe. Take, for simplicity, a scalar field with energy-momentum tensor given by Eq. (2.48). The lowest energy configuration is one where the kinetic energy of the field vanishes while the field is lying at the minimum of its potential

$$T_{\mu\nu} = -V(\phi_0) g_{\mu\nu}, \tag{2.220}$$

where ϕ_0 is the field value at which $V'(\phi_0) = 0$. There is *a priori* no reason for the potential to vanish at the minimum and therefore a term like (2.220) acts as

an effective cosmological constant. All in all, classically, the energy density of the effective cosmological constant reads

$$\rho_\Lambda = m_{\rm P}^2 \Lambda + V(\phi_0), \tag{2.221}$$

where the last term should be interpreted as the sum of the potential densities of all the relevant fields.

In quantum theory, a field may be thought as an infinite collection of harmonic oscillators in momentum space. As in non-relativistic quantum mechanics, these oscillators have a zero-point energy and the sum of all of them in principle gives the energy density of the vacuum[8]. More specifically, taking again a scalar field for simplicity, the Hamiltonian reads

$$H = \int \frac{{\rm d}^3 k}{(2\pi)^3} \sqrt{k^2 + m^2} \left(a_{\mathbf{k}}^\dagger a_{\mathbf{k}} + \frac{1}{2} (2\pi)^3 \delta^{(3)}(0) \right), \tag{2.222}$$

where m is the mass of the field. As we learn in quantum field theory courses, the divergence coming from the delta function can be dealt with by working with energy densities rather than absolute energies. This is because in a finite volume $(2\pi)^3 \delta^{(3)}(0)$ is simply the volume. Therefore, the energy density of the vacuum reads

$$\rho_{\rm vac} = \frac{\langle 0 | \, H \, | 0 \rangle}{V} = \frac{1}{2} \int \frac{{\rm d}^3 k}{(2\pi)^3} \sqrt{k^2 + m^2} = \int \frac{{\rm d}k}{(2\pi)^2} k^2 \sqrt{k^2 + m^2}, \tag{2.223}$$

where in the second step we have switched to spherical coordinates in momentum space. However, the theory is in general only valid until some ultraviolet momentum $k_{\rm max}$. Introducing this cutoff in the integral (2.223), *i.e.*, discarding high-momentum modes, we have

$$\rho_{\rm vac} = \int_0^{k_{\rm max}} \frac{{\rm d}k}{(2\pi)^2} k^2 \sqrt{k^2 + m^2} \simeq \frac{1}{16\pi^2} k_{\rm max}^4, \tag{2.224}$$

where we have taken into account that the integral is dominated by the modes close to the cutoff. In quantum field theory this energy is typically discarded (by normal-ordering) under the grounds that we can not measure absolute energies: we can

[8] Vacuum energy was first experimentally measured by Casimir [125].

only measure differences in energy. However, the situation changes when gravity is included, as any kind of energy contributes to the gravitational interactions. Choosing $k_{\max}$ to be the Planck scale, where quantum gravity effects are expected to become relevant, gives

$$\rho_{\text{vac}} \simeq \frac{m_{\text{P}}^4}{16\pi^2} \sim m_{\text{P}}^4, \tag{2.225}$$

where in the last step we have gotten rid of the numerical pre-factor as it depends on the specific field theory under consideration and we expect contributions to the vacuum energy from all the SM fields.

Comparing Eq. (2.225) with the experimental value of the density of dark energy in Eq. (2.214), we find that the theoretical contribution is many orders of magnitude larger than the experimental value. Taking also into account the bare cosmological constant Λ, it could be that they all cancel out to give the precise value in Eq. (2.214), but they would need to do so with a precision of 60 significant digits in energy (the dimensions of Λ are $[\Lambda] = E^2$). This is the cosmological constant problem [123].

In the present work we take the approach that due to some unknown symmetry, all contributions to the cosmological constant cancel out (as was routinely assumed before the observation of dark energy). In this way, dark energy needs to be explained via other means. In our case, it will be quintessence.

2.2.3 An Interlude: The Hubble tension

The Planck CMB measurements suggest a value for the Hubble parameter today given by Eq. (2.212). This value is not only at odds with the vacuum energy density expected from theoretical considerations, as detailed in the last section. For very different reasons, it is also at odds with local measurements (although the difference in magnitude is much less dramatic), in what is called the Hubble tension [126]. More generally, the Hubble tension may be defined as the discrepancy between the locally *measured* and cosmologically *inferred* values for the expansion rate today H_0 (for reviews on the Hubble tension see, *e.g.*, Refs. [127, 128, 129, 130, 13, 131, 132, 133]

and Refs. [13, 134] for a focus on the different models that have been proposed to explain it). Let us first start by elucidating the difference between both.

Obtaining H_0 involves the measurement of cosmological distances. These measurements are difficult to carry out, although not impossible. The strategy that is often followed is to take advantage of either standard candles, *i.e.*, objects of known intrinsic brightness, or standard rulers, *i.e.*, objects of known size. With the former, comparing the measured flux of light with the theoretical value and taking into account the FRW geometry of the Universe as well as the redshift of light, one can infer the distance to the source. As for the latter, if an object has a known size, *e.g.*, the typical separation between hot and cold spots in the CMB, it can be compared to the observed angular size, which depends on distance.

More specifically, for local measurements, *i.e.*, with redshift $z < 1$, one can Taylor expand the scale factor around the present time t_0 to second order in the look-back time $|t - t_0|$

$$a(t) = 1 + H_0(t - t_0) - \frac{1}{2} q_0 H_0^2 (t - t_0)^2, \tag{2.226}$$

where we have used the normalization $a(t_0) = 1$ and $q_0 \equiv -\ddot{a}(t_0)/(a(t_0)H_0^2)$ is the deceleration parameter today. The redshift then reads

$$z = \frac{1}{a} - 1 = H_0(t_0 - t) + \frac{1}{2}(q_0 + 2)H_0^2(t_0 - t)^2. \tag{2.227}$$

On the other hand, from the flat FRW metric (2.20), the radial comoving distance reads

$$x(t) = c\int_t^{t_0} \frac{\mathrm{d}t}{a(t)} = c\int_t^{t_0} \mathrm{d}t\,[1 - H_0(t - t_0)] = c(t_0 - t) + \frac{cH_0}{2}(t_0 - t)^2, \tag{2.228}$$

where we have reinstated the speed of light c. Noting that Eq. (2.227) can be inverted to give $H_0(t_0 - t) = z - z^2(2 + q_0)/2$ and plugging this in Eq. (2.228) gives the comoving distance as a function of redshift

$$x(z) = \frac{c}{H_0}\left[z - \frac{1}{2}(1 + q_0)z^2\right]. \tag{2.229}$$

But, of course, we do not measure comoving distances. Rather, when using the method of standard candles, the useful definition of distance is that of luminosity distance

$$d_L \equiv (1+z)x = \frac{c}{H_0}\left[z + \frac{1}{2}(1-q_0)z^2 + \mathcal{O}(z^3)\right]. \tag{2.230}$$

Since the measured flux of light coming from, *e.g.*, a Type Ia supernova (SN Ia), is given by

$$F = \frac{L}{4\pi^2 d_L^2}, \tag{2.231}$$

where L is the (known) luminosity, *i.e.*, energy radiated per unit of time, relative distances are easily obtained simply by measuring the brightness of different SN Ia. This, in turn, leads to the determination of the deceleration parameter by using Eq. (2.230). Note, however, that H_0 drops out of the calculation. Indeed, in order to obtain the expansion rate we need to measure absolute distances. This can be done by constructing a distance ladder, starting with distances that can be directly resolved by using parallax to then move to larger distances by using Cepheid variables and SN Ia. Cepheids are bright ($\sim 10^5$ solar luminosities) stars with brightness that changes periodically. In turn, this period is correlated with their intrinsic brightness, due to the κ-mechanism, where the opacity κ of the gas depends on its temperature [135]. The most recent implementation of this technique by the SH0ES team yields a value for the expansion rate at present given by [136]

$$H_0 = 73.04 \pm 1.04 \, \frac{\text{km}}{\text{s} \cdot \text{Mpc}}, \tag{2.232}$$

and

$$H_0 = 73.30 \pm 1.04 \, \frac{\text{km}}{\text{s} \cdot \text{Mpc}}, \tag{2.233}$$

when including high-redshift SN Ia from the Pantheon+ data [137]. This value disagrees at 5σ with the one obtained by the Planck collaboration (see below). Of course, there are other values obtained by a variety of experiments, although all early-time indirect measurements, such as CMB or BAO, which assume ΛCDM, agree between themselves, and likewise for all the late-time ΛCMD-independent measurements, such as distance ladders or strong lensing (see Fig. 2.7).

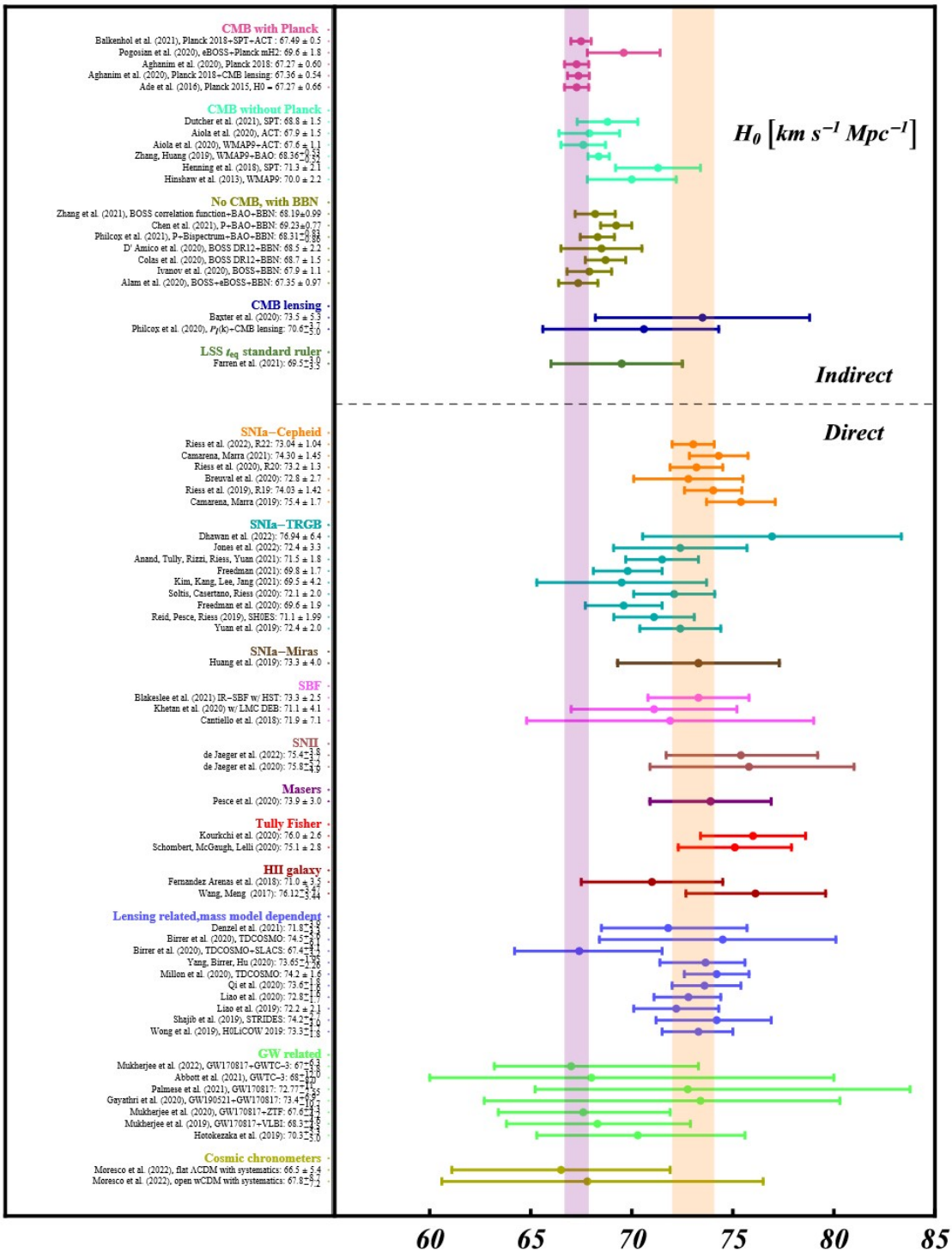

Figure 2.7: Constraints on H_0 coming from different cosmological probes (at 68% C.L.). Figure adapted from Ref. [12] (which is based on Refs. [13, 14]).

The value of the Hubble constant can also be inferred from cosmological observations. The most notable example comes from the peak structure in the angular power spectrum of the temperature anisotropies of the CMB (see Fig. 2.3). The multiple moment l_s of the first acoustic peak is tightly related to the angle subtended by the sound horizon at last scattering θ_s. In fact, the latter has been very precisely determined by Planck to be [8]

$$\theta_s = (1.04109 \pm 0.00030) \times 10^{-2}\,\mathrm{rad}. \tag{2.234}$$

Since θ_s is small we can work in the small angle approximation to write

$$\theta_s = \frac{r_s}{D_A}, \tag{2.235}$$

where r_s is the comoving sound horizon at last scattering and D_A is the comoving angular diameter distance to the surface of last scattering. The former is given by

$$r_s = \int_{z_{\rm ls}}^{\infty} \frac{c_s(z)\mathrm{d}z}{H(z)} = \int_{z_{\rm ls}}^{\infty} \frac{c\,\mathrm{d}z}{\sqrt{3}H_{\rm ls}\sqrt{\Omega_{\rm m,ls}(1+z)^3 + \Omega_{\rm r,ls}(1+z)^4}}, \tag{2.236}$$

where $z_{\rm ls} = 1089.95 \pm 0.27$ [8] is the redshift of last-scattering, $c_s(z) \simeq c/\sqrt{3}$ is the sound speed of the photon-baryon fluid and $\Omega_{\rm m,ls}$ and $\Omega_{\rm r,ls}$ are the density parameters at last scattering of matter and radiation, respectively. Here, the Hubble parameter at last scattering is given by

$$H_{\rm ls}^2 = H_0^2 \left[\Omega_{\rm m,0}(1+z_{\rm ls})^3 + \Omega_{\rm r,0}(1+z_{\rm ls})^4\right], \tag{2.237}$$

where we have omitted the contribution from dark energy as it is negligible at $z_{\rm ls}$.

The comoving angular diameter distance is given by

$$D_A = \int_0^{z_{\rm ls}} \frac{c\,\mathrm{d}z}{H(z)} = \frac{c}{H_0}\int_0^{z_{\rm ls}} \frac{\mathrm{d}z}{\sqrt{\Omega_{\rm m,0}(1+z)^3 + (1-\Omega_{\rm m,0})(1+z)^{3(1+w)}}}, \tag{2.238}$$

where we have assumed wCDM and neglected the contribution from radiation, since the integral is dominated by its lower limit. For ΛCDM, $w = -1$. Combining, Eqs. (2.235)-(2.238) we have

$$H_0 = \sqrt{3}\theta_s H_{\rm ls} \frac{\int_0^{z_{\rm ls}} \frac{\mathrm{d}z}{\sqrt{\Omega_{\rm m,0}(1+z)^3 + (1-\Omega_{\rm m,0})(1+z)^{3(1+w)}}}}{\int_{z_{\rm ls}}^{\infty} \frac{\mathrm{d}z}{\sqrt{\Omega_{\rm m,ls}(1+z)^3 + \Omega_{\rm r,ls}(1+z)^4}}}. \tag{2.239}$$

It should be noted that, strictly speaking, this is an implicit equation for H_0. Indeed, in the right-hand-side, the quantities $\Omega_{\mathrm{m},0} \equiv \omega_{\mathrm{m}}/h^2$ and $\Omega_{\mathrm{r},0} \equiv \omega_{\mathrm{r}}/h^2$ depend on $h = H_0/(100\,\mathrm{km\,s^{-1}\,Mpc^{-1}})$[9]. Furthermore, the density parameters at last scattering are related to their counterparts evaluated at present time via a simple rescaling, so they also depend on H_0. In practice, however, all unknown cosmological parameters are obtained simultaneously by numerically fitting the ΛCDM model to the data. The value for the Hubble parameter obtained by the Planck collaboration using this method is [8] (excluding BAO)

$$H_0 = 67.36 \pm 0.54\,\frac{\mathrm{km}}{\mathrm{s}\cdot\mathrm{Mpc}}. \tag{2.240}$$

This implies a 8% discrepancy with respect to the value obtained by the SH0ES collaboration [136] (see Eq. (2.232)) at a confidence level of 5σ.

Although determining H_0 via Eq. (2.239) is heuristic, it is a good approximation and it serves well to gain some intuition regarding solutions to the Hubble tension. Indeed, although ω_{m} and ω_{b} carry an h dependence, they mainly depend on the characteristics of the CMB power spectrum and, in fact, it has been found [127] that the fractional change of the Hubble parameter with these quantities is mild, $\Delta H_0/H_0 \simeq 0.1\Delta\omega_{\mathrm{b}}/\omega_{\mathrm{b}}$ and $\Delta H_0/H_0 \simeq -0.77\Delta\omega_{\mathrm{m}}/\omega_{\mathrm{m}}$. Then, for example, the value of the Hubble parameter can be increased by increasing the number of additional relativistic degrees of freedom N_{eff}. This is because H_{ls} in the numerator of Eq. (2.239) depends on $\Omega_{\mathrm{r},0}$, which, in turn, depends on the photon density parameter $\Omega_{\gamma,0}$ via the relation

$$\Omega_{\mathrm{r},0} = \left[1 + \frac{7}{8}N_{\mathrm{eff}}\left(\frac{4}{11}\right)^{4/3}\right]\Omega_{\gamma,0}. \tag{2.241}$$

In ΛCDM we have $N_{\mathrm{eff}} = 3.06$ coming from the three neutrino mass eigenstates [138]. However, if N_{eff} were increased it would lead to a higher H_{ls} and therefore to a larger H_0.

[9] Although we have used the approximation $c_s \simeq c/\sqrt{3}$, $c_s(z)$ depends on $\Omega_{\mathrm{b}} \equiv \omega_{\mathrm{b},0}/h^2$, *i.e.*, the baryonic density parameter at present, so it indirectly depends on H_0.

2.2.3.0.1 Solving the Hubble tension

Assuming that the Hubble tension is not due to unknown systematic errors, its resolution calls for the introduction of new physics [139, 140, 141, 142]. Since local measurements of the Hubble constant are largely model independent, most theoretical attempts involve the introduction of new physics, beyond the ingredients of ΛCDM, such that the value of H_0 inferred from CMB measurements is increased. Looking at Eq. (2.239), these can be classified in early-time and late-time solutions, depending on whether they change the denominator or the numerator of this expression, respectively. Early-time solutions usually involve an increase in the energy density before recombination such that the comoving sound horizon at last scattering is decreased. For example, increasing $N_{\rm eff}$ is an early-time solution.

Late-time solutions require that the energy density between recombination and the present time is smaller than in ΛCDM, with the constraint that the current energy density is fixed [143], *i.e.*, $\rho(z)/\rho_0 < \rho(z)/\rho_0|_{\Lambda\rm CDM}$, such that the comoving angular diameter distance to the last scattering surface is increased. Since the redshift scaling of matter and radiation are known, this can be achieved by introducing an exotic component with energy density that *increases* with time. A popular candidate has been a phantom field [144] with barotropic parameter $w = p/\rho < -1$ and, more specifically, dark energy with a phantom crossing [145, 146, 147]. However, these models not only imply a violation of the dominant energy condition (DEC), but lead to discrepancies in the sound horizon seen from the galaxy correlation function [132, 148], as well as with constraints on the barotropic parameter of dark energy coming from high-redshift SNe Ia data [137]. Other possible late-time solutions include a vaccuum phase transition [149, 150, 151, 152] or interacting dark energy [153, 154]. Late-time solutions, which seem to be disfavoured [155, 156], are beyond the scope of the present work, so we do not further comment on them.

One of the most promising early-time solutions for the Hubble tension is EDE, a name coined in Ref. [157] (see also Refs. [158, 159, 160] for early works). The

nature of EDE is well described by its name: it simply is a subdominant dark energy component in the early Universe. In Ref. [161] it was first suggested that EDE might alleviate the Hubble tension, but it was soon realised that the analysis was too simplistic and another model that fully resolves the tension was proposed in Ref. [162]. Since then, EDE in the context of the Hubble tension has become a very active area of research (see, *e.g.*, Refs. [163, 164, 165, 166, 167, 168, 169, 170, 171, 172, 173, 174, 175, 176, 162, 177, 178, 179, 180, 181, 182, 183, 184, 185, 186, 187, 188, 189, 190] for a non-comprehensive list).

EDE provides an increase to the energy density before recombination, leading to a smaller comoving sound horizon at last scattering and therefore to a larger value for H_0 inferred from the CMB. It usually contributes $\sim 10\%$ to the total energy density for a brief time, to then quickly redshift away, leaving the subsequent evolution of the Universe unchanged. More specifically, EDE is generally modelled as a frozen scalar field ϕ that becomes dynamical at redshift $z_{\rm c}$, when its density parameter is $f_{z_{\rm c}} \equiv \Omega_\phi(z_{\rm c})/\Omega_{\rm tot}(z_{\rm c})$. In most of its successful realizations, ϕ then undergoes oscillations, with its energy density decaying faster than radiation. Models are parametrized by three quantities: $z_{\rm c}$, $f_{z_{\rm c}}$ and the effective sound speed c_s^2.

Of course, EDE is highly constrained by the peak structure of the angular power spectrum of the CMB temperature anisotropies (see Fig. 2.3). Indeed, although the multiple moment of the first peak is related to scales corresponding to last scattering, the highest multiple moments, with $l_s \sim 3000$, correspond to scales the re-entered the horizon at redshifts $z \sim 10^6$, deep inside the radiation dominated era and well before equality. Constraints vary depending on the specific model under consideration. However, it is usual to find $z_{\rm c} \simeq z_{\rm eq}$ and $0.015 \lesssim f_{z_{\rm c}} \lesssim 0.107$, so that the contribution of EDE is enough to solve the tension while not impeding structure formation. By last scattering, the density parameter should already be $f_{z_{\rm ls}} < 0.015$.

It has been argued [133, 191] that upcoming ground-based measurements of the CMB, *e.g.*, by the SPT and ACT collaborations or the Simmons Observatory, providing independent measurements of intermediate angular scales and extending

those of small scales, may uniquely probe EDE, possibly discarding it as a viable model. However, if the evidence in favor of EDE became stronger, connecting it with "late" DE would be one of the most pressing questions.

A toy model attempting to unify EDE and late DE is given in the original research in Chapter 7. There, a scalar field with a non-minimal kinetic term, in the context of α-attractors, acts as EDE to then free-fall with energy density $\rho \propto a^{-6}$ and freeze. At late times the field becomes dominant and accounts for the DE observations. Furthermore, it may even be possible to have the scalar field be responsible for the period of cosmic inflation in the early Universe, as in quintessential inflation [15].

2.2.4 Quintessence

After our digression into the Hubble tension, we return to the topic of dark energy. In Sec. 2.2.2 we explained the extreme fine-tuning problem associated with a cosmological constant, in what is called the cosmological constant problem. Our approach in the present work is to ignore this issue by assuming that, due to some unknown symmetry, all contributions to the cosmological constant cancel out. Dark energy then needs to be explained via other means.

Among the plethora of proposed mechanisms, we focus on, arguably, the simplest: a scalar field (see Ref. [113] for a review). And among the plethora of available scalar field models[10] we focus again on, arguably, the simplest: quintessence [208, 209] (see also Ref. [210] and Ref. [211] for a review).

Quintessence is defined as a scalar field ϕ governed by the action

$$S_\phi = \int \mathrm{d}^4x\sqrt{-g}\left[-\frac{1}{2}g^{\mu\nu}\partial_\mu\phi\partial_\nu\phi - V(\phi)\right]. \tag{2.242}$$

This is the same action as the one we introduced for the inflaton in Eq. (2.47). Thus, the analysis given in Sec. 2.1.2 regarding the background dynamics directly applies

[10] A non-comprehensive list includes chameleon fields [192, 193], k-essence [194, 195, 196], modified gravity [197, 198, 199], Chaplygin gas [200, 201, 202], tachyons [203, 204], Phantom Dark Energy [144], the Cyclic Universe [205] and Ghost Condensates [206, 207].

here, with the caveat that during inflation the dominant component of the energy density is the inflaton. After the hot Big Bang, the Universe goes through periods of radiation and matter domination, during which the quintessence field needs to be subdominant, until it comes to dominate at the present time. Therefore, in order to correctly study the dynamics of quintessence we need to study the dynamics of a subdominant scalar field.

The Friedmann equations are modified as

$$H^2 = \frac{1}{3m_{\rm P}^2}\left[\frac{1}{2}\dot{\phi}^2 + V(\phi) + \rho_{\rm b}\right], \tag{2.243}$$

and

$$\dot{H} = -\frac{1}{2m_{\rm P}^2}\left[\dot{\phi}^2 + (1+w_{\rm b})\rho_{\rm b}\right], \tag{2.244}$$

where $\rho_{\rm b}$ is the density of a background perfect fluid with barotropic parameter $w_{\rm b} = p_{\rm b}/\rho_{\rm b}$ and b is label standing for the possible different components, such as pressureless dust or radiation. The energy density ρ_ϕ and pressure p_ϕ of the field remain as in Eqs. (2.51)-(2.52). Both the field and the background perfect fluid obey continuity equations

$$\dot{\rho}_\phi + 3H\rho_\phi(1+w_\phi) = 0, \tag{2.245}$$

where $w_\phi = p_\phi/\rho_\phi$, and

$$\dot{\rho}_{\rm b} + 3H\rho_{\rm b}(1+w_{\rm b}) = 0. \tag{2.246}$$

The solution to Eqs. (2.243) and (2.246) in the case of a subdominant field $\rho_\phi \ll \rho_{\rm b}$ reads

$$\rho_{\rm b}(a) \propto a^{-n} \quad \Rightarrow \quad a(t) \propto t^{2/n} \quad \Rightarrow \quad H(t) = \frac{2}{nt}, \tag{2.247}$$

where, for convenience $n \equiv 3(1+w_{\rm b})$. With this, the KG equation takes the following form

$$\ddot{\phi} + \frac{6}{nt}\dot{\phi} + V'(\phi) = 0. \tag{2.248}$$

Let us obtain the potentials $V(\phi)$ that allow the density evolution of the field to be

$$\rho_\phi \propto a^{-m}, \tag{2.249}$$

where m is a constant. Note that the power of the scaling behaviour of quintessence is bounded as $0 \leq m \leq 6$. The cases $m = 0$ and $m = 6$ correspond to the limiting cases of potential and kinetic domination, with $w_\phi = -1$ and $w_\phi = 1$, respectively. Furthermore, the scaling in Eq. (2.249) requires that the ratio of the kinetic density of the field and its total density remains constant. This can be easily seen by taking a time derivative of ρ_ϕ and combining it with the KG equation to obtain

$$\dot{\rho}_\phi = -3H\dot{\phi}^2. \tag{2.250}$$

Dividing this expression by ρ_ϕ and noting that, from Eq. (2.249), $\dot{\rho}_\phi/\rho_\phi = -m\dot{a}/a$ we find

$$\frac{\dot{\phi}^2/2}{\rho_\phi} = \frac{m}{6}. \tag{2.251}$$

We now can also find the time dependence of $\dot{\phi}$. Combining Eq. (2.251) with Eqs. (2.247) and (2.249) gives

$$\dot{\phi}(t) \propto t^{-m/n}. \tag{2.252}$$

Plugging this back in the KG equation it is straightforward to integrate for $V(\phi)$ [209, 212].

Let us first focus on the $m = n$ case. Integration of Eq. (2.252) gives

$$\phi(t) = \frac{2m_\mathrm{P}}{\lambda} \ln t/t_0, \tag{2.253}$$

and

$$t(\phi) = t_0 e^{\lambda\phi/(2m_\mathrm{P})}, \tag{2.254}$$

where we have chosen the integration constant by convenience. Plugging Eq. (2.253) in the KG equation gives

$$\frac{2m_\mathrm{P}}{\lambda}\left(\frac{6}{n} - 1\right)\frac{1}{t^2} + V'(\phi) = 0. \tag{2.255}$$

Plugging Eq. (2.254) in Eq. (2.255) and integrating gives the exponential potential

$$V(\phi) = \frac{2m_\mathrm{P}^2}{\lambda^2 t_0^2}\left(1 - \frac{6}{n}\right)e^{-\lambda\phi/m_\mathrm{P}}. \tag{2.256}$$

In the current limit of a subdominant field $\rho_\phi \ll \rho$, this potential gives rise to a scaling behaviour for the field such that its energy density mimics that of the background. We prove this by showing that the density parameter of the field is constant as well as by obtaining w_ϕ. First, combining (the time derivative of) Eq. (2.253) and Eq. (2.256) we find the energy density of the field to be

$$\rho_\phi = \frac{1}{2}\dot{\phi}^2 + V(\phi) = \frac{12m_{\rm P}^2}{n\lambda^2 t^2}. \tag{2.257}$$

The energy density of the background can be obtained from the Hubble parameter in Eq. (2.247) via the Friedmann equation as

$$\rho = \frac{12m_{\rm P}^2}{n^2 t^2}. \tag{2.258}$$

Thus,

$$\Omega_\phi = \frac{\rho_\phi}{\rho} = \frac{n}{\lambda^2} = \frac{3(1+w_{\rm b})}{\lambda^2}, \tag{2.259}$$

which is constant. Then, combining (the time derivative of) Eq. (2.253) and Eq. (2.257) we find

$$\frac{\dot{\phi}^2/2}{\rho_\phi} = \frac{n}{6}. \tag{2.260}$$

Plugging this back in Eq. (2.251) gives

$$w_\phi = w_{\rm b}, \tag{2.261}$$

as we wanted to show. Note that in order for the process of BBN not to be disturbed, the contribution of the field to the energy budget of the Universe should be small enough. The bound reads [27]

$$\Omega_\phi(t_{\rm BBN}) < 0.045, \tag{2.262}$$

which combined with Eq. (2.259) (and $w_{\rm b} = 1/3$) leads to

$$\lambda > 9.4. \tag{2.263}$$

It is clear that, in the regime under consideration, it is not possible for a field rolling along an exponential potential to behave as dark energy. Not only its density

remains a constant fraction of the total, but its barotropic parameter is that of the background and therefore can never fulfill the requirement for accelerated expansion $w_\phi < -1/3$, much less the observational bound $w_\phi < -0.95$.

We have obtained the only potential that can give rise to the scaling behaviour in Eq. (2.249), with $n = m$. However, the KG equation is non-linear and there is no guarantee that given an exponential potential the field with generally follow the assumed scaling solution. In other words, the phase-plane analysis of the system should be carried out. This was first done in Refs. [213, 214], where it is found that the solution we have obtained is indeed an attractor, for $\lambda^2 > 3(w_\mathrm{b} + 1)$. Furthermore, there is another attractor for $\lambda^2 < 3(w_\mathrm{b} + 1)$ where the energy density of the field dominates the Universe $\Omega_\phi = 1$. Since in this dominant attractor the barotropic parameter of the field is given by Eq. (2.187), accelerated expansion can only occur for $\lambda^2 < 2$.

Is it possible for exponential quintessence to successfully describe dark energy? The scaling attractor is very attractive (no pun intended!) from a model-building point of view, since given any initial conditions the field stays subdominant, while having a constant non-negligble contribution to the total density, mimicking the scaling of the background. However, precisely for this reason, the field can never lead to accelerated expansion with $w_\phi < -1/3$. On the other hand, the dominant attractor corresponds to total domination of the field. This means that, since $\Omega_\mathrm{de} \simeq 0.69$, at present the field should have not reached this attractor yet, but be in the transition between both attractors. Following this reasoning, in Ref. [215], T. Barreiro, E. J. Copeland and N. J. Nunes proposed the potential

$$V(\phi) = V_1 e^{\alpha\phi/m_\mathrm{P}} + V_2 e^{\beta\phi/m_\mathrm{P}}, \tag{2.264}$$

where V_1 and V_2 are constant density scales and $\alpha \gg \beta$. Therefore, at early times the first term dominates over the second, while the opposite is true at late times. In this way, the field follows the scaling attractor during the radiation and matter domination eras, while towards the present it transitions to the dominant attractor. From the BBN constraint in Eq. (2.263) we have $\alpha > 9.4$, while V_1 is basically a free

parameter, since the scaling regime does not depend on the density scale. As for the second exponential, we can impose the observational constraint for quintessence in Eq. (2.211) to obtain $\beta < 0.39$, while the mass scale V_2 should be comparable to the critical density today $V_2 \sim 10^{-120} m_{\rm P}^4$, in order for the transition between attractors to happen close to the present, with $V(\phi_0) = \Omega_{\rm de}\rho_0$. Of course, this corresponds to the same amount of fine-tuning as for ΛCDM, tarnishing the nice logic behind the mechanism.

Finally, exponential quintessence could also work if the field overshoots both attractors with $\lambda \ll \sqrt{2}$, transiently freezing to then unfreeze close to the present time and approach the dominant attractor. This scenario is called thawing quintessence. However, here one needs to give up the idea of an attractor as the initial condition, *i.e.*, the value $\phi_{\rm F}$ at which the field freezes accounting for the critical density today $V(\phi_{\rm F}) = \Omega_{\rm de}\rho_0$, needs to be explained.

In the original research in Chapter 5 we consider a quintessential inflation model with a quintessential sector governed by the exponential potential (2.256), in the context of modified gravity in the Palatini formalism. The inclusion of a running in the coupling constant ξ of the non-minimal coupling between the field and gravity $\xi\phi^2 R$ [82] generates a minimum in the potential at large field values. When the field reaches this minimum, it essentially behaves as an effective cosmological constant, accounting for dark energy. In this way, we are able to utilise the exponential as a successful quintessence potential in a novel way, without using either the scaling or the dominant attractors.

We now focus on the $m \neq n$ case. Integration of Eq. (2.252) gives

$$\frac{\phi}{\phi_0} = B\left(\frac{t}{t_0}\right)^{1-m/n}, \tag{2.265}$$

and

$$\frac{t}{t_0} = \left(\frac{\phi}{B\phi_0}\right)^{n/(n-m)}, \tag{2.266}$$

where ϕ_0 is an arbitrary field value, t_0 is an arbitrary time value, the integration constant B is dimensionless and we have set the other integration constant to zero

$A = 0$ since it leads to a potential that does not satisfy the constraint in Eq. (2.251). The KG equation now reads

$$t_0^{-2} B\phi_0 \left(1 - \frac{m}{n}\right)\left(\frac{6}{n} - \frac{m}{n}\right)\left(\frac{t}{t_0}\right)^{-(n+m)/n} + V'(\phi) = 0. \tag{2.267}$$

Plugging Eq. (2.266) in Eq. (2.267) and integrating gives the power-law potential

$$V(\phi) = t_0^{-2}(B\phi_0)^2 \left[\frac{2}{q(q-2)}\right]\left(\frac{6}{n} + \frac{q}{2-q}\right)\left(\frac{\phi}{B\phi_0}\right)^q, \tag{2.268}$$

where

$$q \equiv \frac{2m}{m-n}. \tag{2.269}$$

The power of the potential is positive $q > 0$ for $m > n$. In this case, the density of quintessence diminishes faster than that of the background. Conversely, a negative power $q < 0$, first investigated in Refs. [209, 216], corresponds to $m < n$, and the density of the field diminishes slower than that of the background. Solving for m in Eq. (2.269) gives

$$m = \left(\frac{q}{q-2}\right) n. \tag{2.270}$$

It follows that if q is positive then it must be $q > 2$, since both m and n are positive. For negative powers, all values are allowed $q < 0$.

It is straightforward to fix the integration constant B. We simply use Eq. (2.270) in Eq. (2.265) to rewrite the field as

$$\frac{\phi}{\phi_0} = B\left(\frac{t}{t_0}\right)^{2/(2-q)}. \tag{2.271}$$

It is also important to note that given a potential $V(\phi) = V_0\phi^q$, the constant potential density V_0 in front of the V' term in the KG equation can be absorbed into a rescaling of time $t \mapsto \hat{t}(t) = \sqrt{V_0}t$. With this, and plugging Eq. (2.271) in the KG equation (2.248), we obtain

$$B = \left[\frac{1}{q}\left(\frac{2}{q-2}\right)\left(\frac{6}{n} - \frac{q}{q-2}\right)\right]^{1/(q-2)}. \tag{2.272}$$

Finally, noting that $\left(t_0^{-2}\phi_0^{2-q}\right)^{1/(4-q)}$ has dimensions of mass, we rewrite the potential as

$$V(\phi) = M^{4-q}\phi^q, \tag{2.273}$$

where M is a mass scale. For negative values of q, this is typically called the inverse-power-law potential.

We have now derived *all* potentials that lead to a scaling solution of the field given by $\rho_\phi \propto a^{-m}$, assuming that the background scales like $\rho \propto a^{-n}$. However, as we have commented for the exponential potential, the attractor structure should be analysed out in order to find out how general these scaling solutions are. This was first done in Ref. [217] for negative q and $n = 3, 4$ and in Ref. [212] for arbitrary q and arbitrary n. For $q < 0$, it turns out that the scaling solution is an attractor if

$$q < 2\left(\frac{6+n}{6-n}\right). \tag{2.274}$$

Since n is positive, this condition is always satisfied and scaling solutions are attractors for all $q < 0$. Conversely, for $q > 0$ we have an attractor if

$$q > 2\left(\frac{6+n}{6-n}\right). \tag{2.275}$$

Thus, during matter domination, with $n = 3$, the scaling solution is an attractor as long as $q > 6$. During radiation domination the condition is $q > 10$.

Although positive power-law potentials are used in other contexts, such as in EDE (see the discussion towards the end of Sec. 2.2.3) or inflation, they are not so relevant in the context of dark energy. This is because they lead to a scaling behaviour for the field with $m < n$, *i.e.*, the energy density of the field diminishes faster than that of the background, a property that is not desirable since dark energy needs to approach domination towards the present time. Negative power-law potentials are *a priori* better equipped to describe dark energy as they lead to a similar field evolution as for positive power-law, only with $m > n$, so that the density parameter of quintessence grows with time. However, precisely because of this reason, there is a certain amount of tuning in these models. This has to do with the fact that for the BBN process not to be disturbed, the density parameter of the field at that time should satisfy [27] $\Omega_\phi(t_{\rm BBN}) < 0.045$. For the exponential potential, the mass scale of the potential is unaffected by this bound, as the only condition for the field to follow the scaling attractor is on the strength of the exponential

λ. If λ is large enough, not only the field follows the scaling attractor, but its density parameter is small (see Eq. (2.259)). This is not so in inverse-power-law quintessence, for which the scaling solution is an attractor irrespective of the value q takes. Therefore M should be appropriately tuned. Related to this issue is the fact that the field should be starting to dominate at the present time. An estimate for the corresponding field value can be calculated by noting that the density of the field catches up with the background fluid when its mass squared becomes comparable to the Hubble parameter (also known as the coincidence constraint)

$$\frac{\rho_\phi}{\phi_0^2} \simeq \frac{\mathrm{d}^2 V}{\mathrm{d}\phi^2} = m_\phi^2 \simeq H^2 \simeq \frac{\rho_\phi}{m_\mathrm{P}^2}, \tag{2.276}$$

which means that the value of the field at present is of the order of the Planck mass

$$\phi_0 = \mathcal{O}(m_\mathrm{P}). \tag{2.277}$$

Since $V(\phi_0) \simeq \Omega_\mathrm{de}\rho_0 \simeq 10^{-120} m_\mathrm{P}^4$ (see Eq. (2.214)), we obtain the mass scale

$$M \simeq 10^{-120/(4-q)} m_\mathrm{P}. \tag{2.278}$$

For example, if $q = -4$, we have $M \simeq 10^3\,\mathrm{GeV}$, close to the electroweak scale. It seems the severe fine-tuning of ΛCDM is alleviated.

There is a more serious problem when considering the barotropic parameter of the field. From Eqs. (2.268) and (2.271), after a bit of algebra, it is straightforward to obtain

$$w_\phi = \frac{q w_\mathrm{b} + 2}{q - 2} = \frac{|q| w_\mathrm{b} - 2}{|q| + 2}. \tag{2.279}$$

For a background dominated by pressureless dust, with $w_\mathrm{b} = 0$, the observational constraint $w_\phi < -0.95$ leads to

$$|q| < 0.1, \tag{2.280}$$

which, from Eq. (2.278) leads to $M \simeq 10^{-12}\,\mathrm{GeV}$, a mass scale difficult to find in particle physics. We conclude that trying to explain dark energy via inverse-power-law quintessence in the scaling attractor leads to an amount of fine tuning comparable with ΛCDM.

However, Eq. (2.279) has been calculated under the assumption that the field is subdominant $\rho_\phi \ll \rho$. Since the field is beginning to dominate at present, it is reasonable to expect it to be undergoing slow-roll in its potential. In this regime, the barotropic parameter reads [27]

$$w_\phi = \frac{q^2 m_{\rm P}^2 - 6\phi^2}{q^2 m_{\rm P}^2 + 6\phi^2}. \tag{2.281}$$

Imposing the constraint $w_\phi < -0.95$ at present gives $\phi_0 > 2.55|q|m_{\rm P}$, which is consistent with our estimation in Eq. (2.277) for reasonable values of q. Of course, the field is neither in the scaling nor in the dominant attractor, but transition between both. However, as mentioned above, the scenario where the scaling attractor brings the field to dominate today is not feasible due to the amount of fine-tuning involved. In contrast, it could be that the field overshoots the attractor, transiently freezing to later unfreeze close to the present time and approach the dominant attractor. In this scenario, just as we explained for the $\lambda \ll \sqrt{2}$ case in exponential quintessence, the idea of an attractor has to be given up and the initial condition for the field, *i.e.*, the value $\phi_{\rm F}$ at which the field freezes, needs to be explained. Again, this behaviour is called thawing quintessence.

In the original research in Chapter 4 we consider a quintessential inflation model with a quintessential sector governed by the potential in Eq. (2.273). On top of the ingredients described so far, we add an R^2 term to the gravitational action and work in the Palatini formalism. We obtain successful dark energy in the scenario of thawing quintessence, for $q = 4$ and a mass scale close to the electroweak scale, which are rather natural values.

2.2.5 Quintessential Inflation

In the previous section we found that, although it is possible to endow quintessence models with attractor properties, it is generally hard to successfully satisfy the observational constraints on dark energy without either giving up the idea of an attractor or including an amount of fine-tuning comparable to ΛCDM. For example,

the scenario of thawing quintessence does not seem to lead to unreasonable amounts of fine-tuning on the parameters. However, the value $\phi_{\rm F}$ at which the field freezes becomes a free parameter. It seems the fine-tuning has reappeared via the initial conditions of the field. But, what if we could explain the value $\phi_{\rm F}$?

Quintessential inflation is a framework that identifies the inflaton and quintessence scalar fields[11]. In principle this is a natural idea, since in both cases the acceleration of the Universe is driven by a potential-dominated scalar field. In its original form, proposed by P. J. E. Peebles and A. Vilenkin [15] in 1999 (see Refs. [220, 221, 222, 223, 224, 225, 226, 227, 228, 229, 230, 231, 232, 233, 234, 235, 236, 237, 238, 239, 240, 241, 242, 243, 244, 245, 246, 247, 248, 249, 250, 251, 252, 253, 254, 255, 256, 257, 258, 259, 260, 261, 262, 263, 264, 265, 266, 267, 268, 16, 269, 270, 271, 272, 273, 274, 275, 276, 277, 278, 279, 280, 281, 282, 283] for a non-comprehensive list of successful quintessential inflation models and Refs. [284, 285] for reviews), the potential reads (see left panel in Fig. 2.8)

$$V(\phi) = \begin{cases} \lambda(\phi^4 + M^4), & \phi < 0 \\ \frac{\lambda M^8}{\phi^4 + M^4}, & \phi \geq 0 \end{cases}, \tag{2.282}$$

where M is a constant mass scale and λ is the self-coupling of the inflaton. For large negative values of the field $|\phi| \gg M$ the potential reduces to quartic chaotic inflation, which, as we described by the end of Sec. 2.1.4, is discarded by observations, unless, *e.g.*, the gravitational action is extended with an R^2 term in the Palatini formalism (see Chapter 4 for further details). Conversely, for large positive values of the field $\phi \gg M$, the potential reduces to quartic inverse-power-law quintessence. As described in the previous section, the attractor properties of this potential cannot be utilised and we are basically left with a thawing quintessence scenario. However, the situation is now different. Crucially, due to the identification of the inflaton and quintessence fields, the value at which the field freezes $\phi_{\rm F}$ is not a free parameter anymore, but is given by a combination of the inflationary attractor and the mechanism that generates the radiation of the hot Big Bang. We show this, but

[11] The idea of unifying inflation and quintessence can be traced back to Refs. [218, 219].

in order to do so we first need to understand the dynamics of kination, a new period of expansion of the Universe typical of quintessential inflation.

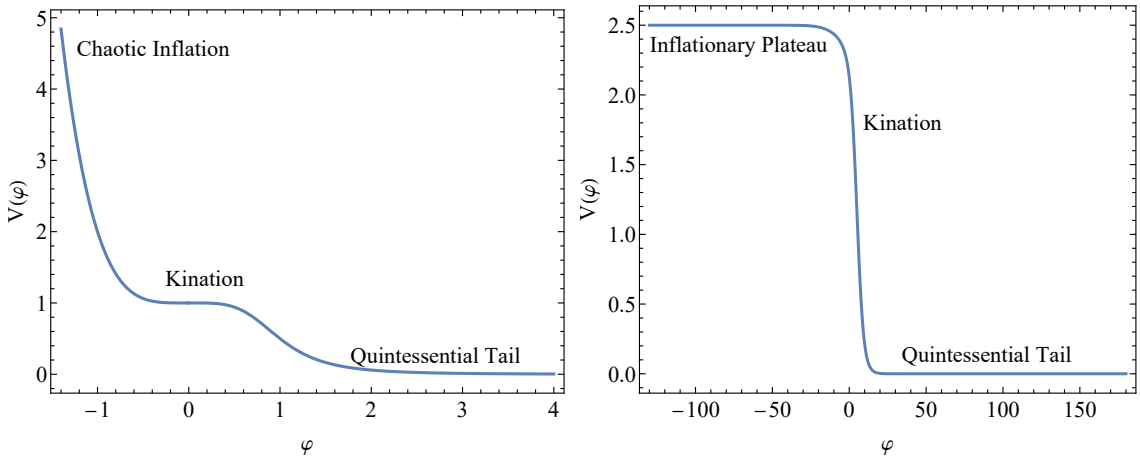

Figure 2.8: Left: Original Peebles-Vilenkin potential [15] (see Eq. (2.282)) in arbitrary units. Quartic chaotic inflation has been discarded by observations, so the model is no longer valid. Right: Typical quintessential inflation potential, in arbitrary units. It features an inflationary plateau, which is observationally favoured.

Kination, a name coined in Ref. [286], takes place after the end of inflation, as the potential becomes very steep. It was first considered as a means of terminating inflation in Ref. [287] and later as a source for a strongly first-order electroweak phase transition that could enhance baryogenesis in Ref. [288]. During this period the energy density of the Universe is still dominated by that of the inflaton field. The defining property is that the inflaton becomes kinetically dominated, oblivious to the potential. Importantly, as a consequence, the properties of the kination period are model-independent. The total energy density of the Universe ρ reads

$$\rho = \rho_\phi = \frac{\dot{\phi}^2}{2} \quad \Rightarrow \quad H = \frac{\dot{\phi}}{\sqrt{6} m_{\rm P}}. \tag{2.283}$$

It immediately follows that the barotropic parameter (see Eq. (2.53)) is $w = 1$. Since the field still obeys its continuity equation, it follows that its energy density scales as

$$\rho = \rho_\phi \propto a^{-6}. \tag{2.284}$$

Using Eq. (2.283), the KG equation during kination reads

$$\ddot{\phi} + \frac{\sqrt{6}}{2m_{\rm P}}\dot{\phi}^2 = 0. \tag{2.285}$$

Assuming that the start of kination happens at the end of inflation, this expression can be readily integrated between then until some arbitrary time during kination to obtain

$$\frac{1}{\dot{\phi}} - \frac{1}{\dot{\phi}_{\rm end}} = \frac{\sqrt{6}}{2m_{\rm P}}\left(t - t_{\rm end}\right), \tag{2.286}$$

where "end" stands for the end of inflation. If kination lasts long enough, *i.e.*, if $t \gg t_{\rm end}$, then, since $\dot{\phi} \propto a^{-3}$, it is a good approximation to use that $\dot{\phi}_{\rm end} \gg \dot{\phi}(t)$. With this and integrating Eq. (2.286) we obtain

$$\phi(t) = \phi_{\rm end} + \sqrt{\frac{2}{3}} m_{\rm P} \ln\left(\frac{t}{t_{\rm end}}\right). \tag{2.287}$$

Of course, even if the inflaton survives until the present day, the Universe needs to be somehow reheated, *e.g.*, via gravitational reheating [97], Ricci reheating [98, 99, 289], curvaton reheating [290, 291], instant preheating [100, 228], primordial black hole evaporation [267] or in the context of warm quintessential inflation [272]. Here we assume this is the case, without choosing one specific mechanism. Since the radiation density scales slower ($\rho_{\rm r} \propto a^{-4}$) than the field density ($\rho_\phi \propto a^{-6}$), it will at some point become dominant. We call this moment reheating. After reheating, since $H = 1/(2t)$, the KG equation reads

$$\ddot{\phi} + \frac{3}{2t}\dot{\phi} = 0. \tag{2.288}$$

Integrating this expression from reheating until some later time during the radiation domination epoch, we obtain

$$\dot{\phi} = \dot{\phi}_{\rm reh}\left(\frac{t_{\rm reh}}{t}\right)^{3/2} = \sqrt{\frac{2}{3}}\frac{m_{\rm P}\sqrt{t_{\rm reh}}}{t^{3/2}}, \tag{2.289}$$

where "reh" stands for reheating and in the second step we have evaluated the time derivative of Eq. (2.287) at reheating in order to obtain $\dot{\phi}_{\rm reh}$. Integrating again we find

$$\phi(t) = \phi_{\rm reh} + 2\sqrt{\frac{2}{3}} m_{\rm P}\left(1 - \sqrt{\frac{t_{\rm reh}}{t}}\right). \tag{2.290}$$

It is obvious that for times $t \gg t_{\rm reh}$, the field freezes at a value given by

$$\phi_{\rm F} = \phi_{\rm reh} + 2\sqrt{\frac{2}{3}} m_{\rm P}. \tag{2.291}$$

We can express $\phi_{\rm reh}$ as a function of the field value and the density parameter of radiation, both at the time at which radiation is generated. The latter is usually referred to as the *reheating efficiency*. As we say above, we assume that reheating happens via some unspecified mechanism. Let the moment at which radiation is created be $t_{\rm rad}$, with $t_{\rm end} < t_{\rm rad} < t_{\rm reh}$. We can integrate Eq. (2.285) between $t_{\rm rad}$ and $t_{\rm reh}$ twice to obtain

$$\phi_{\rm reh} = \phi_{\rm rad} + \sqrt{\frac{2}{3}} m_{\rm P} \ln\left(\frac{t_{\rm reh}}{t_{\rm rad}}\right), \tag{2.292}$$

where we have assumed that $\dot{\phi}_{\rm reh} \ll \dot{\phi}_{\rm rad}$, as before. The ratio $t_{\rm reh}/t_{\rm rad}$ can be estimated by using that the density of parameter of radiation $\Omega_{\rm r}$ during kination scales as

$$\Omega_{\rm r} = \frac{\rho_{\rm r}}{\rho} \propto \frac{a^{-4}}{a^{-6}} = a^2. \tag{2.293}$$

Since at reheating the dominant component of the Universe is radiation, we then have

$$1 = \Omega_{\rm r}^{\rm reh} = \Omega_{\rm r}^{\rm rad} \left(\frac{a_{\rm reh}}{a_{\rm rad}}\right)^2 = \Omega_{\rm r}^{\rm rad} \left(\frac{t_{\rm reh}}{t_{\rm rad}}\right)^{2/3}, \tag{2.294}$$

where in the last step we have used that during kination $a \propto t^{1/3}$. Thus,

$$\frac{t_{\rm reh}}{t_{\rm rad}} = \left(\Omega_{\rm r}^{\rm rad}\right)^{-3/2}. \tag{2.295}$$

Putting everything together, the value at which the field freezes reads

$$\phi_{\rm F} = \phi_{\rm rad} + \sqrt{\frac{2}{3}} \left(2 - \frac{3}{2} \ln \Omega_{\rm r}^{\rm rad}\right) m_{\rm P}. \tag{2.296}$$

Note that the smaller $\Omega_{\rm r}^{\rm rad}$ is, the larger $\phi_{\rm F}$ is. Indeed, smaller values of the reheating efficiency mean that radiation takes longer to dominate. Since the field starts slowing down after radiation becomes dominant, it has a longer time to free-fall and freeze at larger values.

As an example, for gravitational reheating $t_{\rm rad} = t_{\rm end}$. In this case, the value at which the field freezes is given by the inflationary attractor and the reheating efficiency

$$\phi_{\rm F} = \phi_{\rm end} + \sqrt{\frac{2}{3}}\left(2 - \frac{3}{2}\ln\Omega_{\rm r}^{\rm end}\right) m_{\rm P}, \tag{2.297}$$

where "end" stands for the end of inflation. For prompt reheating, with $\Omega_{\rm r}^{\rm end} = 1$, the field transverses the lowest possible distance in field space, given by

$$\phi_{\rm F} = \phi_{\rm end} + 1.63 m_{\rm P}. \tag{2.298}$$

The opposite is true for gravitational reheating, the most inefficient of all reheating mechanisms. For GUT-scale inflation, the reheating efficiency reads $\Omega_{\rm r}^{\rm end} \simeq 10^{-13}$ (see below), leading to

$$\phi_{\rm F} = \phi_{\rm end} + 36.82 m_{\rm P}. \tag{2.299}$$

Needless to say, due to these super-Planckian field displacements, quintessential inflation generically suffers from the same problems that plague quintessence (see end of Sec. (2.2.4)).

The existence of the kination period also increases the number of inflationary e-folds. According to our result by the end of Sec. 2.1.1, the increase with respect to, *e.g.*, a period of an oscillating condensate with $w = 0$ is

$$\Delta N = -\frac{2}{3}\ln\left(\frac{T_{\rm reh}}{V_{\rm end}^{1/4}}\right). \tag{2.300}$$

We can estimate the maximum allowed value for the total number of e-folds if inflation is followed by kination, by using Eq. (2.43). For this, we need to consider the lowest possible reheating temperature, coming gravitational reheating.

Combining Eq. (2.205) with the Friedmann equation at the end of inflation gives the density parameter of the gravitationally produced radiation at the end of inflation

$$\Omega_{\rm r}^{\rm end} = \frac{\rho_{\rm r}(t_{\rm end})}{\rho(t_{\rm end})} = \frac{10^{-2} H_{\rm end}^4}{3 m_{\rm P}^2 H_{\rm end}^2} \simeq 10^{-2}\left(\frac{H_{\rm end}}{m_{\rm P}}\right)^2. \tag{2.301}$$

Since the density parameter of radiation during kination scales as $\Omega_{\rm r} \propto a^2$, we have

$$\frac{a_{\rm end}}{a_{\rm reh}} = \sqrt{\Omega_{\rm r}^{\rm end}} \simeq 10^{-1}\frac{H_{\rm end}}{m_{\rm P}}, \tag{2.302}$$

where we have used that $\Omega_{\rm r}^{\rm reh} = 1$. With this, and using again Eq. (2.205), the radiation density at reheating reads

$$\rho_{\rm r}(t_{\rm reh}) = \rho_{\rm r}(t_{\rm end}) \left(\frac{a_{\rm end}}{a_{\rm reh}}\right)^4 \simeq 10^{-6} \frac{H_{\rm end}^8}{m_{\rm P}^4}. \tag{2.303}$$

Combining this with Eq. (2.41), we finally obtain the reheating temperature of the gravitationally produced radiation

$$T_{\rm reh} = 10^{-2} \frac{H_{\rm end}^2}{m_{\rm P}} \simeq \frac{10^{-2}}{3} \frac{V_{\rm end}}{m_{\rm P}^3}, \tag{2.304}$$

where we have used that for gravitationally produced radiation $g_* \sim 10^2$ and the slow-roll approximation. Plugging this in Eq. (2.43) gives

$$N = 64.26 - \frac{1}{3} \ln \left(\frac{V_{\rm end}^{3/4}}{m_{\rm P}^3}\right) + \ln \left(\frac{V_{\rm end}^{1/4}}{10^{16}\,{\rm GeV}}\right) = 64.26 + \ln \left(\frac{m_{\rm P}}{10^{16}{\rm GeV}}\right) = 70. \tag{2.305}$$

We conclude that the usual 50-60 e-folds of inflation considered in the literature in the canonical case is raised to 60-70 e-folds if inflation is followed by kination.

To end our discussion of quintessential inflation, we address one last consequence of the existence of the period of kination, having to do with the overproduction of GWs. Briefly put, the density parameter of GWs during kination is inversely proportional to scale. Therefore, we expect that GW modes that re-enter the horizon soon after inflation ends to have a large contribution to the energy density, possibly challenging BBN. In what follows we give a summarised account of this phenomenom, leaving most technical details to Appendix A.3. We emphasize that this problem is unique to the period of kination, while the problems associated with a super-Planckian $\phi_{\rm F}$ are also ubiquitous in most models of quintessence.

The quantity we need to consider is the spectral energy density of the primordial GW background, defined as

$$\Omega_{\rm GW}(k,\eta) \equiv \frac{1}{\rho(\eta)} \frac{{\rm d}\rho_{\rm GW}(k,\eta)}{{\rm d}\ln k}, \tag{2.306}$$

where $\rho(\eta)$ is the total energy density of the universe and ${\rm d}\rho_{\rm GW}(k,\eta)$ is the contribution to $\Omega_{\rm GW}(k,\eta)$ from the tensor modes in the interval ${\rm d}\ln k$. In the

literature, Eq. (2.306) is typically evaluated at present, and we simply write

$$\Omega_{\rm GW}(k) \equiv \frac{1}{\rho_{\rm c}} \frac{{\rm d}\rho_{\rm GW}(k,\eta_0)}{{\rm d}\ln k}. \tag{2.307}$$

Since the energy density of the tensor modes reads (see Chapter 6 for a full derivation)

$$\langle \hat{\rho}_{\rm GW} \rangle \simeq \int_{k=aH} \frac{{\rm d}\ln k}{\pi^2} \frac{k^4}{a^4} |\alpha_-|^2, \tag{2.308}$$

where α_- are the coefficients that multiply the negative frequency modes, Eq. (2.307) can be rewritten as

$$\Omega_{\rm GW}(k) = \frac{1}{\rho_{\rm c}} \frac{k^4}{\pi^2 a^4(\eta_0)} |\alpha_-|^2. \tag{2.309}$$

This equation can be simplified even further by noting that the energy density of radiation scales as

$$\rho_{\rm r}(\eta) = \rho_{\rm r}(\eta_{\rm end}) a^{-4}(\eta) = \Omega_{\rm r}^{\rm end} \rho_{\rm end} a^{-4}(\eta), \tag{2.310}$$

where we have used the normalization condition $a(\eta_{\rm end}) = 1$ at the end of inflation. Thus,

$$\Omega_{\rm GW}(k) = \frac{\Omega_{\rm r}^0}{\rho_{\rm end} \Omega_{\rm r}^{\rm end}} \frac{k^4}{\pi^2} |\alpha_-|^2. \tag{2.311}$$

The basic method we use in order to obtain the coefficients α_-, after imposing the Bunch-Davies vacuum as an initial condition, is to match the mode functions and their derivates at the transitions between the different cosmological epochs. We carry out this procedure in detail in Appendix A.3 for kination (see Ref. [292] for the original work of V. Sahni and Refs. [293, 294] for subsequent early works specific to kination) and in the original research in Chapter 6 for the novel period of hyperkination. Plugging Eq. (A.88) in Eq. (2.311), we find that the GW spectrum for a period of kination followed by a period of radiation domination, in the scale-

invariant limit, reads[12]

$$\Omega_{\rm GW}(k) = \frac{\Omega_{\rm r}^0}{\pi^2}\frac{H}{m_{\rm P}} \begin{cases} \frac{k}{3\Omega_{\rm r}^{\rm end}\pi m_{\rm P}} & k_{\rm end} > k > k_{\rm reh} \\ \frac{H}{12 m_{\rm P}} & k_{\rm reh} > k > k_{\rm BBN} \end{cases} \tag{2.312}$$

where $k_{\rm end} = H$ and $k_{\rm reh} = 1/(2\eta_{\rm reh}) = \Omega_{\rm r}^{\rm end} H$. Decreasing the value of $\Omega_{\rm r}^{\rm end}$ makes kination last longer, *i.e.*, decreases the value of $k_{\rm reh}$, and leaves the amplitude of the branch of the spectrum corresponding to radiation domination unchanged. The amplitude of the latter depends solely on the energy scale at the end of inflation. To showcase this behaviour we plot the spectrum in Fig. 2.9 for a few different values of H and $\Omega_{\rm r}^{\rm end}$. In the left panel we fix H at the GUT scale and we find that indeed decreasing the value of $\Omega_{\rm r}^{\rm end}$ shifts the kination peak to lower frequencies. In the right panel we fix $\Omega_{\rm r}^{\rm end}$ and we find that decreasing H indeed lowers the amplitude of the radiation branch of the spectrum. Note that in Fig. 2.9 we show the spectrum as a function of frequency, which is related to the wavenumber via

$$f = \frac{k}{2\pi a_0} = \frac{1}{2\pi}\left(\frac{\Omega_{\rm r}^0 H_0^2}{\Omega_{\rm r}^{\rm end} H^2}\right)^{1/4} k\,, \tag{2.313}$$

where we have used Eq. (2.310) and $\Omega_{\rm r}^0 = 9.15 \times 10^{-5}$. We also show the frequency corresponding to BBN, which reads

$$f_{\rm BBN} = \frac{1}{2\pi}\frac{a_{\rm BBN} H_{\rm BBN}}{a_0} = \frac{1}{2\pi}\left(\frac{\rho_{\rm r}^0}{\rho_{\rm BBN}}\right)^{1/4}\left(\frac{\rho_{\rm BBN}}{3m_{\rm P}^2}\right)^{1/2} \simeq 1.36 \times 10^{-11}\,{\rm Hz}, \tag{2.314}$$

where we used $\rho_{\rm BBN} \simeq 3 \times 10^{-86} m_{\rm P}^4$.

The process of BBN places strong bounds on the energy density parameter of GWs. Indeed, the contribution of GWs at the time of BBN $\Omega_{\rm GW}^{\rm BBN} = \rho_{\rm GW}(\eta_{\rm BBN})/\rho(\eta_{\rm BBN})$ should be small enough so as not to disturb the process. Using

[12] Since our aim is to study the spike in the spectrum generated by kination, we do not take into account the period of matter domination. We simply calculate the spectrum at some time deep into the radiation-dominated era, chosen to be BBN for convenience, and redshift it until the present time. In any case, although the spectrum is boosted during matter domination as $\Omega_{\rm GW}(k) \propto k^2$, the corresponding frequencies are too small to be detected by any upcoming experiment, such as LISA or ET, to name a couple.

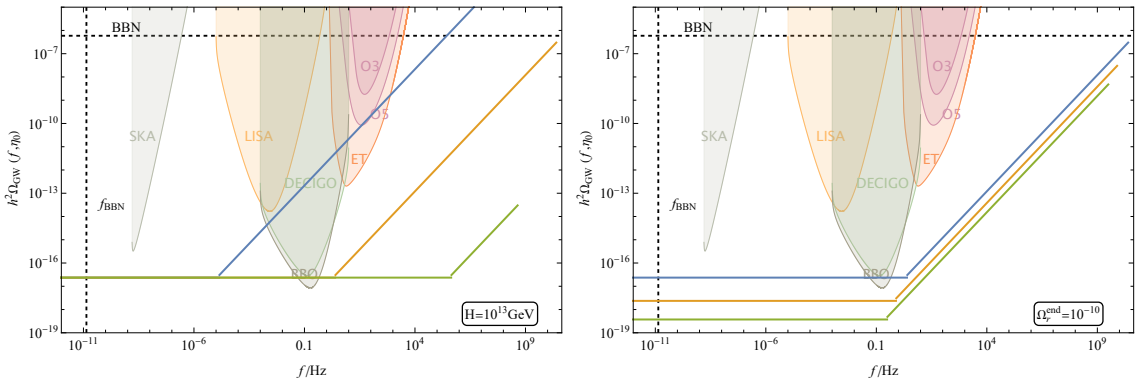

Figure 2.9: GW density spectrum as a function of frequency for a period of kination followed by a period of radiation domination (see Eq. (2.312)), for different values of H and $\Omega_{\rm r}^{\rm end}$, superimposed with the power law integrated curves of different gravitational-wave experiments. Left: $H = 10^{13}\,\text{GeV}$ and $\Omega_{\rm r}^{\rm end} = 10^{-17}$ (blue), $\Omega_{\rm r}^{\rm end} = 10^{-10}$ (orange) and $\Omega_{\rm r}^{\rm end} = 10^{-3}$ (green). Right: $\Omega_{\rm r}^{\rm end} = 10^{-10}$ and $H = 10^{13}\,\text{GeV}$ (blue), $H = 5\times10^{12}\,\text{GeV}$ (orange) and $H = 10^{12}\,\text{GeV}$ (green). The vertical dotted line represents the frequency corresponding to BBN in Eq. (2.314) and the horizontal dotted line represents the approximate BBN bound in Eq. (2.316). The different spectra have a high-frequency cutoff given by $f_{\rm end} = H/(2\pi a_0)$.

Eqs. (2.306) and (2.311) we can relate $\Omega_{\rm GW}^{\rm BBN}$ to present-day quantities. Using the latest observational constraints [295], the BBN bound reads

$$h^2\Omega_{\rm GW}^0 = \int \frac{\mathrm{d}f}{f} h^2\Omega_{\rm GW}(f) < 1.12\times10^{-6}\,. \tag{2.315}$$

If the spectrum does not feature a very narrow peak, we can approximate

$$h^2\Omega_{\rm GW}(f) < 1.12\times10^{-6}. \tag{2.316}$$

This is the bound that we show in Fig. (2.9), as a horizontal dotted line. We can be a bit more careful and compute the integral by using Eq. (2.312). The results reads (barring the negligible contribution coming from modes $k < k_{\rm BBN}$)

$$\begin{aligned} 1.12\times10^{-6} > h^2\Omega_{\rm GW}^0 &= \frac{h^2\Omega_{\rm r}^0 H}{\pi^2 m_{\rm P}}\left[\frac{k_{\rm end}-k_{\rm reh}}{3\Omega_{\rm r}^{\rm end}\pi m_{\rm P}} + \ln\left(\frac{k_{\rm reh}}{k_{\rm BBN}}\right)\frac{H}{12m_{\rm P}}\right] \\ &\simeq 1.28\times10^{-6}\left(\frac{H}{m_{\rm P}}\right)^2\left\{\frac{1}{\Omega_{\rm r}^{\rm end}\pi} + \frac{1}{8}\ln\left[(\Omega_{\rm r}^{\rm end})^{3/2}\frac{H}{m_{\rm P}}\right] + 12.38\right\}, \end{aligned} \tag{2.317}$$

where we have used $\Omega_{\rm r}^0 \simeq 8.37 \times 10^{-5}$, $h \simeq 0.67$, $k_{\rm end} = H$, $k_{\rm reh} = \Omega_{\rm r}^{\rm end} H$, $k_{\rm BBN} = (\rho_{\rm r}(\eta_{\rm end})/\rho_{\rm r}(\eta_{\rm BBN}))^{1/4} (\rho(\eta_{\rm BBN})/(3m_{\rm P}^2))^{1/2}$ and $\Omega_{\rm r}^{\rm end} < 1$. Eq. (2.317) directly relates the model parameters to the BBN bound. For typical parameter values, the last two terms approximately cancel each other, and the BBN bound takes the simple form

$$\frac{1}{\pi \Omega_{\rm r}^{\rm end}} \left(\frac{H}{m_{\rm P}} \right)^2 < 1. \tag{2.318}$$

As an example, the blue line in the left panel of Fig. (2.9) has $H^2/(\pi m_{\rm P}^2 \Omega_{\rm r}^{\rm end}) = 1.06 \times 10^6$, which clearly violates the condition in Eq. (2.318), while the the green line has $H^2/(\pi m_{\rm P}^2 \Omega_{\rm r}^{\rm end}) = 1.06 \times 10^{-8}$ in agreement with Eq. (2.318), as they should.

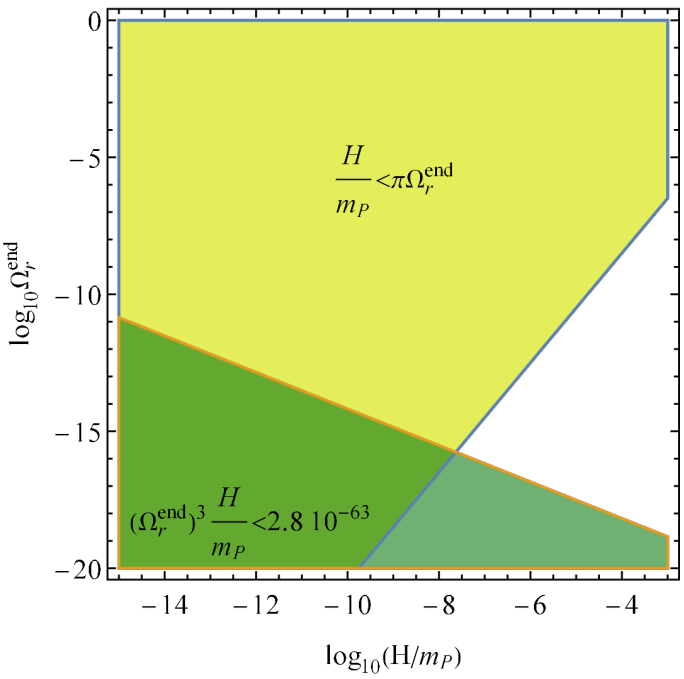

Figure 2.10: Regions in the $(H/m_{\rm P}, \Omega_{\rm r}^{\rm end})$ plane (in logarithmic units) such that the BBN bound in Eq. (2.318) is satisfied (light green) and such that the (approximate) observability condition in Eq. (2.320) is satisfied (dark green). Both conditions are met simultaneously in the locus of points where both regions intersect.

Let us estimate the parameter values needed for the spectrum to be simultaneously detected by most of the upcoming GW observations, including LISA, ET and DECIGO. Looking at Fig. (2.9), it is a good approximation to set

$f_{\rm min} = 10^{-5}\,{\rm Hz} = 2.70 \times 10^{-48} m_{\rm P}$ as the frequency such that if $f_{\rm reh} < f_{\rm min}$ the signal is observable (note that $f_{\rm reh}$ cannot be much smaller than this, otherwise the signal would have been already detected by LVK O3). We then have

$$f_{\rm reh} = \frac{1}{2\pi}\left(\frac{\Omega_{\rm r}^0 H_0^2}{\Omega_{\rm r}^{\rm end} H^2}\right)^{1/4} \Omega_{\rm r}^{\rm end} H < 2.70 \times 10^{-48} m_{\rm P} = f_{\rm min}. \tag{2.319}$$

Simplifying gives

$$(\Omega_{\rm r}^{\rm end})^3 \left(\frac{H}{m_{\rm P}}\right)^2 < 2.82 \times 10^{-63}. \tag{2.320}$$

We show the conditions in Eqs. (2.318) and (2.320) superimposed with each other in the $(H/m_{\rm P}, \Omega_{\rm r}^{\rm end})$ plane (in logarithmic units) in Fig. 2.10. It is clear that it is hard to obtain an observable signal that does not clash with the BBN bound. For this, it is needed both low-scale inflation and a small reheating efficiency. For example, for GUT-scale inflation, with $H \simeq 10^{-5} m_{\rm P}$, the signal is only observable for $\Omega_{\rm r}^{\rm end} < 10^{-17}$, while it clearly violates the BBN bound.

In the original research in Chapter 6 we propose a novel period of cosmic expansion, named hyperkination, after inflation and prior to kination. The defining property of hyperkination is that the inflaton, which still is the dominant component of the density of the Universe, is dominated by a quartic kinetic term. Such a setup can be obtained by adding an R^2 term to the gravitational action and working in the Palatini formalism (although it can also be motivated by k-essence). We find that hyperkination truncates the peak corresponding to kination, thereby making it possible to bring the spectrum within observable frequencies, without violating the BBN bound.

Chapter 3

Modified Gravity

This chapter is based on the introductory sections of the original research articles published in Physical Review D and Journal of Cosmology and Astroparticle Physics, and Galaxies [1, 2, 3] by the author, in collaboration with Konstantinos Dimopoulos, Alexandros Karam and Eemeli Tomberg.

3.1 Introduction

In this chapter we present the background material regarding modified gravity required to follow the original research in Chapters 4, 5 and 6. Our aim is to make the presentation self-consistent, without going into unnecessary detail. Modified gravity is a vast area of research and we do not attempt to give a comprehensive review.

We focus on $f(R)$ theories of gravity (for reviews see Refs. [199, 296, 297, 298, 299]), which was first studied in Ref. [300]. This means that the action now reads

$$S = \frac{m_{\rm P}^2}{2}\int \mathrm{d}^4x\sqrt{-g}f(R) + S_{\rm m}[g_{\mu\nu},\psi], \tag{3.1}$$

where f can be any function of the Ricci scalar R and ψ collectively denotes all matter fields. Note that, for $f(R) = R$, Einstein-Hilbert gravity is recovered. In Chapter 5 we focus on $f(R,\varphi)$, but the results are straightforwardly generalised.

General relativity is one of the most successful physical theories in history, having passed all experimental tests to date, so why should we consider modifications? As explained in Secs. 2.2.1 and 2.2.2, ΛCDM provides an excellent fit to the data, but it does not explain the nature of dark matter or of the inflaton field. Furthermore, the cosmological constant is subject to an extreme amount of fine tuning. Introducing quintessence in order to alleviate the cosmological constant problem also does not provide very satisfactory answers. As we saw in Sec. 2.2.4, it is difficult to endow quintessence with attractor properties without including an amount of fine tuning comparable to ΛCDM. However, could it be that general relativity provides a good description of gravity at the scales it has been put to test, but not at the scales relevant for the description of the dark components of the Universe? This possibility, coupled to the fact that questioning the gravitational theory will lead to a better understanding of it, warrants further investigation of modified theories of gravity.

Importantly, the metric formalism of general relativity is not the only possible choice. The Palatini formulation of gravity (originally introduced by Einstein [18]) has recently gained considerable popularity as an alternative to the usual metric formulation. It treats the metric and the connection as independent variables, which means that one has to vary the action with respect to both of them. For a minimally coupled scalar field and an action linear in R the two formulations result in the same equations of motion and the connection turns out to be the Levi-Civita one. However, when the field is non-minimally coupled to gravity [301, 302, 303, 304, 305, 306, 307, 308, 309, 310, 311, 312, 313, 314, 315, 316, 317, 318, 319, 320, 321, 322, 323, 324, 325, 326, 327, 328, 329, 330, 331, 332, 333, 334, 335, 336, 337, 338, 339, 340, 341, 342, 343] and/or quadratic or higher curvature terms are included [298, 344, 345, 346, 347, 348, 349, 350, 351, 352, 353, 354, 355, 356, 357, 358, 359, 360, 361, 362, 363, 364, 365, 366, 367, 2, 368, 369], significant differences arise. In the case of the non-minimal coupling, the difference can be readily seen when one transforms the Jordan frame action to the Einstein frame one. Because the Riemann tensor only depends on the connection in the Palatini formalism, this means that the Ricci

scalar (which is a contraction of the metric with the Riemann tensor) transforms differently under a Weyl transformation in the two formalisms. As a result, the scalar picks up an extra coefficient in its kinetic term which is absent in the Palatini version of the theory. Therefore, the field redefinition which renders the scalar field canonical is different and the resulting Einstein frame potential is usually flatter in the Palatini formulation. Similarly, when an αR^2 term is added to the action, the auxiliary field which is usually introduced in order to eliminate this term turns out to be non-dynamical in the Palatini formulation, in contrast to the metric version. Consequently, while the metric theory becomes two-field and therefore complicated to analyze, in the Palatini version the auxiliary field can be eliminated through its equation of motion and the resulting action is single-field, albeit modified. The main modification concerns the inflaton potential which is divided by a factor that again renders it asymptotically flat.

In the present chapter we study the differences between metric and Palatini $f(R)$ gravity at the level of the gravitational action, while in Chapters 4 and 5 we include in the analysis a scalar field that acts as the inflaton and as the quintessence field, in the context of quintessential inflation.

3.2 Metric vs. Palatini formalisms

In order to obtain the gravitational field equations, we must apply the variational principle to the action in Eq. (3.1). To do so, we first need to specify what are the gravitational degrees of freedom. Typically, in the metric formalism, the only independent gravitational field is the metric and the field equations read

$$\frac{\delta S}{\delta g^{\mu\nu}} = 0. \tag{3.2}$$

Assuming metric compatibility $\nabla_\alpha g_{\mu\nu} = 0$, the connection takes the usual Levi-Civita form

$$L^\alpha_{\mu\nu} = \frac{1}{2} g^{\alpha\beta} \left(\partial_\mu g_{\beta\nu} + \partial_\nu g_{\beta\mu} - \partial_\beta g_{\mu\nu} \right). \tag{3.3}$$

However, *a priori*, there is no reason why the connection could not be an independent quantity. This is so in the Palatini formalism, where connection and metric are taken to be independent. For example, the Riemann and Ricci tensors are functionals of the connection only, *i.e.*,

$$R^{\lambda}{}_{\mu\lambda\nu}[\Gamma] = R_{\mu\nu}[\Gamma] = \partial_\lambda \Gamma^\lambda_{\mu\nu} - \partial_\nu \Gamma^\lambda_{\mu\lambda} + \Gamma^\lambda_{\lambda\rho}\Gamma^\rho_{\mu\nu} - \Gamma^\rho_{\mu\lambda}\Gamma^\lambda_{\nu\rho}, \tag{3.4}$$

while the Ricci scalar also depends on the metric via the contraction

$$R[g,\Gamma] = g^{\mu\nu}R_{\mu\nu}. \tag{3.5}$$

The field equations read

$$\frac{\delta S}{\delta g^{\mu\nu}} = 0 \quad \text{and} \quad \frac{\delta S}{\delta \Gamma^\mu_{\alpha\beta}} = 0. \tag{3.6}$$

Importantly, it is assumed that matter only couples to the metric, so that $S_{\rm m}$ does not depend on the independent connection[1]. Since the matter action generally includes covariant derivatives of the matter fields, this assumption means that the independent connections does not define parallel transport or the covariant derivative [371]. Instead, these are defined with respect to the Levi-Civita connection as

$$\nabla_\mu A^\nu = \partial_\mu A^\nu + L^\nu_{\mu\gamma} A^\gamma, \tag{3.7}$$

where A^ν is a given 4-vector and analogous expressions hold for different rank tensors. Below we use covariant derivatives with respect to the independent connection, which we denote with a bar as

$$\bar{\nabla}_\mu V^\nu = \partial_\mu V^\nu + \Gamma^\nu_{\mu\gamma} V^\gamma, \tag{3.8}$$

where V^ν is a general 4-vector, unrelated to the matter action.

For simplicity, we also assume that the theory is torsionless, meaning that the torsion tensor, defined as

$$S^\mu_{\mu\nu} \equiv \frac{1}{2}\left(\Gamma^\mu_{\alpha\beta} - \Gamma^\mu_{\beta\alpha}\right), \tag{3.9}$$

[1]Such a coupling is allowed in the metric-affine formalism [370], but this possibility lies beyond the scope of the present work.

is zero. This means that the connection is taken to be symmetric in its lower indices

$$\Gamma^{\mu}_{\alpha\beta} = \Gamma^{\mu}_{\beta\alpha}, \tag{3.10}$$

something that is *a priori* also not required.

When $f(R)$ is a linear function of R, as in general relativity, both metric and Palatini formalisms agree (this is the reason why Einstein preferred the metric formalism). However, for any other function of the Ricci scalar they do not, leading to the different theories of metric $f(R)$ gravity and Palatini $f(R)$ gravity [300].

We can first do some manipulations irrespective of the chosen formalism. Variation of Eq. (3.1) gives

$$\delta S = \frac{m_{\rm P}^2}{2}\int \mathrm{d}^4x\sqrt{-g}\left[\left(f_R R_{(\mu\nu)} - \frac{1}{2}g_{\mu\nu}f\right)\delta g^{\mu\nu} + f_R g^{\mu\nu}\delta R_{\mu\nu}\right] + \delta S_{\rm m}, \tag{3.11}$$

where parenthesis around indices indicate the symmetric part of a tensor, $f_R \equiv \partial_R f$, and

$$\delta R_{\mu\nu} = \bar{\nabla}_\lambda \delta\Gamma^{\lambda}_{\nu\mu} - \bar{\nabla}_\nu \delta\Gamma^{\lambda}_{\lambda\mu}\,, \tag{3.12}$$

which follows from elemental manipulations of Eq. (3.4) and the covariant derivative of $\delta\Gamma^{\mu}_{\alpha\beta}$ (notice that $\Gamma^{\mu}_{\alpha\beta}$ is not a tensor but $\delta\Gamma^{\mu}_{\alpha\beta}$ is). Importantly, the reader should note that, in the Palatini formalism, the covariant derivatives in Eq. (3.12) are with respect to the independent connection. Of course, in the metric formalism $\bar{\nabla}_\mu = \nabla_\mu$.

Let $I = \int \mathrm{d}^4x\sqrt{-g}f_R g^{\mu\nu}\delta R_{\mu\nu}$. Using Eq. (3.12) and integrating by parts gives

$$I = \int \mathrm{d}^4x \bar{\nabla}_\lambda(\sqrt{-g}A^\lambda) - \int \mathrm{d}^4x\left[\bar{\nabla}_\lambda(\sqrt{-g}f_R g^{\mu\nu}) - \bar{\nabla}_\gamma(\sqrt{-g}f_R g^{\gamma(\mu}\delta^{\nu)}_{\lambda}\right]\delta\Gamma^{\lambda}_{\nu\mu}, \tag{3.13}$$

where A^λ is a 4-vector given by

$$A^\lambda = f_R\left(g^{\mu\nu}\delta\Gamma^{\lambda}_{\nu\mu} - g^{\mu\lambda}\delta\Gamma^{\sigma}_{\sigma\mu}\right). \tag{3.14}$$

Using that $\bar{\nabla}_\lambda\sqrt{-g} = \partial_\lambda\sqrt{-g} - \Gamma^{\sigma}_{\lambda\sigma}$ [372], we have

$$\bar{\nabla}_\lambda(\sqrt{-g}A^\lambda) = \partial_\lambda(\sqrt{-g}A^\lambda). \tag{3.15}$$

At this point we must choose between metric and Palatini formalisms. We first cover the metric formalism, *i.e.*, $\Gamma^{\alpha}_{\mu\nu} = L^{\alpha}_{\mu\nu}$. Using Eq. (3.3), it is easy to find the variation of the Levi-Civita connection under $g_{\mu\nu} \to g_{\mu\nu} + \delta g_{\mu\nu}$ to be

$$\delta L^{\alpha}_{\mu\nu} = -\frac{1}{2}\left[g_{\gamma\mu}\nabla_{\nu}(\delta g^{\gamma\alpha}) + g_{\gamma\nu}\nabla_{\mu}(\delta g^{\gamma\alpha}) - g_{\mu\sigma}g_{\nu\rho}\nabla^{\alpha}(\delta g^{\sigma\rho})\right]. \tag{3.16}$$

Ignoring the subtleties related to finding an analogous surface term to the Gibbons-Hawking-York term [373][374] in $f(R)$ gravity (see Ref. [375] for more details), the boundary term (3.15) is set to zero. Thus,

$$\begin{aligned} I &= \int \mathrm{d}^4x\sqrt{-g}\left[\delta^{\nu}_{\lambda}g^{\mu\gamma}\nabla_{\gamma}f_R - g^{\mu\nu}\nabla_{\lambda}f_R\right]\delta L^{\lambda}_{\nu\mu} \\ &= \int \mathrm{d}^4x\sqrt{-g}\left[g_{\mu\gamma}\nabla^{\gamma}(\delta g^{\mu\nu})\nabla_{\nu}f_R - g_{\mu\nu}\nabla^{\lambda}(\delta g^{\mu\nu})\nabla_{\lambda}f_R\right] \\ &= \int \mathrm{d}^4x\sqrt{-g}\left[g_{\mu\nu}\nabla^{\sigma}\nabla_{\sigma}f_R - \nabla_{\mu}\nabla_{\nu}f_R\right]\delta g^{\mu\nu}, \end{aligned} \tag{3.17}$$

where we used Eq. (3.16) in the second step and integrated by parts in the third. Putting everything together, we arrive at the metric $f(R)$ field equations

$$f_R R_{\mu\nu} - \frac{1}{2}g_{\mu\nu}f + \left(g_{\mu\nu}\nabla^{\sigma}\nabla_{\sigma} - \nabla_{\mu}\nabla_{\nu}\right)f_R = \frac{T_{\mu\nu}}{m_{\mathrm{P}}^2}, \tag{3.18}$$

where, as usual,

$$T_{\mu\nu} = -\frac{2}{\sqrt{-g}}\frac{\delta S_{\mathrm{m}}}{\delta g^{\mu\nu}}. \tag{3.19}$$

Since matter is minimally coupled to the metric, the energy-momentum tensor is covariantly conserved

$$\nabla_{\mu}T^{\mu\nu} = 0. \tag{3.20}$$

The same result can be obtained by showing that the covariant derivative of the left-hand-side of Eq. (3.18) vanishes [376].

Taking the trace of Eq. (3.18) gives

$$f_R R - 2f + 3\nabla^{\sigma}\nabla_{\sigma}f_R = \frac{T}{m_{\mathrm{P}}^2}, \tag{3.21}$$

which shows that R is dynamically related to T, rather than algebraically as in GR, where $R = -T/m_{\mathrm{P}}^2$, or in the Palatini formalism (see below). We can find

out more about the dynamical structure of metric $f(R)$ gravity by using the Brans-Dicke representation of the theory [377, 378, 379] (see Refs. [380, 381, 382] for early works). We proceed by rewriting the action (3.1) in a dynamically equivalent form

$$S = \frac{m_{\rm P}^2}{2}\int \mathrm{d}^4x\sqrt{-g}\,[f(\chi) + f'(\chi)(R-\chi)] + S_{\rm m}[g_{\mu\nu},\psi]. \tag{3.22}$$

Variation with respect to χ gives

$$f''(\chi)(R-\chi) = 0, \tag{3.23}$$

which implies that, as long as $f''(\chi) \neq 0$, $\chi = R$. Plugging this back in Eq. (3.22) the original action is recovered. Now, making the field redefinition

$$\varphi = f'(\chi) = f_R, \tag{3.24}$$

and defining

$$V(\varphi) = \chi(\varphi)\varphi - f(\chi(\varphi)), \tag{3.25}$$

where $\chi(\varphi)$ is obtained by inverting Eq. (3.24)[2], we have that the action reads

$$S = \frac{m_{\rm P}^2}{2}\int \mathrm{d}^4x\sqrt{-g}\,[\varphi R - V(\varphi)] + S_{\rm m}[g_{\mu\nu},\psi], \tag{3.26}$$

which is a Brans-Dicke theory with Brans-Dicke parameter $\omega = 0$ [384], *i.e.*, the kinetic term of the field in the Jordan frame vanishes. The field equation are obviously equivalent to Eq. (3.18).

The action in Eq. (3.26) can be brought to the Einstein frame, where the field is minimally coupled to gravity and the gravitational action is simply given by the Einstein-Hilbert term, by performing the conformal transformation

$$g_{\mu\nu} \to \bar{g}_{\mu\nu} = \varphi g_{\mu\nu} = f_R g_{\mu\nu}. \tag{3.27}$$

The new action (see, *e.g.*, Appendix G of Ref. [385] for the transformation properties of the Ricci scalar under conformal transformations) reads

$$S = \frac{m_{\rm P}^2}{2}\int \mathrm{d}^4x\sqrt{-\bar{g}}\left[\bar{R} - \frac{3}{2\varphi^2}\bar{g}^{\mu\nu}\partial_\mu\varphi\partial_\nu\varphi - \frac{V(\varphi)}{\varphi^2}\right] + S_{\rm m}[\bar{g}_{\mu\nu}/\varphi,\psi], \tag{3.28}$$

[2]Note that $f''(\chi) \neq 0$ is a sufficient condition for $\varphi = f'(\chi)$ to be invertible. A necessary condition is that $f'(R)$ be continuous and one-to-one [383].

where barred quantities are in terms of the Einstein frame metric (3.27) (note that the *a priori* independent connection is the Levi-Civita connection in the Einstein frame). Finally, performing the field redefinition

$$\frac{\mathrm{d}\phi}{\mathrm{d}\varphi} = \sqrt{\frac{3}{2}}\frac{m_{\mathrm{P}}}{\varphi} \quad \Rightarrow \quad \varphi = e^{\sqrt{\frac{2}{3}}\frac{\phi}{m_{\mathrm{P}}}} \tag{3.29}$$

gives

$$S = \int \mathrm{d}^4x\sqrt{-\bar{g}}\left[\frac{m_{\mathrm{P}}^2}{2}\bar{R} - \frac{1}{2}\bar{g}^{\mu\nu}\partial_\mu\phi\partial_\nu\phi - U(\phi)\right] + S_{\mathrm{m}}[e^{-\sqrt{\frac{2}{3}}\frac{\phi}{m_{\mathrm{P}}}}\bar{g}_{\mu\nu}, \psi], \tag{3.30}$$

where

$$U(\phi) = \frac{m_{\mathrm{P}}^2}{2}\frac{Rf_R - f}{f_R^2}, \tag{3.31}$$

where $R = R(\phi)$. In this representation, the dynamical degree of freedom is the scalar field ϕ, usually called the scalaron. It is related to the Ricci scalar via

$$\phi = m_{\mathrm{P}}\frac{3}{2}\ln f_R. \tag{3.32}$$

In conclusion, metric $f(R)$ gravity introduces an additional degree of freedom. This can be seen either from the dynamical relation between R and T in the trace equation (3.21) or from the Brans-Dicke representation of the theory (3.30).

Let us now deal with the Palatini formalism. Variation of Eq. (3.11) with respect to the metric gives

$$f_R R_{(\mu\nu)} - \frac{1}{2}g_{\mu\nu}f = \frac{T_{\mu\nu}}{m_{\mathrm{P}}^2}, \tag{3.33}$$

where the energy-momentum tensor is defined as in Eq. (3.19). We emphasize that $R_{\mu\nu}$ is given by Eq. (3.4) and is a function of the independent connection $\Gamma^\alpha_{\mu\nu}$ only, while R also depends on the metric, as shown in Eq. (3.5). Variation of Eq. (3.11) with respect to the connection gives

$$\bar{\nabla}_\lambda(\sqrt{-g}f_R g^{\mu\nu}) - \bar{\nabla}_\gamma(\sqrt{-g}f_R g^{\gamma(\mu}\delta^{\nu)}_\lambda = 0. \tag{3.34}$$

Note that the surface term, given by Eqs. (3.14)-(3.15), depends only on the gravitational field (the connection) at the boundary; it does not depend on its derivatives, as it happens in the metric formalism. Therefore, there is no need

to add a total divergence, in the sense of the Gibbons-Hawking-York term, to the action in the Palatini formalism.

We can further simplify the field equation coming from the variation with respect to the connection. Acting with δ^{λ}_{μ} on Eq. (3.34) gives

$$\bar{\nabla}_{\gamma}(\sqrt{-g}f_R g^{\gamma\mu}) = 0. \tag{3.35}$$

Thus, Eq. (3.34) is simplified to

$$\bar{\nabla}_{\lambda}(\sqrt{-g}f_R g^{\mu\nu}) = 0. \tag{3.36}$$

From this equation, we can see why when $f(R)$ is a linear function of R both Palatini and metric formalisms agree. Indeed, in such a case, $f_R = \text{const.}$ and we are left with $\bar{\nabla}_{\lambda}(\sqrt{-g}g^{\mu\nu}) = 0$, which is the definition of the Levi-Civita connection. Note that in the Palatini formalism this is a dynamical characteristic, rather than an assumption. Importantly, however, both formalisms differ when considering any other function $f(R)$ [300, 386, 387, 388, 389], as can be seen from comparing the field equations (3.18) and (3.45).

The energy-momentum tensor is again conserved with respect to the Levi-Civita connection

$$\nabla_{\mu}T^{\mu\nu} = \partial_{\mu}T^{\mu\nu} + L^{\mu}_{\mu\gamma}T^{\gamma\nu} = 0. \tag{3.37}$$

This follows from the fact that, by assumption, the matter action does not depend on the independent connection. Indeed, Eq. (3.37) follows from diffeomorphism invariance, as in the metric formalism. The same result can be show by brute force by taking the covariant derivative of the left-hand-side of the field equations (3.33) [376]. The reader should note that if the matter action was allowed to depend on the independent connection we would not recover the Einstein field equations even for $f(R) = R$, since Eq. (3.36) would acquire a new term of the form

$$H^{\alpha\beta}_{\mu} = \frac{\delta S_{\mathrm{m}}}{\delta\Gamma^{\mu}_{\alpha\beta}}, \tag{3.38}$$

leading to a different connection than the Levi-Civita one and therefore to modifications in Eq. (3.33) when plugging the connection back in the Ricci tensor.

For the FRW metric, Eq. (3.37) takes the same standard form as in GR

$$\dot{\rho} + 3H(\rho + p) = 0. \tag{3.39}$$

Taking the trace of Eq. (3.33) gives

$$f_R R - 2f = \frac{T}{m_{\rm P}^2}. \tag{3.40}$$

It is evident that this equation relates R and T algebraically, as for GR in the metric formalism. The reader should compare with the analogous equation in the metric formalism (3.21), where R is dynamically related to T. This is an indication that considering modifications to the Einstein-Hilbert action in the Palatini formalism does not lead to the introduction of additional dynamical degrees of freedom, something that can also be seen by using the Brans-Dicke representation of the theory. However, before doing so, we need to rewrite the field equations in terms of $g_{\mu\nu}$.

Let us consider the conformal transformation

$$g_{\mu\nu} \mapsto \bar{g}_{\mu\nu} = f_R g_{\mu\nu}. \tag{3.41}$$

Since $\sqrt{-\bar{g}}\bar{g}^{\mu\nu} = \sqrt{-g} f_R g^{\mu\nu}$, Eq. (3.36) simply states that the "independent" connection is compatible with $\bar{g}_{\mu\nu}$, *i.e.*,

$$\begin{aligned}
\Gamma^{\mu}_{\alpha\beta} &= \frac{1}{2}\bar{g}^{\mu\sigma}\left(\partial_\alpha \bar{g}_{\sigma\beta} + \partial_\beta \bar{g}_{\sigma\alpha} - \partial_\sigma \bar{g}_{\alpha\beta}\right) \\
&= \frac{1}{2 f_R} g^{\mu\sigma}\left[\partial_\alpha\left(f_R g_{\sigma\beta}\right) + \partial_\beta\left(f_R g_{\sigma\alpha}\right) - \partial_\sigma\left(f_R g_{\alpha\beta}\right)\right] \\
&= L^{\mu}_{\alpha\beta} + \frac{1}{2}\left[\partial_\alpha\left(\ln f_R\right)\delta^{\mu}_{\beta} + \partial_\beta\left(\ln f_R\right)\delta^{\mu}_{\alpha} + \partial^{\mu}\left(\ln f_R\right) g_{\alpha\beta}\right].
\end{aligned} \tag{3.42}$$

Since, from Eq. (3.40), R (and therefore f_R) is algebraically related to T, we have shown that the *a priori* independent connection can actually be written as the Levi-Civita connection of the metric plus some derivatives of the matter fields.

Plugging Eq. (3.42) in Eq. (3.4) we find

$$R_{\mu\nu}[\Gamma] = R_{\mu\nu}[g] + \frac{3}{2 f_R^2}\nabla_\mu f_R \nabla_\nu f_R - \frac{1}{f_R}\left(\nabla_\mu\nabla_\nu - \frac{1}{2}g_{\mu\nu}\Box\right) f_R, \tag{3.43}$$

where $R_{\mu\nu}[\Gamma]$ is given by Eq. (3.4) and $R_{\mu\nu}[g]$ is the usual Ricci tensor given by the Levi-Civita connection. Taking the trace of this equation gives

$$g^{\mu\nu}R_{\mu\nu}[\Gamma] = R[g] + \frac{3}{2f_R^2}\nabla_\mu f_R \nabla^\mu f_R + \frac{3}{f_R}\Box f_R. \tag{3.44}$$

Putting everything together back in the field equations (3.33) yields

$$\begin{aligned} R_{\mu\nu}[g] - \frac{1}{2}g_{\mu\nu}R[g] &= \frac{T_{\mu\nu}}{m_{\rm P}^2 f_R} - \frac{1}{2}g_{\mu\nu}\left(R - \frac{f}{f_R}\right) + \frac{1}{f_R}\left(\nabla_\mu\nabla_\nu - g_{\mu\nu}\Box\right) f_R \\ &- \frac{3}{2f_R^2}\left[\nabla_\mu f_R \nabla_\nu f_R - \frac{1}{2}g_{\mu\nu}\left(\nabla f_R\right)^2\right]. \end{aligned} \tag{3.45}$$

We emphasize that all quantities on the right-hand-side of this equation are a function of the matter sources, via the trace equation (3.40). We have thus eliminated the "independent" connection and obtained that Palatini $f(R)$ gravity simply changes the relation between geometry and the matter sources, via the new derivatives of the energy-momentum tensor in the right-hand-side of Eq. (3.45). Furthermore, the *a priori* independent connection behaves as an auxiliary field, rather than being a fully fledged dynamical degree of freedom.

Again, if $f(R) = R$, Eq. (3.45) reduces to GR, as expected. Note that if $T = 0$, from Eq. (3.40), we have that R (and f and f_R) is a constant[3]. Letting this constant be R_0, Palatini $f(R)$ gravity in the vacuum (or with a background of conformally invariant matter) is equivalent to GR with a cosmological constant given by

$$\Lambda = \frac{1}{2}\left(R_0 - \frac{f(R_0)}{f_R(R_0)}\right) = \frac{R_0}{4}, \tag{3.46}$$

where we have used Eq. (3.40). In this way, Eq. (3.45) is reduced to

$$G_{\mu\nu} = -\Lambda g_{\mu\nu}. \tag{3.47}$$

To conclude this section, we analyze the lack of additional degrees of freedom by studying the Brans-Dicke representation of the theory. Following the same steps as

[3]Unless $f(R) \propto R^2$. In this case, the left-hand-side of the trace equation (3.40) is identically zero and, therefore, only conformally invariant matter, which has $T = 0$, can be coupled to gravity. This is not a suitable description of low energy gravity, since matter is not generically conformally invariant and so we do not consider this case in the present work.

in Eqs. (3.22)-(3.26) we obtain that Eq. (3.1) is dynamically equivalent to

$$S = \frac{m_{\rm P}^2}{2}\int \mathrm{d}^4x\sqrt{-g}\left\{\varphi R[\Gamma] - V(\varphi)\right\} + S_{\rm m}[g_{\mu\nu},\psi]. \tag{3.48}$$

The difference betweent this equation and Eq. (3.26) is that the Ricci scalar is now a function of $\Gamma^{\mu}_{\alpha\beta}$ only. Plugging Eq. (3.44) in Eq. (3.48) and neglecting surface terms gives

$$S = \frac{m_{\rm P}^2}{2}\int \mathrm{d}^4x\sqrt{-g}\left[\varphi R + \frac{3}{2\varphi^2}g^{\mu\nu}\nabla_\mu\varphi\nabla_\nu\varphi - V(\varphi)\right], \tag{3.49}$$

where, as for the metric formalism, $\varphi = f_R$ and $V(\varphi) = \chi(\varphi)\varphi - f(\chi(\varphi))$. This is a Brans-Dicke theory with Brans-Dicke parameter $\omega = -3/2$. The field equations are obviously equivalent to Eq. (3.45). After performing a conformal transformation

$$g_{\mu\nu} \to \bar{g}_{\mu\nu} = \varphi g_{\mu\nu} = f_R g_{\mu\nu}, \tag{3.50}$$

the action in the Einstein frame reads

$$S = \int \mathrm{d}^4x\sqrt{-\bar{g}}\left[\frac{m_{\rm P}^2}{2}\bar{R} - U(\varphi)\right] + S_{\rm m}[\varphi^{-1}\bar{g}_{\mu\nu},\psi], \tag{3.51}$$

where

$$U(\varphi) = \frac{m_{\rm P}^2}{2}\frac{Rf_R - f}{f_R^2}. \tag{3.52}$$

The reader should note how the kinetic term of φ dissappears in the Einstein frame. We emphasize that $U(\varphi)$ is a function of the energy-momentum tensor, via the trace equation (3.40).

In conclusion, Palatini $f(R)$ gravity does not introduce additional dynamical degrees of freedom. This can be seen either from the algebraic relation between R and T in the trace equation (3.40) or from the Brans-Dicke representation of the theory (3.51).

Finally, it is also possible to express the Einstein equations in terms of the metric $\bar{g}_{\mu\nu} = f_R g_{\mu\nu}$ (below it is explained that this metric is the one corresponding to the Einstein frame). They read [298]

$$G_{\mu\nu}(h) = \frac{1}{m_{\rm P}^2 f_R}T_{\mu\nu} - \Lambda(T)\bar{g}_{\mu\nu}, \tag{3.53}$$

where

$$\Lambda(T) = \frac{Rf_R - f}{2f_R^2}, \tag{3.54}$$

where R and f_R are functions of the matter content, as explained above.

Chapter 4

Power-law Quintessential Inflation in Palatini $f(R)$ Gravity

This chapter is based on the original research article published in Physical Review D [1] by the author, in collaboration with Konstantinos Dimopoulos. At the time of publishing, the observational bound on the tensor-to-scalar ratio was $r < 0.056$ and is therefore used throughout the present chapter.

4.1 Introduction

Apart from employing a scalar field with a suitable potential in Einstein gravity, inflation can also be achieved by suitably modifying gravity, as was discovered early on by Starobinsky, in his seminal paper [11], where he introduced a higher-order term in the gravitational action, schematically $R + \alpha R^2$, where R is the scalar curvature (Ricci scalar) and α is a non-perturbative coupling. Even though it is possible to model primordial inflation is this way, a la Starobinsky inflation or Higgs inflation [390] for example, the task is much harder for late-time inflation. Indeed, many attempts to consider modified gravity theories, *e.g.* with a term proportional to $1/R$

in the gravitational action [198], were shown to be unstable[1] [392]. Moreover, the recent observation confirming that the speed of propagation of GWs is exactly light-speed (to precision of 15 orders of magnitude) [393], as suggested by Einstein gravity, excludes the contemplation of many otherwise motivated modifications of gravity at work in the late Universe, like the Gauss-Bonnet term [394] (see also Refs. [395, 396] for Gauss-Bonnet models in the Palatini formalism). While work still continues in this front [397], in this chapter we investigate a blended quintessential inflation model, which achieves primordial inflation via $f(R)$ gravity, but late-time inflation via a suitable scalar potential of quintessence. However, our approach cannot be clean-cut in that modifications of gravity are expected to affect the kination era, after primordial inflation, and the recent history of the Universe, after the end of the radiation era.

In metric $R + \alpha R^2$ gravity, the higher order gravity term introduces an extra degree of freedom, which can be rendered in the form of a scalar field, the scalaron. Starobinsky inflation is very successful, but if it were to be considered as part of a quintessential inflation model, the scalaron would need to survive until today and become quintessence. In this case though, experimental tests of gravity [398] cannot allow successful primordial inflation. Therefore, we consider Palatini gravity, where the $R + \alpha R^2$ model does not introduce a scalaron and the theory does not conflict with the experimental tests of gravity. The inflaton field is not the scalaron (for the latter does not exist) but it is explicitly introduced, as in conventional inflation.

However, Palatini gravity does affect our scenario. Firstly, it "flattens" the inflaton scalar potential [346, 347, 354, 358, 352] so that the desired inflationary plateau can be attained even with an originally steep scalar potential. Secondly, the theory is expected to introduce modifications to the kination period, after primordial inflation, and also in the late Universe, when the inflaton field becomes

[1]There are still many other viable models of $f(R)$ gravity in the metric formalism that successfully generate late-time acceleration, such as $f(R) = R - \mu R^p$ with $p \in (0, 1)$, originally proposed in [391].

quintessence. We investigate in detail what these effects are, considering a family of models, which is a generalised version of the original Peebles-Vilenkin quintessential inflation potential.

For the inflationary sector, we assume chaotic power-law inflation with $V(\varphi) \propto \varphi^n$, for any $n > 0$. As discussed at the end of Sec. 2.1.4, for this class of inflationary models the Planck constraints can only be satisfied if $n < 0.3$ (and $N \lesssim 32$), ruling out the historically celebrated models $n = 2$ and $n = 4$. For the quintessential sector we assume inverse-power-law quintessence, with $V(\varphi) \propto \varphi^{-q}$, for any $q > 0$. By the end of Sec. 2.2.4, we showed that, in the scaling attractor, during which the quintessence field is subdominant, imposing the observational constraints on the barotropic parameter of dark energy leads to $q < 0.1$ and a mass scale $M \simeq 10^{-12}\,\mathrm{GeV}$. In this way, these recent observations seem to undermine tracker quintessence. Of course, at present, quintessence is not subdominant anymore, so these considerations are expected to be modified when solving the full dynamics accurately. It could also be that the field overshoots the tracking regime, transiently freezing to later unfreeze, close to the present time, and approach the dominant attractor. However, this *thawing* quintessence requires an explanation for its initial condition, *i.e.*, the value at which the field freezes.

Chaotic inflation is ruled out and the tracking behaviour of inverse-power-law quintessence has to be given up, so why should we consider them? In this chapter, we rescue chaotic inflation, bringing it back within observational constraints by including a term proportional to R^2 in the gravitational action, in the Palatini formalism. We also find other attractive properties in this setup, such as a sub-Planckian field displacement, a feature that may help with radiative corrections of the potential as well as with 5-th force problems. Furthermore, we consider thawing quintessence, with the value at which the field is frozen given by the inflationary attractor.

This chapter is structured as follows. In Sec. 4.2 we introduce $R + \alpha R^2$ Palatini gravity with a scalar field and background matter/radiation, with emphasis on the

interaction between them. In Sec. 4.3, we present our family of quintessential inflation models and how they are affected by the assumed modified gravity setup, focusing on the period of primordial inflation. In Sec. 4.4, the period of kination in the context of Palatini $R + \alpha R^2$ gravity is investigated, in a way which is independent on the form of the scalar potential. To obtain concrete inflationary predictions we assume gravitational reheating, but our results are easy to reproduce when considering another, more efficient mechanism, as only the relevant number of inflationary e-folds is affected. In Sec. 4.5, we investigate quintessence in our setup and look for the amount of tuning needed to satisfy the coincidence requirement. In Sec. 4.6, we show how experimental gravity tests are not challenged by the modified gravity theory considered. Finally, we end in Sec. 4.7 with a brief discussion of our findings and our conclusions.

4.2 The Model

We work in $f(R)$ gravity with a Starobinsky term, as in [346, 347, 354]. In this way, we have

$$f(R) = R + \frac{\alpha}{2m_{\rm P}^2}R^2, \tag{4.1}$$

so that the action reads

$$S = \int \mathrm{d}^4x\sqrt{-g}\left[\frac{m_{\rm P}^2}{2}R + \frac{\alpha}{4}R^2 - \frac{1}{2}g^{\mu\nu}\nabla_\mu\varphi\nabla_\nu\varphi - V(\varphi)\right] + S_m[g_{\mu\nu},\psi]. \tag{4.2}$$

Note that, since Palatini $f(R)$ gravity does not introduce any additional dynamical degrees of freedom, we introduce the inflaton field in the action by hand. As a remark, although $S_m[g_{\mu\nu},\psi] = 0$ during inflation, we keep this term explicit in what follows since the treatment is also valid for the kination and quintessential sectors of the theory, when matter and radiation fields are present.

It is straightforward to calculate the matter dependence of the Ricci scalar. The derivatives of the $f(R)$ function read

$$f_R(R) = 1 + \frac{\alpha}{m_{\rm P}^2}R \tag{4.3}$$

and

$$f_{RR}(R) = \frac{\alpha}{m_{\rm P}^2}. \tag{4.4}$$

Taking into account the two main contributions to the energy density of the Universe come from the inflaton (or quintessence, depending on the cosmological era under consideration) and from regular pressureless mater and radiation, the energy momentum tensor can be written as, assuming the background matter and radiation behave as a perfect fluid,

$$T_{\mu\nu}^{\rm tot} = T_{\mu\nu}^{(\varphi)} + T_{\mu\nu}^{\rm B}, \tag{4.5}$$

where

$$T_{\mu\nu}^{(\varphi)} = \partial_\mu\varphi\partial_\nu\varphi - g_{\mu\nu}\left[\frac{1}{2}\partial^\alpha\varphi\partial_\alpha\varphi + V(\varphi)\right] \tag{4.6}$$

and

$$T_{\mu\nu}^{\rm B} = (\rho + p)u_\mu u_\nu + pg_{\mu\nu}, \tag{4.7}$$

where u^μ is the four-velocity of a comoving observer with respect to the fluid (so that $-1 = \eta^{\mu\nu}u_\mu u_\nu$).

It follows that the trace of the energy momentum tensor, remembering $\varphi = \varphi(t)$, reads

$$T^{\rm tot} = T^{(\varphi)} + T^{\rm B}, \tag{4.8}$$

where

$$T^{(\varphi)} = g^{\mu\nu}T_{\mu\nu}^{(\varphi)} = -\partial^\alpha\varphi\partial_\alpha\varphi - 4V(\varphi) = \dot{\varphi}^2 - 4V(\varphi), \tag{4.9}$$

where in the last equation we have taken φ as homogeneous, and

$$T^{\rm B} = g^{\mu\nu}T_{\mu\nu}^{\rm B} = -\rho + 3p = -\rho(1 - 3w), \tag{4.10}$$

where ρ and p are the density and the pressure of the background perfect fluid respectively, and $w \equiv p/\rho$ is its barotropic parameter.

Assuming the Universe is filled up with radiation ($w_{\rm r} = 1/3$) and pressureless matter ($w_{\rm m} = 0$) we have

$$T^{\rm B} = -\rho_{\rm m}. \tag{4.11}$$

Thus, Eq. (3.40) reads

$$\begin{aligned} f_R R - 2f &= \left(1 + \frac{\alpha}{m_{\rm P}^2} R\right) R - 2R - \frac{\alpha}{m_{\rm P}^2} R^2 = -R \\ &= \frac{1}{m_{\rm P}^2}\left(-\rho_{\rm m} + \dot{\varphi}^2 - 4V(\varphi)\right). \end{aligned} \tag{4.12}$$

The curvature scalar is then obtained as a function of the matter content of the Universe as

$$R = \frac{1}{m_{\rm P}^2}\left(\rho_{\rm m} - \dot{\varphi}^2 + 4V(\varphi)\right). \tag{4.13}$$

Depending on the cosmological era under consideration, some approximations can be made to simplify Eq. (4.13). During slow-roll inflation $\rho_{\rm m} = 0$ and $\dot{\varphi}^2 \ll V(\varphi)$ so that the Ricci scalar reads

$$R_{\rm SR} = \frac{4}{m_{\rm P}^2} V(\varphi). \tag{4.14}$$

During kination, remembering the inflaton is kinetically dominated $\dot{\varphi}^2 \gg V(\varphi)$ and the other contribution to the energy-momentum tensor is radiation, which is traceless, we have

$$R_{\rm kin} = -\frac{\dot{\varphi}^2}{m_{\rm P}^2}. \tag{4.15}$$

During the radiation dominated era, $\rho_{\rm r} \gg \rho^{(\varphi)} = \frac{1}{2}\dot{\varphi}^2 + V(\varphi)$. However, since the energy-momentum tensor of a perfect fluid with $w = 1/3$ is traceless, we have

$$R_{\rm RD} = \frac{1}{m_{\rm P}^2}(-\dot{\varphi}^2 + 4V(\varphi)). \tag{4.16}$$

At reheating, the moment at which radiation becomes the dominant component in the Universe, the field is still in free fall as during kination (see below), so that we still have $R_{\rm RD} \simeq -\dot{\varphi}^2/m_{\rm P}^2$. However, not long after reheating, the field stops and

freezes (see Eq. (4.148) below), so that $R_{\rm RD} \simeq 4V(\varphi)/m_{\rm P}^2$, which is extremely small since $V \sim 10^{-120} m_{\rm P}^4$ because of the coincidence requirement (see below).

During the matter dominated era, the Ricci scalar reads

$$R_{\rm MD} = \frac{\rho_{\rm m}}{m_{\rm P}^2}. \tag{4.17}$$

Note also that during this era the energy density of the quintessence field is $\rho \simeq V(\varphi)$ since it stops its roll-down the potential and freezes during the radiation dominated era, as explained above.

During the quintessence era, the Ricci scalar still obeys Eq. (4.13). However, we consider thawing quintessence (see below), which means the inflaton is only starting to unfreeze today, so that

$$R_{\rm quin} = \frac{1}{m_{\rm P}^2}\left(\rho_{\rm m} + 4V(\varphi)\right). \tag{4.18}$$

Finally, in vacuum, where $T_{\mu\nu} = 0$, we have

$$R_{\rm vac} = 0. \tag{4.19}$$

It is interesting that Palatini $f(R)$ gravity with a Starobinski term does not lead to gravity-driven inflation [369], as in its metric $f(R)$ counterpart. As explained in Chapter 3, Palatini $f(R)$ theories do not introduce a new degree of freedom and the change in the gravitational dynamics (compared to conventional GR) can be interpreted as a change in the matter sources. In this way, when $\rho_{\rm m} = \rho_{\rm r} = 0$, we re-obtain the conventional Friedmann equation with $H = 0$, and inflation does not take place in the absense of an inflaton field. If we do introduce a minimally coupled scalar field φ in Palatini $f(R)$ gravity with a Starobinsky term, the standard inflationary dynamics (in the Jordan frame) is not affected when the inflaton is in the slow-roll regime [368] at the level of the background evolution. However, the generation of perturbations, which is behind the inflationary observables, is indeed affected.

Following the procedure through which we obtained the action in Eq. (3.22), the

action in Eq. (4.2) is dynamically equivalent to

$$\begin{aligned} S &= \int \mathrm{d}^4x\sqrt{-g}\left[\frac{1}{2}m_{\rm P}^2\left(1+\frac{\alpha}{m_{\rm P}^2}\chi\right)R-\frac{1}{4}\alpha\chi^2-\frac{1}{2}(\nabla\varphi)^2-V(\varphi)\right] \\ &+ S_m[g_{\mu\nu},\psi]. \end{aligned} \tag{4.20}$$

We emphasize that the original action in Eq. (4.2) can be obtained by imposing the constraint on the auxiliary field

$$\frac{\delta S}{\delta\chi}=0 \tag{4.21}$$

in the action in Eq. (4.20).

We now perform a conformal transformation[2]

$$g_{\mu\nu}\rightarrow\bar{g}_{\mu\nu}=f'(\chi)g_{\mu\nu}=\left(1+\frac{\alpha}{m_{\rm P}^2}\chi\right)g_{\mu\nu}, \tag{4.22}$$

so that

$$\begin{aligned} \mathrm{d}\bar{t} &= \sqrt{f'(\chi)}\mathrm{d}t \\ \bar{a}(\bar{t}) &= \sqrt{f'(\chi)}a(t). \end{aligned} \tag{4.23}$$

After some algebra, the action in the Einstein frame can be found to be

$$\begin{aligned} S &= \int \mathrm{d}^4x\sqrt{-\bar{g}}\left[\frac{1}{2}m_{\rm P}^2\bar{R}-\frac{1}{2}\frac{m_{\rm P}^2(\bar{\nabla}\varphi)^2}{(m_{\rm P}^2+\alpha\chi)}-\frac{m_{\rm P}^4(V(\varphi)+\frac{\alpha}{4}\chi^2)}{(m_{\rm P}^2+\alpha\chi)^2}\right] \\ &+ S_m[(f'(\chi))^{-1}\bar{g}_{\mu\nu},\psi], \end{aligned} \tag{4.24}$$

where barred quantities are calculated using the Einstein frame metric given by Eq. (4.22). Note the new coupling between χ and the matter fields in the matter action. Now, imposing the condition in Eq. (4.21) on the auxiliary field χ, we have

$$\chi=\frac{4V(\varphi)+(\bar{\nabla}\varphi)^2}{m_{\rm P}^2-\frac{\alpha}{m_{\rm P}^2}(\bar{\nabla}\varphi)^2}, \tag{4.25}$$

which implies that

$$f'(\chi(\varphi))=\frac{m_{\rm P}^4+4\alpha V(\varphi)}{m_{\rm P}^4-\alpha(\bar{\nabla}\varphi)^2}. \tag{4.26}$$

[2]As opposed to $f(R)$ gravity in the metric formalism, the Ricci tensor now only depends on the connection, so that it does not transform under the conformal transformation in Eq. (4.22).

Substituting back in the action in Eq. (4.24), one obtains

$$\begin{aligned} S &= \int \mathrm{d}^4x\sqrt{-\bar{g}}\left[\frac{1}{2}m_{\rm P}^2\bar{R} - \frac{\frac{1}{2}(\bar{\nabla}\varphi)^2}{1+\frac{4\alpha}{m_{\rm P}^4}V(\varphi)} - \frac{V(\varphi)}{1+\frac{4\alpha}{m_{\rm P}^4}V(\varphi)} + \frac{\alpha}{4m_{\rm P}^4}\frac{(\bar{\nabla}\varphi)^2(\bar{\nabla}\varphi)^2}{1+\frac{4\alpha}{m_{\rm P}^4}V(\varphi)}\right] \\ &+ S_m\left[(f'(\varphi))^{-1}\bar{g}_{\mu\nu},\psi\right], \end{aligned} \tag{4.27}$$

where $(f'(\varphi))^{-1}$ is given by Eq. (4.26) and the prime denotes a derivative with respect to $\chi = \chi(\varphi)$.

Since we study the behaviour of the inflaton during slow-roll and of quintessence today, when its potential is becoming shallow, higher than quadratic powers of $\bar{\nabla}\varphi$ are not expected to play a role. Furthermore, it can be shown [368] that during a kinetic energy dominated era, such a kination, the kinetic energy of the inflaton (in the Jordan frame) is bounded as

$$\frac{1}{2}\dot{\varphi}^2 < \frac{m_{\rm P}^4}{2\alpha}. \tag{4.28}$$

As it is shown below, during kination the kinetic term in the action is canonical to a very good approximation (since the potential is negligible compared to $m_{\rm P}^4$ during this epoch). This means the canonical field in the Einstein frame ϕ is equal to the canonical field in the Jordan frame φ. Therefore, Eq. (4.28) holds in the Einstein frame during kination and the quartic kinetic term in Eq. (4.27) is negligible compared to the quadratic kinetic term, in the same way as it is during slow-roll inflation and during the quintessence tail. Thus, this term is ignored in what follows.

4.2.1 Coupling to Matter

The conformal transformation in Eq. (4.22) introduces a coupling between the field φ and the matter action in the Einstein frame, as can be seen in, *e.g.*, Eq. (4.27). In this section we investigate the effects of such coupling.

The relation between the energy-momentum tensor in the Jordan and in the Einstein frames reads (remember barred quantities correspond to the Einstein frame

while unbarred quantities correspond to the Jordan frame)

$$\bar{T}^{\rm B}_{\mu\nu} = -\frac{2}{\sqrt{-\bar{g}}}\frac{\delta S_m}{\delta \bar{g}^{\mu\nu}} = -\frac{2}{\sqrt{-\bar{g}}}\frac{\partial g^{\alpha\beta}}{\partial \bar{g}^{\mu\nu}}\frac{\delta S_m}{\delta g^{\alpha\beta}} = \frac{f'(\varphi)}{(f'(\varphi))^2}\left(-\frac{2}{\sqrt{-g}}\frac{\delta S_m}{\delta g^{\mu\nu}}\right) = \frac{1}{f'(\varphi)}T^{\rm B}_{\mu\nu}, \tag{4.29}$$

where we have used

$$\frac{\partial g^{\alpha\beta}}{\partial \bar{g}^{\mu\nu}} = f'(\varphi)\delta^{\alpha}_{\mu}\delta^{\beta}_{\nu} \tag{4.30}$$

and

$$\sqrt{-\bar{g}} = (f'(\varphi))^2\sqrt{-g}, \tag{4.31}$$

which follow from Eq. (4.22). Following Refs. [198, 399], it is then convenient to define the energy-momentum tensor for a perfect fluid in the Einstein frame as

$$\bar{T}^{\rm B}_{\mu\nu} = (\bar{\rho}+\bar{p})\bar{u}_{\mu}\bar{u}_{\nu} + \bar{p}\bar{g}_{\mu\nu}, \tag{4.32}$$

where, comparing with Eq. (4.7) and using Eq. (4.29),

$$\begin{aligned} \bar{u}_{\mu} &= \sqrt{f'(\varphi)}u_{\mu}, \\ \bar{\rho} &= \frac{\rho}{(f'(\varphi))^2}, \\ \bar{p} &= \frac{p}{(f'(\varphi))^2}. \end{aligned} \tag{4.33}$$

During inflation, $S_m[g_{\mu\nu},\psi] = 0$, and so the new coupling in the matter action between φ and the matter fields does not change the dynamics. However, after inflation ends and the Universe is reheated, the matter action is not zero anymore. Indeed, the equation of motion for the inflaton field now reads

$$\frac{\delta S}{\delta \varphi} + \frac{\delta S_m}{\delta \varphi} = 0, \tag{4.34}$$

where the result of the first term depends on the specific form the potential takes.

Let us investigate the second term. We have

$$\begin{aligned} \frac{\delta S_m}{\delta \varphi} = \frac{\partial g^{\mu\nu}}{\partial \varphi}\frac{\delta S_m}{\delta g^{\mu\nu}} = f'_{\varphi}(\varphi)\bar{g}^{\mu\nu}\left(-\frac{1}{2}\sqrt{-g}T^{\rm B}_{\mu\nu}\right) &= \frac{f'_{\varphi}(\varphi)}{f'(\varphi)}\bar{g}^{\mu\nu}\left(-\frac{1}{2}\sqrt{-\bar{g}}\bar{T}^{\rm B}_{\mu\nu}\right) \\ &= -\frac{f'_{\varphi}(\varphi)}{2f'(\varphi)}\sqrt{-\bar{g}}\bar{T}^{\rm B}, \end{aligned} \tag{4.35}$$

where $f'_\varphi = \partial f'/\partial\varphi$ (recall that the prime denotes derivative with respect to $\chi(\varphi)$) and we have used Eqs. (4.22) and (4.29)-(4.31).

Analogously to Eq. (4.10), the trace of the energy-momentum tensor in the Einstein frame reads

$$\bar{T}^{\rm B} = \bar{g}^{\mu\nu}\bar{T}^{\rm B}_{\mu\nu} = -\bar{\rho} + 3\bar{p} = -\bar{\rho}(1 - 3\bar{w}), \tag{4.36}$$

where $\bar{w} = \bar{p}/\bar{\rho}$ is the barotropic parameter of the background perfect fluid. Note that Eq. (4.33) implies the barotropic parameter is the same in both the Jordan and Einstein frames. Indeed,

$$\bar{w} = \frac{\bar{p}}{\bar{\rho}} = \frac{p}{\rho} = w. \tag{4.37}$$

Furthermore, the prefactor in the right-hand-side of Eq. (4.35) reads, from Eq. (4.26),

$$\frac{f'_\varphi(\varphi)}{f'(\varphi)} = \frac{4\alpha}{m_{\rm P}^4}\frac{\partial V}{\partial\varphi}\frac{1}{1 + \frac{4\alpha}{m_{\rm P}^4}V(\varphi)}. \tag{4.38}$$

Putting everything together, we finally have

$$\frac{\delta S_m}{\delta\varphi} = \sqrt{-\bar{g}}\frac{2\alpha}{m_{\rm P}^4}\frac{\partial V(\varphi)}{\partial\varphi}\frac{\bar{\rho}(1 - 3\bar{w})}{1 + \frac{4\alpha}{m_{\rm P}^4}V(\varphi)}. \tag{4.39}$$

It immediately follows that during the radiation dominated epoch ($\bar{w} = 1/3$)

$$\frac{\delta S_m}{\delta\varphi}\Big|_{\rm RD} = 0, \tag{4.40}$$

and the dynamics of φ is unaffected by the new coupling in the matter action. Likewise, during kination, although the dominant contribution to the energy density of the Universe is that of the inflaton and the barotropic parameter of the Universe is $\bar{w} = 1$, the only other matter field present during this epoch is radiation, so that $\bar{w} = 1/3$ in Eq. (4.39) and the dynamics of the inflaton during kination is also unaffected.

As a remark, below is defined a new canonical field ϕ which is identified as the inflaton. Obtaining its equation of motion

$$\frac{\delta S}{\delta\phi} + \frac{\delta S_m}{\delta\phi} = 0 \tag{4.41}$$

is straightforward by simply using the chain rule

$$\frac{\delta S_m}{\delta \phi} = \frac{\mathrm{d}\varphi}{\mathrm{d}\phi}\frac{\delta S_m}{\delta \varphi}. \tag{4.42}$$

Finally, it has been explained above (see Eqs. (3.53)-(3.54)) that the Einstein equations in the Einstein frame read

$$\bar{G}_{\mu\nu} = \frac{1}{m_{\rm P}^2 f'(T)} T_{\mu\nu} - \frac{R(T)f'(T) - f(T)}{2(f'(T))^2}\bar{g}_{\mu\nu}, \tag{4.43}$$

where the Ricci scalar and the function $f'(R)$ depend on the matter content of the specific cosmological epoch under consideration.

4.3 The Inflationary Sector

After the general treatment of the action given in the previous sections, we fix $V(\varphi)$ to be a generalised version of the Peebles-Vilenking potential [15], given by

$$V(\varphi) = \begin{cases} \frac{\lambda^n}{m_{\rm P}^{n-4}}(\varphi^n + M^n), & \varphi < 0 \\ \frac{\lambda^n}{m_{\rm P}^{n-4}}\frac{M^{n+q}}{\varphi^q + M^q}, & \varphi \geq 0, \end{cases}$$

where λ is a dimensionless constant fixed by the inflationary observables and $0 < M \ll m_{\rm P}$ is a suitable energy scale that is fixed by requiring that the potential energy density of the inflaton (see below) at its frozen value ϕ_F corresponds to the vacuum energy density measured today (coincidence requirement). The parameters n and q are of order unity. We will consider integer values of n and q to facilitate our analytic treatment, but this is strictly speaking not necessary, as we elaborate in the discussion section. The original potential of Ref. [15] is recovered when $n = q = 4$. Remember, as we have said above, that $S_m[g_{\mu\nu}, \psi] = 0$ during inflation.

The kinetic term in the action (4.27), when $|\varphi| \gg M$, reads

$$\frac{\frac{1}{2}(\bar{\nabla}\varphi)^2}{1 + \frac{4\alpha}{m_{\rm P}^4}V(\varphi)} \simeq \frac{\frac{1}{2}(\bar{\nabla}\varphi)^2}{1 + \frac{4\alpha\lambda^n}{m_{\rm P}^n}\varphi^n}. \tag{4.44}$$

It can be made canonical by means of the transformation

$$\mathrm{d}\phi = \frac{\mathrm{d}\varphi}{\sqrt{1 + \frac{4\alpha\lambda^n}{m_{\rm P}^n}\varphi^n}} = \frac{m_{\rm P}}{\lambda(4\alpha)^{1/n}}\frac{\mathrm{d}x}{\sqrt{1+x^n}}, \tag{4.45}$$

where we have defined

$$x \equiv \frac{\lambda(4\alpha)^{1/n}\varphi}{m_{\rm P}} \tag{4.46}$$

and ϕ can be identified as the canonical inflaton. For now it is not necessary to obtain $\phi = \phi(x)$. We only need

$$\frac{{\rm d}x}{{\rm d}\phi} = \frac{\lambda(4\alpha)^{1/n}}{m_{\rm P}}\sqrt{1+x^n}. \tag{4.47}$$

The potential in the Einstein frame reads

$$\bar{V} = \frac{V(\varphi)}{1+\frac{4\alpha}{m_{\rm P}^4}V(\varphi)} = \frac{\lambda^n\varphi^n/m_{\rm P}^{n-4}}{1+\frac{4\alpha\lambda^n}{m_{\rm P}^n}\varphi^n} = \frac{m_{\rm P}^4}{4\alpha}\frac{x^n(\phi)}{1+x^n(\phi)}. \tag{4.48}$$

The slow-roll parameters are calculated in terms of the canonical field ϕ, so that

$$\epsilon_V = \frac{1}{2}m_{\rm P}^2\left(\frac{\bar{V}'(\phi)}{\bar{V}(\phi)}\right)^2 = \frac{1}{2}\frac{m_{\rm P}^2}{\bar{V}^2(x)}\left(\frac{{\rm d}x}{{\rm d}\phi}\frac{\partial\bar{V}(x)}{\partial x}\right)^2 = \frac{1}{2}\lambda^2(4\alpha)^{2/n}n^2\frac{1}{x^2(1+x^n)}, \tag{4.49}$$

where from now on the prime denotes a derivative with respect to ϕ, and

$$\begin{aligned}\eta_V = m_{\rm P}^2\frac{\bar{V}''(\phi)}{\bar{V}(\phi)} &= \frac{m_{\rm P}^2}{\bar{V}(x)}\frac{{\rm d}x}{{\rm d}\phi}\frac{\rm d}{{\rm d}x}\left(\frac{{\rm d}x}{{\rm d}\phi}\frac{\partial\bar{V}(x)}{\partial x}\right)\\ &= \lambda^2(4\alpha)^{2/n}\frac{n(n-1)-n(\frac{n}{2}+1)x^n}{x^2(1+x^n)},\end{aligned} \tag{4.50}$$

where we have used Eq. (4.47). We can now calculate the remaining number of inflationary e-folds after the cosmological scales exit the horizon as

$$\begin{aligned}N = -\frac{1}{m_{\rm P}}\int_{\phi_*}^{\phi_{\rm end}}\frac{{\rm d}\phi}{\sqrt{2\epsilon_V(\phi)}} &= -\frac{1}{\lambda^2 n(4\alpha)^{2/n}}\int_{x_*}^{x_{\rm end}}x\,{\rm d}x\\ &= \frac{1}{2\lambda^2 n(4\alpha)^{2/n}}(x_*^2 - x_{\rm end}^2),\end{aligned} \tag{4.51}$$

where ϕ_* is the inflaton value at which the cosmological scales leave the horizon and $\phi_{\rm end}$ is the inflaton value at which inflation ends, *i.e.*, $\epsilon_V(\phi_{\rm end}) = 1$. The value of the field x at the end of inflation $x_{\rm end} \equiv x(\phi_{\rm end})$ can be obtained, using Eq. (4.49), through the condition

$$\epsilon_V(\phi_{\rm end}) = 1 \Leftrightarrow x_{\rm end}^2(x_{\rm end}^n + 1) = \frac{1}{2}\lambda^2(4\alpha)^{2/n}n^2. \tag{4.52}$$

For the typical values of λ and α we consider, and for n not too large, we have

$$|x_{\rm end}| \ll 1 \tag{4.53}$$

so that[3]

$$x_{\rm end}^2 \simeq \frac{1}{2}\lambda^2(4\alpha)^{2/n}n^2 \quad \text{for all } n. \tag{4.54}$$

The value of the field x when the cosmological scales leave the horizon $x_* = x(\phi_*)$ then reads, from Eq. (4.51),

$$x_*^2 = x_{\rm end}^2 + 2\lambda^2 n(4\alpha)^{2/n}N = 2\lambda^2 n(4\alpha)^{2/n}\left(N + \frac{n}{4}\right). \tag{4.55}$$

4.3.1 Inflationary Observables

We can constrain the parameters of our theory by imposing the observational data obtained by Plank [8], listed in Eqs. (2.132)-(2.133). As for the tensor-to-scalar ratio, it is constrained to be

$$r = \frac{A_h}{A_s} < 0.056. \tag{4.56}$$

Let us start with the curvature power spectrum. In the slow-roll approximation, which is valid at the time at which the cosmological scales exit the horizon, it reads

$$A_s = \frac{\bar{V}(\phi_*)}{24\pi^2 m_{\rm P}^4 \epsilon_V(\phi_*)} = \frac{x_*^{n+2}}{48\pi^2 n^2\lambda^2\alpha(4\alpha)^{2/n}} = \frac{2^{n/2}n^{n/2-1}}{6\pi^2}\lambda^n\left(N + \frac{n}{4}\right)^{\frac{n+2}{2}}, \tag{4.57}$$

where we have used the first Friedmann equation and Eq. (4.55) for the value of the field x at horizon exit. It follows that A_s is independent of α. Note that the total number of e-folds N depends on the specific details of the kination period. See Fig. 4.1 for graphs representing the constant λ^n for different values of n as a function

[3]In the opposite limit $|x_{\rm end}| \gg 1$, the term $n/4$ in the parenthesis in Eq. (4.55) is replaced by the complicated expression $2^{\frac{-n-4}{n+2}}n^{\frac{-n+2}{2+n}}(\lambda^2(4\alpha)^{2/n})^{\frac{-n}{2+n}}$. Using the limit $|x_{\rm end}| \gg 1$ it can be shown this expression is bounded from above by $n/4$. Taking into account that $N \gg n$ for reasonable values of n, this means that our results are insensitive to whether $|x_{\rm end}| \gg 1$ or $|x_{\rm end}| \ll 1$. However, we emphasize that, for the typical values of λ and α, $|x_{\rm end}| \ll 1$ holds.

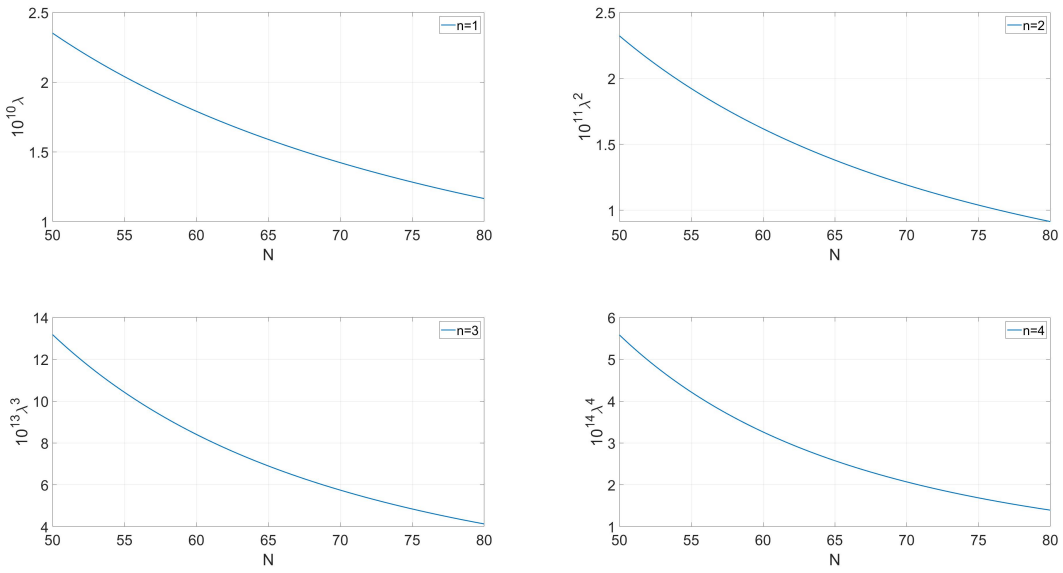

Figure 4.1: Constant λ^n for $n = 1$ (top left), $n = 2$ (top right), $n = 3$ (bottom left) and $n = 4$ (bottom right) as a function of the number of e-folds N in the range of interest for quitenssential inflation.

of the number of e-folds N. Note that in quintessential inflation, we typically have $N \in [60, 70]$.

The scalar spectral index reads

$$\begin{aligned} n_s &= 1 - 6\epsilon_V(\phi_*) + 2\eta_V(\phi_*) = 1 - \lambda^2(4\alpha)^{2/n}\frac{n(n+2) + n(n+2)x_*^n}{x_*^2(1+x_*^n)} \\ &= 1 - \lambda^2(4\alpha)^{2/n}\frac{n(n+2)}{x_*^2} = 1 - \frac{n+2}{2\left(N + \frac{n}{4}\right)}, \end{aligned} \tag{4.58}$$

where we have used Eqs. (4.49), (4.50) and (4.55). It follows that the scalar spectral index depends only on the number of e-folds (and on n) and does not depend on the parameters of the theory α, M and λ. Remember the remaining number of inflationary e-folds N depends on the details of the kination period.

Finally, the tensor-to-scalar ratio reads

$$\begin{aligned} r &= 16\epsilon_V(\phi_*) = \lambda^2(4\alpha)^{2/n}n^2\frac{8}{x_*^2(1+x_*^n)} = \frac{4n}{\left(N + \frac{n}{4}\right)(1+x_*^n)} \\ &= \frac{4n}{\left(N + \frac{n}{4}\right)}\frac{1}{\left[1 + 4(2n)^{n/2}\lambda^n\alpha\left(N + \frac{n}{4}\right)^{n/2}\right]}, \end{aligned} \tag{4.59}$$

where we have used Eq. (4.55).

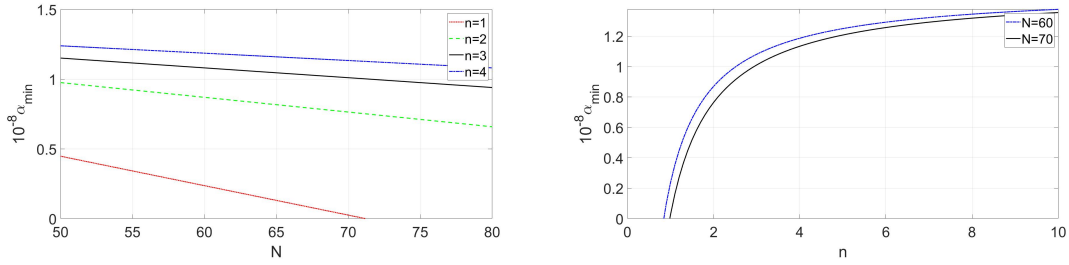

Figure 4.2: Left: Lower bound on α as a function of the number of e-folds N for $n = 1$ (red dotted line), $n = 2$ (green dashed line), $n = 3$ (black solid line) and $n = 4$ (blue dash-dot line) obtained by imposing $r = 0.056$. The lower bound is roughly $\alpha \sim 10^8$ for all values of n for the typical number of e-folds in quintessential inflation models $N \in [60, 70]$. Right: Lower bound on α as a function of n for $N = 60$ (blue dash-dot line) and $N = 70$ (black solid line), obtained by imposing $r = 0.056$. The bound quickly becomes insensitive to the specific value of n taken, independently of the number of e-folds within the range of interest in quintessential inflation.

To better understand the role α plays in the observational bound $r < 0.056$, one can solve for λ^n in Eq. (4.57) and plug it in Eq. (4.59) to obtain

$$r = \frac{16n}{(4N+n)} \frac{1}{\left[1 + \frac{96\pi^2 n}{(4N+n)} \alpha A_s\right]}. \tag{4.60}$$

Therefore, α in terms of r reads

$$\alpha = \frac{\frac{16}{r} - \left(1 + \frac{4N}{n}\right)}{96\pi^2 A_s}. \tag{4.61}$$

This means that α can be small (of order unity) when

$$r \simeq \frac{16}{1 + \frac{4N}{n}}. \tag{4.62}$$

For $n = 2$ and taking taking into account that the existence of a kination period means that the total number of e-folds is typically within the interval $N \in [60, 70]$, α is small (of order unity) when the scalar-to-tensor ratio is approximately in the interval

$$r \in [0.113, 0.132]. \tag{4.63}$$

The 1σ bound $r < 0.056$ does not allow this, but it might be marginally allowed at 2σ, where $r < 0.114$ [8].

For $n = 1$ accompanied by a long period of kination such that $N \simeq 71$, we have

$$r = 0.055, \tag{4.64}$$

which is marginally within the 1σ bounds. See the top left panel of Fig. 4.3 for the $r - n_s$ graph in the $n = 1$ case. Note however, that we expect $N \lesssim 70$ or so, for otherwise kination lasts too long and there is danger that a spike in the spectrum of primordial GWs, corresponding to the scales which reenter the horizon during kination, threatens to destabilise Big Bang Nucleosynthesis [254].

When the tensor-to-scalar ratio takes the value given by Eq. (4.62), α can be very small (of order unity). However, as we have explained above, this in general not the case (when $n = \mathcal{O}(1)$ we have $\alpha \gtrsim 10^8$ as can be seen in Fig. 4.2). Indeed, using $N = 60$ and $A_s = 2 \times 10^{-9}$, we have the following bounds for some values of n by imposing $r < 0.056$

$$\begin{aligned} n = 2 \quad &\Rightarrow \quad \alpha > 0.87 \times 10^8 \\ n = 4 \quad &\Rightarrow \quad \alpha > 1.18 \times 10^8 \\ n = 8 \quad &\Rightarrow \quad \alpha > 1.34 \times 10^8. \end{aligned} \tag{4.65}$$

Note that α is a non-perturbative coefficient that can be much larger than unity without a problem. Note also that these bounds are a direct consequence of the observational value of the scalar power spectrum and cannot be realaxed via the choice of a suitable value of λ^n.

We end this section with a remark regarding the Lyth bound [400]. By expressing the equation of motion of the inflaton (during slow-roll) as a function of the number of e-folds, with the help of Eq. (4.60), it is straightforward to obtain the variation of the inflaton from the time at which the cosmological scales exit the horizon until the end of inflation as

$$\Delta\phi \equiv \phi_{\rm end} - \phi_* = -m_{\rm P}\sqrt{2n}\int_{N_*}^{N_{\rm end}} \frac{{\rm d}N}{\sqrt{4N + n + 96\pi^2 n\alpha A_s}}. \tag{4.66}$$

We consider two different limits. Firstly, for α at least one order of magnitude larger than A_s^{-1}, *e.g.*, the higher bound $\alpha = 10^{10}$ in Fig. 4.3, r is very small (cf. Eq. (4.60)) and the third term in the square root in Eq. (4.66) dominates. It can then be easily found that the displacement of the inflaton, taking $N_* - N_{\rm end} \simeq 70$, as is usual in quintessential inflation, reads

$$\Delta\phi \sim 0.7 m_{\rm P}. \tag{4.67}$$

Note that for arbitrarily large α, $\Delta\phi$ can be made arbitrarily small, *e.g.*, for $\alpha \sim 10^{13}$ we have $\Delta\phi \sim 10^{-2} m_{\rm P}$.

In the opposite limit, when the value of α is around the lower bound given by Eq. (4.65), all terms in the square root in Eq. (4.66) are comparable. However, the integration can easily be carried out, yielding, for $n \sim \mathcal{O}(1)$ and $N = 70$,

$$\Delta\phi \sim 6 m_{\rm P}. \tag{4.68}$$

In order to obtain the displacement of the canonical field in the Jordan frame φ, for a given n, we would need to integrate Eq. (4.45) to obtain the relation between φ and ϕ. In general it is not possible to obtain an analytic expression, except for the $n = 2$ case. This case is studied in detail below and the displacement of φ is calculated there.

4.4 Kination

4.4.1 Dynamics in the Jordan and Einstein Frames

After the inflaton reaches the value given by Eq. (4.54) and inflation ends, a new cosmological era called kination starts. During kination, the dominant contribution to the energy density of the Universe is still that of the inflaton. Furthermore, as the slope the potential becomes larger in magnitude, the inflaton becomes oblivious to the potential and its energy density is dominated by the kinetic part. Varying the action (4.2) with respect to φ we obtain the usual Klein-Gordon equation (remember

in the Jordan frame the field is minimally coupled to gravity). Thus, during kination, the equation of motion of the inflaton reads

$$\ddot{\varphi} + 3H\dot{\varphi} \simeq 0. \tag{4.69}$$

In the Palatini formalism, new effective matter sources are introduced as a consequence of the addition of the αR^2 term to the gravitational action. We can see this by calculating the 00-th component of the Einstein equations (3.45). Using Eq. (4.15) and remembering that during a kinetic dominated era the kinetic energy density of the inflaton is bounded as [368]

$$\frac{1}{2}\dot{\varphi}^2 < \frac{m_{\rm P}^4}{2\alpha}, \tag{4.70}$$

which means that

$$f_R^{-1}(R) = \left(1 - \frac{\alpha}{m_{\rm P}^4}\dot{\varphi}^2\right)^{-1} \simeq 1 + \frac{\alpha}{m_{\rm P}^4}\dot{\varphi}^2, \tag{4.71}$$

the 00-th component of the Einstein equations reads

$$3H^2 = \frac{\dot{\varphi}^2}{2m_{\rm P}^2} + \frac{6H\alpha}{m_{\rm P}^4}\dot{\varphi}\ddot{\varphi} + \frac{3\alpha}{4m_{\rm P}^6}\dot{\varphi}^4 + \frac{3\alpha^2}{m_{\rm P}^8}\dot{\varphi}^2\ddot{\varphi}(2H\dot{\varphi} - \ddot{\varphi}) - \frac{\alpha^2}{4m_{\rm P}^{10}}\dot{\varphi}^6 - \frac{6\alpha^3}{m_{\rm P}^{12}}\dot{\varphi}^4\ddot{\varphi}^2. \tag{4.72}$$

This equation can be further simplified by using Eq. (4.69) to obtain

$$\begin{aligned} 3H^2 m_{\rm P}^2 &= \frac{1}{2}\dot{\varphi}^2 - \frac{2\alpha}{m_{\rm P}^2}\ddot{\varphi}^2 + \frac{3\alpha}{4m_{\rm P}^4}\dot{\varphi}^4 - \frac{5\alpha^2}{m_{\rm P}^6}\dot{\varphi}^2\ddot{\varphi}^2 - \frac{\alpha^2}{4m_{\rm P}^8}\dot{\varphi}^6 - \frac{6\alpha^3}{m_{\rm P}^{10}}\dot{\varphi}^4\ddot{\varphi}^2 \\ &= \frac{1}{2}\dot{\varphi}^2\left[1 + \frac{3\alpha}{2m_{\rm P}^4}\dot{\varphi}^2\left(1 - \frac{\alpha}{3m_{\rm P}^4}\dot{\varphi}^2\right)\right] - \frac{2\alpha}{m_{\rm P}^2}\ddot{\varphi}^2\left[1 + \frac{5\alpha}{2m_{\rm P}^4}\dot{\varphi}^2\left(1 + \frac{6\alpha}{5m_{\rm P}^4}\dot{\varphi}^2\right)\right] \end{aligned} \tag{4.73}$$

If α is not very large, Eq. (4.70) can be strongly satisfied, especially as the kinetic energy density decreases rapidly after the end of inflation. Then, the above is reduced to

$$3H^2 m_{\rm P}^2 \simeq \frac{1}{2}\dot{\varphi}^2 - \frac{2\alpha}{m_{\rm P}^2}\ddot{\varphi}^2 \simeq \frac{1}{2}\dot{\varphi}^2\left(1 - 36\alpha\frac{H^2}{m_{\rm P}^2}\right), \tag{4.74}$$

where we also used Eq. (4.69)[4]. H is diminishing with time, so $H^2 < H_{\rm inf}^2 \sim 10^{-10} m_{\rm P}^2$. Thus, if α is not too large, the second term in the parenthesis above very

[4]Rearranging Eq. (4.74) we obtain $(\dot{\varphi}/H)^2 = 6m_{\rm P}^2 + 36\alpha\dot{\varphi}^2/m_{\rm P}^2$, where one can see that H is not zero for any finite value of α, that is the brackets in Eq. (4.74) are always positive.

soon becomes negligible compared to unity. It follows that the main contribution to the energy density of the Universe is the kinetic energy density of the inflaton

$$3H^2 m_{\rm P}^2 \simeq \frac{1}{2}\dot{\varphi}^2. \tag{4.75}$$

The following expressions immediately follow

$$\rho = \rho_\varphi = \frac{1}{2}\dot{\varphi}^2 \propto a^{-6} \Leftrightarrow w = 1 \Leftrightarrow a \propto t^{1/3} \Leftrightarrow H = \frac{1}{3t}, \tag{4.76}$$

where w is the barotropic parameter of the Universe.

We conclude that the modifications to the kination dynamics coming from the introduction of a αR^2 term in Palatini $f(R)$ gravity are subdominant and the typical situation is recovered.

Equivalent conclusions can be obtained in the Einstein frame. Indeed, close to the origin, the modified Peebles-Vilenkin potential reads

$$V(\varphi) \simeq \frac{\lambda^n M^n}{m_{\rm P}^{n-4}}, \tag{4.77}$$

so that the field redefinition (4.44) for the (non-canonical) kinetic term in the action (4.27) now reads

$$\mathrm{d}\phi = \frac{\mathrm{d}\varphi}{\sqrt{1+\frac{4\alpha\lambda^n M^n}{m_{\rm P}^n}}} \simeq \left(1 - \frac{2\alpha\lambda^n M^n}{m_{\rm P}^n}\right)\mathrm{d}\varphi, \tag{4.78}$$

where we have used that $M \ll m_{\rm P}$ and $\alpha\lambda^n \ll 1$ (see below). It follows that the kinetic term of φ is canonical to a very good approximation, *i.e.*, $\phi \simeq \varphi$. Furthermore, the coupling in the matter action does not affect the dynamics (see the discussion after Eq. (4.39)). Thus, since the inflaton is still oblivious to the potential, in the Einstein frame we have the equation

$$\ddot{\phi} + 3\bar{H}\dot{\phi} \simeq 0. \tag{4.79}$$

As for the 00-th component of the Einstein equations, from Eq. (4.43) and Eq. (4.71) we have

$$3\bar{H}^2 m_{\rm P}^2 = \frac{1}{2}\dot{\phi}^2 + \frac{3\alpha\dot{\phi}^4}{4m_{\rm P}^4} + \frac{\alpha^2\dot{\phi}^6}{2m_{\rm P}^8}. \tag{4.80}$$

where barred quantities are calculated using the metric in the Einstein frame (4.22) and dots represent $\mathrm{d}/\mathrm{d}\bar{t}$. Again, using Eq. (4.70) and $\phi \simeq \varphi$ during kination, the Friedmann equation reads, to a very good approximation,

$$3\bar{H}^2 m_{\mathrm{P}}^2 \simeq \frac{1}{2}\dot{\phi}^2. \tag{4.81}$$

4.4.2 Reheating and Number of e-folds

When there is a cosmological era after inflation with a stiff equation of state with barotropic parameter w, the number of inflationary e-folds is increased by (*cf.* Eq. (2.43))

$$\Delta N = \frac{3w-1}{3(1+w)} \ln\left(\frac{V_{\mathrm{end}}^{1/4}}{T_{\mathrm{reh}}}\right). \tag{4.82}$$

In common inflationary models, after inflation ends, the Universe is perturbately reheated when the inflaton oscillates around the minimum of its potential. It is easy to show that in this situation the effective barotropic of the Universe is $w = 0$, so that the prefactor in Eq. (4.82) is $-1/3$ and the remaining e-folds of inflation are actually decreased. In contrast, during kination, the barotropic parameter of the Universe is $w = 1$ (see Eq. (4.76)), so that the prefactor is $+1/3$. Thus, the remaining number of inflationary e-folds is increased by

$$\Delta N = \frac{1}{3} \ln\left(\frac{\bar{V}^{1/4}(\phi_{\mathrm{end}})}{T_{\mathrm{reh}}}\right), \tag{4.83}$$

where T_{reh} is the temperature of the radiation bath at reheating and $\bar{V}(\phi_{\mathrm{end}})$ is the potential at the end of inflation. In this way, in what follows we consider that the remaining number of inflationary e-folds after the cosmological scales exit the horizon is given by

$$N = 60 + \Delta N. \tag{4.84}$$

The lowest value for T_{reh}, and, therefore, the highest for ΔN, is obtained through gravitational reheating (for which reheating occurs at the end of inflation $t_{\mathrm{reh}} =$

$t_{\rm end}$)[5]. For this reheating mechanism, we have obtained (see Eq. (2.304)) that

$$T_{\rm reh}^{\rm gr} \sim 10^{-2}\frac{H^2(\phi_{\rm end})}{m_{\rm P}}. \tag{4.85}$$

Assuming that the slow-roll approximation is still valid at the end of inflation, we have

$$T_{\rm reh}^{\rm gr} = 10^{-2}\frac{\bar{V}(\phi_{\rm end})}{3m_{\rm P}^3}. \tag{4.86}$$

Thus, the increase in the number of e-folds reads

$$\Delta N = \frac{1}{3}\ln\left(\frac{3m_{\rm P}^3\bar{V}^{1/4}(\phi_{\rm end})}{10^{-2}\bar{V}(\phi_{\rm end})}\right) \simeq 2 + \ln\left(\frac{m_{\rm P}}{\bar{V}^{1/4}(\phi_{\rm end})}\right). \tag{4.87}$$

The potential at the end of inflation $\bar{V}(\phi_{\rm end})$ can be obtained by evaluating Eq. (4.48) at $x_{\rm end}$, given by Eq. (4.54). It reads

$$\bar{V}(\phi_{\rm end}) = \frac{m_{\rm P}^4}{4\alpha}\frac{x^n(\phi_{\rm end})}{1+x^n(\phi_{\rm end})} = \frac{m_{\rm P}^4 n^n\lambda^n}{2^{n/2}+4\alpha n^n\lambda^n}, \tag{4.88}$$

and the remaining number of e-folds is increased by

$$\Delta N = 2 + \frac{1}{4}\ln\left(\frac{2^{n/2}+4\alpha n^n\lambda^n}{n^n\lambda^n}\right). \tag{4.89}$$

Note that, by virtue of Eq. (4.53), Eq. (4.88) is simplified as

$$\bar{V}(\phi_{\rm end}) = \frac{m_{\rm P}^4 n^n\lambda^n}{2^{n/2}}, \tag{4.90}$$

so that Eq. (4.89) is simplified as

$$\Delta N = 2 + \frac{n}{4}\ln\left(\frac{\sqrt{2}}{n\lambda}\right). \tag{4.91}$$

We emphasize that Eq. (4.53), and thus the approximated expressions in Eqs. (4.90) and (4.91), only hold when we work near the lower bound for α (as we do in the present work).

[5]It is important to mention that modifications to the gravitational particle production, due to the R^2 term in the action, are possible. However, during inflation this term and the Einstein-Hilbert one are comparable. Therefore, any possible modifications are of order unity. This is why, for simplicity, we assume the dominant contribution comes from the latter. The study of particle production due to an event horizon in Palatini $f(R)$ gravity will be addressed in a future work.

From Eq. (4.58), taking into account that the remaining number of inflationary e-folds is $N = 60 + \Delta N$ we have

$$n_s = 1 - \frac{n+2}{2\left(60 + \Delta N + \frac{n}{4}\right)}. \tag{4.92}$$

At this point, in order to obtain analytical results we need to choose specific values for n.

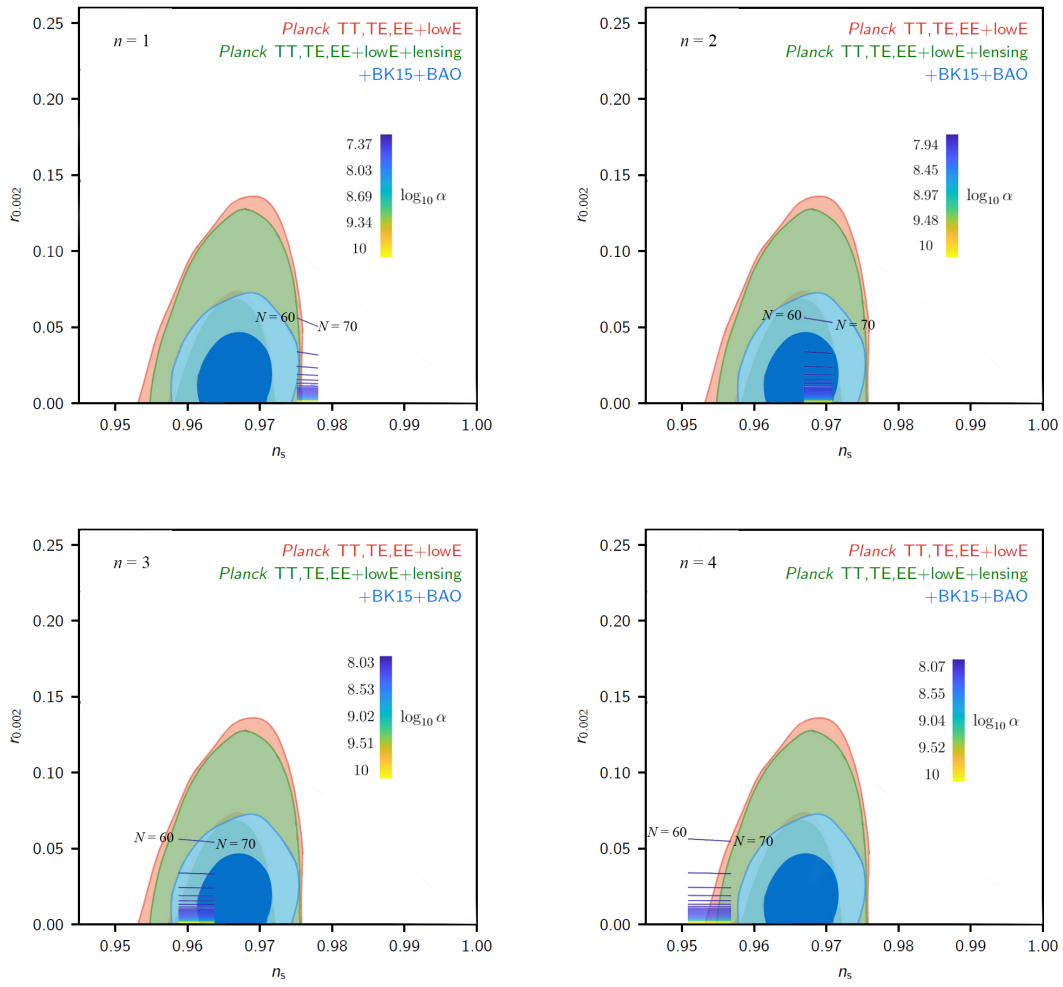

Figure 4.3: $r - n_s$ graph where the predictions derived from our model, for $n = 1$ (top left), $n = 2$ (top right), $n = 3$ (bottom left) and $n = 4$ (bottom right), are compared to the experimental data. The number of e-folds represented range from 60 (left side) to 70 (right side). The parameter α ranges from its lower bound $\alpha_{\min} = 2.36 \times 10^7$ (blue) to $\alpha = 10^{10}$ (yellow). Figure adapted from Ref. [8].

4.4.3 $n = 2$

In this section we focus on the $n = 2$ case. The potential in the Jordan frame, remembering $\varphi \gg M$ during inflation, reads

$$V(\varphi) = \lambda^2 m_{\rm P}^2 \varphi^2. \tag{4.93}$$

We can redefine the coupling constant as

$$\lambda^2 m_{\rm P}^2 \equiv \frac{1}{2} m^2, \tag{4.94}$$

where m is a suitable mass scale.

It is worth mentioning that for $n = 2$ it is possible to obtain an analytical expression for the potential in the Einstein frame. Indeed, the field redefinition (4.45) now reads

$$\mathrm{d}\phi = \frac{m_{\rm P}}{2\lambda\sqrt{\alpha}} \frac{\mathrm{d}x}{\sqrt{1+x^2}}. \tag{4.95}$$

Integrating this expression we obtain

$$\phi(x) = \frac{m_{\rm P}}{2\lambda\sqrt{\alpha}} \sinh^{-1} x \Rightarrow x(\phi) = \sinh\left(\frac{2\lambda\sqrt{\alpha}}{m_{\rm P}}\phi\right). \tag{4.96}$$

Using this in Eq. (4.48) we obtain the potential in the Einstein frame

$$\bar{V}(\phi) = \frac{m_{\rm P}^4}{4\alpha} \tanh^2\left(\frac{2\lambda\sqrt{\alpha}}{m_{\rm P}}\phi\right). \tag{4.97}$$

Choosing $n = 2$ in Eqs. (4.57)-(4.59), the inflationary observables now read

$$A_s = \frac{m^2}{24\pi^2 m_{\rm P}^2}(2N+1)^2, \tag{4.98}$$

$$n_s = 1 - \frac{4}{2N+1}, \tag{4.99}$$

and

$$r = \frac{16}{(2N+1)\left[1 + \frac{4m^2\alpha}{m_{\rm P}^2}(2N+1)\right]}, \tag{4.100}$$

where $N = 60 + \Delta N$ is the total number of inflationary e-folds. Furthermore, Eq. (4.54) now reads

$$x_{\rm end}^2 = 4\frac{m^2}{m_{\rm P}^2}\alpha, \tag{4.101}$$

while the increase in the number of e-folds is

$$\Delta N = 2 + \frac{1}{4}\ln\left(\frac{1 + 4\alpha\frac{m^2}{m_{\rm P}^2}}{\frac{m^2}{m_{\rm P}^2}}\right). \tag{4.102}$$

The above is reduced to $\Delta N = 2 + \frac{1}{2}\ln(m_{\rm P}/m)$ when $|x_{\rm end}| \ll 1$.

In order to obtain the most accurate value for ΔN, one can solve for $m^2/m_{\rm P}^2$ in Eq. (4.98) and use it in Eq. (4.102) to obtain the equation

$$\Delta N = 2 + \frac{1}{4}\ln\left[\frac{(121 + 2\Delta N)^2 + 96\alpha\pi^2 A_s}{24\pi^2 A_s}\right]. \tag{4.103}$$

Using the lower bound for alpha $\alpha \sim 8.7 \times 10^7$, given by Eq. (4.65), and the observational value for the amplitude of the scalar power spectrum, this equation can be numerically solved to obtain

$$\Delta N = 8.103 \simeq 8, \tag{4.104}$$

which means that the total number of inflationary e-folds is

$$N \simeq 68. \tag{4.105}$$

Using this result in Eq. (4.99) immediately gives

$$n_s = 0.9708, \tag{4.106}$$

which is just above the upper 1σ bound and can be easily accommodated by the 2σ bounds [8]. This can be understood as follows. From Eq. (4.99), the number of e-folds in terms of n_s reads

$$N = \frac{1}{2}\left(\frac{2}{1 - n_s} - 1\right), \tag{4.107}$$

so that the 1σ bounds correspond to

$$N \in [52, 66]. \tag{4.108}$$

Thus, the extra 6 e-folds at the upper bound could be explained by a period of kination, although $\Delta N = 8$ would be too large to be within the 1σ bounds.

The mass scale m^2 is fixed by the amplitude of the power spectrum. For $N = 68$, using Eq. (4.98), we obtain

$$\frac{m^2}{m_{\rm P}^2} \in [2.518, 2.773] \times 10^{-11}, \tag{4.109}$$

so that $m \sim 10^{-11/2} m_{\rm P} \sim 10^{13}\,\text{GeV}$. This range of values is in agreement with what was obtained in the top right panel of Fig. 4.1.

We have already obtained (see Eq. (4.65)) that as long as

$$\alpha > 8.7 \times 10^7 \tag{4.110}$$

the observational bound $r < 0.056$ is satisfied. Indeed, using the obtained values for N and m^2 and the lower bound for α in Eq. (4.100) gives

$$r \in [0.050, 0.053], \tag{4.111}$$

which is within observational bounds, as expected.

The results obtained in this subsection are summarized in the $r - n_s$ graph in the top right panel of Fig. 4.3.

We can also obtain the displacement of the canonical field in the Jordan frame φ, as was discussed at the end of Sec. 4.3.1. Using Eq. (4.96) with the obtained value for $m^2/m_{\rm P}^2$, the displacement of the inflaton field $\Delta\phi = 0.7 m_{\rm P}$, in the limit when $\alpha \sim 10^{10}$ (represented by the yellow color in the top right panel of Fig. 4.3) corresponds to

$$\Delta\varphi \sim 0.7 m_{\rm P}. \tag{4.112}$$

In this limit $\Delta\varphi$ behaves as $\Delta\phi$, in the sense that for arbitrarily large α, $\Delta\varphi$ becomes arbitrarily small. We conclude that in this regime, the potential $V(\varphi) = m^2\varphi^2/2$ belongs to the small-field class of inflationary models.

In the opposite regime, when α takes a value around its lower bound $\alpha \sim 10^8$, the displacement of the inflaton $\Delta\phi \sim 6m_{\rm P}$ (cf. Eq. (4.68)) corresponds to

$$\Delta\varphi \sim 6m_{\rm P}. \tag{4.113}$$

To end this subsection, we can verify that the approximations made above are valid. With the obtained values for m^2 and α, the value $x_{\rm end}$ at the end of inflation is

$$x_{\rm end}^2 = 4\frac{m^2}{m_{\rm P}^2}\alpha = 0.0091 \Rightarrow x_{\rm end} = 0.095, \tag{4.114}$$

and the approximation made in Eq. (4.54) is valid.

Finally, the potential (4.88) with the obtained values of m^2 and α is

$$\bar{V}(x_{\rm end}) = \frac{m^2 m_{\rm P}^2}{1 + 4\alpha\frac{m^2}{m_{\rm P}^2}} \simeq m^2 m_{\rm P}^2 \sim 2.5 \times 10^{-11} m_{\rm P}^4, \tag{4.115}$$

which is similar to the typical inflationary energy scale $V \sim 10^{-13} m_{\rm P}^4$ and in the last step we used Eq. (4.53).

4.4.4 $n = 4$

In this section we focus on the $n = 4$ case, following the same steps as in the last subsection. The potential in the Jordan frame, remembering $\varphi \gg M$ during inflation, reads

$$V(\varphi) = \lambda^4\varphi^4. \tag{4.116}$$

Choosing $n = 4$ in Eqs. (4.57)-(4.59), the inflationary observables now read

$$A_s = \frac{8}{3\pi^2}\lambda^4(N+1)^3, \tag{4.117}$$

$$n_s = 1 - \frac{3}{N+1}, \tag{4.118}$$

and

$$r = \frac{16}{(N+1)\left[1 + 256\alpha\lambda^4(N+1)^2\right]}, \tag{4.119}$$

where $N = 60 + \Delta N$ is the total number of inflationary e-folds. Furthermore, Eq. (4.54) now reads

$$x_{\rm end}^2 = 16\lambda^2\sqrt{\alpha}, \tag{4.120}$$

while the increase in the number of e-folds is

$$\Delta N = 2 + \frac{1}{4}\ln\left(\frac{1 + 256\alpha\lambda^4}{64\lambda^4}\right). \tag{4.121}$$

The above is reduced to $\Delta N = 2 - \ln\big(2\sqrt{2}\lambda\big)$ when $|x_{\rm end}| \ll 1$.

In order to obtain the most accurate value for ΔN, one can solve for λ^4 in Eq. (4.117) and use it in Eq. (4.121) to obtain the equation

$$\Delta N = 2 + \frac{1}{4}\ln\left[\frac{(61 + \Delta N)^3 + 96\alpha\pi^2 A_s}{24\pi^2 A_s}\right]. \tag{4.122}$$

Using the lower bound for alpha $\alpha \sim 1.18 \times 10^8$, given by Eq. (4.65), and the observational value for the amplitude of the scalar power spectrum, this equation can be numerically solved to obtain

$$\Delta N = 8.825 \simeq 9, \tag{4.123}$$

which means that the total number of inflationary e-folds is

$$N \simeq 69. \tag{4.124}$$

Using this result in Eq. (4.118) immediately gives

$$n_s = 0.9571, \tag{4.125}$$

which is outside the 1σ bounds but could be accommodated by the 2σ bounds [8].

Using the number of e-folds in Eq. (4.124) and the observational value for the amplitude of the scalar power spectrum, it follows from Eq. (4.117) that the value the coupling constant takes is

$$\lambda^4 \in [2.153, 2.371] \times 10^{-14}. \tag{4.126}$$

This range of values is in agreement with what was obtained in the bottom right panel of Fig. 4.1.

As for the parameter α, we have already obtained (see Eq. (4.65)) that as long as

$$\alpha > 1.18 \times 10^8, \tag{4.127}$$

the bound $r < 0.056$ is satisfied. Indeed, using the obtained values for N, λ^4 and the lower bound for α in Eq. (4.119) gives

$$r \in [0.0507, 0.0546], \tag{4.128}$$

which is within observational bounds, as expected.

The results obtained in this subsection are summarized in the $r - n_s$ graph in the bottom right panel of Fig. 4.3.

With these values for λ^4 and α, the value $x_{\rm end}$ at the end of inflation is

$$x_{\rm end}^2 = 16\lambda^2\sqrt{\alpha} = 0.026 \Rightarrow x_{\rm end} = 0.16, \tag{4.129}$$

and the approximation made in Eq. (4.54) is valid.

Finally, the potential (4.88) with the obtained values of λ^4 and α is

$$\bar{V}(x_{\rm end}) = \frac{64\lambda^4 m_{\rm P}^4}{1 + 256\alpha\lambda^4} \simeq 64\lambda^4 m_{\rm P}^4 \sim 10^{-12} m_{\rm P}^4, \tag{4.130}$$

which is similar to the typical value of the inflationary energy scale $V \sim 10^{-13} m_{\rm P}^4$ and in the last step we used Eq. (4.53).

It is important to emphasize that the results obtained above are indicative only. The parameter n can assume other order unity values, for example $n = 1$ and $n = 3$, or even non-integer values inbetween. In the top and bottom left panels of Fig. 4.3 the cases $n = 1$ and $n = 3$ are also considered. We find that the best results are obtained for $n \simeq 2 - 3$, which suggests that modelling the inflationary plateau as a power-law is a successful choice.

4.5 Quintessential Sector

We have already analysed inflation and kination in this model. In this section we focus on the positive branch of the modified Peebles-Vilenkin potential in Eq. (4.44) to study quintessence.

The kinetic term in the action (4.27) for the field φ in the Einstein frame, at large field values $\varphi \gg M$, reads

$$\frac{\frac{1}{2}(\bar{\nabla}\varphi)^2}{1+\frac{4\alpha}{m_{\rm P}^4}V(\varphi)} \simeq \frac{\frac{1}{2}(\bar{\nabla}\varphi)^2}{1+\frac{4\alpha\lambda^n}{m_{\rm P}^n}\frac{M^{n+q}}{\varphi^q}}. \tag{4.131}$$

It can be made canonical by means of the transformation

$$\mathrm{d}\phi = \frac{\mathrm{d}\varphi}{\sqrt{1+\frac{4\alpha\lambda^n}{m_{\rm P}^n}\frac{M^{n+q}}{\varphi^q}}} = \left(\frac{4\alpha\lambda^n M^{n+q}}{m_{\rm P}^n}\right)^{1/q}\frac{\mathrm{d}y}{\sqrt{1+y^{-q}}}, \tag{4.132}$$

where we have defined

$$y \equiv \left(\frac{m_{\rm P}^n}{4\alpha\lambda^n M^{n+q}}\right)^{1/q}\varphi, \tag{4.133}$$

and ϕ can be identified as the quintessence field, or, in other words, as the inflaton field at large positive values in field space.

The potential in the Einstein frame reads

$$\bar{V} = \frac{V(\varphi)}{1+\frac{4\alpha}{m_{\rm P}^4}V(\varphi)} = \frac{\lambda^n M^{n+q}/m_{\rm P}^{n-4}\varphi^q}{1+\frac{4\alpha\lambda^n}{m_{\rm P}^n}\frac{M^{n+q}}{\varphi^q}} = \frac{m_{\rm P}^4}{4\alpha}\frac{1}{y^q(\phi)+1}. \tag{4.134}$$

Note that in order to obtain an expression of the potential in terms of the inflaton $\bar{V}(\phi)$ we need to solve Eq. (4.132) to obtain $y = y(\phi)$ and then plug this result in Eq. (4.134).

4.5.1 Corrections Coming From the Matter Action

In this section we study the influence of the coupling between the inflaton and the matter action in the Einstein frame (*cf.* Eq. (4.27)), following the results obtained

in Sec. 4.2.1. After making the field redefinition given by Eq. (4.132), the equation of motion for the inflaton reads, using Eqs. (4.41), (4.42) and (4.39),

$$\ddot{\phi} + 3\bar{H}\dot{\phi} + \bar{V}'(\phi) + \frac{\mathrm{d}\varphi}{\mathrm{d}\phi}\frac{2\alpha}{m_{\mathrm{P}}^4}\frac{\partial V(\varphi)}{\partial\varphi}\frac{\bar{\rho}_{\mathrm{m}}}{1+\frac{4\alpha}{m_{\mathrm{P}}^4}V(\varphi)} = 0, \tag{4.135}$$

where we have taken into account that during this era $\bar{w} = 0$. Using Eq. (4.132), this equation can be recast as

$$\ddot{\phi} + 3\bar{H}\dot{\phi} + \bar{V}'(\phi) + \frac{2\alpha\bar{\rho}_{\mathrm{m}}}{m_{\mathrm{P}}^4}\frac{1}{\sqrt{1+\frac{4\alpha}{m_{\mathrm{P}}^4}V(\varphi)}}\frac{\partial V(\varphi)}{\partial\varphi} = 0. \tag{4.136}$$

Furthermore, the third term on the left-hand-side can be written as, using again Eqs. (4.132) and (4.134),

$$\begin{aligned}\bar{V}'(\phi(\varphi)) = \frac{\mathrm{d}\varphi}{\mathrm{d}\phi}\frac{\partial\bar{V}(\varphi)}{\partial\varphi} = \sqrt{1+\frac{4\alpha}{m_{\mathrm{P}}^4}V(\varphi)}\,\frac{\partial V(\varphi)}{\partial\varphi} \\ \times\left(\frac{1}{1+\frac{4\alpha}{m_{\mathrm{P}}^4}V(\varphi)} - \frac{4\alpha}{m_{\mathrm{P}}^4}\frac{V(\varphi)}{\left[1+\frac{4\alpha}{m_{\mathrm{P}}^4}V(\varphi)\right]^2}\right).\end{aligned} \tag{4.137}$$

Putting everything together, Eq. (4.136) now reads

$$\ddot{\phi} + 3\bar{H}\dot{\phi} + \left(1+\frac{2\alpha\bar{\rho}_{\mathrm{m}}}{m_{\mathrm{P}}^4}\right)\frac{1}{\sqrt{1+\frac{4\alpha}{m_{\mathrm{P}}^4}V(\varphi)}}\frac{\partial V(\varphi)}{\partial\varphi} - \frac{4\alpha}{m_{\mathrm{P}}^4}\frac{V(\varphi)}{\left[1+\frac{4\alpha}{m_{\mathrm{P}}^4}V(\varphi)\right]^{3/2}}\frac{\partial V(\varphi)}{\partial\varphi} = 0 \tag{4.138}$$

The second term inside the parenthesis, coming from the coupling of the inflaton in the matter action in the Einstein frame is Planck suppressed and, unless α is unrealistically large[6], is many orders of magnitude smaller than unity (see below the discussion concerning Eq. (4.190) in relation to experimental constraints). Thus, the equation of motion for the inflaton during the quitessence era reads

$$\ddot{\phi} + 3\bar{H}\dot{\phi} + \bar{V}'(\phi) \simeq 0, \tag{4.139}$$

where we have used Eq. (4.137) to combine back together the derivatives of $V(\varphi)$.

[6] $\alpha > \frac{m_{\mathrm{P}}^4}{\bar{\rho}_{\mathrm{m}}} \gtrsim \left(\frac{m_{\mathrm{P}}}{1\,\mathrm{eV}}\right)^4 \sim 10^{108}$.

We conclude the coupling in the matter action is negligible during the quintessence era and is ignored in what follows. Furthermore, note that this conclusion also holds for the matter dominated era. Indeed, the difference between both eras is that during the matter dominated era the matter energy density is the dominant contribution to the total energy density of the Universe, while during the quintessence era it is a subdominant component (accounting for $\sim 30\%$ of the total energy density). However, in both cases $\bar{w} = 0$, whether the energy density of the quintessence field dominates the Universe or not, and the second term in the parenthesis in Eq. (4.138) is negligible in both cases. Furthermore, during kination and during the radiation dominated era $\bar{w} = 1/3$, so that the coupling term (given by Eq. (4.39)) vanishes. Lastly, $S_m[g_{\mu\nu}, \psi] = 0$ during inflation. Thus, the non-minimal coupling with the inflaton in the matter action in the Einstein frame does not affect the dynamics of the inflaton throughout the whole cosmological history of the Universe.

As for the Friedmann equation in the Einstein frame, remembering $R = -T/m_{\rm P}^2$ from the trace equation (3.40), it is easy to show that Eq. (4.43) takes the form

$$3\bar{H}^2 m_{\rm P}^2 = T_{00} + \frac{\alpha T}{m_{\rm P}^4}\left(T_{00} + \frac{T}{4}\right) + \frac{\alpha^2 T^3}{2m_{\rm P}^8}, \tag{4.140}$$

where

$$T_{00} = \frac{1}{2}\dot{\phi}^2 + \bar{V}(\phi) + \rho_{\rm m} \tag{4.141}$$

and

$$T = \dot{\phi}^2 - 4\bar{V}(\phi) - \rho_{\rm m}. \tag{4.142}$$

Remember barred quantities are calculated using the metric in the Einstein frame (4.22) and dots represent $\mathrm{d}/\mathrm{d}\bar{t}$.

Working to first order in $\mathcal{O}(1/m_{\rm P}^2)$, the Friedmann equation reads

$$3\bar{H}^2 m_{\rm P}^2 \simeq T_{00} = \frac{1}{2}\dot{\phi}^2 + \bar{V}(\phi) + \rho_{\rm m} \simeq \bar{V}(\phi) + \rho_{\rm m}, \tag{4.143}$$

where in the last step we have taken into account that we work with thawing quintessence and the scalar field is only starting to roll down its potential today.

Thus, the new effective matter sources that appear due to the treatment of our $f(R)$ function in the Palatini formalism (the terms proportional to powers of α) are negligible compared to T_{00} unless α is unrealistically large, and the usual Friedmann equation is recovered.

4.5.2 Frozen Inflaton

In this section we calculate the value at which the canonically normalized field ϕ freezes after the period of kination. It is important to mention that, although there exist other reheating mechanisms, such as instant preheating [100, 259], curvaton reheating [290, 401, 291], Ricci reheating [98, 99] or considering warm quintessential inflation [258, 402, 277], in the present work we consider gravitational reheating [97, 403, 404]. The reason is twofold. First, it simplifies the calculations and allows for the reader to have a clearer picture of the mechanisms behind quintessential inflation in Palatini $f(R)$ gravity. Second, this reheating mechanism propels the field the furthest after kination, so that it freezes at a value such that the residual potential energy easily fits the observed vacuum energy density. Note that gravitational reheating corresponds to the lowest possible value for $T_{\rm reh}$, so that the increment in the number of e-folds given by Eq. (4.89) is maximised. In this way, other reheating mechanism would correspond to a lower value of ΔN and, specifically, the results obtained for $n = 2$ would be closer to the 1σ bounds for the scalar spectral index (see Eqs. (4.104)-(4.108)).

Since Eqs. (4.79) and (4.81) are the standard Klein-Gordon and Friedmann equations in the kination limit, when $\dot{\phi}^2/2 \gg \bar{V}'(\phi)$, we can use the results obtained in Sec. (2.2.5). There, we found that, for gravitational reheating, the value at which the inflaton freezes is given by

$$\phi_F = \phi_{\rm end} + \sqrt{\frac{2}{3}} m_{\rm P} \left(2 - \frac{3}{2} \ln \Omega_r^{\rm end} \right) . \tag{4.144}$$

In order to obtain an expression for the radiation density parameter at the end of inflation $\Omega_r^{\rm end}$ we remember that the density of particles created by the event

horizon in de Sitter space at the end of inflation reads

$$\rho_{\rm r}^{\rm end} = q\frac{\pi^2}{30}g_*^{\rm gr}\left(\frac{H_{\rm end}}{2\pi}\right)^4 \sim 10^{-2}H_{\rm end}^4, \tag{4.145}$$

where $q \sim 1$ and $g_*^{\rm gr} = \mathcal{O}(100)$ is the effective relativistic degrees of freedom. Dividing this expression by the Friedmann equation $\rho^{\rm end} = 3H_{\rm end}^2 m_{\rm P}^2$ gives

$$\Omega_r^{\rm end} = \frac{\rho_r^{\rm end}}{\rho^{\rm end}} \sim 10^{-2}\left(\frac{H_{\rm end}}{m_{\rm P}}\right)^2 \sim 10^{-2}\frac{V(\phi_{\rm end})}{m_{\rm P}^4}, \tag{4.146}$$

where in the last step we assumed that the slow-roll approximation is valid at the end of inflation. Plugging Eq. (4.146) in Eq. (4.144) gives

$$\phi_F = \phi_{\rm end} + \sqrt{\frac{2}{3}}m_{\rm P}\left[2 + 3\ln 10 - \frac{3}{2}\ln\left(\frac{V(\phi_{\rm end})}{m_{\rm P}^4}\right)\right]. \tag{4.147}$$

Using the obtained an expression for $V(\phi_{\rm end})$ given by Eq. (4.88) we have

$$\phi_F = \phi_{\rm end} + \sqrt{\frac{2}{3}}m_{\rm P}\left[2 + 3\ln 10 - \frac{3}{2}\ln\left(\frac{n^n\lambda^n}{2^{n/2} + 4\alpha n^n\lambda^n}\right)\right]. \tag{4.148}$$

When α takes a value close to its lower bound, using Eqs. (4.53) and (4.90), this equation is simplified as

$$\phi_F = \phi_{\rm end} + \sqrt{\frac{2}{3}}m_{\rm P}\left[2 + 3\ln 10 + \frac{3n}{2}\ln\left(\frac{\sqrt{2}}{n\lambda}\right)\right]. \tag{4.149}$$

Note that in order to obtain $\phi_{\rm end}$ we need to solve the (generally complicated) integral (4.45) and plug the resulting $x = x(\phi)$ in the equation for $x_{\rm end}$ given by (4.54). However, in most cases $\phi_{\rm end}$ is negligible compared to the second term in the right-hand-side of Eq. (4.148). To illustrate this we can choose the simplest case for which Eq. (4.45) can be solved, *i.e.*, for $n = 2$. Indeed,

$$\mathrm{d}\phi = \frac{m_{\rm P}}{\lambda(4\alpha)^{1/2}}\frac{\mathrm{d}x}{\sqrt{1+x^2}} \Rightarrow \phi = \frac{m_{\rm P}}{\lambda(4\alpha)^{1/2}}\sinh^{-1}x. \tag{4.150}$$

Thus,

$$\phi_{\rm end} = \frac{m_{\rm P}}{\lambda(4\alpha)^{1/2}}\sinh^{-1}x_{\rm end} \simeq \frac{m_{\rm P}}{\lambda(4\alpha)^{1/2}}x_{\rm end} = \sqrt{2}m_{\rm P}, \tag{4.151}$$

where we have used Eq. (4.54) and taken into account that unless $\alpha \gtrsim 10^{11}$, $|x_{\rm end}| \ll 1$. Then, remembering (see Eq. (4.109)) that inflation fixes $2\lambda^2 = m^2/m_{\rm P}^2 \sim 10^{-11}$ and taking $\alpha \sim 10^8$, the inflaton freezes at

$$\phi_F = -\sqrt{2}m_{\rm P} + \sqrt{\frac{2}{3}}m_{\rm P}\left(2 + 3\ln 10 + 15\ln 10\right) \simeq 35 m_{\rm P} \gg \phi_{\rm end}. \tag{4.152}$$

Notice that the above is a super-Planckian displacement of the canonical inflaton ϕ and not of φ, which appears in the scalar potential of this model, in Eq. (4.44).

4.5.3 Residual Potential Energy

If we were to obtain the residual potential energy for a general q we would need to solve Eq. (4.132) in order to obtain $y = y(\phi)$ and substitute it in the potential (4.134) to finally use the value at which the inflaton is frozen after kination, given by Eq. (4.148). Although Eq. (4.132) is in general difficult to solve, we can take into account that when the inflaton stops being kinetically dominated, *i.e.*, when it freezes, the potential energy has become many orders of magnitude smaller than the Plank scale (we are on the quintessential tail). In this way, we are in the regime where

$$4\alpha V(\varphi) \ll m_{\rm P}^4 \Leftrightarrow 4\alpha\lambda^n M^{n+q} \ll m_{\rm P}^n \varphi^q \Leftrightarrow y^{-q} \ll 1, \tag{4.153}$$

where we have used Eq. (4.133). Thus, Eq. (4.132) can be approximated by

$$\mathrm{d}\phi = \left(\frac{4\alpha\lambda^n M^{n+q}}{m_{\rm P}^n}\right)^{1/q}\left(1 - \frac{1}{2}y^{-q}\right)\mathrm{d}y. \tag{4.154}$$

This equation can be immediately integrated to obtain, for $q \neq 1$,

$$\phi(y) = \left(\frac{4\alpha\lambda^n M^{n+q}}{m_{\rm P}^n}\right)^{1/q} y\left(1 + \frac{1}{2(q-1)y^q}\right). \tag{4.155}$$

Raising the above to the power of q and using the approximation (4.153) again we have

$$\phi^q(y) \quad = \frac{4\alpha\lambda^n M^{n+q}}{m_{\rm P}^n}\left(y^q + \frac{q}{2(q-1)}\right). \tag{4.156}$$

Therefore, the analytical expression for $y(\phi)$, in the regime defined by Eq. (4.153), is

$$y^q(\phi) = \frac{m_{\rm P}^n \phi^q}{4\alpha\lambda^n M^{n+q}} - \frac{q}{2(q-1)}. \tag{4.157}$$

Evaluating this expression at ϕ_F and plugging it in Eq. (4.134), after some algebra, we obtain the residual potential density

$$\frac{\bar{V}(\phi_F)}{m_{\rm P}^4} = \left(\frac{m_{\rm P}^n \phi_F^q}{\lambda^n M^{n+q}} + \frac{2\alpha(q-2)}{q-1}\right)^{-1}, \tag{4.158}$$

where ϕ_F is given by Eq. (4.148). Note that for most values of α, and for $q \neq 1$, such that the limit $m_{\rm P}^n \phi_F^q \gg 2\alpha\lambda^n M^{n+q}$ holds, the potential can be approximated to first order as

$$\bar{V}(\phi_F) = \frac{\lambda^n M^{n+q}}{m_{\rm P}^{n-4}\phi_F^q}\left[1 - \frac{2(q-2)\alpha\lambda^n M^{n+q}}{(q-1)m_{\rm P}^n \phi_F^q}\right]. \tag{4.159}$$

Also note that to zeroth order this is the same as the original Peebles-Vilenkin potential [15] in the Jordan frame in the limit $\varphi \gg M$, only with φ_F replaced by ϕ_F. Of course, this was expected since we assumed the limit in Eq. (4.153) in the first place.

4.5.3.1 $q = 1$

Before calculating the residual potential energy density for specific values of n and q we focus on the special case $q = 1$. Eq. (4.154) now reads

$$\mathrm{d}\phi = \frac{4\alpha\lambda^n M^{n+1}}{m_{\rm P}^n}\left(1 - \frac{1}{2y}\right)\mathrm{d}y. \tag{4.160}$$

Integrating, we have

$$\phi = \frac{4\alpha\lambda^n M^{n+1}}{m_{\rm P}^n}\left(y - \frac{1}{2}\ln y\right). \tag{4.161}$$

It is not possible to obtain an analytic expression for $y = y(\phi)$. However, in the limit $y \gg 1$, to a good approximation

$$y(\phi) \simeq \frac{m_{\rm P}^n\,\phi}{4\alpha\lambda^n M^{n+1}}, \tag{4.162}$$

so that the residual potential energy reads

$$\bar{V}(\phi_F) \simeq \frac{\lambda^n M^{n+1}}{m_{\rm P}^{n-4}\phi_F}. \tag{4.163}$$

Note this coincides with the 0-th order approximation in Eq. (4.159). Of course, the approximation made in Eq. (4.162) is equivalent to neglecting the second term in Eq. (4.157). We can conclude that similar results to the ones obtained for a general q are obtained for $q = 1$.

4.5.4 $q = 2$ and $n = 2$

An exception for the treatment given above is $q = 2$. Note that in this case the corrections in Eq. (4.159) cancels out and the form of the potential for ϕ is the same as for the non-canonical field φ. Furthermore, an analytical expression for $y(\phi)$ can be obtained. It reads, using $n = 2$,

$$\mathrm{d}\phi = \frac{2\sqrt{\alpha}\lambda M^2}{m_{\rm P}} \frac{\mathrm{d}y}{\sqrt{1+y^{-2}}} \Rightarrow \phi = \frac{2\sqrt{\alpha}\lambda M^2}{m_{\rm P}} \sqrt{1+y^2}. \tag{4.164}$$

Solving for y we have

$$y_F^2 = \frac{m_{\rm P}^2 \phi_F^2}{4\alpha\lambda^2 M^4} - 1, \tag{4.165}$$

so that the potential at the value of the frozen inflaton reads

$$\bar{V}(\phi_F) = \frac{m_{\rm P}^4}{4\alpha} \frac{4\alpha\lambda^2 M^4}{m_{\rm P}^2\phi_F^2} = \frac{\lambda^2 M^4}{1225} \sim 10^{-14} M^4, \tag{4.166}$$

where we have used $\phi_F \simeq 35 m_{\rm P}$ (see Eq. (4.152)) and that inflation fixes $2\lambda^2 = m^2/m_{\rm P}^2 \sim 2.6 \times 10^{-11}$ (see Eq. (4.109)). Note that the residual potential energy is independent of α.

The vacuum energy density today is $\rho_0 \sim 10^{-120} m_{\rm P}^4$, so that the mass scale M is fixed to be

$$M \sim 3.5 \times 10^{-26} m_{\rm P} \sim 8.5 \times 10^{-8} \mathrm{GeV}. \tag{4.167}$$

4.5.5 $q = 4$ and $n = 2$

In this section we study the case where $q = 4$ and $n = 2$. We consider the lower bound $\alpha \sim 10^8$, the fact that inflation fixes $2\lambda^2 = m^2/m_{\rm P}^2 \sim 2.6 \times 10^{-11}$ and the value at which the inflaton freezes $\phi_F \simeq 35 m_{\rm P}$. Thus, using the approximation obtained for the potential in Eq. (4.159), we have

$$\bar{V}(\phi_F) = \frac{\lambda^2 m_{\rm P}^2 M^6}{\phi_F^4}\left(1 - \frac{4\alpha\lambda^2 M^6}{3 m_{\rm P}^2 \phi_F^4}\right) = 8.7 \times 10^{-18}\frac{M^6}{m_{\rm P}^2}\left(1 - 10^{-9}\frac{M^6}{m_{\rm P}^6}\right). \quad (4.168)$$

The residual potential energy should be comparable to the vacuum energy density today $\rho_0 \sim 10^{-120} m_{\rm P}^4$. In this way the mass scale M is fixed by

$$8.7 \times 10^{-18}\frac{M^6}{m_{\rm P}^2}\left(1 - 10^{-9}\frac{M^6}{m_{\rm P}^6}\right) = 10^{-120} m_{\rm P}^4. \quad (4.169)$$

It is straightforward to solve this quadratic equation to obtain

$$M \sim 10^{-17} m_{\rm P} \sim 10\text{GeV}. \quad (4.170)$$

4.6 Constraints Coming From Experimental Tests

$f(R)$ theories in the Palatini formalism should be treated in the same way as general relativity, in the sense that they should agree with experiments and observations on all scales in order to be viable. In this way, $f(R)$ theories proposed to explain cosmic speedup should coincide with the dynamics of the solar system and laboratory experiments. In this section we summarize the most salient results found in the literature, mainly following Ref. [298].

In scales comparable to that of the solar system, the Universe does not behave as a perfect fluid (as opposed to cosmological scales), and it makes sense to make a distinction between the interior and exterior of matter sources. Outside of matter sources $\rho_{\rm m} = 0$ and, in the thawing quintessence scenario we consider, the inflaton freezes at ϕ_F so that $V(\phi_F)$ accounts for the vacuum energy density measured today[7].

[7]Remember that during the quintessence era $\phi \simeq \varphi$ to a very good approximation (cf.

Thus, the Ricci scalar today outside of matter sources reads (cf. Eq. (4.13))

$$R_{\rm out} \equiv R(0) = \frac{4V(\phi_F)}{m_{\rm P}^2} = \text{constant}. \tag{4.171}$$

This means that the Einstein equations in the exterior of matter sources reduce to the form

$$G_{\mu\nu} = \frac{1}{m_{\rm P}^2 f_R} T_{\mu\nu} - \Lambda_{\rm eff} g_{\mu\nu}\,, \tag{4.172}$$

as suggested by Eq. (3.45) with $f_R(R) = \text{constant}$, where $T_{\mu\nu} = -g_{\mu\nu}V(\phi_F)$ and $\Lambda_{\rm eff}$ is given by Eq. (3.46)

$$\Lambda_{\rm eff} = \frac{1}{2}R_{\rm out} - \frac{1}{2}\frac{f(R_{\rm out})}{f_R(R_{\rm out})}. \tag{4.173}$$

In the above, in view of Eqs. (4.1), (4.3) and (4.171) we have

$$f(R_{\rm out}) \equiv f(0) = \frac{4V(\phi_F)}{m_{\rm P}^2} + \frac{8\alpha V^2(\phi_F)}{m_{\rm P}^6} = \frac{4V(\phi_F)}{m_{\rm P}^2}\left(1 + \frac{2\alpha V(\phi_F)}{m_{\rm P}^4}\right), \tag{4.174}$$

and

$$f_R(R_{\rm out}) \equiv f_R(0) = 1 + \frac{4\alpha V(\phi_F)}{m_{\rm P}^4}. \tag{4.175}$$

Since $V(\phi_F) \simeq 10^{-120} m_{\rm P}^4$ accounts for the vacuum energy density today and assuming that α is not unrealistically large, we have $4\alpha V(\phi_F) \ll m_{\rm P}^4$. Thus, the effective cosmological constant is simplified to

$$\Lambda_{\rm eff} \simeq \frac{2V(\phi_F)}{m_{\rm P}^2} - \frac{2V(\phi_F)}{m_{\rm P}^2}\left(1 + \frac{2\alpha V(\phi_F)}{m_{\rm P}^4}\right)\left(1 - \frac{4\alpha V(\phi_F)}{m_{\rm P}^4}\right) \simeq \frac{4\alpha V^2(\phi_F)}{m_{\rm P}^6}\,. \tag{4.176}$$

Considering the 00-component of the Einstein equations in Eq. (4.172) we obtain the Friedman equation, which reads

$$3H^2 m_{\rm P}^2 = \frac{T_{00}}{f_R} + m_{\rm P}^2\Lambda_{\rm eff} \simeq V(\phi_F)\left(1 - \frac{4\alpha V(\phi_F)}{m_{\rm P}^4}\right) + \frac{4\alpha V^2(\phi_F)}{m_{\rm P}^4} = V(\phi_F). \tag{4.177}$$

Thus, the vacuum density is $V(\phi_F)$, which is much larger than $m_{\rm P}^2\Lambda_{\rm eff}$ since

$$\frac{V(\phi_F)}{m_{\rm P}^2\Lambda_{\rm eff}} = \frac{m_{\rm P}^4}{4\alpha V(\phi_F)} \gg 1\,. \tag{4.178}$$

Eq. (4.157)). Also, we are ignoring the fact that quintessence is thawing so, technically, it is unfreezing at present, which means that it has a non-zero kinetic energy density, which, however, is subdominant $\frac{1}{2}\dot{\phi}^2 \ll V(\phi) \simeq V(\phi_F)$.

This means that $V(\phi_F)/m_{\rm P}^2$ is the "true" cosmological constant, as we assumed in the previous section, while the contribution due to Palatini gravity $m_{\rm P}^2\Lambda_{\rm eff}$ is negligible. In the following we redefine $\Lambda_{\rm eff}$ as $\Lambda_{\rm eff} = V(\phi_F)/m_{\rm P}^2$.

4.6.1 Solar System

In Chapter 3 we found (see Eq. (3.47)) that the vacuum equations of motion in Palatini $f(R)$ theories are equivalent to those of GR with a cosmological constant, given by Eq. (4.173). Furthermore, we found that in the quintessential inflation scenario with the $f(R)$ function given by

$$f(R) = R + \frac{\alpha}{2m_{\rm P}^2}R^2, \tag{4.179}$$

the equations of motion are also equivalent to those of GR with a cosmological constant, now given by $\Lambda_{\rm eff} = V(\phi_F)/m_{\rm P}^2$. It follows that, if one considers a spherically symmetric non-rotating mass distribution, such as the Sun, the metric outside is the Schwarzschild-de Sitter solution

$$\mathrm{d}s^2 = -A(r)\mathrm{d}t^2 + \frac{\mathrm{d}r^2}{A(r)} + r^2\mathrm{d}\Omega^2, \tag{4.180}$$

where $A(r) = 1 - 2GM/r - \Lambda_{\rm eff}r^2/3$, with M identified as the mass of the star and $\Lambda_{\rm eff}$ is the cosmological constant. In the vacuum case, some authors [405, 406] conclude that Palatini $f(R)$ theories are compatible with solar system observations, based on the fact that for a suitable region in the parameter space of the theory $\Lambda_{\rm eff}$ can be made small enough and predictions are virtually indistinguishable from those of the Schwarzschild solution in general relativity (which pass all experimental tests). In the quintessential inflation case, $\Lambda_{\rm eff} = V(\varphi_F)/m_{\rm P}^2$ is obviously very small and the metric effectively takes the Schwarzschild form.

However, as it is pointed out in Ref. [298], Eq. (3.45) departs from GR with an effective cosmological constant in the regions of space where R, and therefore f_R, is no longer constant (and the ∂f_R in the right-hand-side of Eq. (3.45) are no longer zero), such as in the interior of stars. In this way, the transition from the interior

to the exterior solution is, in general, not as simple as in GR, due to the modified dynamics in the interior of the sources.

We now give a brief overview of the study of the transition from the interior to the exterior solution in Palatini $f(R)$ theories. The reader is referred to Ref. [298] for further details. It is convenient to perform a conformal transformation $g_{\mu\nu} \to h_{\mu\nu} = \gamma(T) g_{\mu\nu} \equiv \frac{f_R(T)}{f_R(0)} g_{\mu\nu}$ under which Eq. (3.45) reads[8]

$$G_{\mu\nu}(h) = \frac{1}{\tilde{m}_{\rm P}^2 \gamma(T)} T_{\mu\nu} - \tilde{\Lambda}(T) h_{\mu\nu}, \tag{4.181}$$

where we have relabelled $f_{R_{\rm out}} \equiv f_R(0)$ (see Eq. (4.175)), $\tilde{m}_{\rm P}^2 = m_{\rm P}^2 f_R(0)$ and $\tilde{\Lambda}(T) = (R f_R - f)/(2 f_R(0) \gamma^2)$, so that $\tilde{\Lambda}(0) = \Lambda_{\rm eff}$.

We now focus on spherically symmetric pressureless bodies, for which an analytical solution for an arbitrary $f(R)$ can be obtained [407] by using the ansatz

$$\mathrm{d}s^2 = g_{\mu\nu} \mathrm{d}x^\mu \mathrm{d}x^\nu = \frac{1}{\gamma(T)} h_{\mu\nu} \mathrm{d}x^\mu \mathrm{d}x^\nu = \frac{1}{\gamma(T)} \left[-B(r) \mathrm{e}^{2\Phi(r)} \mathrm{d}t^2 + \frac{1}{B(r)} \mathrm{d}r^2 + r^2 \mathrm{d}\Omega^2 \right]. \tag{4.182}$$

The explicit form of $B(r)$ and $\Phi(r)$, obtained from the field equations (4.181), can be found in Ref. [407]. For our current purposes it suffices to say that both functions are well defined and provide a complete solution for a nonrotating, pressureless, spherically symmetric body. Furthermore, in the exterior of matter sources, where $\gamma(0) = 1$, the line element in Eq. (4.182) is the same as the Schwarzschild-de Sitter one given by Eq. (4.180), just by absorbing the $\mathrm{e}^{2\Phi}$ factor with a time coordinate redefinition and identifying $A(r)$ with $B(r)$. As for the interior of the body, the usual GR expressions are recovered by choosing $\gamma = 1$ and $\tilde{\Lambda} = 0$. In this way, the Newtonian limit of the general solution (4.182) can be studied. In particular, we focus on the time-time component of the metric[9]

$$g_{tt} = -\frac{1}{\gamma(T)} \left[1 - \frac{2\tilde{G} M(r)}{r} \right] \mathrm{e}^{2(\Phi(r) - \Phi_0)}. \tag{4.183}$$

[8] Note Eq. (4.181) is the same as Eq. (3.53), only with $\bar{g}_{\mu\nu}$ replaced by $h_{\mu\nu}$, $f_R(T)$ by $\gamma(T)$ and $m_{\rm P}$ by $\tilde{m}_{\rm P}$. Indeed, $\bar{g}_{\mu\nu} = f_R(0) h_{\mu\nu}$, but the Einstein tensor is invariant under constant rescalings of the metric $G_{\mu\nu}(\bar{g}) = G_{\mu\nu}(f_R(0)\bar{g})$.

[9] We have redefined $B(r) = 1 - 2\tilde{G} M(r)/r$.

The conclusions presented in Ref. [298] imply that, for a Palatini $f(R)$ theory to be viable, the function $f(R)$ has to be chosen such that $\gamma(T)$ (or $f_R(T)$) is not very sensitive to density variations over the range of densities accessible to the corresponding experiments. In other words, $\gamma(T)$ must be almost constant since then, with a simple constant rescaling of the metric, the constant $\gamma(T) \simeq \gamma_0 + \text{corrections}$ can be brought to the form $\tilde{\gamma}(T) = 1 + \text{corrections}$. This, in turn, implies that the metric has the standard form $g_{\mu\nu} = \eta_{\mu\nu} + \text{corrections}$.

From a more analytical perspective, we require that a change $\Delta\gamma$ relative to γ induced by a change $\Delta\rho$ relative to ρ must be small

$$\left|\frac{\rho}{\gamma}\frac{\partial\gamma}{\partial\rho}\right| = \left|\frac{\rho}{f_R}\frac{\partial f_R}{\partial\rho}\right| \ll 1. \tag{4.184}$$

This condition is equivalent to [408]

$$\left|\frac{\rho}{m_{\rm P}^2 R f_R}\right|\left|\frac{1}{1 - f_R/(R f_{RR})}\right| \ll 1. \tag{4.185}$$

We now have the tools to determine whether our $f(R)$ function, given by

$$f(R) = R + \frac{\alpha}{2m_{\rm P}^2}R^2, \tag{4.186}$$

satisfies Solar System bounds or not. Using Eqs. (4.3), (4.4) and (4.18) we have the following expressions inside the matter sources

$$f(T) = \frac{1}{m_{\rm P}^2}[\rho_{\rm m} + 4V(\varphi_F)] + \frac{\alpha}{2m_{\rm P}^6}[\rho_{\rm m} + 4V(\varphi_F)]^2 \simeq \frac{\rho_{\rm m}}{m_{\rm P}^2}\left(1 + \frac{\alpha\rho_{\rm m}}{2m_{\rm P}^4}\right), \tag{4.187}$$

$$f_R(T) = 1 + \frac{\alpha}{m_{\rm P}^4}[\rho_{\rm m} + 4V(\varphi_F)] \simeq 1 + \frac{\alpha}{m_{\rm P}^4}\rho_{\rm m}, \tag{4.188}$$

and

$$f_{RR}(T) = \frac{\alpha}{m_{\rm P}^2}, \tag{4.189}$$

where we have taken into account that $V(\varphi_F) \ll \rho_{\rm m}$ inside matter sources. Plugging these results in Eq. (4.184) gives

$$\frac{\alpha\rho_{\rm m}}{m_{\rm P}^4} \ll 1. \tag{4.190}$$

It is obvious that this bound is satisfied for most values of the coupling constant α, and in particular for the lower bounds given by Eq. (4.65). For example, the density of the Sun is $\rho = 1.41\text{g/cm}^3 = 1.3 \times 10^{-91} m_{\rm P}^4$, so that

$$10^{-91}\alpha \ll 1. \tag{4.191}$$

We conclude that our model passes the Solar System constraints. However, this is not the end of the story: We have overlooked one important subtlety by taking the approximation that the considered matter distributions are perfectly homogeneous. Indeed, the real structure of matter is discrete and our results could be modified. Specifically, the condition that $\gamma(T)$ has to be almost constant does not necessarily hold when one considers microscopic experiments, since it would be always possible to find regions of space where $\gamma(T)$ could take any possible value.

4.6.2 Microscopic Experiments

In this section we make use of the results found in Refs. [298, 409, 410]. The first experimental constraint is obtained by considering the non-relativistic Schrödinger equation for an electron in an external electromagnetic field, derived from the equation for a Dirac field in curved space-time. It is found that the $\gamma(T)$ term in the metric in Eq. (4.182) induces a miss-match in $\tilde{m} \equiv m\gamma^{-1/2}$, where m is the mass of the electron, calculated in vaccuum and in the interior of sources. This miss-match in turn corresponds to a change in the potential in the outermost part of the atom, which could induce a probability flux towards infinity reducing its half-life. In order for the miss-match to be small enough, any viable $f(R)$ theory must have a negligible [409]

$$\Delta_m = m_0 \left(\sqrt{\frac{f_R(\infty)}{f_R(0)}} - 1 \right), \tag{4.192}$$

where m_0 is a constant of the order of the mass of the electron m and $f_R(\infty)$ is f_R evaluated in the regions of space where the matter energy-density is much larger

than the vacuum energy-density. From the results obtained in the previous section, we have

$$\Delta_m = m_0 \left(\sqrt{1 + \frac{\alpha \rho_e}{m_{\rm P}^4}} - 1 \right) \simeq \frac{m_0 \alpha \rho_e}{2 m_{\rm P}^4}. \tag{4.193}$$

Since the vacuum-density scale $m_{\rm P}^2/\alpha$ is much larger than any matter-density scale that the wavefunction of the electron can reach, unless α is unrealistically large, we conclude that our choice for the $f(R)$ function is compatible with experiments related to the stability of the Hydrogen atom.

Another constraint was obtained in Ref. [410] from the variation in the energy levels of Hydrogen, for models in which the constraint given by Eq. (4.192) is satisfied, *i.e.*, Δ_m is negligibly small, such as ours. It reads

$$\left| \frac{f_{RR}(0) H_0^2}{f_R(0)} \right| \leq 4 \times 10^{-40}. \tag{4.194}$$

Using the results obtained in the previous section and the first Friedmann equation we obtain

$$\left| \frac{\alpha \rho_0}{3 m_{\rm P}^4} \right| \leq 4 \times 10^{-40}, \tag{4.195}$$

where ρ_0 is the energy-density of the Universe today, which value is

$$\rho_0 \simeq 8.5 \times 10^{-30} \frac{\rm g}{\rm cm^3} \simeq 10^{-120} m_{\rm P}^4. \tag{4.196}$$

The bound in Eq. (4.195) is obviously satisfied unless, again, α is unrealistically large.

This concludes the section about constraints coming from experimental tests. We have found that our choice for $f(R)$ passes the constraints coming from both Solar System and microscopic experiments. Furthermore, they are compatible with the bound in Eq. (4.127) coming from inflationary dynamics.

4.7 Discussion

The emphasis in this work is put on investigating quintessential inflation in the context of an $R + \alpha R^2$ Palatini modified gravity theory. In the Palatini formalism,

$R + \alpha R^2$ gravity does not introduce an extra dynamical degree of freedom (the scalaron) as is the case in the metric formalism. Instead, inflation is driven by an explicitly introduced inflaton field. What the Palatini setup does is it "flattens" the scalar potential leading to an effective inflationary plateau even though the original inflaton potential might be steep. As such, we have shown that a theory with e.g. $V \propto \varphi^2$ is successful in accounting for the inflationary observables.

However, thus far this is not a new result, as inflation in the Palatini context has been studied before. In our work we have also investigated other implications of our Palatini modified gravity theory after inflation. During radiation domination $R = 0$, which implies that our $R + \alpha R^2$ Palatini modified gravity does not really differ from standard Einstein gravity. However, this is not true during kination and subsequently during the recent history of the Universe, after the end of the radiation era. In principle, these periods may be affected and we have studied this in detail. We have shown that the Palatini corrections are largely subdominant to negligible during the kination era if the coupling α of the R^2 term in our theory is not too large[10]. We also showed that, as far as the Universe dynamics is concerned, the recent matter era is also unaffected.

There is an additional level on which our Palatini setup outperforms $R + \alpha R^2$ modified gravity theory in the metric setup, and it has to do with constraints from experimental tests on the coupling α of the R^2 term. The inflationary observables are satisfied when $\alpha \gtrsim 10^8$ or so. In the metric formalism, such values are excluded by solar system observational constraints and other microscopic experimental tests. The tightest constraint comes from time-delay effect of the Cassini tracking for the Sun, enforcing a stringent bound on post-Newtonian parameter $|\gamma - 1| < 2.3 \times 10^{-5}$ [398]. This implies $\alpha < 5.8 \times 10^{-6}$. However, this is not so in the Palatini formalism, where experimental tests allow for large values of α without problems. Thus, $R+\alpha R^2$ quintessential inflation is possible only in the context of the Palatini and not the metric formalism.

[10]Recall that the Lagrangian density of gravity is actually $\mathcal{L} = \frac{1}{2} m_{\rm P}^2 R + \frac{1}{4} \alpha R^2$.

To obtain specific predictions and demonstrate the analytic treatment of quintessential inflation in our Palatini modified gravity theory, we have investigated a family of models based on a generalised version of the original Peebles-Vilenkin quintessential inflation model [15], introduced in Eq. (4.44). This model is not to be taken too seriously though. The reason is that only two small regions of the scalar potential are really relevant. During inflation, the observable part of the scalar potential corresponds to the region traversed in slow-roll of the canonical inflaton field ϕ in no more than about 10 e-folds. For the non-canonical field φ (cf. Eq. (4.45)), this region is even smaller. For thawing quintessence, the region traversed corresponds to the field unfreezing and starting to roll. This region is again rather small. The model approximates the two regions as power-laws, with a positive power n for inflation and a negative power $-q$ for quintessence.

For inflation, we have shown that the correct spectral index of the primordial curvature perturbation is obtained when $n = 2 - 3$, in the case when reheating is due to gravitational particle production. This is the least effective mechanism for reheating, which corresponds to about $N \simeq 68$ e-folds of remaining inflation when the cosmological scales exit the horizon. The problem of gravitational reheating is that the subsequent kination period is so long that the amplification of primordial gravitational waves challenges the process of Big Bang Nucleosynthesis. A more efficient mechanism would reduce N somewhat down to $N \simeq 65$ or so. This would mean that $n \simeq 2$ or even less. The observed amplitude of the primordial curvature perturbation determines the value of the constant λ. When $n = 2$ we find that $\lambda \sim 10^{-6}$. Finally, regarding the generated primordial tensors, we find that we are within the observational limits if $\alpha \gtrsim 10^8$. If we are near this value, the produced primordial tensors are within reach of observations in the near future (*e.g.* by the BICEP3 or Simons observatories).

For quintessence, we have shown that coincidence can be achieved by avoiding the extreme fine-tuning of ΛCDM. Indeed, for $q = 4$ we found $M \sim 10\,\mathrm{GeV}$, which is rather reasonable. We have shown that this value substantially grows if q becomes

larger ($M \sim 10^{-7}\,\text{GeV}$ when $q = 2$). However, the negative power q cannot be much larger because the barotropic parameter of thawing quintessence today would be too large [258], the observational bound being $-1 \leq w < -0.95$ [8]. Future observations (e.g. Euclid or the Nancy Grace Roman missions), will pinpoint w further, resulting in a better estimate of q. It will be interesting if $w = -1$ was excluded and ΛCDM was in trouble. We should note that the power-law approximations of the scalar potential in the inflation and quintessence regions are only indicative. In this sense, one can envisage non-integer powers.

After inflation there is a period of kination where the inflaton field is oblivious of the scalar potential. Our treatment of kination within the Palatini setup is therefore independent of the specific model chosen for the scalar potential. We found that the canonical field ϕ is propelled over super-Planckian distances. However, the non-canonical field φ for both inflation and quintessence (cf. Eqs. (4.45) and (4.132)) is expected to vary much less, as is the case of α-attractors [258]. This means that the radiative stability of the quintessential tail is protected and the 5th force problem of quintessence is overcome [259].

Summing up, we have investigated quintessential inflation in the context of an $R + \alpha R^2$ Palatini modified gravity theory. We have shown that inflation is successful with a quadratic scalar potential for the inflaton field, while quintessence is successful with a quartic inverse power-law potential without the extreme fine-tuning of ΛCDM. He have found that the Palatini setup introduces subdominant corrections to the kination and quintessence periods and does not lead to violations on experimental tests of gravity. Our treatment is able to provide concrete predictions for the primordial tensors and the barotropic parameter of dark energy, which will be tested in the near future.

Chapter 5

Exponential Quintessential Inflation in Palatini $f(\varphi, R)$ Gravity

This chapter is based on the original research articles published in Journal of Cosmology and Astroparticle Physics [3] and in Galaxies [2] by the author, in collaboration with Konstantinos Dimopoulos, Alexandros Karam, and Eemeli Tomberg.

5.1 Introduction

In this chapter, we study a model of quintessential inflation in the context of $R+R^2$ Palatini gravity where the scalar field has a running non-minimal coupling to gravity. Employing Palatini gravity to study quintessential inflation was first considered in Chapter 4, considering a variation of the original quintessential inflation model in Ref. [15]. This toy-model investigation demonstrated that modeling quintessential inflation with Palatini gravity is promising. In this, much more elaborated and realistic approach, we consider a simple negative exponential potential in the Jordan frame. When we transform the action to the Einstein frame, the potential becomes flat for both negative and positive field values with a steep transition region in-between, resembling a step function. The two flat regions are suitable for inflation

and quintessence. Working in the Palatini formulation allows us to modify the inflationary plateau, in particular, through the R^2 term. The running of the non-minimal coupling allows us to obtain the correct quintessence behaviour. To study the full time evolution of the system throughout its cosmic history, we provide the equations of motion of the scalar field and an ideal fluid component representing other matter sources in the universe. We solve these equations numerically and scan over the parameter space, finding working scenarios matching both the CMB and late-time observations for parameter values that are free of fine-tuning. A preliminary study of the model can be found in Ref. [2]. In the present chapter, our treatment and findings are more complete and comprehensive.

This chapter is structured as follows. In the next section, we describe our model and perform the Jordan to Einstein frame transformation. Then, in Sec. 5.3, we describe the model's time evolution in a cosmological setup. We employ the slow-roll approximation and discuss the inflationary behaviour of the model, adopt Ricci reheating as the mechanism responsible for reheating the Universe and describe its details, and outline the post-inflationary expansion history, namely, kination, radiation/matter domination, and quintessence. Numerical results for inflationary and late-universe observables are presented in Sec. 5.4, and we conclude in Sec. 5.5. Further computational details are relegated to the appendices.

5.2 Setup

In this section, we first present the action of the model in the Jordan frame. After a frame transformation we bring the action to its Einstein frame form. Then, we compute the equations of motion in both Jordan and Einstein frames and show how one can easily transition between them.

5.2.1 The model

We start by considering the action in the Palatini formalism

$$S = \int \mathrm{d}^4x\sqrt{-g}\left[\frac{m_\mathrm{P}^2}{2}f(\varphi,R) - \frac{1}{2}g^{\mu\nu}\partial_\mu\varphi\partial_\nu\varphi - V(\varphi)\right] + S_\mathrm{m}[g_{\mu\nu},\psi]\,, \tag{5.1}$$

where m_P is the reduced Plank mass, ψ collectively represents the matter fields other than the inflaton φ, and we take them to behave as an ideal fluid. The function $f(\varphi, R)$ takes the form

$$f(\varphi,R) = \left(1 + \frac{\xi}{m_\mathrm{P}^2}\varphi^2\right)R + \frac{\alpha}{2m_\mathrm{P}^2}R^2\,. \tag{5.2}$$

We let the non-minimal coupling ξ run as

$$\xi(\varphi) = \xi_*\left[1 + \beta\ln\left(\frac{\varphi^2}{\mu^2}\right)\right]\,, \tag{5.3}$$

with $\xi_* > 0$ and $\beta < 0$ constants, and μ an arbitrary reference scale.

In the Palatini formalism, the connection Γ is independent of the metric $g_{\mu\nu}$. The connection features in the Ricci tensor, which is a function of the connection Γ only, with

$$R = g^{\mu\nu}R_{\mu\nu}(\Gamma)\,. \tag{5.4}$$

The form of the connection is determined by constraint equations obtained by varying the action with respect to Γ, and, in the presence of the non-minimal gravitational physics introduced by the non-zero ξ and α, it will differ from the standard Levi-Civita form.

The real scalar field φ, which plays the role of the inflaton and quintessence in quintessential inflation, is governed by an exponential potential

$$V(\varphi) = M^4\mathrm{e}^{-\kappa\varphi/m_\mathrm{P}}\,. \tag{5.5}$$

The exponential form is well-motivated in particle physics (it usually appears in string theory and supergravity models, e.g. in gaugino condensation [411, 412, 413]). It can produce quintessence in agreement with observations in its flat tail at $\varphi > 0$,

and it is also suitable for quintessence from a theoretical point of view: we do not introduce a fine-tuned cosmological constant by hand, but instead $V \to 0$ for large φ, and the late time dark energy density arises dynamically from the equations of motion.

The action (5.1) is dynamically equivalent (as long as $\partial_\chi^2 f \neq 0$) to

$$S = \int \mathrm{d}^4x\sqrt{-g}\left[f(\varphi,\chi) + \partial_\chi f(\varphi,\chi)(R-\chi) - \frac{1}{2}g^{\mu\nu}\partial_\mu\varphi\partial_\nu\varphi - V(\varphi)\right] + S_\mathrm{m}[g_{\mu\nu},\psi]\,, \tag{5.6}$$

as can be seen by obtaining the equation of motion for the auxiliary field χ and plugging it back in Eq. (5.6). Using this, the action can be cast in the form

$$S = \int \mathrm{d}^4x\sqrt{-g}\left[\frac{m_\mathrm{P}^2}{2}\left(1 + \frac{\xi}{m_\mathrm{P}^2}\varphi^2 + \frac{\alpha}{m_\mathrm{P}^2}\chi\right)R - \frac{\alpha}{4}\chi^2 - \frac{1}{2}g^{\mu\nu}\partial_\mu\varphi\partial_\nu\varphi - V(\varphi)\right] + S_\mathrm{m}[g_{\mu\nu},\psi]\,. \tag{5.7}$$

As is standard, we employ a conformal transformation (note that, in the Palatini formalism, this does not change Γ)

$$g_{\mu\nu} \to \bar{g}_{\mu\nu} = \Omega^2 g_{\mu\nu} \equiv \left(1 + \frac{\xi}{m_\mathrm{P}^2}\varphi^2 + \frac{\alpha}{m_\mathrm{P}^2}\chi\right)g_{\mu\nu} \tag{5.8}$$

to express the action in the Einstein frame where the gravitational part takes the standard Einstein–Hilbert form:

$$S = \int \mathrm{d}^4x\sqrt{-\bar{g}}\left[\frac{m_\mathrm{P}^2}{2}\bar{R} - \frac{1}{2}\frac{m_\mathrm{P}^2(\bar{\partial}\varphi)^2}{(m_\mathrm{P}^2 + \xi\varphi^2 + \alpha\chi)} - \frac{m_\mathrm{P}^4\left(V(\varphi) + \frac{\alpha}{4}\chi^2\right)}{(m_\mathrm{P}^2 + \xi\varphi^2 + \alpha\chi)^2}\right] + S_\mathrm{m}[\Omega^{-2}\bar{g}_{\mu\nu},\psi]\,. \tag{5.9}$$

Note that, essentially, $\Omega^2 = \partial_R f(\varphi, R) \equiv f_R$. We have introduced the short-hand notation $(\bar{\partial}\varphi)^2 \equiv \bar{g}_{\mu\nu}\bar{\partial}^\mu\varphi\bar{\partial}^\nu\varphi$, where $\bar{\partial}$ denotes a derivative with respect to the Einstein frame coordinates. Throughout the chapter, we will use an overbar to denote Einstein frame quantities. Due to the standard form of the gravity sector, we will interpret all the usual cosmological observations in the Einstein frame.

To make the calculations that follow less cluttered, we define

$$h(\varphi) \equiv m_\mathrm{P}^2 + \xi\varphi^2\,. \tag{5.10}$$

We then get rid of the auxiliary field by obtaining its equation of motion. Let us,

for a moment, ignore all matter except for the inflaton; then, we have

$$\frac{\delta S}{\delta \chi} = 0 \quad \Leftrightarrow \quad \chi = \frac{4m_{\rm P}^2 V + h(\varphi)(\bar{\partial}\varphi)^2}{h(\varphi)m_{\rm P}^2 - \alpha(\bar{\partial}\varphi)^2}\,, \tag{5.11}$$

giving

$$\Omega^2 = \frac{h^2 + 4\alpha V}{h m_{\rm P}^2 - \alpha(\bar{\partial}\varphi)^2}\,. \tag{5.12}$$

Plugging both expressions back into the action gives [345, 346]

$$S = \int \mathrm{d}^4x\sqrt{-\bar{g}}\left[\frac{m_{\rm P}^2}{2}\bar{R} - \frac{1}{2}\frac{(\bar{\partial}\varphi)^2 h m_{\rm P}^2}{h^2 + 4\alpha V} + \frac{\alpha}{4}\frac{(\bar{\partial}\varphi)^4}{h^2 + 4\alpha V} - \frac{V m_{\rm P}^4}{h^2 + 4\alpha V}\right]. \tag{5.13}$$

Note that, because we were able to get rid of the non-dynamical auxiliary field through its equation of motion, the above action contains only one scalar field. This is in contrast to the metric version of the theory, where the auxiliary field is dynamical and the Einstein frame action contains two fields.

The field can be made canonical via the redefinition

$$\frac{\mathrm{d}\phi}{\mathrm{d}\varphi} = \sqrt{\frac{h(\varphi)m_{\rm P}^2}{h(\varphi)^2 + 4\alpha V(\varphi)}}\,. \tag{5.14}$$

Note that for large negative φ, this gives $\mathrm{d}\phi/\mathrm{d}\varphi \propto e^{\kappa\varphi/(2m_{\rm P})}$, which, after integration, shows that ϕ approaches a constant as $\varphi \to -\infty$. We choose this constant to be equal to zero, so that ϕ is restricted to take positive values.

The field redefinition leads finally to

$$S = \int \mathrm{d}^4x\sqrt{-\bar{g}}\left[\frac{m_{\rm P}^2}{2}\bar{R} - \frac{1}{2}(\bar{\partial}\phi)^2 + \frac{\alpha}{4}\frac{h^2 + 4\alpha V}{h^2 m_{\rm P}^4}(\bar{\partial}\phi)^4 - \frac{V m_{\rm P}^4}{h^2 + 4\alpha V}\right]. \tag{5.15}$$

Note the appearance of the higher-order kinetic terms for the scalar. As we will see below, they are negligible for most of cosmological evolution. Note also the form of the Einstein frame potential,

$$\bar{V}(\phi) \equiv \frac{V m_{\rm P}^4}{h^2 + 4\alpha V} = \frac{m_{\rm P}^4 M^4 e^{-\kappa\varphi(\phi)/m_{\rm P}}}{(m_{\rm P}^2 + \xi\varphi(\phi)^2)^2 + 4\alpha M^4 e^{-\kappa\varphi(\phi)/m_{\rm P}}}\,, \tag{5.16}$$

which chiefly determines the cosmological evolution of the model. An example case is depicted in Fig. 5.1. The appealing features of the model are evident in the potential. For $\varphi < 0$, the potential decreases with increasing φ, but only slowly: the

α term makes the potential flat and suitable for slow-roll inflation. For $\varphi > 0$, the α term is subleading, and the potential decreases quasi-exponentially, modified by the change of variables (5.14). The ξ contribution modifies the potential; its running enables it to fix both the inflationary CMB observables and the late-time dark energy to values that match observations. For large enough φ, ξ runs to negative values, causing $\bar{V}$ to first flatten and then start growing, forming a local minimum and a nearby peak when $1 + \xi(\varphi)\varphi^2/m_{\rm P}^2$ becomes zero. For the parameters in Fig. 5.1, the zero occurs at $\varphi = 890.99 m_{\rm P}$, and at this point the height of the Einstein frame potential is $\bar{V}(890.99) = 1.14 \times 10^{-94} m_{\rm P}^4$ (notice the second term in the denominator in the potential regularizes the peak). Beyond the peak, the kinetic term in (5.13) changes sign. In practice, as we will see below, dynamics never probe this region.

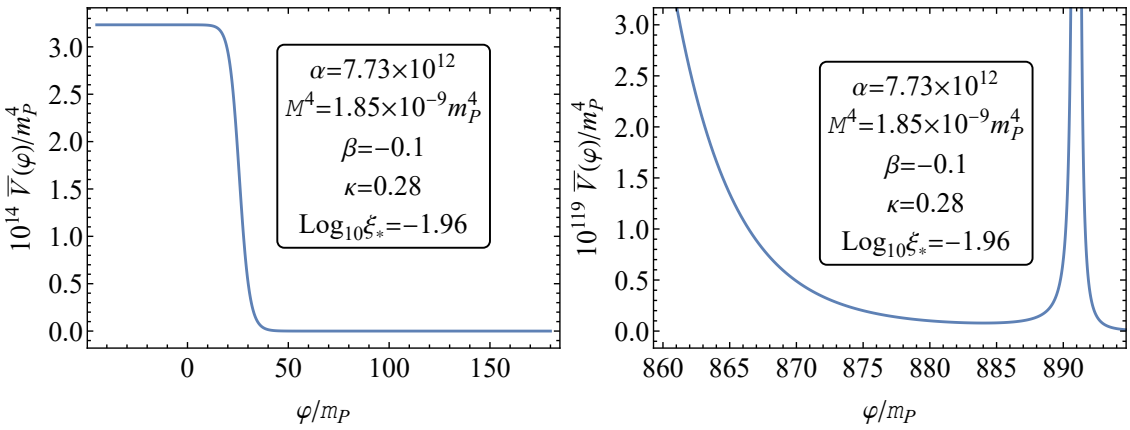

Figure 5.1: Potential in the Einstein frame $\bar{V}$ as a function of the field φ (in Planck units), with the presented parameter values, in two regions: around the inflation scale, $\varphi \sim 0$ (left), and around the point at which $1 + \xi(\varphi)\varphi^2/m_{\rm P}^2$ becomes zero, *i.e.*, $\varphi = 890.99\, m_{\rm P}$ (right). The height of the potential at this point is $\bar{V}(890.99) = 1.14 \times 10^{-94}\, m_{\rm P}^4$.

5.2.2 Equations of motion in the Jordan frame

While the Einstein frame discussed in the previous section is useful for physical interpretation of the results, the equations of motion are easier to formulate in

the Jordan frame, especially when we wish to include the non-inflaton matter contribution from (5.1) and thus go beyond the simplified Einstein frame action (5.15). To obtain the equivalent of Einstein equations for our system, we follow the same steps as in Sec. 3.2.

We take the matter energy-momentum tensor to be of the ideal fluid form with energy density ρ and pressure p, $T^{(\mathrm{m})}_{\mu\nu} = (\rho + p)u_\mu u_\nu + p g_{\mu\nu}$. We define the fluid's barotropic parameter as $w \equiv p/\rho$. The energy-momentum tensor of the field takes the standard form $T^{(\varphi)}_{\mu\nu} = \partial_\mu\varphi\partial_\nu\varphi - g_{\mu\nu}\left(\frac{1}{2}(\partial\varphi)^2 + V\right)$.

Using Eq. (5.2), the trace equation (3.40) becomes

$$R = -\frac{T}{m_{\mathrm{P}}^2 + \xi\varphi^2}\,, \tag{5.17}$$

and the R-derivative of the f function reads

$$f_R = \left(1 + \frac{\xi}{m_{\mathrm{P}}^2}\varphi^2\right) - \frac{\alpha T}{m_{\mathrm{P}}^4 + \xi m_{\mathrm{P}}^2\varphi^2}\,, \tag{5.18}$$

where trace of the energy-momentum tensor reads

$$T = -g^{\mu\nu}\partial_\mu\varphi\partial_\nu\varphi - 4V(\varphi) - \rho(1 - 3w)\,. \tag{5.19}$$

Adopting now the flat FLRW metric, the metric Einstein tensor $G_{\mu\nu}$ can be written in terms of the scale factor a and its time derivatives such as the Hubble parameter $H \equiv \dot{a}/a$ in a standard way. Dot refers to a derivative with respect to the cosmic time. The zeroth-zeroth component of Eq. (3.45) then reads

$$3H^2 = \frac{1}{m_{\mathrm{P}}^2 f_R}T_{00} + \frac{1}{2}\left(R - \frac{f}{f_R}\right) - \frac{3H\partial_0 f_R}{f_R} - \frac{3}{4f_R^2}\left(\partial_0 f_R\right)^2\,, \tag{5.20}$$

while the ij components read

$$\dot{H} = -\frac{1}{2m_{\mathrm{P}}^2 f_R}(p + \rho + \dot{\varphi}^2) - \frac{\ddot{f}_R}{2f_R} + \frac{3}{4f_R^2}(\dot{f}_R)^2 + \frac{H\dot{f}_R}{2f_R}\,, \tag{5.21}$$

where R and f_R are given in terms of the matter content by Eq. (5.17) and (5.18) and

$$T_{00} = \rho + \frac{1}{2}\dot{\varphi}^2 + V(\varphi)\,. \tag{5.22}$$

Eq. (5.20) is a second-order algebraic equation for H, which can be solved in terms of the field and fluid variables φ, $\dot{\varphi}$, ρ, and w. A complication arises from the time derivatives of f_R: these contain also factors such as $\ddot{\varphi}$ and $\dot{\rho}$, which must be eliminated using the field and fluid equations introduced below. The procedure is explained in detail in Appendix B.1.

As discussed in Sec. 3.2, the energy-momentum tensor of the fluid is conserved [376], so that

$$\nabla_\mu T^{\mu\nu}_{(\mathrm{m})} = 0 \quad \Rightarrow \quad \dot{\rho} + 3H\rho(1+w) = 0\,. \tag{5.23}$$

Finally, varying the action with respect to φ, we have

$$\ddot{\varphi} + 3H\dot{\varphi} + V'(\varphi) - \left(\xi(\varphi) + \frac{\xi'(\varphi)\varphi}{2}\right)\varphi R = 0\,, \tag{5.24}$$

which, using Eq. (5.3), becomes

$$\ddot{\varphi} + 3H\dot{\varphi} + V'(\varphi) - \tilde{\xi}\varphi R = 0\,, \tag{5.25}$$

where we have defined

$$\tilde{\xi} \equiv \xi_* \left[1 + \beta\left(1 + \ln\frac{\varphi^2}{\mu^2}\right)\right]. \tag{5.26}$$

Equations (5.23) and (5.25), with (5.17) and (5.20) for R and H, form a complete set of equations from which the dynamics of the system can be solved.

5.2.3 Between the Jordan and Einstein frames

To give a physical interpretation for the dynamics, we want to relate the Jordan frame quantities to the Einstein frame ones. In both frames, we use a flat FLRW coordinate system with the metrics $g_{\mu\nu} = \mathrm{diag}(-1, a^2, a^2, a^2)$ and $\bar{g}_{\mu\nu} = \mathrm{diag}(-1, \bar{a}^2, \bar{a}^2, \bar{a}^2)$. We remind the reader that we use an overbar to denote the Einstein frame quantities. The spatial coordinates of these two flat FLRW coordinate systems match, but the time coordinates are rescaled. As per our convention, we call the Jordan frame coordinates $x^\mu = (t, x^i)$ and the Einstein frame coordinates $\bar{x} = (\bar{t}, x^i)$, and the conformal transformation gives for spacetime

intervals

$$\begin{aligned} ds^2 &= \mathrm{d}x^\mu \mathrm{d}x^\nu g_{\mu\nu} = \mathrm{d}\bar{x}^\mu \mathrm{d}\bar{x}^\nu \bar{g}_{\mu\nu}\Omega^{-2} \\ \Leftrightarrow\ (\mathrm{d}x^i)^2 a^2 &= (\mathrm{d}x^i)^2 \bar{a}^2 \Omega^{-2}\,, \quad -\mathrm{d}t^2 = -\mathrm{d}\bar{t}^2\Omega^{-2}\,, \end{aligned} \tag{5.27}$$

where $\Omega^2 = f_R$ depends on time only. We obtain the relationships

$$\frac{\mathrm{d}\bar{t}}{\mathrm{d}t} = \sqrt{f_R}\,, \qquad \bar{a} = a\sqrt{f_R} \tag{5.28}$$

as the master equations for moving between the two frames. With these, we can express various Einstein frame quantities in terms of the Jordan frame ones. In particular,

$$\frac{\mathrm{d}}{\mathrm{d}\bar{t}}\phi \equiv \mathring{\phi} = \frac{1}{\sqrt{f_R}}\frac{d\phi}{d\varphi}\dot{\varphi}\,, \qquad \bar{H} \equiv \frac{\mathring{\bar{a}}}{\bar{a}} = \frac{H}{\sqrt{f_R}} + \frac{1}{2}\frac{\dot{f}_R}{f_R^{3/2}}\,, \tag{5.29}$$

where a dot still denotes a derivative with respect to the Jordan frame time, and we introduced a circle over a symbol to indicate a derivative with respect to the Einstein frame time, so that $\mathring{x} = f_R^{-1/2}\dot{x}$.

The relation between the fluid energy-momentum tensors in the Jordan and Einstein frames is [1]

$$\bar{T}^{(\mathrm{m})}_{\mu\nu} = -\frac{2}{\sqrt{-\bar{g}}}\frac{\delta S_\mathrm{m}}{\delta \bar{g}^{\mu\nu}} = -\frac{2}{\sqrt{-\bar{g}}}\frac{\partial g^{\alpha\beta}}{\partial \bar{g}^{\mu\nu}}\frac{\delta S_\mathrm{m}}{\delta g^{\alpha\beta}} = \frac{f}{f^2}\left(-\frac{2}{\sqrt{-g}}\frac{\delta S_\mathrm{m}}{\delta g^{\mu\nu}}\right) = \frac{1}{f}T^{(\mathrm{m})}_{\mu\nu}\,, \tag{5.30}$$

where we used $\partial g^{\alpha\beta}/\partial \bar{g}^{\mu\nu} = f\delta^\alpha_\mu\delta^\beta_\nu$ and $\sqrt{-\bar{g}} = f^2\sqrt{-g}$.

The Jordan frame ideal fluid is still ideal fluid in the Einstein frame; following Refs. [198, 399], we write its energy-momentum tensor as

$$\bar{T}^{(\mathrm{m})}_{\mu\nu} = (\bar{\rho} + \bar{p})\bar{u}_\mu\bar{u}_\nu + \bar{p}\bar{g}_{\mu\nu}\,, \qquad \bar{u}_\mu = \sqrt{f}u_\mu\,, \quad \bar{\rho} = \frac{\rho}{f^2}\,, \quad \bar{p} = \frac{p}{f^2}\,, \tag{5.31}$$

where the last equations relate the Jordan and Einstein frame quantities. It follows that the barotropic parameter has the same expression in both frames:

$$\bar{w} \equiv \frac{\bar{p}}{\bar{\rho}} = \frac{p}{\rho} = w\,. \tag{5.32}$$

Below, we will always refer to the Einstein frame when talking of the barotropic parameter; we will omit the bar for simplicity of notation.

5.2.4 Equations of motion in the Einstein frame

We are now ready to examine the Einstein frame equations of motion. Their full form is complicated—in the Einstein frame action (5.9), the field and fluid components are coupled through the conformal factor Ω^{-2} inside $S_{\rm m}$. In a general case with $\alpha \neq 0$, the fluid may even modify the χ constraint equation (5.11) and, as a consequence, the field transformation (5.14). We only present here approximate forms of the equations, free of some of these complications and valid during specific cosmological eras. Exact expressions can always be obtained by starting from the Jordan frame equations of Sec. 5.2.2 and applying the transformations of Sec. 5.2.3.

During inflation and right after it, the fluid is subdominant and can be ignored in the field equations. Varying the action (5.15) then gives [345]

$$\begin{aligned}\left[1+3\alpha\left(1+\frac{4\alpha V}{h^2}\right)\frac{\mathring{\phi}^2}{m_{\rm P}^4}\right]\mathring{\mathring{\phi}}+3\left[1+\alpha\left(1+\frac{4\alpha V}{h^2}\right)\frac{\mathring{\phi}^2}{m_{\rm P}^4}\right]\bar{H}\mathring{\phi}\\ +3\alpha^2\frac{\mathring{\phi}^4}{m_{\rm P}^4}\frac{\mathrm{d}}{\mathrm{d}\phi}\left(\frac{V}{h^2}\right)+\frac{\mathrm{d}}{\mathrm{d}\phi}\bar{V}=0\,,\end{aligned} \tag{5.33}$$

with h defined in (5.10). The energy density and pressure of the field read [362]

$$\begin{aligned}\bar{\rho}_\phi&=\frac{1}{2}\left[1+\frac{3}{2}\alpha\left(1+\frac{4\alpha V}{h^2}\right)\frac{\mathring{\phi}^2}{m_{\rm P}^4}\right]\mathring{\phi}^2+\bar{V}\,,\\ \bar{p}_\phi&=\frac{1}{2}\left[1+\frac{1}{2}\alpha\left(1+\frac{4\alpha V}{h^2}\right)\frac{\mathring{\phi}^2}{m_{\rm P}^4}\right]\mathring{\phi}^2-\bar{V}\,,\end{aligned} \tag{5.34}$$

and the Hubble parameter can be written as $3m_{\rm P}^2\bar{H}^2=\bar{\rho}_\phi$. The higher-order kinetic terms are the only complication compared to a standard canonical scalar field.

At later times, the fluid becomes important, but the α terms turn out to be negligible. In this limit, the field transformation (5.14) can be solved explicitly to yield[1]

$$\sqrt{\xi}\varphi=m_{\rm P}\sinh\left(\sqrt{\xi}\phi/m_{\rm P}\right), \tag{5.35}$$

[1]Note that, when $\alpha=0$, we have $\phi\to-\infty$ as $\varphi\to-\infty$, contrary to the discussion below Eq. (5.14). When working in the $\alpha=0$ limit, we normalize the field so that $\phi=0$ when $\varphi=0$.

with the Einstein frame potential

$$\bar{V}(\phi) = M^4 \frac{\exp\left[-\frac{\kappa}{\sqrt{\xi}}\sinh\left(\frac{\sqrt{\xi}}{m_{\rm P}}\phi\right)\right]}{\cosh^4(\frac{\sqrt{\xi}}{m_{\rm P}}\phi)} \equiv \tilde{V}(\phi)\,. \tag{5.36}$$

The field is coupled to the fluid; action (5.15) with the fluid contribution added in gives in the $\alpha \to 0$ limit:

$$\mathring{\mathring{\phi}} + 3\bar{H}\mathring{\phi} + \frac{d\bar{V}}{d\phi} - \frac{1}{2f_R}\frac{df_R}{d\phi}(1-3w)\bar{\rho} = 0\,, \tag{5.37}$$

where f_R is given by (5.18), so that $\partial_\phi f_R/(2f_R) = \sqrt{\xi}\tanh\sqrt{\xi}\phi$, and we used

$$\frac{1}{\sqrt{-\bar{g}}}\frac{\delta S_{\rm m}}{\delta\phi} = \frac{\partial\Omega^2}{\partial\phi}\bar{g}^{\mu\nu}\left(\frac{1}{\sqrt{-\bar{g}}}\frac{\delta S_{\rm m}}{\delta g^{\mu\nu}}\right) = -\frac{1}{\Omega^2}\frac{\partial\Omega^2}{\partial\phi}\bar{T}_m\,, \qquad \bar{T}_m = -(1-3w)\bar{\rho}\,. \tag{5.38}$$

Throughout the cosmic history, the fluid continuity equation in the Einstein frame can be obtained from the Jordan frame version (5.23), using the transformations of Sec. 5.2.3. The result is

$$\mathring{\bar{\rho}} + 3\bar{H}\bar{\rho}(1+w) + \frac{1}{2f_R}\mathring{f}_R(1-3w)\bar{\rho} = 0\,. \tag{5.39}$$

Multiplying the field equation (5.37) by $\mathring{\phi}$ gives the continuity equation for the field energy density. The inflaton-fluid coupling terms there and in (5.39) are identical but have opposite signs: the coupling simply transfers energy from one component to the other. The coupling vanishes in the early universe when the fluid behaves like radiation, $w = 1/3$, but it can be non-negligible during matter domination. We will discuss the effects of this coupling in more detail in Sec. 5.4.

Note that these expressions are still written partly in terms of the Jordan frame field φ, hidden in quantities like h, V, and f_R. In a general case, it is not possible to solve the field ϕ from φ analytically. This is why, in our practical numerical computations, we work in the Jordan frame. The Einstein frame expressions of this section are for the benefit of developing a physical intuition of the system.

5.3 Cosmic history with quintessential inflation

Let us now turn to the time evolution of our model in a cosmological setup. In this section, we explore the cosmic history qualitatively through its many stages, starting

from inflation and ending with quintessence domination. To make contact with the standard formalism discussed in the literature, we mostly work in the Einstein frame.

5.3.1 Inflation

We start with the field at the plateau with $\varphi < 0$ and high $\bar{V}$, with other matter components being negligible. We assume the high potential energy density dominates over the scalar's kinetic energy, giving rise to cosmic inflation, where the expansion of space accelerates. The plateau in $\bar{V}$ is suitable for *slow-roll inflation*, where the field slowly moves towards positive values so that the potential gradient is balanced by Hubble friction. In this limit, the Einstein frame equations of motion (5.33) take the standard form

$$3\bar{H}\mathring{\phi} + \frac{\mathrm{d}\bar{V}}{\mathrm{d}\phi} = 0\,, \qquad 3\bar{H}^2 m_P^2 = \bar{V}\,, \tag{5.40}$$

where we neglected higher-order kinetic terms as subleading slow-roll corrections [345]. The evolution is characterized by the slow-roll parameters:

$$\epsilon_V \equiv \frac{1}{2}\left(\frac{\mathrm{d}\bar{V}}{\mathrm{d}\phi}\frac{m_P}{\bar{V}}\right)^2, \qquad \eta_V \equiv \frac{\mathrm{d}^2\bar{V}}{\mathrm{d}\phi^2}\frac{m_P^2}{\bar{V}}\,. \tag{5.41}$$

For slow roll to be possible, we must have $\epsilon_V < 1$ and $|\eta_V| < 1$ at the corresponding field values. We can compute the slow-roll parameters for our potential (5.16) in the limit of constant ξ, that is, with $\beta = 0$. To make the computation simpler, we use a result from [345] that relates ϵ_V and η_V to their counterparts in the $\alpha = 0$ limit (here $\tilde{\epsilon}$ and $\tilde{\eta}$, respectively). The results, by using Eq. (5.14) and the chain rule, can be expressed terms of the Jordan frame field φ as

$$\eta_V = \tilde{\eta} - 3\frac{4\alpha\tilde{V}}{1+4\alpha\tilde{V}}\,, \qquad \epsilon_V = \frac{\tilde{\epsilon}}{1+4\alpha\tilde{V}}\,,$$
$$\tilde{\epsilon} = \frac{1}{2}\frac{\left[\kappa\left(1+\frac{\xi\varphi^2}{m_\mathrm{P}^2}\right)+4\xi\frac{\varphi}{m_\mathrm{P}}\right]^2}{1+\frac{\xi\varphi^2}{m_\mathrm{P}^2}}\,, \quad \tilde{\eta} = \frac{7\kappa\xi\frac{\varphi}{m_\mathrm{P}}\left(1+\frac{\xi\varphi^2}{m_\mathrm{P}^2}\right)+\kappa^2\left(1+\frac{\xi\varphi^2}{m_\mathrm{P}^2}\right)-4\xi+16\xi^2\frac{\varphi^2}{m_\mathrm{P}^2}}{1+\frac{\xi\varphi^2}{m_\mathrm{P}^2}}\,, \tag{5.42}$$

and $\tilde{V}$ is defined in (5.36). The expression for ϵ_V reveals possible extrema with $\tilde{V}' = 0$ at $\kappa\varphi/m_\mathrm{P} = -2 \pm \sqrt{4-\kappa^2/\xi}$. We demand that the potential is monotonic,

i.e. $\tilde{V}' < 0$ everywhere; this sets the restriction $\kappa^2 > 4\xi$ on the allowed parameter space.

Asymptotically, $\tilde{\epsilon} \sim \varphi^2$, diverging for both positive and negative φ. However, ϵ_V is suppressed by the exponential $\alpha\tilde{V}$ contribution so that $\epsilon_V \ll 1$ for $\varphi \ll -m_{\rm P}/\kappa$. This allows the system to undergo inflation even for large negative φ. Indeed, this was the motivation for us to introduce the αR^2 term to our model (5.1) in the first place. The asymptotic behaviour $\eta_V \sim \tilde{\eta} \sim \varphi$ also reveals divergences for $|\varphi| \to \infty$, this time not removed by the α terms, making slow roll impossible for $\varphi \ll -m_P/(\kappa\xi)$. This leaves us with a range of field values near $\varphi = 0$ that are compatible with slow-roll inflation. We start our inflationary evolution in slow-roll in this field range. As we will see in Sec. 5.4, typical values of the model parameters support the 60 or so e-folds of inflation needed for a successful inflationary scenario.

As discussed in Chapter 2, the motivation for slow-roll inflation is that it produces a nearly scale-invariant spectrum of perturbations, compatible with the CMB observations [10, 9]

$$A_s = 2.1 \times 10^{-9}\,, \quad n_s = 0.9649 \pm 0.0042\,, \quad \alpha_s = -0.0045 \pm 0.0067\,, \quad r < 0.036\,. \tag{5.43}$$

Here A_s is the scalar power spectrum amplitude, n_s is the scalar spectral index, α_s its running, and r is the tensor-to-scalar ratio at the CMB pivot scale $k_* = 0.05\,\mathrm{Mpc}^{-1}$. In the slow-roll limit, the perturbations read

$$\begin{aligned} A_s &= \frac{\bar{V}}{24\pi^2 m_P^4 \epsilon_V} = \frac{\bar{H}^2}{8\pi^2 m_P^2 \epsilon_H}\,, \\ n_s &= 1 - 6\epsilon_V + 2\eta_V = 1 - 4\epsilon_H + 2\eta_H\,, \qquad r = 16\epsilon_V = 16\epsilon_H\,, \end{aligned} \tag{5.44}$$

where we also gave the forms based on the Hubble slow-roll parameters,

$$\epsilon_H \equiv \frac{\mathring{\phi}^2}{2\bar{H}^2 m_P^2} \approx \epsilon_V\,, \qquad \eta_H \equiv -\frac{\mathring{\mathring{\phi}}}{\bar{H}\mathring{\phi}} \approx \eta_V - \epsilon_V\,, \tag{5.45}$$

where the approximations apply during slow roll. The expression for α_s depends on higher-order slow-roll parameters, which we omit for brevity; these can be found in

e.g. [39]. Using the results (5.42), we can also write down the full expression

$$n_s - 1 = -\kappa^2\left(1 + \frac{\xi\varphi^2}{m_{\rm P}^2}\right) - 10\xi\kappa\frac{\varphi}{m_{\rm P}} - 8\xi\frac{1 + 2\frac{\xi\varphi^2}{m_{\rm P}^2}}{1 + \frac{\xi\varphi^2}{m_{\rm P}^2}}\,. \tag{5.46}$$

In our numerical results, we have $\beta \neq 0$, so the results (5.42), (5.46) will be modified slightly. We will use these expressions as guidance when scanning over the parameter space, but we will compute the CMB observables from the Hubble slow-roll parameters as laid out in (5.44). The modifications of inflation due to a non-zero β turn out to be minor; β is more important for the later evolution of the system, in particular, for fixing the final dark energy density.

5.3.2 Kination

Inflation ends when the field rolls down from the inflationary plateau to positive φ values. As the field drops off the potential 'cliff', see Fig. 5.1, its velocity increases and the kinetic terms in the action (5.15) start to dominate over the potential. During this stage, the extra kinetic terms proportional to $\alpha\mathring{\phi}^4$ may play a role in the evolution (see Chapter 6). However, as the field velocity decreases due to Hubble friction, these terms die out quicker than the canonical $\mathring{\phi}^2$ kinetic term, which soon dominates. Analogously, in the Jordan frame, the αR^2 term becomes subdominant compared to the linear R term as the energy density of the universe, and thus its curvature, decreases, and it stays subdominant until today. Thus, the α term is only important during and right after inflation.

After a transition period (lasting less than 10 e-folds according to the numerics of Sec. 5.4), the scalar field follows standard kination [287, 288, 286, 239, 240, 245] with the equations of motion

$$\mathring{\bar{\phi}} + 3\bar{H}\mathring{\bar{\phi}} = 0\,, \qquad 3\bar{H}^2 m_P^2 = \frac{1}{2}\mathring{\bar{\phi}}^2\,, \tag{5.47}$$

with the solution

$$\mathring{\bar{\phi}} \propto \bar{a}^{-3}\,, \qquad \bar{\rho}_\phi = \bar{p}_\phi = \frac{1}{2}\mathring{\bar{\phi}}^2 \propto \bar{a}^{-6}\,. \tag{5.48}$$

Note that the exponentially suppressed potential does not play a role during this stage. The evolution (5.48) corresponds to a barotropic parameter $w = 1$, which is quite distinct from the standard radiation or cold matter domination ($w = 1/3$ and 0, respectively). The period of kination leads to a non-standard expansion history of the universe, which, in particular, shifts the number of e-folds of inflation left at the Hubble exit of the CMB pivot scale $k = 0.05\text{Mpc}^{-1}$ from the standard 50–60 to 60–70. We will return to this point in Sec. 5.4, where we match the CMB scale based on the full expansion history.

5.3.3 Reheating

In many conventional models of inflation, reheating occurs through the inflaton decaying into matter particles, which then take over the energy density and start the standard Hot Big Bang era. In quintessential inflation[2], the field condensate must be preserved and serve as dark energy later on. Therefore, radiation has to be created in some other way. There are many mechanisms which can facilitate this.

As an example, we consider one such mechanism, called Ricci reheating. Ricci reheating was first considered by Ref. [98]. Then, it was refined first by Ref. [99], which also coined the name, and further by Ref. [289]. In a nutshell, the idea behind Ricci reheating is as follows. The mechanism is based on the fact that, for a flat FRW Universe, the Ricci scalar (in the Einstein frame) is $\bar{R} = 3(1 - 3w_{\text{tot}})\bar{H}^2$, where w_{tot} is the barotropic parameter of the whole Universe. During slow-roll inflation we expect $w_{\text{tot}} = -1$, while after the end of inflation during kination we have $w_{\text{tot}} = 1$. This implies that the sign of $\bar{R}$ changes in the transition from inflation to kination. If one considers also a spectator scalar field ψ with non-minimal coupling to gravity $\propto \bar{R}\psi^2$, then this change of sign in $\bar{R}$ would correspond to a change of sign in the effective mass-squared of ψ generated due to the non-minimal coupling. Assuming that this effective mass-squared is positive during inflation, we can safely consider that the expectation value of ψ is zero by the end of inflation. However, as we switch

[2]and in general in non-oscillating inflation models

to kination, the effective mass of ψ becomes tachyonic and the field is displaced from zero (which corresponds to a potential hilltop, after inflation) and begins oscillations in its effective potential. The oscillating ψ has a particle interpretation and can decay into radiation, which eventually reheates the Universe, because its density is diluted less efficiently by the expansion than that of the free-falling inflaton during kination.

The mechanism has a number of advantages compared to other reheating mechanisms considered in quintessential inflation. It can be very efficient, in contrast to gravitational reheating [97, 403], which means it would not challenge Big Bang Nucleosynthesis (BBN); it does not require a coupling between the spectator field and the quintessential inflaton in an enhanced symmetry point, as would be the case of instant preheating [100, 228]; it does not need tuning of initial conditions for the spectator field, as does the curvaton reheating mechanism [290, 291] and finally it does not presuppose a quintessential inflaton with dissipating properties as in warm quintessential inflation [272] or the generation of primordial black holes [414]. It only employs the fact that renormalisation in curved spacetime results generically in a non-minimal coupling of scalar fields to gravity.

The additional Lagrangian density of the scalar field is

$$\delta\bar{\mathcal{L}} = -\frac{1}{2}\hat{\xi}\bar{R}\psi^2 - \frac{1}{2}\bar{g}^{\mu\nu}\bar{\partial}_\mu\psi\bar{\partial}_\nu\psi - V(\psi)\,, \tag{5.49}$$

where $V(\psi)$ is the part of the scalar potential which involves ψ and $\hat{\xi}$ is a non-perturbative coupling, which should not be confused with ξ, the non-minimal coupling of the quintessential inflaton field.

Technically, the addition of the above in the Lagrangian density of the theory is yet another modification of gravity, which must be taken into account when switching between the Jordan and Einstein frames. However, we consider that $\sqrt{\hat{\xi}}|\psi| \ll m_P$ always, which means that the influence of ψ on gravity remains always negligible. Thus, in effect, we can consider that the only effect of the above non-minimal coupling is to provide a contribution to the effective mass-squared of the spectator field. Additionally, the condition $\sqrt{\hat{\xi}}|\psi| \ll m_P$ allows us to consider a perturbative scalar potential, which around the expectation value of the field during

inflation, can be written as

$$V(\psi) = \frac{1}{2}m^2\psi^2 + \frac{1}{4}\lambda\psi^4 + \cdots , \tag{5.50}$$

where the ellipsis denotes higher-order non-renormalisable terms, presumed negligible. We will consider at first that the non-minimal coupling overwhelms the bare effective mass-squared $|m^2| \ll |\hat{\xi}\bar{R}|$ so we can ignore the first term on the right-hand-side above. This sets a limit on the mass which we discuss in Appendix B.2. We will also consider a positive perturbative self-coupling $0 < \lambda < 1$, so that the potential is stabilised by the quartic term and not by non-renormalisable terms, although a modification of our results in the latter case is straightforward.

In Ref. [289] it was shown that after the end of inflation, the field ψ oscillates as determined by the terms in (5.50) that stabilize $V(\psi)$, while the effect of the central potential hill (generated by the non-minimal coupling) is diminishing (and negligible) because $\bar{R} \sim \bar{H}(t)$ is decreasing after inflation. If the stabilising potential is quartic, as is the case of Eq. (5.50), then the density of the oscillating condensate decays as radiation, $\bar{\rho}_\psi \propto \bar{a}^{-4}$ [106]. However, if the potential were stabilised by a non-renormalisable term, this would not have been so. Fortunately, Ref. [289] demonstrated that it is largely irrelevant which term stabilises the potential $V(\psi)$. This is because in Ref. [289] it was shown that the primary reheating effect is not the perturbative decay of the coherently oscillating ψ condensate, but the non-perturbative particle production on the hilltop, right after the end of inflation. At this moment, the field finds itself on top of a potential hill, leading to ample production of radiation due to a tachyon instability. In Ref. [289], it was claimed that the produced radiation dominates over the one corresponding to the oscillating condensate. Because the latter is diluted (at least) as fast as radiation, it never becomes important, at least as long as the quadratic term in Eq. (5.50) remains negligible. These considerations simplify our treatment, because they suggest that radiation is immediately produced at the end of inflation, and the further evolution of the oscillating ψ condensate is irrelevant. The only question is how much radiation is produced.

An estimate of the size of the spread of a scalar field condensate on top of a potential hill is given by $\langle\psi^2\rangle \simeq |m_{\rm eff}|^2$ [415], where the effective mass squared in our case is $m_{\rm eff}^2 = -6\hat{\xi}\bar{H}^2$ during kination, which takes place near the end of inflation. Therefore, the density of radiation at the end of inflation is

$$\bar{\rho}_r^{\rm end} = \frac{1}{2}|m_{\rm eff}^2|\langle\psi^2\rangle \simeq 18\,\hat{\xi}^2\bar{H}_{\rm end}^4\,, \tag{5.51}$$

where 'end' denotes the end of inflation. Thus, we obtain

$$\Omega_r^{\rm end} = \frac{\bar{\rho}_r^{\rm end}}{\bar{\rho}_{\rm tot}^{\rm end}} \simeq \frac{18\,\hat{\xi}^2\bar{H}_{\rm end}^4}{3\bar{H}_{\rm end}^2 m_P^2} = 6\,\hat{\xi}^2\left(\frac{\bar{H}_{\rm end}}{m_P}\right)^2. \tag{5.52}$$

During kination, the total density of the Universe decreases as $\bar{\rho}_{\rm tot} \propto \bar{a}^{-6}$, while for radiation we have $\bar{\rho}_r \propto \bar{a}^{-4}$, which means that $\bar{\rho}_r/\bar{\rho}_{\rm tot} \propto \bar{a}^2$. Therefore,

$$\left.\frac{\bar{\rho}_r}{\bar{\rho}_{\rm tot}}\right|_{\rm end} = \left(\frac{\bar{a}_{\rm end}}{\bar{a}_{\rm reh}}\right)^2 \left.\frac{\bar{\rho}_r}{\bar{\rho}_{\rm tot}}\right|_{\rm reh} \Rightarrow \left(\frac{\bar{a}_{\rm end}}{\bar{a}_{\rm reh}}\right)^2 \simeq 6\,\hat{\xi}^2\left(\frac{\bar{H}_{\rm end}}{m_P}\right)^2, \tag{5.53}$$

where 'reh' denotes reheating, which is the moment that radiation takes over and we have $\bar{\rho}_r \simeq \bar{\rho}_{\rm tot}$. The density of the Universe at reheating is straightforward to find, by considering that $\bar{\rho}_{\rm tot} \propto \bar{a}^{-6}$. Indeed, we get

$$\bar{\rho}_{\rm tot}^{\rm reh} = \left(\frac{\bar{a}_{\rm end}}{\bar{a}_{\rm reh}}\right)^6 \bar{\rho}_{\rm tot}^{\rm end} \simeq 648\,\hat{\xi}^6\frac{\bar{H}_{\rm end}^8}{m_P^4}\,, \tag{5.54}$$

where we used Eq. (5.53) and $\bar{\rho}_{\rm tot}^{\rm end} = 3\bar{H}_{\rm end}^2 m_P^2$. Therefore, using that at reheating $\bar{\rho}_{\rm tot} \simeq \bar{\rho}_r = \frac{\pi^2}{30}g_* T^4$, the reheating temperature is

$$T_{\rm reh} \simeq 6\left(\frac{15}{\pi^2 g_*}\right)^{1/4}\hat{\xi}^{3/2}\,\frac{\bar{H}_{\rm end}^2}{m_P}\,, \tag{5.55}$$

where g_* is the number of effective relativistic degrees of freedom at reheating.

The allowed reheating efficiency for successful reheating is

$$10^{-18} \lesssim \Omega_r^{\rm end} < 1\,. \tag{5.56}$$

The lower bound in the range of the reheating efficiency in Eq. (5.56) is obtained from gravitational reheating [97, 403], which challenges the process of BBN due to an over-enhancement of primordial GWs during kination. Indeed, gravitational reheating

suggests $\bar{\rho}_r^{\rm gr} \sim 10^{-2}\bar{H}_{\rm end}^4$, where $\bar{H}_{\rm end} \sim 10^{-8} m_P$ and we used that $\bar{V}_{\rm end}^{1/4} \sim 10^{-4} m_P$, as the numerical scans of Sec. 5.4 give. The value of $\bar{V}_{\rm end}^{1/4}$ roughly corresponds to $m_{\rm P}/(4\alpha)^{1/4}$, that is, $\bar{V}^{1/4}$ on the plateau during inflation. Using Eq. (5.52), we obtain the range of the non-minimal coupling of the spectator field

$$0.1 \lesssim \hat{\xi} < 10^8 \,. \tag{5.57}$$

This range includes values of $\hat{\xi} \sim 1$, which means that no fine-tuning is required for our mechanism to work. A similar lower bound on $\hat{\xi}$ is obtained when considering the density of the primordial GWs generated by inflation. Indeed, the density of the gravitational radiation at the end of inflation is $\bar{\rho}_{\rm GW}^{\rm end} \simeq \frac{1}{4\pi^2}\bar{H}_{\rm end}^4$ (see appendix B.3). We require that $\bar{\rho}_r/\bar{\rho}_{\rm GW} > 20$ at BBN, but because both $\bar{\rho}_r$ and $\bar{\rho}_{\rm GW}$ decrease with the expansion as $\bar{a}^{-4}$, we have the same requirement at the end of inflation. In view of Eq. (5.51), this requirement becomes $\hat{\xi} > 1/6\sqrt{2}\,\pi \simeq 0.038$, which agrees with the range in Eq. (5.57).

Equations (5.55) and (5.57) suggest that the reheating temperature ranges as

$$10 \text{ GeV} \lesssim T_{\rm reh} < 10^{14} \text{ GeV} \,. \tag{5.58}$$

5.3.4 Radiation and matter domination

After reheating, the universe is dominated by hot radiation, and the barotropic parameter settles to $w = 1/3$. As the univserse cools, particles in the thermal bath start to become non-relativistic, and this cold matter eventually takes over. We approximate this to happen instantaneously when $\bar{\rho}_r \simeq 10^{-110} m_P^4$, corresponding to a temperature of ~ 0.8 eV [39].

At the same time, the field follows the equation of motion (5.37), veering away from kination once radiation starts to take over. While the fluid is relativistic, $w = 1/3$, the field and fluid don't mix directly. However, in the presence of radiation the Hubble parameter is larger than it would be if induced by ϕ alone, and this increases the importance of the friction term. The field velocity $\mathring{\phi}$ starts to decrease dramatically, until the field essentially freezes to a near-constant value $\phi_{\rm fr}$. Using

the known scalings of the scalar and radiation energy densities, and assuming a negligible scalar potential, we can write

$$\bar{\rho}_{\rm tot} = \bar{\rho}_\phi^{\rm kin}\left(\frac{\bar{a}}{\bar{a}_{\rm kin}}\right)^{-6} + \bar{\rho}_r^{\rm kin}\left(\frac{\bar{a}}{\bar{a}_{\rm kin}}\right)^{-4}, \tag{5.59}$$

where 'kin' refers to a moment at the beginning of standard kination with $\bar{\rho}_r^{\rm kin}/\bar{\rho}_\phi^{\rm kin} \equiv \Omega_r^{\rm kin} \ll 1$. With this and $3\bar{H}^2 m_P^2 = \bar{\rho}_{\rm tot}$, we can solve the frozen field value as

$$\begin{aligned}
\phi_{\rm fr} - \phi_{\rm kin} &= \int_{\bar{t}_{\rm kin}}^{\infty} \mathrm{d}\bar{t}\,\mathring{\phi} = \int_{\bar{a}_{\rm kin}}^{\infty} \mathrm{d}\bar{a}\frac{\mathring{\phi}}{\bar{a}\bar{H}} \\
&= \int_{\bar{a}_{\rm kin}}^{\infty} \frac{\mathrm{d}\bar{a}}{\bar{a}_{\rm kin}} \frac{\sqrt{2\bar{\rho}_\phi^{\rm kin}}(\bar{a}/\bar{a}_{\rm kin})^{-4}}{\sqrt{\left[\bar{\rho}_\phi^{\rm kin}(\bar{a}/\bar{a}_{\rm kin})^{-6} + \bar{\rho}_r^{\rm kin}(\bar{a}/\bar{a}_{\rm kin})^{-4}\right]/(3m_P^2)}} \\
&= \sqrt{6} m_P \sinh^{-1}\left(1/\sqrt{\Omega_r^{\rm kin}}\right) \approx m_{\rm P}\sqrt{6}\ln 2 - m_{\rm P}\sqrt{\frac{3}{2}}\ln\Omega_r^{\rm kin}\,.
\end{aligned} \tag{5.60}$$

As the kinetic energy of the field drops, the potential again starts to play an important role in field evolution, complicating the dynamics. Two basic behaviours emerge: the field may completely freeze, so that its potential energy comes to dominate over the kinetic one and the field's barotropic parameter becomes -1, or the field may start to follow a scaling attractor with slow time evolution [208, 416, 213]. To estimate which fate is more likely, we can approximate the potential locally around $\phi = \phi_0$ with the exponential

$$\begin{gathered}
\bar{V}(\phi) \approx M_{\rm eff}^4 e^{-\kappa_{\rm eff}\phi/m_P}\,, \\
M_{\rm eff}^4 \equiv \frac{e^{-\frac{\kappa}{\sqrt{\xi(\phi_0)}}}\sinh\left(\sqrt{\xi(\phi_0)}\phi_0/m_P\right) + \kappa\phi_0\cosh\left(\sqrt{\xi(\phi_0)}\phi_0/m_P\right)}{\cosh^4(\sqrt{\xi(\phi_0)}\phi_0/m_P^2)}\,, \qquad \kappa_{\rm eff} \equiv \kappa\cosh\left(\sqrt{\xi(\phi_0)}\phi_0/m_P\right).
\end{gathered} \tag{5.61}$$

If $\kappa_{\rm eff}$ is approximately a constant, then $\kappa_{\rm eff} < \sqrt{2}$ leads to freezing, and $\kappa_{\rm eff} > \sqrt{2}$ gives the scaling solution. In our model in the examples below, we find $\kappa_{\rm eff}$ to be small and slowly changing, leading indeed to a freezing behaviour.

After matter becomes non-relativistic with $w \neq 1/3$, time evolution is further complicated by the direct coupling between the fluid and the field in (5.37), (5.39). In practice, the dynamics have to be solved numerically; we do this in Sec. 5.4.

5.3.5 Quintessence domination

As the field rolls, ξ from Eq. (5.3) runs to smaller and smaller values, and the Einstein frame potential (5.16) becomes flatter and flatter, becoming more suitable for quintessence with a slowly rolling field. Indeed, as mentioned in Sec. 5.2.1, eventually ξ runs to negative values; around this point, the Einstein frame potential develops a local minimum and then starts to grow again, with a high positive peak near $\xi(\varphi)\varphi^2 = -m_{\rm P}^2$. The coupling to matter can cause the field to overshoot the minimum and oscillate around it a few times, but eventually, as the fluid energy density dilutes away, the field will settle into the potential minimum at $\varphi \equiv \varphi_{\rm fin}$. Its barotropic parameter $w_\phi = -1$ and its energy density, given by the height of the potential, become constant. The quintessence field then behaves as dark energy. To match observations, we need $\bar{V}(\varphi_{\rm fin}) = 7.23 \times 10^{-121} m_P^4$, computed assuming that $\bar{H} = 67.66$km/s/Mpc and that roughly 70% of the energy density of the universe today is in dark energy. To be more precise, the dark energy fraction today is [8]

$$\Omega_\phi = \Omega_{\rm DE} = 0.6889 \pm 0.0056\,. \tag{5.62}$$

Since we live in the transition period where both dark energy and matter have non-negligible roles, the quintessence field is not necessarily completely frozen yet. In our numerical results, we demand that the barotropic parameter of the field today respects the observational bounds of the CPL parametrisation [114],

$$w_{\rm DE} = w_{\rm DE}^0 + w_{\rm a}\left(1 - \frac{\bar{a}}{\bar{a}_0}\right), \qquad w_{\rm a} \equiv -\left.\frac{{\rm d}w_{\rm DE}}{{\rm d}\bar{a}}\right|_{\bar{a}_0}, \tag{5.63}$$

where '0' refers to today, and the limits are [8]

$$-1 \leq w_{\rm DE}^0 < -0.95 \qquad \text{and} \qquad w_{\rm a} \in [-0.55, 0.03]\,. \tag{5.64}$$

5.4 Numerical results

In this section, we explain the details concerning the numerical side of our work. As it is explained above, in order to numerically solve the dynamics of the system, we

work in the Jordan frame. It is then straightforward to obtain the corresponding quantities in the Einstein frame, where our intuition applies, by following the discussion in Sec. 5.2.3. To be more explicit, we need to solve for the scale factor $a(t)$, the inflaton field $\varphi(t)$ and the fluid density $\rho(t)$ (remember that, at a classical level, homogeneity and isotropy impose that the fields depend on time only), since every other quantity depends on these. In principle this could be done by solving the system of ordinary differential equations given by Eqs. (5.21), (5.23), and (5.25). However, the Hubble factor can be algebraically solved to be

$$H = -\frac{A}{B + 2f_R} + \frac{\sqrt{3f_R(4T_{00} + \alpha R^2)}}{3(B + 2f_R)}\,, \tag{5.65}$$

where the specific forms of A and B, as well as the details of the calculation, can be found in Appendix B.1. For our current discussion it suffices to know that A and B depend on $\varphi(t)$ (and its first derivative) and $\rho(t)$ only. This means that the initial system of ordinary differential equations given by Eqs. (5.25), (5.21) and (5.23) is reduced to Eqs. (5.25) and (5.23), where H is given by Eq. (5.65). These are the equations that we numerically solve.

It is also worth commenting on our choice of the Jordan frame over the Einstein frame. One obvious advantage of working in the Einstein frame is that the gravitational sector of the action is simply the Einstein–Hilbert term. However, were we to work in the Einstein frame, Eq. (5.14) would need to be solved and inverted in order to obtain $\varphi(\phi)$, to then be plugged back in the action (5.13) in order to express all the quantities in terms of the canonical Einstein frame field ϕ. Furthermore, the action in the Einstein frame features a quartic kinetic term and a coupling between the inflaton and the background matter fields through a conformal factor in the matter action. Although during inflation the matter action is zero, during the subsequent cosmological eras this extra coupling is present, complicating the setup. Likewise, the quartic kinetic term, which complicates the equations of motion even further, cannot be *a priori* discarded (although after solving the dynamics it is found to be in general negligible, see Fig. 5.8). All of these considerations outweigh the only hurdle in the Jordan frame: gravity is non-linear. As a matter of fact, due to

working in the Palatini formalism, we can profit from further simplifications as the one explained above, where the Hubble factor can be algebraically solved in terms of the inflaton and the background fields. In this way, we find the solution of the system to be much more approachable in the Jordan frame than in the Einstein frame. Finally, it is important to keep in mind that, as we have mentioned, once the dynamics is solved in the Jordan frame it is straightforward to obtain the analogous quantities in the Einstein frame by following the discussion in Sec. 5.2.3.

5.4.1 Initial conditions

During the inflationary era the only existing field is the inflaton (even if some matter fields existed they would be inflated away), so that $\rho(t) = 0$. Therefore, the only equation to solve for is Eq. (5.25) (with H given by Eq. (5.65)), which is a second order ordinary differential equation. Thus, only two initial conditions are needed, $\varphi(t_i)$ and $\dot{\varphi}(t_i)$. We choose $\varphi(t_i)$ sufficiently negative to capture all the possible evolution histories when scanning over the parameter space, while respecting the bound that imposes that the field should not be much smaller than $-m_{\rm P}/(\kappa\xi)$ (*c.f.* Sec. 5.3.1), for which slow-roll is not possible. This usually amounts to having $\varphi(t_i) \sim -30\, m_{\rm P}$ and as it can be seen from Fig. 5.3 (see also the discussion in Sec. 5.4.3), using a smaller value would be of no help, since the region of the parameter space compatible with observations restricts $\varphi(t_i) > -30\, m_{\rm P}$. Furthermore, for simplicity, since the field will eventually reach the slow-roll attractor, we choose $\dot{\varphi}(t_i)$ such that slow-roll is satisfied. Effectively this means neglecting the second order derivative in Eq. (5.25). With $\varphi(t_i)$ fixed, this equation only depends on $\dot{\varphi}(t_i)$, for which we can (numerically) solve to obtain the initial value.

The end of inflation gives way to kination. During this era, some reheating mechanism transfers the energy density of the inflaton to the particles of the SM, which are modelled in our setup by a perfect fluid with energy density $\rho(t)$. In this way, the last needed initial condition is the initial energy density of radiation, at

the end of inflation, $\rho(t_{\rm end})$. It can be found by the following simple calculation

$$\mathrm{e}^{\bar{N}} \equiv \frac{\bar{a}_{\rm end}}{\bar{a}_*} = \frac{\bar{a}_{\rm end}}{\bar{a}_0}\frac{\bar{a}_0}{\bar{a}_*} = \frac{\bar{a}_{\rm end}}{\bar{a}_0}\frac{\bar{H}_*}{\bar{a}_*\bar{H}_*} = \frac{T_0}{T_{\rm end}}k_*^{-1}\bar{H}_*\,, \tag{5.66}$$

where $*$ corresponds to the time at which the CMB pivot scale exits the horizon during inflation (with $k_* = \bar{a}_*\bar{H}_* = 0.05$ Mpc^{-1}), "end" corresponds to the end of inflation, and '0' corresponds to the present time. We have also set $\bar{a}_0 = 1$ and made the approximation $\bar{a} \propto T^{-1}$ from the end of inflation until today, where T is the temperature of radiation. Using Eq. (5.28), we can relate the number of e-folds in the Einstein and Jordan frames as [417, 418]

$$\bar{N} = N + \frac{1}{2}\ln\frac{f_R^{\rm end}}{f_R^*}\,. \tag{5.67}$$

Thus,

$$\mathrm{e}^{N} = \frac{T_0}{T_{\rm end}}k_*^{-1}\sqrt{\frac{f_R^*}{f_R^{\rm end}}}\bar{H}_*\,, \tag{5.68}$$

where $T_0 \approx 2.7$K. The initial energy density of radiation at the end of inflation can be written as

$$\bar{\rho} = \frac{\pi^2}{30}g_*T^4\,, \tag{5.69}$$

where $g_* = 106.75$ is the number of relativistic degrees of freedom. Relating $\bar{\rho}$ to ρ via (5.31) and gathering the above results together, we get

$$\rho(t_{\rm end}) = (f_R^*)^2\frac{\pi^2 g_*}{30}\left[\frac{T_0}{\mathrm{e}^N}k_*^{-1}\bar{H}_*\right]^4\,, \tag{5.70}$$

written in terms of quantities that are either known or fixed by inflation. Note the cancellation of $(f_R^{\rm end})^2$ due to the extra factor of f_R^2 coming from expressing the energy density in the Jordan frame. It is important to mention that when scanning over the parameter space we require that $\bar{\rho}(t_{\rm end})$ satisfies two bounds, the upper one such that the inclusion of the radiation fluid at the end of inflation is a small perturbation to the overall dynamics, *i.e.*, $\Omega_r^{\rm end} < 0.1$, and the lower one corresponding to the gravitational reheating limit, which is the least efficient reheating mechanism. Thus, we impose $\bar{\rho}(t_{\rm end}) > \bar{\rho}_{\rm grav} = qg_*(\bar{H}_{\rm end})^4/(480\pi^2) \simeq 2.25\times10^{-2}(\bar{H}_{\rm end})^4$ [27], where we have introduced $q \sim 1$ because the spectrum is not exactly thermal.

5.4.2 The parameter space

The model has six parameters, namely κ, ξ_*, β, μ, α, and M^4. It would be computationally costly to perform a scan over such a six-dimensional space. However, there are some simplifications that allow us to reduce the dimensionality of the parameter space.

The first thing to notice is the scaling law the model obeys. Indeed, let us rescale the coordinates, background density and parameters in the Jordan frame as[3]

$$x^\mu \to \lambda x^\mu, \quad \rho \to \lambda^{-2}\rho, \quad \alpha \to \lambda^2\alpha \quad \text{and} \quad M^4 \to \lambda^{-2}M^4\,. \tag{5.71}$$

From Eq. (5.17) it immediately follows that under this transformation the Ricci scalar scales as

$$R \to \lambda^{-2}R\,. \tag{5.72}$$

Likewise, from Eq. (5.1), the action scales as

$$S \to \lambda^2 S\,. \tag{5.73}$$

Of course, the equations of motion are invariant under such a rescaling of the action. Furthermore, the quantity αM^4 is also invariant. Looking at the expressions for the inflationary observables in Eq. (5.45), one can see that the parameters α and M^4 only enter the expressions for n_s and r through the combination αM^4, *i.e.*, they are invariant under the rescaling (5.71). It is not so for A_s, where M^4 enters its expression alone.

From this discussion we conclude that it is enough to scan over the quantity αM^4. For each value of αM^4 we can fix M^4 such that A_s satisfies the observational requirements from (5.43). In this way we have reduced the dimensionality of the parameter space to five.

There is one extra simplification that can be made by taking into account that μ in Eq. (5.3) is an arbitrary scale that can be changed by reabsorbing it into

[3]Note that here λ is just a constant factor and should not be confused with the ψ field self-coupling in Eq. (5.50).

ξ_*. Therefore it can be chosen to take the most convenient value, which, for us, is the field value at which the cosmological scales leave the horizon, φ_*. This way, around this scale the effect of the running is minimal and the non-minimal coupling is roughly just ξ_*. The dimensionality of the parameter space is now four.

Having defined the degrees of freedom of the system, *i.e.*, $\varphi(t)$, $a(t)$ and $\rho(t)$, the initial conditions, *i.e.*, $\varphi(t_i)$, $\dot{\varphi}(t_i)$, and $\rho(t_{\rm end})$, and the parameters over which to scan, *i.e.*, κ, αM^4, ξ_* and β, we first focus on the inflationary regime of the theory. In this way, we start with the initial conditions discussed above and numerically solve the system until the end of inflation, defined by the condition[4] $\epsilon_H \equiv \mathring{\phi}^2/(2\bar{H}^2 m_{\rm P}^2) = 1$. We take discrete slices in αM^4, ranging from 0.0143 to 1.43×10^6 in steps of factor 10 and a region in β around the central value of -0.1 with a resolution of 10^{-3} and scan over the parameters κ and $\log_{10}\xi_*$ with values in the intervals $[0.2, 0.7]$ and $[-2.5, -0.9]$, respectively, with resolutions of 5×10^{-3}. The reason behind choosing such a central value for β is that we have found that a correct behaviour for quintessence is strongly peaked around it.

As the values for the field and its velocity at the end of inflation will serve as the initial conditions for the beginning of the next cosmological era, we impose a set of conditions on the points obtained from the scan through which we obtain the valid region in the parameter space. In addition to fixing $A_s = 2.1 \times 10^{-9}$ as discussed above, we require that:

- The value of the scalar spectral index is equal to the central value obtained by Planck [8], *i.e.*, $n_s = 0.9649$.

- The value of the tensor-to-scalar ratio is within the latest observational bounds [9], *i.e.*, $r < 0.036$.

- The value of the running of the scalar spectral index is within the 2σ bounds obtained by Planck [8], *i.e.*, $-0.0179 < \alpha_s < 0.0089$.

[4]Note that the first slow-roll parameter in Eq. (5.42) is only an approximation. In the numerical study we also take into account the presence of the running in ξ.

- The initial energy density of radiation at the end of inflation, obtained via Eq. (5.70), amounts to a small perturbation of the system, *i.e.*, $\Omega_r^{\rm end} < 0.1$.

- The initial energy density of radiation at the end of inflation is larger than the energy density corresponding to gravitational reheating, *i.e.*, $\bar{\rho}(t_{\rm end}) > 2.25 \times 10^{-2} (\bar{H}^{\rm end})^4$.

The last two conditions translate to the available range in the number of e-folds from the time at which the cosmological scales exit the horizon until the end of inflation (see the right panel in Fig. 5.2). It is usually between 60 and 75. Also note that we have not imposed a correct value for the amplitude of the power spectrum A_s as a condition since every single point in the parameter space already satisfies this, by exploiting the scaling property of the model explained above.

When inflation ends, and after imposing the above set of conditions to obtain the valid region of the parameter space, we use the final values of the field and its velocity as the initial conditions for the next cosmological era, as well as Eq. (5.70) for the radiation energy density, in order to solve Eqs. (5.23) and (5.25), with H given by Eq. (5.65). The barotropic parameter of the fluid is of course $1/3$ up until the transition to the matter domination era, when it becomes $w = 0$. We model this transition by a jump from $1/3$ to 0 in the barotropic parameter of the background at the time when the energy density of radiation is equal to its value at matter-radiation equality, $\bar{\rho}_{\rm eq} = 1.27 \times 10^{-110} m_{\rm P}^4$ [8]. The simulation is finished when the energy density ratio of the field, corresponding now to dark energy, is equal to the central value obtained by Planck [8] of its value today, *i.e.*, $\Omega_\phi^0 = 0.6889$. At this point we impose another set of conditions, which we list here.

- The temperature of the universe at the onset of radiation domination is above $T_{\rm BBN} \simeq 0.1{\rm MeV}$.

- The barotropic parameter of the field is within the latest observational bounds [8], *i.e.*, $w_\phi^0 < -0.95$.

- The running of the barotropic parameter of the field in the CPL parametrization is within the latest observational bounds [8], *i.e.*, $-0.55 < w_a^0 < 0.03$.

- The energy density of the field at present is within one order of magnitude from the central value obtained by Planck, $\bar{\rho}_{\rm DE}^{\rm Planck} = 7.26 \times 10^{-121} m_{\rm P}^4$ [8].

Importantly, we also consider the bound on the density parameter of GWs coming from BBN constraints, $20\,\Omega_{\rm GW}^{\rm end} < \Omega_r^{\rm end}$, as discussed in Sec. 5.3.3. By using Eq. (5.52) this bound translates to an allowed range of values for the non-minimal coupling between the reheaton and gravity $\hat{\xi}$. The successful values of $\hat{\xi}$ for each point in the parameter space are presented in Table 5.1. The two points, for which $\hat{\xi}$ is the largest ($\hat{\xi} \sim \mathcal{O}(1)$), are highlighted in black in Fig. 5.11 (while the rest are in red).

The points that satisfy this extra set of conditions are the successful points of our model. For them we have successful inflation, with correct inflationary predictions, as well as a correct evolution during the expansion history of the universe, with successful dark energy at the present time.

5.4.3 Numerical results for inflation

In this section, we present and analyze the obtained results for inflation. We remind the reader that the power spectrum strength at the pivot scale, A_s, is fixed to its observed value in all our results. In the left panel in Fig. 5.2 we show an example slice of the parameter space in the $(\log_{10}\xi_*, \kappa)$ plane with fixed $\beta = -0.1$ and $\alpha M^4/m_{\rm P}^4 = 1.43$. The blue points have a correct value for n_s while the orange points satisfy the full set of conditions for inflation stated in Sec. 5.4.2. In order to understand the shape of the parameter space let us consider the $\beta = 0$ case, for simplicity. First, we remember we have imposed the potential to be monotonic, *i.e.*, $\kappa^2 > 4\xi = 4\xi_*$. The lower boundary of the parameter space region corresponds to this requirement. The other consideration to take into account is Eq. (5.46), which, since in the $\beta = 0$ case the expressions for the slow-roll parameters in Eq.

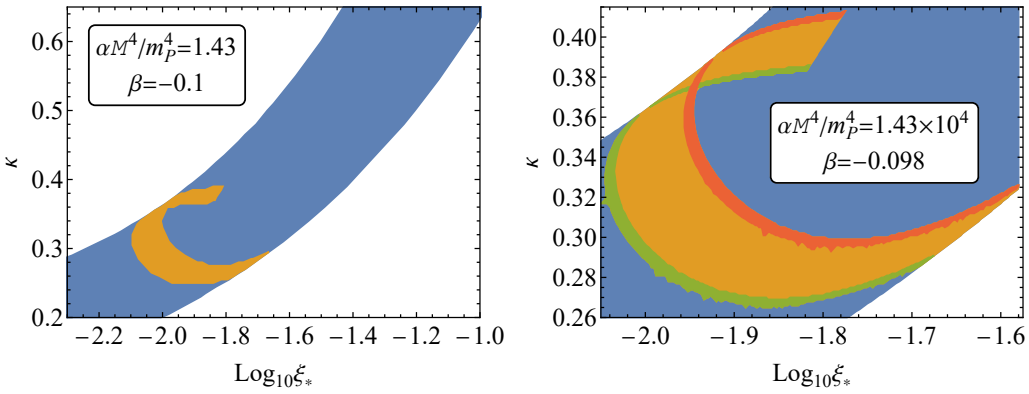

Figure 5.2: Left: Slice of the parameter space in the $(\log_{10}\xi_*, \kappa)$ plane with $\beta = -0.1$ and $\alpha M^4/m_{\rm P}^4 = 1.43$. The blue points have a correct value of the scalar spectral index, while the orange points satisfy all observational constraints for inflation. Right: A zoomed-in slice with $\beta = -0.098$ and $\alpha M^4/m_{\rm P}^4 = 1.43 \times 10^4$, depicting the bounds in parameter space corresponding to the bounds in the number of inflationary e-folds. The red region is close to saturating the gravitational reheating bound $\bar{\rho}(t_{\rm end}) > 2.25 \times 10^{-2} (\bar{H}^{\rm end})^4$ (which corresponds to the upper limit in the number of e-folds), while the green region is close to saturating the bound $\Omega_r^{\rm end} < 0.1$ (which corresponds to the lower limit in the number of e-folds).

(5.42) are exact, is an exact expression for the scalar spectral index (in the slow-roll approximation). Since this is a quadratic equation in κ, it can be algebraically solved for, giving an expression depending on ξ_* and φ_* (the field at horizon exit), $\kappa = \kappa(\xi_*, \varphi_*)$. In Fig. 5.3 we plot in green the curve $\kappa(\xi_*)|_{n_s=0.9649}$, for many values of the field at horizon exit, ranging from $-30\, m_{\rm P}$ to 0 (in steps of $0.5\, m_{\rm P}$). We can see that the upper boundary of the parameter space coincides with the asymptotic upper bound that the top curves form. In other words, above the upper boundary of the blue region, the value of the scalar spectral index is incorrect, for any φ_*.

Increasing the range for φ_* does not change the shape of the upper boundary of the parameter space in the $(\log_{10}\xi_*, \kappa)$ plane. Indeed, we also plot more $\kappa(\xi_*)|_{n_s=0.9649}$ curves, now in purple, with φ_* ranging from $-200\, m_{\rm P}$ to $-30\, m_{\rm P}$. We find that in the range $-30\, m_{\rm P}$ to 0 we cover almost the entirety of the shown

parameter space, while approaching more negative values simply covers a region of the parameter space discarded by observations, located at smaller and smaller values of κ.

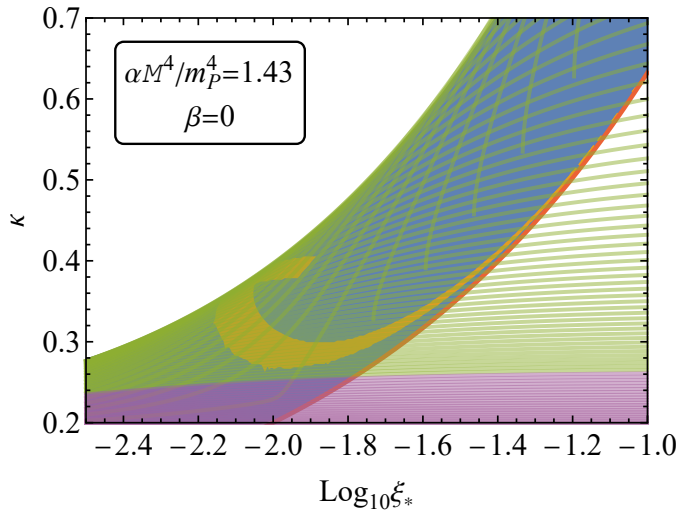

Figure 5.3: Slice of the parameter space in the $(\log_{10}\xi_*, \kappa)$ plane with $\beta = 0$ and $\alpha M^4/m_{\rm P}^4 = 1.43$, where we plot many curves $\kappa(\xi_*)|_{n_s=0.9649}$ with φ_* ranging from $-30\,m_{\rm P}$ to 0 (green) and from $-200\,m_{\rm P}$ to $-30\,m_{\rm P}$ (purple), as well as the curve $\kappa^2 = 4\xi(= 4\xi_*)$ (red), so that the condition for a monotonic potential $\kappa^2 > 4\xi(= 4\xi_*)$ is satisfied above it. The upper boundary of the parameter space coincides with the asymptotic upper bound from the green curves. Increasing φ_* to more negative values explores a region of the parameter space that is not in agreement with observations, towards smaller and smaller κ, as can be seen from the purple curves. The parameter space of the theory lies between the asymptotic upper bound from the $\kappa(\xi_*)|_{n_s=0.9649}$ curves and the condition $\kappa^2 = 4\xi(= 4\xi_*)$, as it should.

It could also be that changing αM^4 would change the shape of the parameter space. However, we find that the main effect of this is on r. Indeed, there exists a bound, given by $\alpha M^4/m_{\rm P}^4 \simeq 0.143$ below which the size of the orange region in the parameter space is reduced in size (although it never fully disappears, see the left panel in Fig. 5.5), and above which its position shifts towards larger values of κ and ξ. This can be seen by comparing the middle and right panels in Fig. 5.5. It is also

straightforward to see from Eqs. (5.42) and (5.44) that r can be made arbitrarily small by making αM^4 larger, as we have obtained in our numerical study (see Fig. 5.4). However, it is important to note that the shift in the orange region of the parameter towards larger κ and ξ can change the subsequent cosmological evolution after inflation ends, since these points serve as the initial conditions for the later evolution.

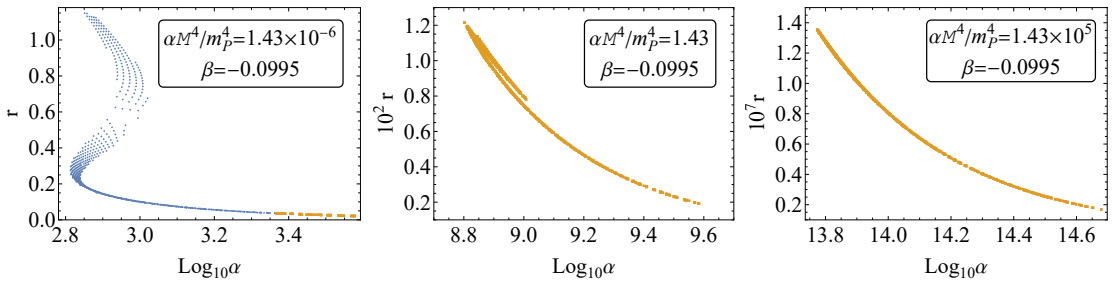

Figure 5.4: The tensor-to-scalar ratio r as a function of $\log_{10}\alpha$ for different values of αM^4, with fixed $\beta = -0.0995$. Blue points have a correct n_s, α_s and N while orange points also have a correct r. As we make αM^4 larger we lower the values r takes. Below the threshold value of $\alpha M^4/m_{\rm P}^4 \simeq 0.143$ there still exists an orange region (left), while above it all blue points become orange (middle and right).

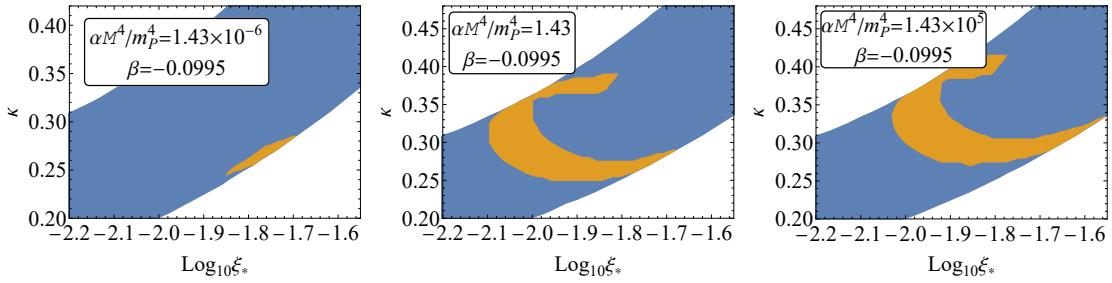

Figure 5.5: Slices of the parameter space in the $(\log_{10}\xi_*, \kappa)$ plane with $\beta = -0.0995$ and $\alpha M^4/m_{\rm P}^4 = 1.43 \times 10^{-6}$ (left), $\alpha M^4/m_{\rm P}^4 = 1.43$ (middle) and $\alpha M^4/m_{\rm P}^4 = 1.43 \times 10^5$ (right). The shape of the parameter space is identical for both the panels in the center and right, although the region with correct observational predictions is shifted toward larger κ and ξ_* as we make αM^4 larger. Even for very small values of αM^4 the orange region never disappears (left).

We conclude that the shape of the blue region shown in Fig. 5.2 is an universal feature of the model, with the caveat that the analysis concerning Fig. 5.3 is for the $\beta = 0$ case. We expect only minor modifications to this figure when studying the general non-zero β case, since during slow-roll inflation the value of the field barely changes and we choose the scale μ to be approximately equal to the field value at horizon exit φ_*, making the running in ξ negligible. In the same spirit, it is obvious that the shapes of the blue and orange regions in Fig. 5.3, for which $\beta = 0$, are very similar to the analogous regions in Fig. 5.2, for which $\beta = -0.1$.

To conclude this section, in Fig. 5.6, we show an example plot of the scalar spectral index as a function of the number of e-folds before the end of inflation in the Einstein frame. The shape of $n_s(\bar{N})$ in Fig. 5.6 is general and for most of the valid points of the parameter space, the equation $n_s(\bar{N}) = 0.9649$ has two solutions, *e.g.*, $\bar{N} = 73.7$ and $\bar{N} = 110.8$ in the specific case of the figure under consideration. Of course, only one of the two is selected via the bounds imposed on the initial radiation energy density. We have not found a trend where only the first (or the second) of the solutions are the correct ones. Indeed, depending on the region of the parameter space under consideration we can have one or the other giving the correct value for the number of e-folds.

5.4.4 Numerical results for post-inflationary evolution

In order to gain some understanding about the model, we start this section by studying one specific benchmark point of the parameter space which leads to correct dark energy predictions. After this we show the full parameter space of our quintessential inflation model.

Let us look at the point in parameter space with parameter values given by

$$\begin{gathered} \kappa = 0.284\,, \quad \log_{10}\xi_* = -1.960\,, \quad \alpha = 7.73 \times 10^{12}\,, \\ M^4/m_{\rm P}^4 = 1.85 \times 10^{-9}\,, \quad \beta = -0.100\,, \quad \text{and} \quad \mu = -6m_{\rm P}\,, \end{gathered} \tag{5.74}$$

which satisfies all the conditions listed above required for correct inflation and dark energy. This can be immediately confirmed by looking at Figs. 5.7 and 5.8. In the

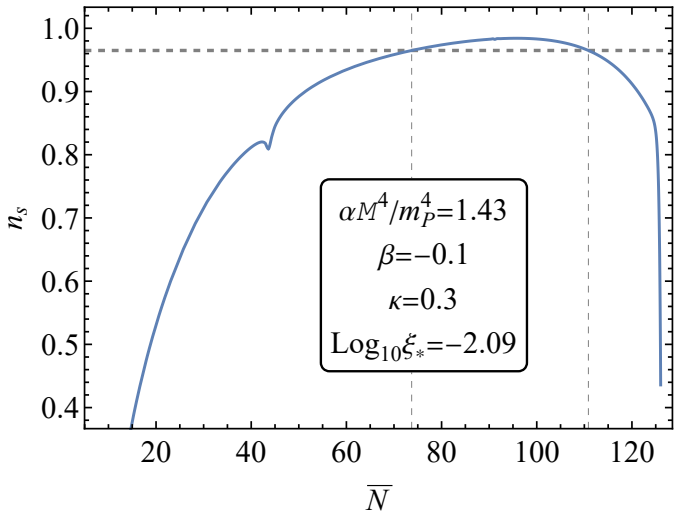

Figure 5.6: Scalar spectral index as a function of the number of e-folds before the end of inflation in the Einstein frame, for $\alpha M^4 = 1.43 m_{\rm P}^4$, $\beta = -0.1$, $\kappa = 0.30$ and $\log_{10}\xi_* = -2.09$. $\bar{N} = 0$ corresponds to the end of inflation. The horizontal dashed line is located at $n_s = 0.9649$, and it intersects $n_s(\bar{N})$ at $\bar{N} = 73.7$ and at $\bar{N} = 110.8$.

left panel in Fig. 5.7 we show the barotropic parameter of the inflaton and of the whole universe, which are given by

$$w_\phi = \frac{\bar{p}_\phi}{\bar{\rho}_\phi} \quad \text{and} \quad w_{\rm tot} = \frac{w_{\rm r,m}\bar{\rho}_{\rm r,m} + \bar{p}_\phi}{\bar{\rho}_{\rm r,m} + \bar{\rho}_\phi}\,, \tag{5.75}$$

where $w_{\rm r,m}$ is equal to either 1/3 or 0 for a radiation (r) or a pressureless dust (m) background with energy density $\bar{\rho}_{\rm r,m}$, respectively, and $\bar{\rho}_\phi$ and $\bar{p}_\phi$ are given by Eq. (5.34). At the present time, which corresponds to $\bar{N} = 0$ in both figures, the energy fraction of the field is $\Omega_\phi^0 = 0.6889$ (see the right panel in Fig. 5.7) and its barotropic parameter and running are $w_\phi^0 = -0.95895$ and $w_a^0 = -0.17034$, in agreement with dark energy observations. As for the energy densities at present it can be confirmed by looking at the right panel in Fig. 5.8, that the energy density of the field is $\bar{\rho}_\phi = 1.7 \times 10^{-120} m_{\rm P}^4$ while that of the fluid is $\bar{\rho}_{\rm m} = 7.5 \times 10^{-121} m_{\rm P}^4$, which are within an order of magnitude of observations. Finally, the temperature of the universe at the onset of radiation domination, *i.e.*, when $w_{\rm tot} = 0.36$ and $\Omega_\phi = 0.05$, is $T = (30\rho/(\pi^2 g))^{1/4} \simeq 2.49 \times 10^{-23} m_{\rm P} = 0.15\,{\rm MeV}$, which is slightly above $T_{\rm BBN}$.

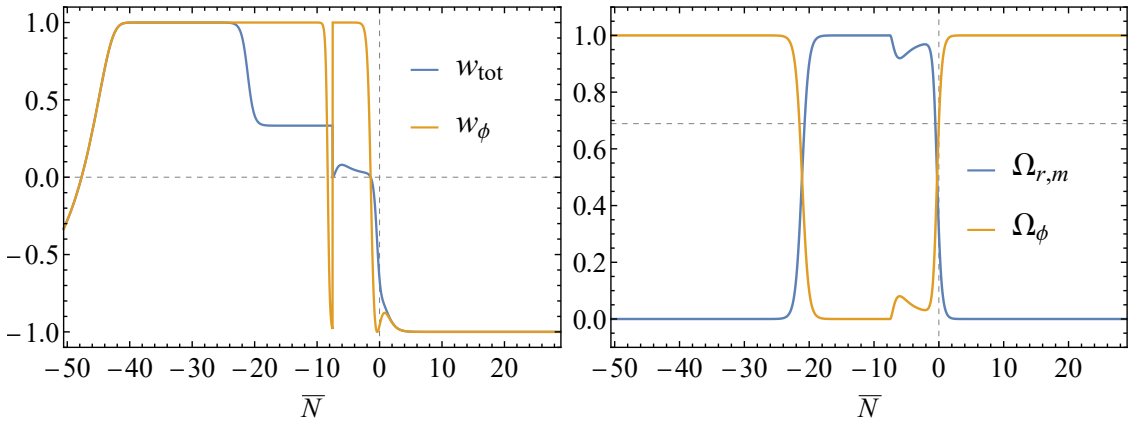

Figure 5.7: Left: Barotropic parameter of the universe (blue) and of the inflaton (orange) as a function of the elapsing number of e-folds in the Einstein frame. Right: Energy density parameter of the background fluid (blue), which is radiation (r) before and pressureless dust (m) after equality, and of the field (orange) as a function of the elapsing number of e-folds in the Einstein frame. The horizontal dashed line is located at 0.6889. For both graphs $\bar{N} = 0$ corresponds to the present time and $\bar{N} = -7.5$ to matter-radiation equality.

As a far as inflationary observables and dark energy predictions go, the point given by Eq. (5.74) is fine. However, as the careful reader might have noticed, there are two issues with the matter dominated era. As it can be seen in the left panel in Fig. 5.7, its duration $\bar{N}_{\rm mat} = 7.5$ is below what would be expected in a standard cosmology, where $\bar{N}_{\rm mat} \sim 8$. Furthermore, the barotropic parameter of the universe is not exactly zero (although it stays below 0.1). We can explain this behaviour by taking a closer look at our model. We remind the reader that, as shown in Eqs. (5.37) and (5.39), there is a coupling between the inflaton and the fluid (the last term in both equations) coming from the conformal factor that appears in the matter action after the conformal transformation to the Einstein frame. During inflation we have $\bar{\rho}_{\rm r,m} = 0$ and during kination and the radiation dominated era we have that the barotropic parameter of the fluid is $w = 1/3$, so that the coupling is not present until matter-radiation equality. However, as soon as we have a pressureless dust-dominated universe, with $w = 0$, the coupling is turned on. In order to better

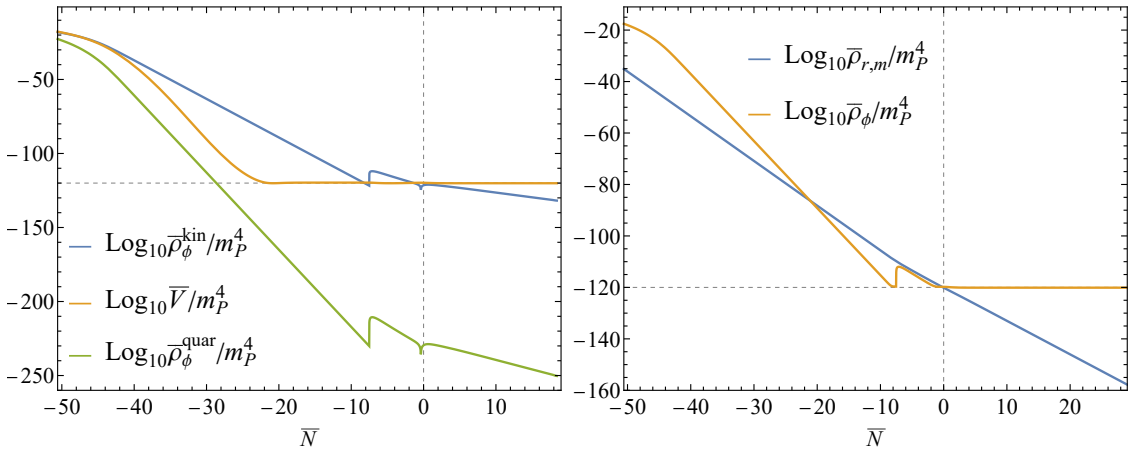

Figure 5.8: Left: Contributions from the kinetic energy energy density $\bar{\rho}_{\phi}^{\mathrm{kin}} = \mathring{\bar{\phi}}^2/2$ (blue), potential energy density $\bar{V}$ (orange) and quartic kinetic term $\bar{\rho}_{\phi}^{\mathrm{quar}} = 3\alpha(1+4\alpha V/h^2)\mathring{\bar{\phi}}^4/4$ (green) to the total energy density of the inflaton in the Einstein frame in Planck units, as a function of the elapsing number of e-folds in the Einstein frame. These contributions correspond to the first, second and third terms in the action (5.15), respectively. Right: Einstein frame energy densities of the background fluid (blue), which can be either radiation (r) or pressureless dust (m), and of the inflaton (orange) as a function of the elapsing number of e-folds in the Einstein frame. The horizontal dashed lines are located at $\log_{10}(\bar{\rho}/m_{\mathrm{P}}^4) = -120$, $\bar{N} = 0$ corresponds to the present time, and $\bar{N} = -7.5$ corresponds to matter-radiation equality.

understand this, after some simple algebra, one can rewrite Eq. (5.39) as

$$\mathring{\bar{\rho}} + 3\bar{H}\bar{\rho}(1+w_{\mathrm{eff}}) = 0\,, \tag{5.76}$$

where

$$w_{\mathrm{eff}} = w + \frac{(1-3w)}{3\left(\frac{2f_R H}{\dot{f}_R}+1\right)} = \frac{1}{3\left(\frac{2f_R}{f_R'}+1\right)}\,, \tag{5.77}$$

where the last equality follows from working in the matter dominated era and a prime denotes a derivative with respect to the Jordan frame number of e-folds. Thus, w_{eff} will only be close to zero when the rate of change of f_R satisfies

$$\frac{f_R'}{f_R} \ll 1\,. \tag{5.78}$$

However, looking at the expression for f_R in Eq. (5.18), and remembering that the terms coming from the α contribution are negligible at late times, the rate of change from Eq. (5.78) is approximately $f_R'/f_R \sim \varphi'/\varphi$. By noticing that the field is in free fall, and, thus, has a non-negligible rate of change, during the matter dominated era (its barotropic parameter is one[5] as can be seen in Fig. 5.7) it immediately follows that f_R'/f_R cannot be very small and $w_{\rm eff}$ will be generally larger than zero, as we find.

As for the number of e-folds of the matter dominated era $\bar{N}_{\rm mat}$, noting that from Eq. (5.76) follows that $\bar{\rho} \propto \bar{a}^{-3(1+w_{\rm eff})}$, a simple calculation reveals

$$\bar{N}_{\rm mat} = \log\frac{\bar{a}_0}{\bar{a}_{\rm eq}} = \frac{1}{3(1+w_{\rm eff})}\log\frac{\bar{\rho}_{\rm eq}}{\bar{\rho}_0} \simeq \frac{1}{3}\log\frac{\bar{\rho}_{\rm eq}}{\bar{\rho}_0} - \frac{w_{\rm eff}}{3}\log\frac{\bar{\rho}_{\rm eq}}{\bar{\rho}_0}\,, \tag{5.79}$$

where we have taken into account that $w_{\rm eff} \lesssim 0.1$, as is the case for most of the valid parameter space. Thus, $\bar{N}_{\rm mat}$ will generally be smaller than its canonical value in standard Einstein–Hilbert gravity, where there is no coupling between the fluid and the inflaton so that $w_{\rm eff} = 0$. Introducing the values of the energy density of the fluid at equality, $\bar{\rho}_{\rm eq} = 1.27 \times 10^{-110} m_{\rm P}^4$, and at the present time, $\bar{\rho}_0 = 3.28 \times 10^{-121} m_{\rm P}^4$, we find that $\bar{N}_{\rm mat}$ could be decreased by as much as about one e-fold. We take this into account in the parameter space scans, not neglecting points that *a priori* would have been considered to have a too short matter dominated era. In this way, we choose six as the smallest value $\bar{N}_{\rm mat}$ can take when scanning over the parameter space, although, as we will see below, for all valid points $\bar{N}_{\rm mat}$ will always be larger than seven, in agreement with the approximation $w_{\rm eff} \lesssim 0.1$ that we have taken above.

In conclusion, we have obtained that the barotropic parameter of the universe during the matter dominated era will generally be larger than zero and that the length of this era will generally be shorter than in Einstein–Hilbert gravity. These

[5]It could be that the higher order kinetic terms that appear in the Einstein frame modify the barotropic parameter of the field from its usual expression $w_\phi = (\frac{1}{2}\mathring{\phi}^2 - \bar{V})/(\frac{1}{2}\mathring{\phi}^2 + \bar{V})$. This is not the case, as can be seen in Fig. 5.8, where it is clear that the quartic kinetic term plays a subdominant role throughout the expansion history of the universe.

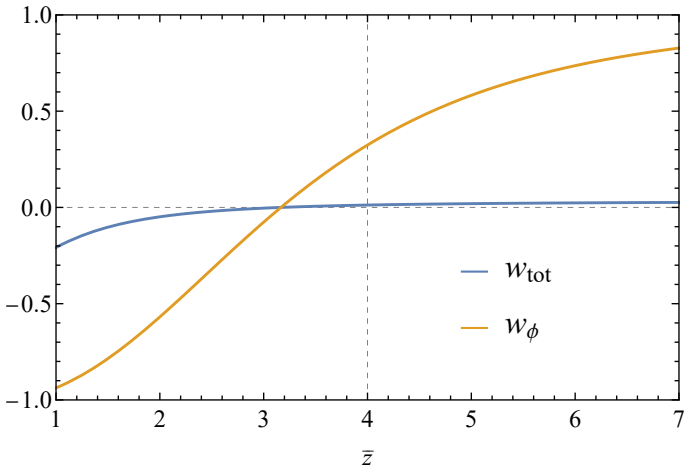

Figure 5.9: Barotropic parameter of the universe (blue) and of the inflaton (orange) as a function of the redshift in the Einstein frame. The vertical dashed line is located at $\bar{z} = 4$, corresponding to galaxy formation. The barotropic parameter of the universe is very close to zero around this redshift, making structure formation largely unimpeded.

effects are an inevitable consequence of working in our modified gravity setup. However, we find that for most of the parameter space $w_{\rm eff} \lesssim 0.1$ (and discard the points which do not satisfy this), and in fact, around redshifts corresponding to galaxy formation, *i.e.*, $\bar{z} \sim 4$ (where $\bar{z} \equiv \bar{a}^{-1} - 1$) [419], the barotropic parameter is very close to zero, thereby not significantly impeding structure formation (see Fig. 5.9).

Having discussed the effect of the inflaton-fluid coupling, modified gravity manifests itself in the Einstein frame through one other effect: the existence of a quartic kinetic term in the action (see the third term in Eq. (5.15)), which *a priori* cannot be discarded. However, as it can be seen from the left panel in Fig. 5.8, it remains subdominant throughout the expansion history of the universe. This is a general behaviour in all the valid parameter space. In what follows we neglect this term.

Let us next examine the evolution of the system more carefully, stage by stage. As the field approaches the end of the inflationary plateau and its velocity starts increasing, the condition $\epsilon_H = 1$ is satisfied and inflation ends. After the end of inflation there is a transition period where the field is gaining kinetic energy although its total energy density is still not dominated by it. This can be seen from Fig. 5.10, where we show the energy density ratios

$$\frac{\bar{\rho}_\phi^{\rm kin}}{\bar{\rho}_\phi} = \frac{\frac{1}{2}\mathring{\phi}^2}{\frac{1}{2}\mathring{\phi}^2 + \bar{V}} \quad \text{and} \quad \frac{\bar{\rho}_\phi^{\rm pot}}{\bar{\rho}_\phi} = \frac{\bar{V}}{\frac{1}{2}\mathring{\phi}^2 + \bar{V}} \,. \tag{5.80}$$

Indeed, after the end of inflation, at $\bar{N} = -50.6$, it is not until $\bar{N} \sim -40$ that the

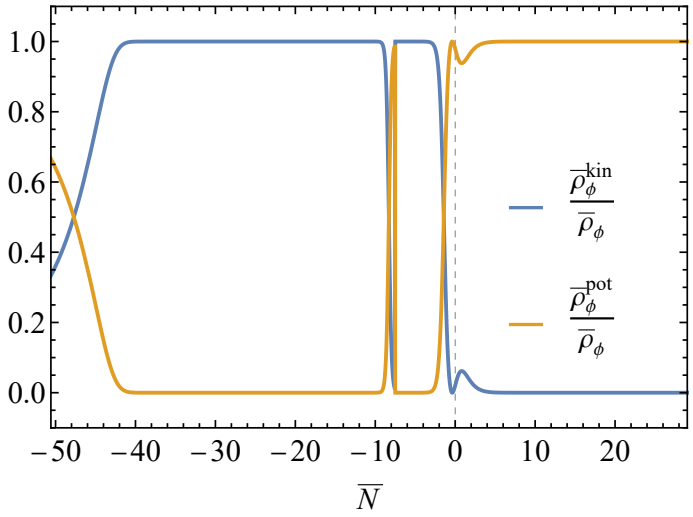

Figure 5.10: Kinetic energy density of the field over its total energy density (blue) and potential energy density of the field over its total energy density (orange) in the Einstein frame as a function of $\bar{N}$, from the end of inflation, at $\bar{N} = -50.6$ to the present time, at $\bar{N} = 0$. The end of kination (reheating) occurs at $\bar{N} = -19.6$ and matter-radiation equality at $\bar{N} = -7.5$.

energy density of the inflaton is kinetically dominated, while the energy density of the universe is still dominated by that of the field (Ω_ϕ is still equal to one as can be seen from the right panel in Fig. 5.7), giving way to the kination era. This can also be seen from the left panel in Fig. 5.7, where the barotropic parameter of the field does not become equal to one until $\bar{N} \sim -40$. Of course, at the moment when

the field becomes kinetically dominated, remembering the quartic kinetic terms are negligible, we have

$$w_\phi = \frac{\frac{1}{2}\overset{\circ}{\phi}^2 - \bar{V}}{\frac{1}{2}\overset{\circ}{\phi}^2 + \bar{V}} = \frac{\frac{1}{2}\overset{\circ}{\phi}^2}{\frac{1}{2}\overset{\circ}{\phi}^2} = 1\,. \tag{5.81}$$

During kination, the radiation energy density fraction approaches that of the field, until it takes over and approaches one around $\bar{N} = -19.6$, see Fig. 5.7. This moment corresponds to reheating. It is important to note that the scaling of the energy density of the universe between $\bar{N} = -50.6$ and $\bar{N} = -40$ is not $\bar{\rho} \propto \bar{a}^{-6}$ (but slower), and thus the exponent 6 on the right-hand-side of Eq. (5.54) is only an approximation. Effectively this means that we are able to have a reheating temperature close to $T_{\rm BBN}$ without violating the bound on $\Omega_{\rm GW}^{\rm end}$ discussed in Sec. 5.3.3.

After reheating, the universe is dominated by the background radiation, while the field is still in free-fall, with its energy density being kinetically dominated. This can be seen from the left panel in Fig. 5.7, where the barotropic parameter of the field is still equal to one, as well as from the left panel in Fig. 5.8 and from Fig. 5.10. This behaviour continues until briefly before matter-radiation equality, when the field runs out of kinetic energy and starts to freeze (see Eq. (5.60)). Indeed, its barotropic parameter approaches minus one (this can also be seen from Fig. 5.10, where the kinetic density ratio goes from one to zero and vice versa for the potential density ratio). However, the field never fully freezes. This is due to the change in the barotropic parameter of the background from 1/3 to 0 at matter-radiation equality. As explained above, at this point the coupling between the field and the fluid is turned on and there is an energy transfer between the components. One way to understand this is by noting that $w_{\rm eff}$ is larger than zero, meaning that the background dilutes faster than in the canonical case, feeding its energy into the kinetic energy of the field. Indeed, the barotropic parameter of the field jumps back to unity and the inflaton goes back into free-fall during the entirety of the matter-dominated era, only to run out of kinetic energy and freeze again (its barotropic parameter going back to minus one) at the end of it.

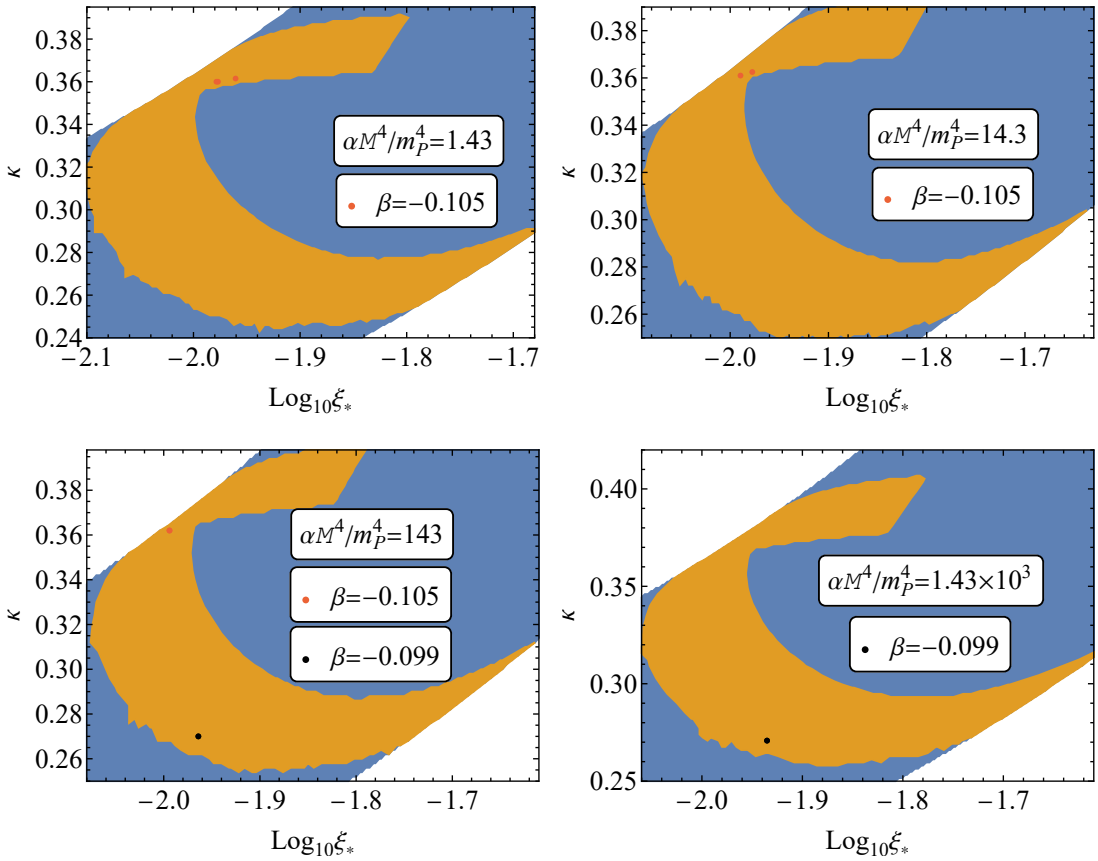

Figure 5.11: Slices of the parameter space in the $(\log_{10}\xi_*, \kappa)$ $\alpha M^4/m_{\rm P}^4 = 1.43$ (up left), $\alpha M^4/m_{\rm P}^4 = 14.3$ (up right), $\alpha M^4/m_{\rm P}^4 = 143$ (down left) and $\alpha M^4/m_{\rm P}^4 = 1.43 \times 10^3$ (down right). Points in the blue region have a correct value of n_s, while points in the orange region satisfy the whole set of constraints for inflation. Red points satisfy the constraints for dark energy, while black points also satisfy strongest the bound on $\Omega_{\rm GW}^{\rm end}$ coming from BBN (where $\hat{\xi} \sim \mathcal{O}(1)$). In the blue and orange regions β takes values from the interval $[-0.108, -0.099]$ in steps of 10^{-3}, while points giving rise to correct dark energy are only found when either $\beta = -0.099$ or $\beta = -0.105$.

Finally, the field does not simply slow down and freeze. If it did, we would not find the small bump in its barotropic parameter after $\bar{N} = 0$ in Fig. 5.7. The same bump can be found in Fig. 5.10. This is due to the local minimum of the potential in the Einstein frame, located slightly before the local maximum around

$1 + \xi(\varphi_{\max})\varphi_{\max}^2/m_{\rm P}^2 = 0$ (see discussion in Sec. 5.2.1). Indeed, the field overshoots the minimum and gains some kinetic energy, only to fall back to the minimum at $\varphi_{\min} = 884.03 m_{\rm P}$ and finally freeze. The present time $\bar{N} = 0$ corresponds to some time briefly after overshooting the minimum but before turning back.

Having characterised the dynamics of a typical valid parameter space point, including the effects of the modified gravity terms, let us now turn our attention to the location and shape of the full valid parameter space. We show some example slices in the $(\log_{10}\xi_*, \kappa)$ plane for different values of αM^4 in Fig. 5.11. We also scan over the parameter β, which in the orange and blue regions in the figure takes values in the interval $[-0.11, -0.098]$ in steps of 10^{-3}. We find that points giving rise to correct dark energy (shown in red and black), which satisfy the whole set of constraints given above, are only found for $\beta = -0.099$ and $\beta = -0.105$. We also show in Tab. 5.1 the actual parameter values all of the successful points take. We find they form no specific shape in the $(\log_{10}\xi_*, \kappa)$ plane, but expect a higher-resolution scan to reveal more working points. Lowering the required minimum temperature of the universe at the onset of the radiation dominated era, such that it is no longer larger than $T_{\rm BBN}$, makes the valid parameter space follow a curved area inside the orange region. However, imposing the appropriate bound spoils this behaviour. It is worth mentioning that although our selection criteria regarding the length of the matter dominated era is for it to be longer than 6 e-folds, allowing for a non-zero $w_{\rm eff}$ to decrease $\bar{N}_{\rm mat}$, all valid points actually have at least 7 e-folds, although they are always below 8 e-folds. It is possible that the rest of constraints regarding the energy density and the barotropic parameter make the parameter space to lie in this interval.

To conclude, in this section we have characterised the behaviour, both for the field dynamics and for the modified gravity effects, of a typical successful point in the parameter space. We have also found the location of the valid points in the $(\log_{10}\xi_*, \kappa)$ plane, having scanned over β in the $[-0.11, -0.098]$ interval in steps of 10^{-3} and over $\alpha M^4/m_{\rm P}^4$ in the interval $[1.43, 1.43 \times 10^3]$ in steps of factor 10. We

Successful Parameter Space Points									
	κ	$\log_{10}\xi_*$	αM^4	β	$H_{\rm CMB}/m_{\rm P}$	$10^{120}\bar{\rho}_0$	w_ϕ^0	w_a^0	$\hat{\xi}$
1	0.36	-1.96	1.43	-0.105	$9.22\cdot10^{-6}$	2.31	-0.954	-0.185	0.36
2	0.36	-1.98	1.43	-0.105	$9.17\cdot10^{-6}$	6.69	-0.960	-0.168	0.48
3	0.36	-1.97	1.43	-0.105	$9.17\cdot10^{-6}$	6.05	-0.969	-0.149	0.39
4	0.36	-1.98	14.3	-0.105	$2.95\cdot10^{-6}$	1.26	-0.955	-0.179	0.35
5	0.36	-1.99	14.3	-0.105	$2.96\cdot10^{-6}$	3.66	-0.959	-0.168	0.45
6	**0.27**	**-1.96**	**143**	**-0.099**	$9.78\cdot10^{-7}$	2.44	**-0.951**	**-0.184**	**1.01**
7	0.36	-1.99	143	-0.105	$9.56\cdot10^{-7}$	1.92	-0.960	-0.166	0.39
8	**0.27**	**-1.92**	**1430**	**-0.099**	$2.89\cdot10^{-7}$	3.63	**-0.951**	**-0.194**	**0.90**

Table 5.1: Parameter values for the parameter space points which give rise to successful inflation and dark energy. For each point we also show the value of $\hat{\xi}$, the Hubble parameter at the time at which the cosmological scales exit the horizon (in Planck units), energy density of the universe (in Planck units), the barotropic parameter of the field and its running, all at the present cosmic time. The two points which satisfy strongest the lower bound on $\hat{\xi}$ are highlighted in bold. αM^4 and $\bar{\rho}_0$ are given in Planck units.

obtain definite predictions for all of the parameters of our model except from αM^4, which just needs to be larger than a given lower bound $\alpha M^4 \sim 0.1$[6]. Indeed, the most successful points have $\kappa = 0.27$, $\log_{10}\xi_* = -1.9$ and $\beta = -0.099$.

5.5 Discussion

In this chapter we studied a relatively simple model of quintessential inflation where a single scalar field can unify the two epochs of accelerated expansion in the history

[6]This can be understood by remembering that $r = 16\epsilon_V$, with ϵ_V given by Eq. (5.42), and noting how αM^4 enters the denominator, so that r can be made arbitrarily small by making αM^4 arbitrarily large.

of the Universe: inflation and dark energy domination. We worked in the framework of Palatini gravity where the metric and the connection are treated as independent variables. The three main ingredients in our action are:

- An exponential potential of the form $M^4 e^{-\kappa\varphi/m_{\rm P}}$ which for large positive values of the scalar field produces the quintessential tail.
- An αR^2 term which asymptotically flattens the potential for large negative values and produces inflation in agreement with observations.
- A non-minimal coupling $\xi\varphi^2 R$ between the quintessence/inflaton field and gravity, where $\xi \approx \xi_*$ is approximately constant and positive during inflation but then runs to negative values with a slope β in order to reproduce the correct late-time dark energy. Note that the region where $\xi(\varphi)$ is negative is never probed since the field freezes before that.

The main advantage of employing the Palatini formalism is that the auxiliary field introduced in order to parametrise the R^2 term turns out to be non-dynamical and can therefore be eliminated through its equation of motion. The resulting action is then single field, but contains a quartic kinetic term and a modified effective potential. For sufficiently large values of α, the effective potential is always asymptotically flat and can therefore accommodate slow-roll inflation.

In addition to the quintessence/inflaton field, we considered an ideal fluid representing the matter and radiation content of the universe. We began our analysis by examining the equations of motion for the field and the fluid in both the Jordan and Einstein frames, while at the same time relating the quantities of interest in the two frames. We determined the Jordan frame equations to be easier to solve numerically. We then studied separately all the phases arising during the time evolution of our model in a cosmological setup, namely, inflation, kination, reheating, radiation and matter domination, and finally quintessence. To produce the radiation component after inflation, we considered as an example Ricci reheating [98, 99, 289], where an additional scalar field with a non-minimal coupling to gravity reheats the

universe during a period of kination. For quintessence, we showed that the Einstein frame scalar field potential develops a local minimum where the field eventually gets stuck, behaving like dark energy afterwards. The minimum is generated by the non-minimal coupling of the scalar field running to negative values. The dark energy density there is generated through the interplay of the different parameters, all taking natural values, avoiding the extreme fine-tuning of the cosmological constant in the standard ΛCDM scenario.

In the end, we presented a thorough analysis of our numerical procedure and results. We scanned over the inflationary parameter space and showed that, for correct choices of the parameter values, the inflationary predictions of the model match the Planck observations [10]. For late-time evolution, we noted the emergence of a coupling between the fluid and the scalar field, present in the Einstein frame during matter domination. This coupling turned out to be the biggest obstacle for our model building, threatening to disrupt the standard cosmic evolution by transferring energy from the matter fluid to the rolling field. Nevertheless, we found example points that satisfy all the criteria we set for a successful cosmological scenario, in particular for the present-time energy density and barotropic parameter of the quintessential dark energy component. We obtain definite predictions for all of the parameters of our model. The preferred parameter values which give rise to successful results are $\kappa = 0.27$, $\log_{10}\xi_* = -1.9$ and $\beta = -0.099$. We did not find a preference for any specific value for the combination αM^4, as long as it is above the threshold $\alpha M^4/m_{\rm P}^4 \sim 0.1$, below which the tensor-to-scalar ratio is too large to be compatible with observations. In addition to satisfying all the available observational constraints, our model also offers testable predictions, to be probed in the future by experiments such as EUCLID [420]. Indeed, a non-zero derivative of the barotropic parameter of dark energy with respect to the scale factor (w_a in the CPL parametrization), as is the case in our model, would favor dynamical dark energy models over a cosmological constant (as in ΛCDM). Our model offers specific predictions for w_a, which will be useful to discern between dynamical dark energy

models as measurements become more precise. It also features a non-zero barotropic parameter of the universe, probing redshifts between galaxy formation and equality, *i.e.*, $\bar{z}$ ∼500–1500.

To conclude, our model produces successful inflation and quintessential dark energy from the above-listed simple set of ingredients alone, without the extreme fine-tuning of ΛCDM. Our model is the first one (barring the toy-model in Ref. [1]) to produce successful quintessential inflation using modified gravity as the main ingredient.

Chapter 6

Observable Gravitational Waves from Hyperkination in Palatini Modified Gravity and Beyond

This chapter is based on the original research article published in The European Physical Journal C [6] by the author, in collaboration with Konstantinos Dimopoulos, Alexandros Karam, and Eemeli Tomberg. In recognition of the fact that the author made the primary contribution, his name is put first against alphabetical order.

6.1 Introduction

As we discuss in Chapter 2 (see Eq. (2.140) and below), the production of a stochastic background of primordial GWs is a generic prediction of inflation. These GWs, which are coming within reach of observability in the near future [421, 422, 423, 424, 425], are tensor perturbations of the spacetime metric, generated in much the same way as the scalar curvature perturbations behind the primordial density perturbations, for which there is overwhelming evidence in the CMB. Because of this, great interest has been developed in recent years for the observability of the inflation-produced GWs either indirectly, through the B-mode polarization of the

CMB [421], or directly from interferometers [422].

GWs were predicted by Einstein's general relativity at the beginning of the twentieth century. Almost exactly a hundred years afterwards, GWs were directly observed by LIGO (Laser Interferometer Gravitational-Wave Observatory) and Virgo in 2015 [426, 427]. This seminal observation heralded the birth of GW astronomy, which enables the study of compact objects, such as astrophysical black holes, which are typically shrouded by opaque accretion disks. It also allows, in principle, a glimpse of the very early Universe, well beyond the last-scattering surface, where the CMB was emitted. As such, there is hope to detect the stochastic primordial GW background from Cosmic Inflation. Such observations will allow the study of inflation at scales much different than the ones which correspond to the CMB primordial anisotropy, opening up a new window in the understanding of fundamental physics at extremely high energies (comparable to the energy of grand unification), which is behind the process of Cosmic Inflation and remains a mystery to this day.

This has, in part, motivated a number of future GW detection missions. In the near future, Advanced LIGO (plus Virgo and KAGRA) [428, 429, 430, 431, 432] (LVK) and the space interferometer LISA (Laser Interferometer Space Antenna) [433, 434, 435] are coming online; the launch date of LISA is in 2037. Another space interferometer DECIGO (DECi-hertz Interferometer GW Observatory) [436, 437, 438] is also planned to be launched in the 2030s. More are to follow, such as BBO (Big Bang Observer) [439], a proposed successor to LISA. It seems an ideal time to investigate GW production by inflation and its potential observational signatures.

However, there is a challenge in the study of the inflation-produced primordial GW background. The background signal is too weak for any currently operational GW detector to observe, and it may be decades before such an observation can be made. Indeed, were the early Universe dominated by radiation, as assumed by the concordance model, the primordial GW spectrum would be flat, *i.e.* like white

noise, where the GW density parameter per logarithmic frequency interval $\Omega_{\rm GW}(f)$ is constant over the range of frequencies f corresponding to the GW modes that re-enter the horizon during the radiation dominated period (they have been pushed out of the horizon during inflation). The constant value of the flat spectrum is very low, and the hope of detecting in the near future such inflation-generated primordial GWs is little [423].

Fortunately, this is not the end of our hopes for detecting primordial GWs. While there is observational evidence of the early Universe being radiation dominated, provided by the delicate process of Big Bang Nucleosynthesis (BBN) taking place a mere few seconds after the Big Bang itself, what the state of affairs was before BBN is still unknown. If the Universe's history before BBN was not dominated by radiation, then the primordial GW spectrum does not need to be flat. This opens up the possibility of a boosted GW spectrum, possible to detect even in the near future.

An early realisation of this possibility was provided by modelling quintessential inflation [15] (see Sec. 2.2.5 and Refs. [284, 285] for recent reviews). Quintessential inflation aims to explain in a unified way both Cosmic Inflation in the early Universe and Dark Energy at present. Most quintessential inflation models consider non-oscillatory inflation [100, 440] driven by a scalar field (the inflaton) with a runaway potential, which can play the role of quintessence at late times and explain the accelerated expansion of the Universe at present [229, 239, 242, 441, 233, 442, 258, 257, 259, 260, 256, 16]. In such models, there is a period after the end of inflation but before reheating (*i.e.* the onset of the radiation era) when the kinetic energy density of the inflaton field dominates the Universe. This period is called kination [286] (see also [443, 444, 445]), characterised by a stiff equation of state with a barotropic parameter $w = p/\rho = 1$. In Sec. 2.2.5 (see Eq. (2.306) and below), we show that, for GW modes that re-enter the horizon during kination, the spectrum is peaked with $\Omega_{\rm GW}(f) \propto f$ [294, 293, 446, 447, 448, 449, 450, 451, 452]. Unfortunately, this peak corresponds to very high frequencies, which will be unobservable in the near future.

Extending the period of kination does extend the peak to lower, possibly observable frequencies, but then the peak becomes too large and the resulting primordial GWs cannot but affect and destabilise the BBN process [294, 293, 453, 229] (see Figs. 2.9 and 2.10).

After the direct detection of GWs, there has been much interest in considering modifications of the history of the Universe, safely before BBN, to boost the primordial GW signal at observable frequencies. In Ref. [454], it was shown that $\Omega_{\rm GW}(f) \propto f^{-2(\frac{1-3w}{1+3w})}$, where w is the barotropic parameter of the Universe ($w = 1/3$ for radiation domination). In Refs. [455] and [456] models were considered where there is a period of matter domination followed by kination, which would create a mountain-like peak in $\Omega_{\rm GW}$ (see also Ref. [454]). Another possibility is to consider a stiff period after inflation that is not kination with $w = 1$, but has a milder value of $w \approx 1/2$ and can be extended down to observable frequencies without destabilising the BBN because the peak is not so steep as in usual kination [457]. A realisation of this in hybrid inflation with a non-canonical waterfall field was investigated in Refs. [458, 459].

In this chapter, we consider a different possibility, motivated by Palatini modified gravity. The cosmological consequences of Palatini modified gravity with $\mathcal{L} \propto R + \alpha R^2$ and a non-minimally coupled scalar field in in the context of quintessential inflation are considered in Chapters 4 and 5 (see also Refs. [460, 350]) and in Refs. [345, 346] in the context of inflation (see also Refs. [325, 461] for reviews). When switching to the Einstein frame, the scalar field obtains an additional quartic kinetic term[1]. In most cases considered, this term plays a negligible role in the dynamics of the scalar field. However, there are models for which this is not the case. We investigate in detail what happens when the scalar field dominating the Universe is governed by the quartic kinetic term in a period we call *hyperkination*. We show that the barotropic parameter of the Universe

[1]In Ref. [462] it was shown that the addition of the Holst and Holst^2 terms in the usual Palatini quadratic action can generate a modification of the higher-order kinetic term.

during hyperkination is the same as that of radiation domination, $w = 1/3$. As a result, in a realistic model of non-oscillatory inflation with a runaway inflaton potential, we consider a post-inflationary period of hyperkination, followed by a period of regular kination, when the kinetic energy of the inflaton is quadratic as usual. Kination is followed by radiation domination after reheating. This evolution results in a truncated peak in the GW spectrum, which can be safely extended down to observable frequencies without destabilising BBN. We calculate analytically the GW spectrum during all phases of hyperkination, kination and radiation and we verify our findings numerically. We explore the parameter space and show that we can obtain a boosted primordial GW signal with unique characteristics, which will be well-detectable by forthcoming observations. If such a signal is indeed detected, it will be a strong hint of non-canonical kinetic terms for the inflaton field from Palatini modified gravity or some other appropriate k-inflation or k-essence model.

This chapter is organized as follows. In Sec. 6.2, we introduce hyperkination, in the context of Palatini R^2 gravity, and embed it into the full expansion history of the Universe. In Sec. 6.3, we consider the primordial GWs, including their initial conditions as fluctuations of the quantum vacuum. Sec. 6.4 details our analytical computation of the GW evolution. We compare our GW spectra to observational bounds in Sec. 6.5 and conclude in Sec. 6.6. Further technical and computational details are relegated to the appendices.

6.2 Hyperkination

6.2.1 Quartic kinetic terms from Palatini R^2 inflation

We consider the same action in the Jordan frame as in Eq. (5.1) and follow the same procedure as in Sec. 5.2 to arrive at the action in the Einstein frame [345, 346]

$$S = \int \mathrm{d}^4x\sqrt{-\bar{g}}\Big[\frac{m_\mathrm{P}^2}{2}\bar{R} - \frac{1}{2}(\bar{\partial}\phi)^2 + \frac{\alpha}{4}\frac{h^2+4\alpha V}{h^2 m_\mathrm{P}^4}(\bar{\partial}\phi)^4 - U\Big] + S_\mathrm{m}[\Omega^{-2}\bar{g}_{\mu\nu},\psi]\,, \quad (6.1)$$

where

$$U \equiv \frac{V m_{\rm P}^4}{h^2 + 4\alpha V}\,, \tag{6.2}$$

and we employed a field redefinition of the form

$$\frac{{\rm d}\phi}{{\rm d}\varphi} = \sqrt{\frac{h(\varphi) m_{\rm P}^2}{h(\varphi)^2 + 4\alpha V(\varphi)}} \tag{6.3}$$

in order to render the quadratic kinetic term canonical, where the bars indicate quantities in the Einstein frame. Note that the process of transforming from the Jordan to the Einstein frame has generated a quartic kinetic term[2] and a modified potential U which will in general display a plateau for growing V, approaching the asymptotic value $m_{\rm P}^4/(4\alpha)$ [345]. Also, importantly, in the present work, we concentrate on the early era when the other matter components ψ are a perfect fluid of radiation. In this limit, the coupling between the inflaton and the matter action in the last term of Eq. (6.1) disappears [1, 3].

Neglecting the last term for the moment, we can rewrite the action as

$$S = \int {\rm d}^4x \sqrt{-\bar{g}} \left[\frac{m_{\rm P}^2}{2} \bar{R} + P\left(\phi, X\right) \right], \tag{6.4}$$

with

$$P\left(\phi, X\right) = X + L(\phi) X^2 - U\,, \tag{6.5}$$

where

$$X \equiv -\frac{(\bar{\partial}\phi)^2}{2} \qquad \text{and} \qquad L(\phi) \equiv \frac{\alpha}{4} \frac{h^2 + 4\alpha V}{h^2 m_{\rm P}^4}\,. \tag{6.6}$$

The action in Eq. (6.4) belongs to the general class of k-inflation [463] (where inflation is kinetically driven) or k-essence [194, 195, 196] (where the non-canonical kinetic terms can behave as quintessence).[3]

[2]Note that, in the context of Palatini gravity, models that contain a non-minimal derivative coupling term $G_{\mu\nu}\partial^\mu\varphi\partial^\nu\varphi$ [334] or $R_{(\mu\nu)}R^{(\mu\nu)}$ terms [363, 365] in the Jordan frame, can lead to actions similar to (6.1) in the Einstein frame after applying a disformal transformation of the metric.

[3]In Ref. [352] it was shown that the Palatini R^2 models share common features with k-inflation models.

Varying the action in Eq. (6.1) we can obtain the equation of motion for ϕ, which reads [345]

$$\left[1+3\alpha\left(1+\frac{4\alpha V}{h^2}\right)\frac{\dot{\phi}^2}{m_{\rm P}^4}\right]\ddot{\phi}+3\left[1+\alpha\left(1+\frac{4\alpha V}{h^2}\right)\frac{\dot{\phi}^2}{m_{\rm P}^4}\right]\bar{H}\dot{\phi}+3\alpha^2\frac{\dot{\phi}^4}{m_{\rm P}^4}\frac{\mathrm{d}}{\mathrm{d}\phi}\left(\frac{V}{h^2}\right)+\frac{\mathrm{d}}{\mathrm{d}\phi}U=0\,. \tag{6.7}$$

Then, from the non-zero components of the energy-momentum tensor we can obtain the energy density and pressure of the field, which read [362]

$$\begin{aligned}\bar{\rho}_\phi &= \frac{1}{2}\left[1+\frac{3}{2}\alpha\left(1+\frac{4\alpha V}{h^2}\right)\frac{\dot{\phi}^2}{m_{\rm P}^4}\right]\dot{\phi}^2+U\,,\\ \bar{p}_\phi &= \frac{1}{2}\left[1+\frac{1}{2}\alpha\left(1+\frac{4\alpha V}{h^2}\right)\frac{\dot{\phi}^2}{m_{\rm P}^4}\right]\dot{\phi}^2-U\,.\end{aligned} \tag{6.8}$$

To complete the equations of motion, the Hubble parameter can be written as

$$3m_{\rm P}^2\bar{H}^2=\bar{\rho}_\phi\,. \tag{6.9}$$

Again, the above equations differ from those of a standard canonical scalar field due to the higher-order kinetic terms. In the limit $\alpha\to 0$ they reduce to the minimal case. The bars are dropped in what follows to avoid clutter. Unless otherwise stated we always work in the Einstein frame.

The plateau in U mentioned above is ideal for slow-roll inflation, and can easily produce CMB observables compatible with observations for simple forms of the potential V [345, 346]. However, it restricts the inflationary—and thus post-inflationary—energy density to values lower than $m_{\rm P}^4/(4\alpha)$. Unfortunately, this severely restricts the parameter space considered in the following sections. One way to overcome this problem is to consider an α that experiences a drastic change at the end of inflation but remains constant afterwards. This is possible if α depends on a degree of freedom that changes its value when inflation ends. A toy model discussing this possibility is presented in C.1. Another example of a model describing the full inflationary history may be the one studied in Chapter 5, as long as it is enhanded with the hybrid mechanism discused in C.1. Moreover, we point out that the Palatini R^2 models considered here act as an inspiration for the extra quartic kinetic terms

in the action, but our analysis is more general, and we do not specify the details of the inflationary part of the model.

6.2.2 Kinetic domination

While the quartic kinetic terms in Eq. (6.1) are negligible during slow-roll inflation [345], they may play an important role in the post-inflationary Universe. We consider next such a scenario; a period of kinetic domination, where the potential V is negligible and the field rolls forward freely. In this limit, Eqs. (6.7) and (6.9) become

$$\Big(1+3\alpha\frac{\dot\phi^2}{m_{\rm P}^4}\Big)\ddot\phi+3\Big(1+\alpha\frac{\dot\phi^2}{m_{\rm P}^4}\Big)H\dot\phi=0\,,\quad 3H^2m_{\rm P}^2=\rho_\phi\,, \tag{6.10}$$

and the energy and pressure become

$$\begin{aligned}\rho_\phi &= \frac{1}{2}\Big(1+\frac{3}{2}\alpha\frac{\dot\phi^2}{m_{\rm P}^4}\Big)\dot\phi^2\,,\\ p_\phi &= \frac{1}{2}\Big(1+\frac{1}{2}\alpha\frac{\dot\phi^2}{m_{\rm P}^4}\Big)\dot\phi^2\,.\end{aligned} \tag{6.11}$$

It is instructive to change the time variable to the number of elapsing e-folds $N=\ln a$, with $\mathrm{d}N=H\mathrm{d}t$, and eliminate H. We can assume $\dot\phi>0$ without loss of generality. The field time derivatives are related as[4]

$$\dot\phi=m_{\rm P}^2\sqrt{\frac{2(6m_{\rm P}^2-\phi'^2)}{3\alpha\phi'^2}}\,. \tag{6.12}$$

Note that, due to the scaling with the heavily $\dot\phi$-dependent H, the limit $\dot\phi\to0$ corresponds to $\phi'\to\sqrt{6}m_{\rm P}$, and $\dot\phi\to\infty$ corresponds to $\phi'\to0$. Eqs. (6.10) and

[4]A prime denotes a derivative with respect to N in this section only. In the rest of the thesis, it denotes a derivative with respect to the conformal time η, $\mathrm{d}\eta=\mathrm{d}t/a$. As an exception, ϕ_0' in Eq. (6.16), which is used throughout this chapter, is always equal to $\phi_0'=\dot\phi/H$ evaluated at the end of inflation.

(6.11) become

$$\begin{aligned}
\phi'' &= \frac{\phi'(6m_{\rm P}^2-\phi'^2)(12m_{\rm P}^2+\phi'^2)}{6m_{\rm P}^2(12m_{\rm P}^2-\phi'^2)}\,,\\
\rho_\phi &= \frac{2m_{\rm P}^6}{\alpha\phi'^2}\left(\frac{6m_{\rm P}^2}{\phi'^2}-1\right)\,,\\
p_\phi &= \frac{2m_{\rm P}^6}{3\alpha\phi'^2}\left(\frac{6m_{\rm P}^2}{\phi'^2}+1\right)-\frac{2m_{\rm P}^4}{9\alpha}\,,\\
w_\phi &= \frac{1}{9}\left(3+\frac{\phi'^2}{m_{\rm P}^2}\right)\,,
\end{aligned} \tag{6.13}$$

where $w_\phi \equiv p_\phi/\rho_\phi$ is the barotropic parameter of the field. Note that α dropped out of the equation of motion: changing α rescales the time and energy density but leaves quantities like ϕ, N, and w_ϕ untouched.

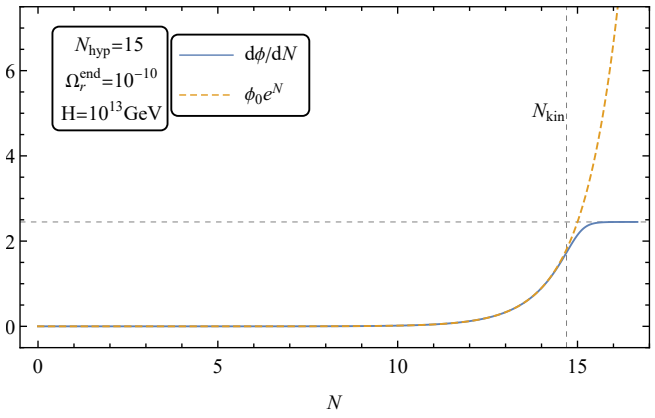

Figure 6.1: N-derivative of the field obtained from the numerical simulation (full blue line) and its initial approximation given in Eq. (6.16) (dashed orange line) as functions of N. The dashed vertical line, labelled $N_{\rm kin}$, corresponds to the time at which kination starts in the numerical simulation, defined here as the moment at which both addends inside the parenthesis in the energy density in Eq. (6.11) become equal, while the dashed horizontal line corresponds to $\phi' = \sqrt{6}m_{\rm P}$. In the legend, H denotes the Hubble parameter at the end of inflation $H_{\rm end}$.

If $\dot\phi$ is small—that is, $\frac{3}{2}\alpha\dot\phi^2 \ll m_{\rm P}^4$ and $\phi' \approx \sqrt{6}m_{\rm P}$—the quartic extra kinetic

terms are small, and Eq. (6.13) give

$$\begin{aligned}\phi'' &\approx 6(\sqrt{6}m_{\rm P} - \phi') \quad \Rightarrow \quad \phi' \approx \sqrt{6}m_{\rm P}\left(1 - ce^{-6N}\right)\,,\\ \rho_\phi &\propto (6m_{\rm P}^2 - \phi'^2) \propto e^{-6N} \propto a^{-6}\,, \quad w_\phi \approx 1\,,\end{aligned} \tag{6.14}$$

where c is an integration constant and we are concerned with the large N limit. We see that $\phi' = \sqrt{6}m_{\rm P}$ is an attractor. It corresponds to standard *kination* [287, 288, 286, 239, 240, 245] with a quickly diluting energy density and $w_\phi \approx 1$.

In the opposite limit of $\frac{3}{2}\alpha\dot{\phi}^2 \gg m_{\rm P}^4$ and $\phi' \approx 0$, the quartic kinetic terms dominate, and Eq. (6.13) gives

$$\begin{aligned}\phi'' &\approx \phi' \quad \Rightarrow \quad \phi' \approx ce^N \propto a\,,\\ \rho_\phi &\propto (\phi')^{-4} \propto a^{-4}\,, \quad w_\phi \approx \frac{1}{3}\,.\end{aligned} \tag{6.15}$$

We name this phase *hyperkination*. The extra kinetic terms modify the dynamics so that the energy density dilutes only as fast as radiation with $w_\phi \approx 1/3$.

Hyperkination only lasts for a limited time. As spatial expansion dilutes the field's kinetically dominated energy density, $\dot{\phi}$ decreases and ϕ' grows. The quartic kinetic terms are diluted faster than the quadratic ones, and eventually the latter take over. Consequently, the field transitions into standard kination. We can use Eqs. (6.14) and (6.15) to approximate the time evolution of ϕ' as it approaches the kination attractor as

$$\phi' \approx \begin{cases} \phi'_0 e^N & N < \ln\left(\sqrt{6}m_{\rm P}/\phi'_0\right)\,,\\ \sqrt{6}m_{\rm P} & N > \ln\left(\sqrt{6}m_{\rm P}/\phi'_0\right)\,,\end{cases} \tag{6.16}$$

where ϕ'_0 is the initial value of ϕ' at $N = 0$, taken below to be the end of inflation. Tuning ϕ'_0 lets us modify the length of hyperkination, which we define as[5]

$$N_{\rm hyp} \equiv \ln\left(\sqrt{6}m_{\rm P}/\phi'_0\right)\,. \tag{6.17}$$

[5]With the restriction $\rho_\phi < m_{\rm P}^4/(4\alpha)$ discussed at the end of section 6.2.1, we would have $\phi'_0 > 2m_{\rm P}$ at $N = 0$, and Eq. (6.16) restricts hyperkination to last less than 0.20 e-folds, a negligible amount. As mentioned, we omit this restriction in this paper.

Figure 6.1 compares Eq. (6.16) to a numerical solution of Eq. (6.13) in an example case.

Due to the exponential growth of ϕ', the transition from hyperkination to kination is fast. Let us define the beginning of standard kination $N_{\rm kin}$ as the moment when both addends inside the parenthesis in the energy density in Eq. (6.11) become equal. Using Eqs. (6.12) and (6.16), this condition reads

$$1 = \frac{3\alpha\dot{\phi}^2}{2m_{\rm P}^4} = e^{2(N_{\rm hyp}-N_{\rm kin})} - 1 \;\Leftrightarrow\; N_{\rm kin} = N_{\rm hyp} - \ln\sqrt{2}\,. \tag{6.18}$$

Thus, $N_{\rm hyp} \simeq N_{\rm kin}$ and we conclude that it is a good approximation to assume an instantaneous transition between hyperkination and kination.

We end this section with a relation between α, the energy density at the start of hyperkination (end of inflation) $\rho_{\rm end}$, and $N_{\rm hyp}$. Equation (6.13) together with the definition of $N_{\rm hyp}$ gives

$$\alpha\rho_{\rm end} = \frac{m_{\rm P}^4(1-e^{-2N_{\rm hyp}})}{3e^{-4N_{\rm hyp}}} \simeq \frac{m_{\rm P}^4 e^{4N_{\rm hyp}}}{3}\,, \tag{6.19}$$

where we have assumed a non-negligible duration for hyperkination $\mathcal{O}(N_{\rm hyp}) \sim 1$ in the last step. Note that $N_{\rm hyp} = 0$ corresponds to $\alpha = 0$, as it should.

6.2.3 Full cosmic evolution

Let us now embed a period of kination into a full history of the Universe. Initially, during cosmic inflation, the field energy density is dominated by potential energy. Once inflation ends, the potential drops to zero and the field's velocity increases as the potential energy is transformed into kinetic energy. In typical models, the field is trapped into a potential minimum, oscillating there and decaying into a thermal bath of particles, reheating the Universe. In our models of interest, the post-inflationary potential is of the runaway type—that is, flat and low—and the field keeps rolling onward under kinetic domination. If the quartic kinetic terms dominate, this phase starts with hyperkination, transitioning into standard kination later, as described above.

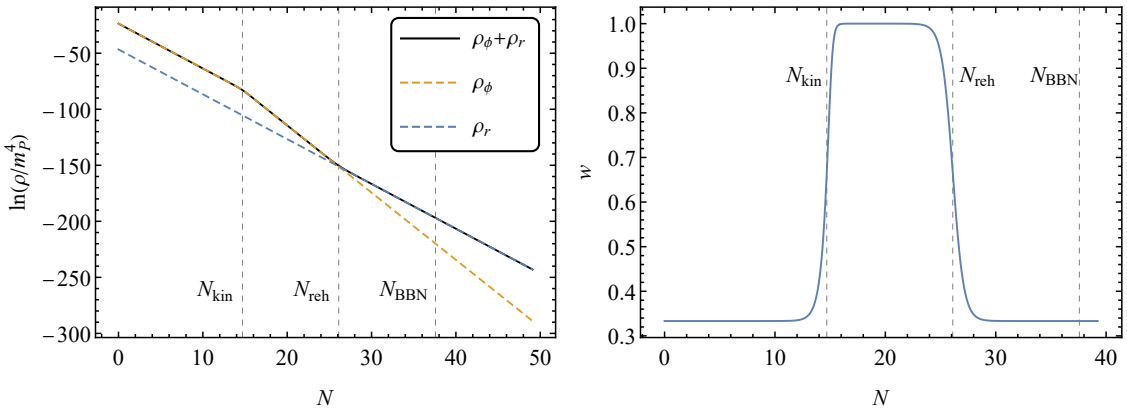

Figure 6.2: Left: Logarithm of the energy density of the Universe (full black), the field (dashed orange) and the background radiation fluid (dashed blue) as a function of the number of e-folds calculated from the end of inflation, obtained by numerically solving the system. Right: Barotropic parameter of the Universe from the same computation. The vertical dashed lines correspond to the start of kination, reheating, and the BBN. The parameters for both panels are $N_{\rm hyp} = 15$, $\Omega_{\rm r}^{\rm end} = 10^{-10}$ and $H = 10^{13}$ GeV.

To reheat the Universe, we assume a small amount of radiation is produced at the end of inflation e.g. through Ricci reheating [98, 99, 289]. During hyperkination, the radiation energy density is diluted as fast as that of the field, $\rho_{{\rm r},\phi} \propto a^{-4}$, so radiation stays subdominant. However, when standard kination starts, the field energy density dilutes faster, $\rho_\phi \propto a^{-6}$, and the radiation fraction grows until it overtakes the field. The Universe is reheated and radiation domination starts. We assume this to take place at high energies, above the BBN temperature $T_{\rm BBN} \approx 1$ MeV; afterwards, the Universe follows the standard ΛCDM expansion history.

The behaviour of the system can be solved from the Friedmann equations

$$3H^2 m_{\rm P}^2 = \rho_{\rm r} + \rho_\phi\,, \quad \rho_{\rm r} = 3(H_{\rm end})^2 m_{\rm P}^2 \times \Omega_{\rm r}^{\rm end} \left(\frac{a}{a_{\rm end}}\right)^{-4}\,, \tag{6.20}$$

combined with the first equations from Eqs. (6.10) and (6.11). Here $\Omega_{\rm r}^{\rm end}$ is the radiation energy density fraction (parameter) at the end of inflation and $a_{\rm end}$ and $H_{\rm end}$ are the scale factor and Hubble parameter at the end of inflation.

Figure 6.2 shows the behaviour of the energy densities solved numerically; for details on the numerical implementation, see Appendix C.2. It also shows the corresponding evolution of the barotropic parameter w, defined as the ratio between the total pressure and energy density of the Universe, taking values from $w = 1/3$ (hyperkination) to $w = 1$ (standard kination) back to $w = 1/3$ (radiation domination).

In summary, we assume a cosmological evolution where inflation is followed by two phases: hyperkination and kination, in this order. Reheating, which takes places at temperatures larger than $T_{\rm BBN}$, signals the end of these phases. After reheating, the conventional cosmic evolution with radiation and matter dominated eras follows[6].

The non-standard expansion history opens the door for new phenomenology. For one, it changes the matching between scales in the early and late Universe. Indeed, when inflation is followed by a stiff cosmological era with barotropic parameter w, the number of inflationary e-folds is increased by [258, 445, 1, 272] (see Eq. (2.43))

$$\Delta N = \frac{3w-1}{3(1+w)} \ln\left(\frac{V_{\rm end}^{1/4}}{T_{\rm reh}}\right). \tag{6.21}$$

It follows that hyperkination, for which $w = 1/3$, has a vanishing contribution. This is not the case for kination, with $w = 1$. Thus, in our scenario we have

$$\Delta N = \frac{1}{3} \ln\left(\frac{\rho_{\rm kin}^{1/4}}{T_{\rm reh}}\right), \tag{6.22}$$

where $\rho_{\rm kin} \ll V_{\rm end}$ is the energy density at the end of hyperkination and the onset of kination proper. Typically, this increases the remaining number of inflationary efolds after the cosmological scales exit the horizon to at most $N_* \simeq 65$, which implies $\Delta N \lesssim 5$, something that must be taken into account when calculating the

[6]Some authors (see Ref. [455] and the discussion on page 6 in Ref. [464]) have considered that the stiff era takes place after BBN, but before recombination. This would relax the lower bound for the temperature of the stiff phase to $T < 6\,\text{keV}$. However, this possibility is not considered in the present work.

inflationary observables.[7]

All in all, the CMB scales exit the Hubble radius approximately 60–65 e-folds before the end of inflation instead of the standard 50–60, see e.g. [1, 36]. This affects inflationary model building, although the effects are mitigated with respect to the standard kination scenario. In addition, the spectrum of primordial GWs is altered in ways that are sensitive to the duration of hyperkination.

6.3 Gravitational waves

6.3.1 Tensor perturbations and quantization

In this section we review the quantization of the primordial GWs, mainly following Sec. 2.1.3 (see Eq. (2.140) and below). To study the behaviour of GWs, we write the metric tensor as $g_{\mu\nu} = a^2\,(\eta_{\mu\nu} + h_{\mu\nu})$, where $\eta_{\mu\nu}$ is the Minkowski metric so that $a^2\eta_{\mu\nu} \equiv \bar{g}_{\mu\nu}$ is the unperturbed FLRW metric, and $h_{\mu\nu}$ is a small perturbation. We expand the action in Eq. (6.1) to second order in $h_{\mu\nu}$, keeping only the tensor modes[8], which evolve independently of other perturbations in linear perturbation theory. We obtain

$$\delta^{(2)}S = \sum_{s=\oplus,\otimes} \frac{m_{\rm P}^2}{4} \int \mathrm{d}\eta\, a^2 \int \mathrm{d}^3k \left(|h_{\vec{k}}^{s\prime}|^2 - k^2|h_{\vec{k}}^{s}|^2\right) , \tag{6.23}$$

where s indexes the two GW polarisations, and the polarization amplitudes h^s are defined through the Fourier decompositions

$$h^s(\vec{x}) = \int \frac{\mathrm{d}^3k}{(2\pi)^{3/2}}\, h_{\vec{k}}^{s}\, e^{i\vec{k}\cdot\vec{x}} , \tag{6.24}$$

so that $h_{\vec{k}}^{s}$ describes oscillations of a given polarization in directions perpendicular to the wave vector $\vec{k}$.

[7] Such an increase has some effect on the inflationary observables, but this effect is minimal. For example, in Starobinsky inflation [11] or Higgs inflation [390] (or α-attractors [465]), the scalar spectral index is $n_s \simeq 1 - \frac{2}{N_*}$. With $N_* = 60$ this results in $n_s = 0.966$. If we have $N_* = 65$ instead, then $n_s = 0.969$, which is still within the 1-σ contour of the Planck satellite observations [10].

[8] The tensor perturbations obey $\partial_\mu h^{\mu\nu} = 0$ and $h^\mu{}_\mu = 0$.

The amplitudes h^s behave as massless scalar fields, up to normalization, following the Klein–Gordon equation

$$h^{s\prime\prime} + 2\mathcal{H}h^{s\prime} + \nabla^2 h^s = 0 \tag{6.25}$$

with wave solutions. Here $\mathcal{H} \equiv a'/a$ and $\nabla^2 \equiv \partial_i\partial_i$ where i is summed over the spatial indices. The corresponding energy-momentum tensor is

$$T^{\mathrm{GW}}_{\mu\nu} = -\frac{2}{\sqrt{-\bar{g}}}\frac{\delta(\delta^{(2)}S)}{\delta\bar{g}^{\mu\nu}} = \sum_{s=\oplus,\otimes}\frac{m_{\mathrm{P}}^2}{2}\left(\partial_\mu h^s\partial_\nu h^s - \frac{1}{2}\bar{g}_{\mu\nu}\bar{g}^{\alpha\beta}\partial_\alpha h^s\partial_\beta h^s\right), \tag{6.26}$$

so that the GW energy density reads

$$\rho_{\mathrm{GW}} = a^{-2}T^{\mathrm{GW}}_{00} = \sum_{s=\oplus,\otimes}\frac{m_{\mathrm{P}}^2}{4a^2}\left[(h^{s\prime})^2 + (\nabla h^s)^2\right]. \tag{6.27}$$

In order to quantize the primordial GWs, we first go to the canonically normalized variables $v^s = m_{\mathrm{P}}ah^s/\sqrt{2}$, so that (after integration by parts) the action in Eq. (6.23) becomes

$$\delta^{(2)}S = \sum_{s=\oplus,\otimes}\frac{1}{2}\int \mathrm{d}\eta\,\mathrm{d}^3k\left[|v^{s\prime}_{\vec{k}}|^2 - \left(k^2 - \frac{a''}{a}\right)|v^s_{\vec{k}}|^2\right]. \tag{6.28}$$

This is the Minkowski space action for a free field with mass a''/a, quantized the standard way by writing

$$\hat{v}^s(\eta,\vec{x}) = \int\frac{\mathrm{d}^3k}{(2\pi)^{3/2}}\left[v^s_k(\eta)\hat{a}^s_{\vec{k}}e^{i\vec{k}\cdot\vec{x}} + v^{s*}_k(\eta)\hat{a}^{s^\dagger}_{\vec{k}}e^{-i\vec{k}\cdot\vec{x}}\right], \tag{6.29}$$

where $\hat{a}^s_{\vec{k}}$, $\hat{a}^{s^\dagger}_{\vec{k}}$ are the ladder operators following the canonical commutation relations

$$[\hat{a}^{s'}_{\vec{k}'}, \hat{a}^{s^\dagger}_{\vec{k}}] = \delta^{s's}\delta^{(3)}(\vec{k}' - \vec{k}). \tag{6.30}$$

Time evolution is delegated to the mode functions v^s_k, which follow the Mukhanov–Sasaki equations derived from Eq. (6.28),

$$v^{s\prime\prime}_k + \left(k^2 - \frac{a''}{a}\right)v^s_k = 0. \tag{6.31}$$

Note that, due to the ladder operators, the mode functions v^s_k differ in normalization from the classical Fourier modes $v^s_{\vec{k}}$. Abusing the notation slightly, we differentiate

these by writing k instead of $\vec{k}$ as the mode function index—in an FLRW background, the quantum mode functions only depend on the magnitude of the wave vector and not its direction. Analogously, we define $\hat{h}^s = \sqrt{2}\hat{v}^s/(am_{\rm P})$, $h^s_k = \sqrt{2}v^s_k/(am_{\rm P})$.

Deep inside the Hubble radius, $k \gg \mathcal{H}$, the GWs do not feel the expansion of space, the mass term a''/a is negligible, and Eq. (6.31) has the standard vacuum solution

$$v^s_k = \frac{1}{\sqrt{2k}} e^{-ik\eta}\,, \qquad v^{s\prime}_k = -ikv^s_k\,. \tag{6.32}$$

When the mode functions follow Eq. (6.32), the state annihilated by $\hat{a}^s_k$ is the Bunch–Davies vacuum [82]; we take the perturbations to start in this vacuum state during inflation. Over their cosmic evolution, the modes stretch and exit the Hubble radius, evolving beyond Eq. (6.32). After inflation, they re-enter the Hubble radius, this time following the general sub-Hubble form

$$v^s_k = \frac{1}{\sqrt{2k}} \left[\lambda_+(k)e^{-ik\eta} + \lambda_-(k)e^{ik\eta}\right]\,. \tag{6.33}$$

We will solve the coefficients $\lambda_\pm(k)$ for a given cosmic history in section 6.4.2; since the Mukhanov–Sasaki equation conserves the Wronskian of its solutions, we have $|\lambda_+|^2 - |\lambda_-|^2 = 1$, set by the initial vacuum in Eq. (6.32). The coefficient λ_- contains the GW excitations, the part beyond the vacuum solution in Eq. (6.32).

Let us next consider the energy density of the GWs induced by the above process. The late-time GW energy density is dominated by high-k, sub-Hubble modes, for which Eq. (6.33) applies. Using this result, we replace h^s by $\hat{h}^s$ in the energy-momentum tensor in Eq. (6.26) and compute its expectation value. The result is

$$\begin{aligned}\langle\hat{\rho}_{\rm GW}\rangle \quad &= \sum_{s=\oplus,\otimes} \frac{m_{\rm P}^2}{2} \int \frac{(\mathrm{d}\ln k)\,k^3}{4\pi^2 a^2}\left(|h^{\prime s}_k|^2 + k^2|h^s_k|^2\right) \approx \int_{k=\mathcal{H}} \frac{(\mathrm{d}\ln k)}{2\pi^2}\frac{k^4}{a^4}\left(|\lambda_+|^2 + |\lambda_-|^2\right) \\ &= \int_{k=\mathcal{H}} \frac{(\mathrm{d}\ln k)}{\pi^2}\frac{k^4}{a^4}\left(|\lambda_-|^2 + \frac{1}{2}\right)\,,\end{aligned} \tag{6.34}$$

where we used the Wrosnkian condition, and the fact that the integration limit $k > \mathcal{H}$ restricts us to sub-Hubble modes. In the last line, we have taken the polarization sum (starting from the Bunch–Davies vacuum, $\lambda_\pm$ are identical for both polarizations).

Note that, regardless of $\lambda_\pm$, the final term of 1/2 makes Eq. (6.34) diverge for large k—this is the usual energy density vacuum divergence of quantum field theory. One can regularize the result by normal ordering the ladder operators in $\hat{\rho}_{\rm GW}$. However, this has to be done with the late-time ladder operators which annihilate the late-time Bunch–Davies vacuum. These are related to the original ladder operators $\hat{a}_k^s$ by a Bogoliubov transformation; for a detailed discussion, see e.g. Ref. [82]. The regularized energy density becomes

$$\langle\hat{\rho}_{\rm GW}\rangle \approx \int_{k=\mathcal{H}} \frac{(\mathrm{d}\ln k)}{\pi^2}\frac{k^4}{a^4}|\lambda_-|^2\,. \tag{6.35}$$

In practice, all of our modes of interest are highly excited with $|\lambda_-| \gg 1$, so that Eqs. (6.34) and (6.35) are approximately equal. In this limit, the vacuum contribution is negligible and the GWs are essentially classical.

6.3.2 Energy density scaling and the problem with kination

From Eq. (6.35), we see that the sub-Hubble GWs scale as radiation, with $\rho_{\rm GW} \propto a^{-4}$, as expected for massless degrees of freedom. In cosmology with a standard expansion history, only a small amount of GWs are generated during inflation, and they always stay subdominant compared to the background radiation energy density. However, during kination, the background dilutes faster than radiation, and the GW fraction grows. The resulting GW spectrum is peaked and tends to either clash with bounds on the number of relativistic degrees of freedom during BBN or be hard to observe in GW experiments [294, 293, 446, 447, 448, 449]. In the following sections, we will demonstrate that adding a period of hyperkination helps with this issue, opening a wider parameter space for allowed GW spectra.

6.4 Analytical solution

6.4.1 Solving the background

Let us move on to solve the GW spectrum analytically. The first step is to solve the background dynamics, in particular the scale factor a, in the presence of radiation, as a function of the conformal time η. This provides us with a''/a, allowing us to later solve the Mukhanov–Sasaki equation for the GW mode functions.

The scale factor evolves through different epochs during the cosmic history: inflation, hyperkination, kination, and radiation domination. The transitions between the epochs, assumed to be instantaneous, happen at conformal times $\eta_{\rm end}$ (end of inflation and start of hyperkination), $\eta_{\rm kin}$ (end of hyperkination and start of kination), and $\eta_{\rm reh}$ (end of kination and start of radiation domination, *i.e.*, reheating), which we will also solve in terms of the model parameters below. We use the same indices to refer to various variables evaluated at these times. We require the continuity of $a(\eta)$ and its derivative at the transition times; between them, we solve $a(\eta)$ from

$$\mathrm{d}\eta = \frac{\mathrm{d}t}{a} = \frac{\mathrm{d}a}{a^2 H} = \frac{\mathrm{d}a}{a^2}\sqrt{\frac{3m_{\rm P}^2}{\rho}}\,. \tag{6.36}$$

If we know how the Universe's energy density ρ scales in a, we can integrate and invert Eq. (6.36) to obtain $a(\eta)$ epoch by epoch. We will normalize the scale factor so that

$$a(\eta_{\rm end}) = 1\,, \tag{6.37}$$

and write $a = e^N$, so that N counts the e-folds since the end of inflation.

For inflation, we assume a generic slow-roll inflationary phase, with the end of inflation $\eta_{\rm end} < 0$ determined by the usual condition

$$\epsilon \equiv -\frac{\dot{H}}{H^2} = 1\,, \tag{6.38}$$

where ϵ is the first Hubble slow-roll parameter. For the reader's benefit, we will express our GW mode functions as a function of ϵ, approximated to be constant. In

the example spectra we consider in section 6.5, we work in the pure de Sitter limit $\epsilon = 0$. To avoid clutter (and slightly abusing the notation), we will use H, as for pure de Sitter, to refer to the Hubble parameter at the end of inflation $H_{\rm end}$.

For hyperkination, we get $\rho(N)$ from Eq. (6.13), where ϕ' follows the first branch of Eq. (6.16) and we write the initial field velocity ϕ_0' in terms of $N_{\rm hyp}$ as explained below the equation. For kination and radiation domination, we use the standard results $\rho \propto a^{-6}$ and $\rho \propto a^{-4}$. With these, the full behaviour of the scale factor becomes

$$a = \begin{cases} \left[-\frac{1}{(1-\epsilon)H\eta}\right]^{1/(1-\epsilon)}, & \eta \leq \eta_{\rm end}\,, \\ e^{N_{\rm hyp}} \sin\left[e^{-N_{\rm hyp}}(H\eta+1) + \sin^{-1} e^{-N_{\rm hyp}}\right], & \eta_{\rm end} \leq \eta \leq \eta_{\rm kin}\,, \\ a_{\rm kin}\sqrt{2\mathcal{H}_{\rm kin}(\eta-\eta_{\rm kin})+1}\,, & \eta_{\rm kin} \leq \eta \leq \eta_{\rm reh}\,, \\ a_{\rm reh}[\mathcal{H}_{\rm reh}(\eta-\eta_{\rm reh})+1]\,, & \eta_{\rm reh} \leq \eta\,. \end{cases} \tag{6.39}$$

For the hyperkination expression, we used

$$\eta_{\rm end} = -\frac{1}{(1-\epsilon)H} \simeq -\frac{1}{H}\,, \tag{6.40}$$

which follows from Eq. (6.37) and the first line in Eq. (6.39). We also used Eq. (6.19) with $3H^2 m_{\rm P}^2 = \rho_{\rm end}$ to eliminate α. For a long hyperkination period with $N_{\rm hyp} \gtrsim 1$, we can approximate the expression as

$$a(\eta) \simeq e^{N_{\rm hyp}} \sin\left[e^{-N_{\rm hyp}}(H\eta+2)\right] \simeq H\eta + 2\,, \tag{6.41}$$

where the right-hand-side is exactly the scale factor for a radiation-dominated universe, compare to the last line in Eq. (6.39). Note that the last approximation stops being valid at large times $\eta \sim e^{N_{\rm hyp}}/H$ and one needs to use the middle expression instead. This is the case below, when we obtain an analytical estimate for $\eta_{\rm kin}$.

For kination and radiation domination, the constants in Eq. (6.39) are to be read

off from the end values during the previous phase. Using Eq. (6.41), we have

$$\begin{aligned} a_{\rm kin} &= e^{N_{\rm hyp}} \sin\left[e^{-N_{\rm hyp}}(H\eta_{\rm kin}+2)\right] , \\ a_{\rm reh} &= a_{\rm kin}\sqrt{2\mathcal{H}_{\rm kin}(\eta_{\rm reh}-\eta_{\rm kin})+1}\,, \end{aligned} \tag{6.42}$$

and

$$\begin{aligned} \mathcal{H}_{\rm kin} &= \frac{He^{-N_{\rm hyp}}}{\tan\left[e^{-N_{\rm hyp}}(H\eta_{\rm kin}+2)\right]}\,, \\ \mathcal{H}_{\rm reh} &= \frac{\mathcal{H}_{\rm kin}}{2\mathcal{H}_{\rm kin}(\eta_{\rm reh}-\eta_{\rm kin})+1}\,. \end{aligned} \tag{6.43}$$

In practice, it is a good approximation to use

$$a_{\rm kin} = H\eta_{\rm kin}+2\,, \qquad \mathcal{H}_{\rm kin} = \frac{H}{H\eta_{\rm kin}+2}\,. \tag{6.44}$$

Let us next estimate the conformal times for the rest of the transition points. We do this by solving an equation where a is expressed in two different ways, through Eq. (6.39) and through a condition related to our model parameters.

As a reminder, we define the beginning of kination as the time at which both addends inside the parenthesis in the energy density in Eq. (6.11) become equal. Since this happens at large times $\eta \sim e^{N_{\rm hyp}}/H$, we use the middle expression in Eq. (6.41) together with Eq. (6.18) to obtain

$$a_{\rm kin} = e^{N_{\rm hyp}} \sin\left[e^{-N_{\rm hyp}}(H\eta_{\rm kin}+2)\right] = e^{N_{\rm kin}} = \frac{e^{N_{\rm hyp}}}{\sqrt{2}}, \tag{6.45}$$

so that

$$\eta_{\rm kin} = \frac{\frac{\pi}{4}e^{N_{\rm hyp}}-2}{H} \simeq \frac{\pi e^{N_{\rm hyp}}}{4H}\,. \tag{6.46}$$

The time of reheating $\eta_{\rm reh}$ can be estimated by noting that the total energy density during kination scales as $\rho \propto a^{-6}$, while that of the radiation scales as $\rho_{\rm r} \propto a^{-4}$. Thus, the density parameter of radiation during kination scales as $\Omega_{\rm r} \propto a^2$. By reheating, radiation is the dominant component, that is,

$$1 \approx \Omega_{\rm r}^{\rm reh} \approx \Omega_{\rm r}^{\rm kin}\left(\frac{a_{\rm reh}}{a_{\rm kin}}\right)^2 = \Omega_{\rm r}^{\rm end}\frac{2H^2\eta_{\rm kin}\eta_{\rm reh}}{e^{2N_{\rm hyp}}/2}\,, \tag{6.47}$$

so that

$$\eta_{\rm reh} = \frac{e^{N_{\rm hyp}}}{\pi \Omega_{\rm r}^{\rm end} H}\,, \tag{6.48}$$

where we used $\Omega_{\rm r}^{\rm kin} \approx \Omega_{\rm r}^{\rm end}$, since the field and radiation redshift similarly during hyperkination, together with the approximation $|\eta_{\rm end}| \ll \eta_{\rm kin} \ll \eta_{\rm reh}$ yielding $a_{\rm reh} \approx H\sqrt{2\eta_{\rm kin}\eta_{\rm reh}}$ from Eqs. (6.42) and (6.43). We also used Eq. (6.45) for $a_{\rm kin}$ and Eq. (6.46) for $\eta_{\rm kin}$.

6.4.2 The gravitational wave mode functions

The next step is to obtain expressions for the GW mode functions. We proceed by matching the solutions and their derivatives at the transitions between epochs. To simplify the expressions, we do the matching in the super-Hubble limit, which gives an excellent approximation except for modes entering the horizon around the transitions. Our goal is to obtain the coefficients $\lambda_-(k)$ from Eq. (6.33) for each mode so that we can read off their asymptotic, sub-Hubble behaviour. We report the details of the somewhat technical calculations in Appendix C.3, while in the present section we simply give the main results, as well as a comparison between the analytical and numerical solutions in Fig. 6.3 (for details on the numerics see AppendixC.2).

We can summarize the scale factor time dependence from the last section as

$$a = \left(\frac{\eta}{\eta_c}\right)^{1/2-\nu}\,, \qquad \nu \equiv \frac{3(w-1)}{2(1+3w)}\,, \tag{6.49}$$

where w is the corresponding barotropic parameter of the Universe, so that $\nu = 3/2$ ($w = -1$) for de Sitter, $\nu = 3/2 + \epsilon \equiv \nu_I$ for a more realistic quasi-de Sitter inflation [425], $\nu = 0$ ($w = 1$) for kination and $\nu = -1/2$ ($w = 1/3$) for hyperkination and radiation domination. We then get

$$\frac{a''}{a} = -\left(\frac{1}{4} - \nu^2\right)\frac{1}{\eta^2}\,. \tag{6.50}$$

The constants η_c can be read from the previous section, giving

$$\frac{a''}{a} = \begin{cases} \frac{2+3\epsilon}{\eta^2}\,, & \eta \leq \eta_{\rm end}, \\ 0\,, & \eta_{\rm end} \leq \eta \leq \eta_{\rm kin}, \\ -\frac{1}{4z^2}\,, & \eta_{\rm kin} \leq \eta \leq \eta_{\rm reh}, \\ 0\,, & \eta_{\rm reh} \leq \eta, \end{cases} \tag{6.51}$$

where we defined for kination

$$z \equiv \eta - \frac{\eta_{\rm kin}}{2} + \frac{1}{H}\,. \tag{6.52}$$

Note that $a'' = 0$ during hyperkination. This feature is shared with the period of radiation domination, during which the spectrum is flat, a result that was originally derived in Ref. [292]. Therefore we expect the peak from kination to be truncated by a secondary plateau.

With this, we can proceed to solve the Mukhanov–Sasaki equation (6.31). Making the change of variables $x = k\eta$ ($x = -k\eta$ during inflation when $\eta < 0$) and redefining the mode functions as $v = \sqrt{x}g$, it can be recast as a Bessel equation

$$x^2\frac{{\rm d}^2 g}{{\rm d}x^2} + x\frac{{\rm d}g}{{\rm d}x} + (x^2 - \nu^2)g = 0\,, \tag{6.53}$$

the most general solution of which is given by

$$g(x) = c_1 H_\nu^{(1)}(x) + c_2 H_\nu^{(2)}(x)\,, \tag{6.54}$$

where $H_\nu^{(1)}$ and $H_\nu^{(2)}$ are Hankel functions of the first and second kind respectively. Using the values of ν from above, the solutions during inflation, hyperkination, kination, and radiation domination become

$$v_k^s(\eta) = \begin{cases} \sqrt{\frac{\pi}{4k}}\sqrt{-k\eta}\,e^{i\frac{\pi}{4}(1+2\nu_I)}H_{\nu_I}^{(1)}(-k\eta)\,, & \eta \leq \eta_{\rm end}\,, \\ \frac{1}{\sqrt{2k}}\left[\alpha_+(k)e^{-ik\eta} + \alpha_-(k)e^{ik\eta}\right]\,, & \eta_{\rm end} \leq \eta \leq \eta_{\rm kin}\,, \\ \sqrt{\frac{\pi z}{4}}\left[\beta_+(k)e^{-i\pi/4}H_0^{(2)}(kz) + \beta_-(k)e^{i\pi/4}H_0^{(1)}(kz)\right]\,, & \eta_{\rm kin} \leq \eta \leq \eta_{\rm reh}\,, \\ \frac{1}{\sqrt{2k}}\left[\gamma_+(k)e^{-ik\eta} + \gamma_-(k)e^{ik\eta}\right]\,, & \eta_{\rm reh} \leq \eta\,, \end{cases} \tag{6.55}$$

where we fixed the coefficients $c_{1,2}$ during inflation so that in the initial sub-Hubble regime, $-k\eta \gg 1$, the mode functions obey the Bunch–Davies vacuum conditions in Eq. (6.32). The constants and phases in the other branches have been chosen so that the coefficients $\alpha_\pm$, $\beta_\pm$, and $\gamma_\pm$ correspond to the $\lambda_\pm$ of Eq. (6.33) in the late sub-Hubble limit $k\eta \gg 1$. Their values are fixed by requiring the continuity of v_k^s and its derivative at the transition times $\eta_{\rm end}$, $\eta_{\rm kin}$, and $\eta_{\rm reh}$. Matching the branches in the super-Hubble limit yields

$$\alpha_\pm(k) = \mp\frac{f(\epsilon)}{2}\left(\frac{H}{k}\right)^{2+\epsilon}, \tag{6.56}$$

$$\beta_\pm(k) = 2ie^{\pm i\pi/4}\alpha_-(k)\sqrt{\frac{k\eta_{\rm kin}}{\pi}}, \tag{6.57}$$

$$\gamma_\pm(k) = \mp\alpha_-(k)\sqrt{\frac{\eta_{\rm kin}}{2z_{\rm reh}}}, \tag{6.58}$$

where

$$f(\epsilon) \equiv e^{i\pi\epsilon/2}\frac{\Gamma(3/2+\epsilon)}{\Gamma(3/2)}2^\epsilon, \tag{6.59}$$

and $z_{\rm reh} \simeq \eta_{\rm reh}$ is z from (6.52) evaluated at $\eta_{\rm reh}$. For the scale-invariant case with $\epsilon \to 0$, $f(\epsilon) \to 1$, the moduli squared of the coefficients take the simplified forms

$$\begin{aligned}|\alpha_-(k)|^2 &= \frac{H^4}{4k^4}, \\ |\beta_-(k)|^2 &= \frac{H^4}{\pi k^4}k\eta_{\rm kin}, \\ |\gamma_-(k)|^2 &= \frac{H^4}{4k^4}\frac{\eta_{\rm kin}}{2\eta_{\rm reh}}.\end{aligned} \tag{6.60}$$

Note that since we did the matchings at the super-Hubble limit, the expressions in Eqs. (6.56)–(6.58) and (6.60) only apply for modes that are super-Hubble during the corresponding transition. To find the final behaviour of a mode, we take the last transition where this applies, track the following mode function from Eq. (6.55) to the sub-Hubble limit, where it takes the form in Eq. (6.33), and equate the α_-, β_-, or γ_- with the coefficient λ_-. Indeed, after a mode has settled to its asymptotic sub-Hubble behaviour, its evolution is trivial—redshfiting gently like radiation—and it won't be sensitive to further changes in the equation of state of the Universe.

From the Mukhanov–Sasaki solutions in Eq. (6.55) we can also deduce the metric perturbations h_k^s. Using the scale factor expressions, $a \simeq H\eta$, $a \simeq H\sqrt{2\eta_{\rm kin}\eta}$, and $a \simeq H\sqrt{\eta_{\rm kin}/(2\eta_{\rm reh})}\eta$ during hyperkination, kination, and radiation domination, respectively, and using Eqs. (6.56)–(6.58), we get

$$h_k^s(\eta) = \begin{cases} \frac{iH}{m_{\rm P}k^{3/2}} f(\epsilon) \left(\frac{k}{H}\right)^{-\epsilon} j_0(k\eta)\,, & \eta_{\rm end} \leq \eta \leq \eta_{\rm kin}\,, \\ \frac{iH}{m_{\rm P}k^{3/2}} f(\epsilon) \left(\frac{k}{H}\right)^{-\epsilon} J_0(kz)\,, & \eta_{\rm kin} \leq \eta \leq \eta_{\rm reh}\,, \\ \frac{iH}{m_{\rm P}k^{3/2}} f(\epsilon) \left(\frac{k}{H}\right)^{-\epsilon} j_0(k\eta)\,, & \eta_{\rm reh} \leq \eta\,, \end{cases} \tag{6.61}$$

where $j_0(k\eta) = \sqrt{\pi/(2k\eta)}J_{1/2}(k\eta) = \sin k\eta/(k\eta)$ is a spherical Bessel function of the first kind and J_0 is a Bessel function of the first kind. For a comparison with the numerical solutions in the scale-invariant case, see Fig. 6.3. We do not include the inflationary metric perturbations in Eq. (6.61) as they do not simplify as nicely as the others.

Note that in the super-Hubble limit, all the expressions in Eq. (6.61) freeze to

$$h_k^s(\eta) \xrightarrow{k|\eta|\to 0} \frac{iH}{m_{\rm P}k^{3/2}} f(\epsilon) \left(\frac{k}{aH}\right)^{-\epsilon} \xrightarrow{\epsilon\to 0} \frac{iH}{m_{\rm P}k^{3/2}}\,, \tag{6.62}$$

where the last one is the standard scale-invariant result. Note that this result holds also for inflation. In principle, one can use this as an initial condition and solve the Klein–Gordon equation (6.25) to obtain Eq. (6.61) separately in each phase without the matching procedure described above[9]. One can then use Eq. (6.34) to obtain the unregularized GW energy density. We use this method in our numerical solutions. The expressions for $\alpha_\pm$, $\beta_\pm$, and $\gamma_\pm$ are still needed to regularize the integral in Eq. (6.34), and they are the conventional way to express the GW excitations in the literature.

[9]In particular, GWs at the CMB scales stay frozen throughout the kination and hyperkination periods and are thus not affected by the non-standard background evolution. The same is true for the curvature perturbation $\mathcal{R}$—see [466] for a linear treatment of $\mathcal{R}$ in a model with a non-standard kinetic sector, Appendix B of [362] for an application to Palatini R^2 models, and [467] for a general proof that $\mathcal{R}$ freezes at super-horizon scales.

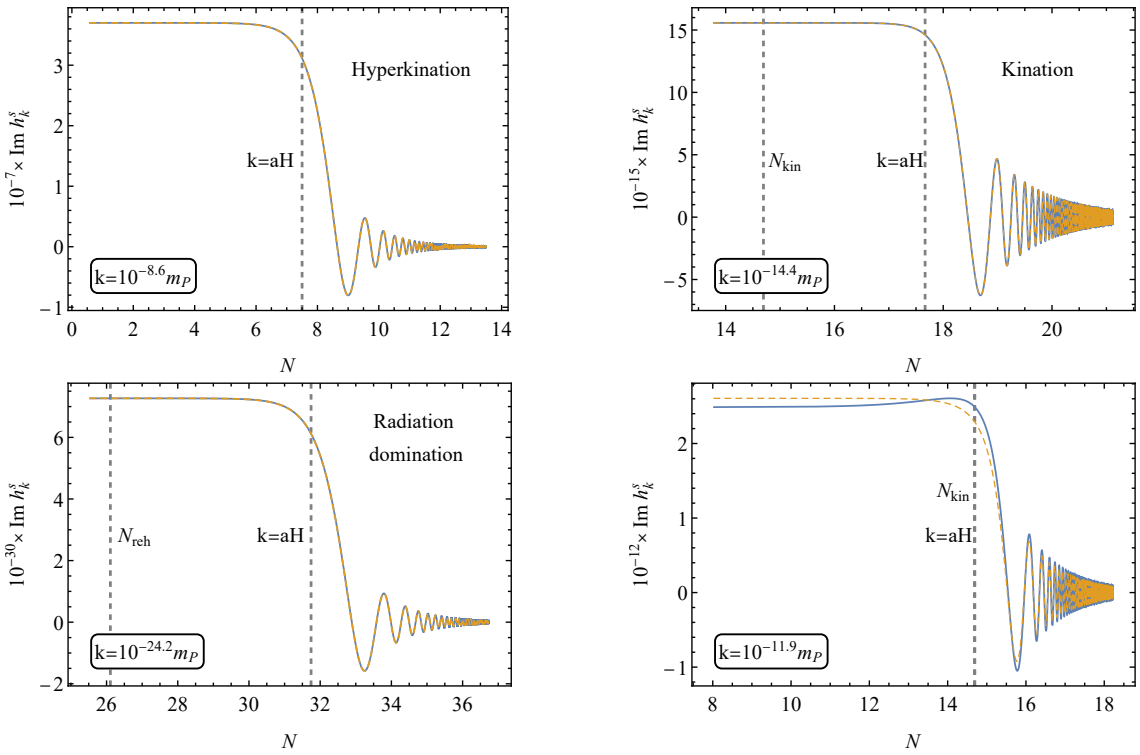

Figure 6.3: Comparison between the analytical solution (solid blue lines) and its numerical counterpart (dashed orange) of the imaginary part of the mode functions h_k^s as a function of the elapsing number of e-folds when the mode enters the horizon during the hyperkination (top left), kination (top right) and radiation domination (bottom left) periods. The match is excellent, except when the wavenumber of the mode is comparable to the horizon size at a transition (bottom right). The vertical dashed lines represent the time of horizon crossing $k = aH$ and the times at which kination starts $N_{\rm kin}$ and reheating happens $N_{\rm reh}$. The parameters for all panels are $N_{\rm hyp} = 15$, $\Omega_{\rm r}^{\rm end} = 10^{-10}$ and $H = 10^{13}$ GeV.

6.5 Gravitational wave observations

6.5.1 Gravitational wave spectrum

We are finally in a position to calculate the spectral energy density of the primordial GW background. It is defined as

$$\Omega_{\rm GW}(k,\eta) \equiv \frac{1}{\rho(\eta)}\frac{{\rm d}\rho_{\rm GW}(k,\eta)}{{\rm d}\ln k} = \frac{1}{\rho(\eta)}\frac{k^4|\lambda_-(k)|^2}{\pi^2 a^4(\eta)}\,, \tag{6.63}$$

where ρ is the total energy density of the Universe and $\rho_{\rm GW}(k,\eta)$ is the contribution to the GW energy density from modes around k, given by Eq. (6.35) for the dominant, sub-Hubble modes. Here λ_- is to be matched to α_-, β_-, or γ_- as explained above.

To evaluate Eq. (6.63) at a specific time, we note that the radiation energy density can be written as (remember our normalization $a_{\rm end}=1$)[10]

$$\rho_{\rm r}(\eta)=\Omega_{\rm r}(\eta)\rho(\eta)=\Omega_{\rm r}^{\rm end}\rho_{\rm end}a^{-4}(\eta)\,, \tag{6.64}$$

so that

$$\rho(\eta)a^4(\eta)=\rho_{\rm end}\frac{\Omega_{\rm r}^{\rm end}}{\Omega_{\rm r}(\eta)}\,. \tag{6.65}$$

In particular, using the current radiation temperature and total energy density, $T_0=2.7\ {\rm K}=0.23\times10^{-9}$ MeV and $\rho_0=1.05\times10^{-120}m_{\rm P}^4$ [8], we obtain $\rho_{\rm r}^0=8.79\times10^{-125}m_{\rm P}^4$ and $\Omega_{\rm r}^0=8.37\times10^{-5}$. We use the index '0' to refer to quantities today. With this and the de Sitter limit results in Eq. (6.60) together with Eqs. (6.46) and (6.48), the GW spectrum today becomes

$$\Omega_{\rm GW}(k,\eta_0)=\begin{cases}\frac{\Omega_{\rm r}^0}{96}\left(\frac{H}{m_{\rm P}}\right)^2, & k<k_{\rm reh},\\ \frac{\Omega_{\rm r}^0}{12\pi^2\Omega_{\rm r}^{\rm end}}\left(\frac{H}{m_{\rm P}}\right)^2\frac{k}{H}e^{N_{\rm hyp}}, & k_{\rm reh}<k<k_{\rm kin},\\ \frac{\Omega_{\rm r}^0}{12\pi^2\Omega_{\rm r}^{\rm end}}\left(\frac{H}{m_{\rm P}}\right)^2, & k_{\rm kin}<k<k_{\rm end}.\end{cases} \tag{6.66}$$

Below, we will refer to the different branches as $\Omega_{\rm GW}^{\rm rad}$, $\Omega_{\rm GW}^{\rm kin}$, and $\Omega_{\rm GW}^{\rm hyp}$. The boundary values are given by $k=\mathcal{H}$ at the end of inflation and at the transition times. Using Eqs. (6.42) and (6.43), we get

$$\begin{aligned}k_{\rm end}&=H\,,\\ k_{\rm kin}&\simeq\frac{1}{\eta_{\rm kin}}=\frac{4H}{\pi e^{N_{\rm hyp}}}\,,\\ k_{\rm reh}&\simeq\frac{1}{2\eta_{\rm reh}}=\frac{\pi\Omega_{\rm r}^{\rm end}H}{2e^{N_{\rm hyp}}}\,,\end{aligned} \tag{6.67}$$

[10] We neglect the change in the effective number of relativistic species contributing to the entropy $g_{*S}(T)$ and to the energy density $g_*(T)$. This introduces an additional mild scale dependence into the spectrum. For further details, we refer the reader to Ref. [468], and in particular to Fig. 4 therein.

where we approximated $|\eta_{\rm end}| \ll \eta_{\rm kin} \ll \eta_{\rm reh}$.

In our figures, we show the spectrum as a function of f, the GW frequency today. To relate f to our wavenumber[11] k, we use Eq. (6.64) and $\rho = 3H^2 m_{\rm P}^2$, yielding

$$f = \frac{k}{2\pi a_0} = \frac{1}{2\pi}\left(\frac{\Omega_{\rm r}^0 H_0^2}{\Omega_{\rm r}^{\rm end} H^2}\right)^{1/4} k\,. \tag{6.68}$$

An important frequency is the one that corresponds to BBN. It does not depend on the early expansion history, and we can solve it explicitly as

$$\begin{aligned} f_{\rm BBN} = &\quad \frac{1}{2\pi}\frac{a_{\rm BBN} H_{\rm BBN}}{a_0} = \frac{1}{2\pi}\left(\frac{\rho_{\rm r}^0}{\rho_{\rm BBN}}\right)^{1/4}\left(\frac{\rho_{\rm BBN}}{3m_{\rm P}^2}\right)^{1/2} \\ \simeq &\quad 1.36\times 10^{-11}\,{\rm Hz}\,, \end{aligned} \tag{6.69}$$

where we used $\rho_{\rm BBN} \simeq 3\times 10^{-86} m_{\rm P}^4$. We present $f_{\rm BBN}$ as a vertical dotted line in our graphs.

We show a comparison between the numerical and analytical spectra, for an example set of parameters, in Fig. 6.4. We see that the analytical expressions for the spectrum are very accurate. In Fig. 6.5 we present some example analytical spectra superimposed with the power-law integrated curves (PLICs) for future GW experiments.

From Eqs. (6.66) and (6.67), we can straightforwardly understand the shape of the spectrum. The height of the first plateau, corresponding to hyperkination, is given by the combination $H^2/(\Omega_{\rm r}^{\rm end} m_{\rm P}^2)$, *i.e.*, the larger the energy density at the end of inflation and the smaller the reheating efficiency, the larger the energy density spectrum amplitude will be. The third free parameter of our theory, the number of e-folds of hyperkination $N_{\rm hyp}$, controls the length of the boosted spectrum; the longer the hyperkination period lasts, the more stretched the boosted spectrum is. In contrast, the height of the second plateau depends on $H^2/m_{\rm P}^2$, *i.e.*, it depends on the energy scale at the end of inflation only, the standard result from a scenario

[11] Note that, since we have set $a = 1$ at the end of inflation instead of today as is customary, the numerical values of our k differ from those of the usual comoving wavenumber. Equation (6.68) takes this into account.

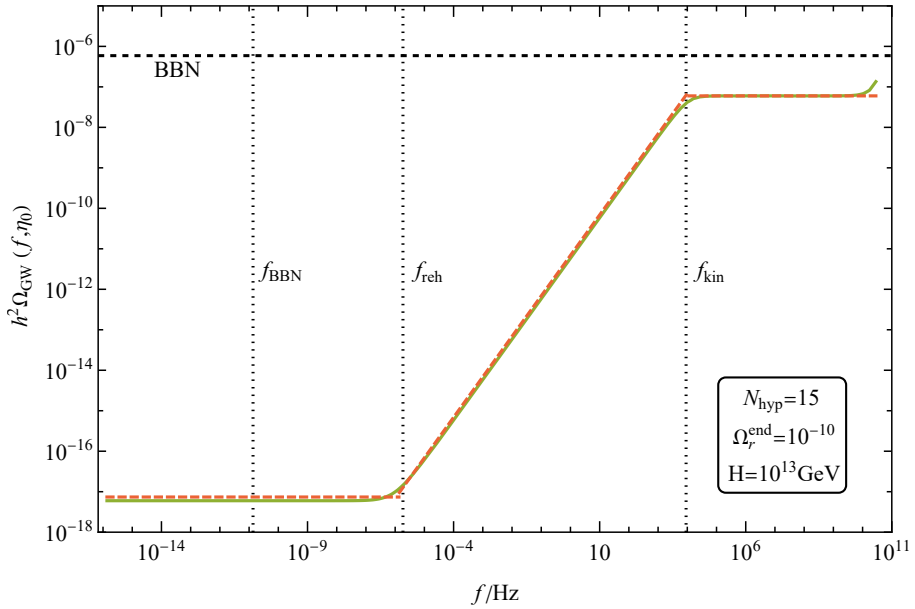

Figure 6.4: Analytical spectral energy density of the primordial GWs (dashed orange) and its numerical counterpart (full green). For details on the numerical solution, we refer the reader to Appendix C.2. The vertical dotted lines represent the frequencies associated with the start of kination, reheating and BBN, while the horizontal dashed line represents the BBN bound on the spectrum. The numerical spectral energy density is not well resolved at the largest frequencies because the modes re-entering the horizon right after inflation are never frozen as assumed in the code. This leads to the unphysical upslope around 10^{11} Hz. The parameters used are $N_{\rm hyp} = 15$, $\Omega_{\rm r}^{\rm end} = 10^{-10}$ and $H = 10^{13}$ GeV.

with no period of kinetic domination, originally derived in Ref. [292]. Both plateaus are connected via a region growing linearly with the frequency f, corresponding to the kination period. At large frequencies, the spectrum is cut off at the last mode to be excited by inflation. At small frequencies, there is no cutoff; the first line in Eq. (6.66) applies to all modes that re-enter during radiation domination.

Although it is easier to understand the shape of the spectrum in terms of $N_{\rm hyp}$, the free parameter in the action in Eq. (6.1) is α. For this reason, we present below our results regarding the parameter space of the theory in terms of α and not $N_{\rm hyp}$.

The two are related by Eq. (6.19). For completeness, we present here the spectrum in terms of α, and with k replaced with f:

$$\Omega_{\rm GW}(f,\eta_0) = \begin{cases} \frac{\Omega_{\rm r}^0}{96}\left(\frac{H}{m_{\rm P}}\right)^2 , & f < f_{\rm reh}\,, \\ \left(\frac{\Omega_{\rm r}^0}{\Omega_{\rm r}^{\rm end}}\right)^{3/4} \frac{H^{3/2}}{6\pi H_0^{1/2} m_{\rm P}^2} \left(\frac{1+\sqrt{1+36\alpha H^2/m_{\rm P}^2}}{2}\right)^{\frac{1}{2}} f\,, & f_{\rm reh} < f < f_{\rm kin}\,, \\ \frac{\Omega_{\rm r}^0}{12\pi^2\Omega_{\rm r}^{\rm end}}\left(\frac{H}{m_{\rm P}}\right)^2 , & f_{\rm kin} < f < f_{\rm end}\,, \end{cases} \tag{6.70}$$

where

$$f_{\rm end} = \frac{1}{2\pi}\left(\frac{\Omega_{\rm r}^0 H_0^2 H^2}{\Omega_{\rm r}^{\rm end}}\right)^{1/4} , \qquad f_{\rm kin} = \frac{2}{\pi^2}\left(\frac{\Omega_{\rm r}^0 H_0^2 H^2}{\Omega_{\rm r}^{\rm end}}\right)^{1/4} \left(\frac{1+\sqrt{1+36\alpha H^2/m_{\rm P}^2}}{2}\right)^{-\frac{1}{2}} , \tag{6.71}$$

$$f_{\rm reh} = \frac{\left[\Omega_{\rm r}^0 (\Omega_{\rm r}^{\rm end})^3 H_0^2 H^2\right]^{1/4}}{4} \left(\frac{1+\sqrt{1+36\alpha H^2/m_{\rm P}^2}}{2}\right)^{-\frac{1}{2}} . \tag{6.72}$$

Note that the frequencies of the modes that cause the truncated peak, corresponding to hyperkination and kination, are always between $f_{\rm reh}$ and $f_{\rm end}$, given by Eqs. (6.72) and (6.71), respectively. The specific values depend on the Hubble parameter at the end of inflation H, the density parameter of radiation at the end of inflation $\Omega_{\rm r}^{\rm end}$ and α. In order to give some indicative values, let us assume GUT scale inflation $H \simeq 10^{13}\,\text{GeV}$ and electroweak-scale reheating $\rho(\eta_{\rm reh}) \simeq (200\,\text{GeV})^4$, corresponding to $\Omega_{\rm r}^{\rm end} = 10^{-10}$. Changing α obviously leaves $f_{\rm end}$ unchanged. In Table 6.1, we show $f_{\rm reh}$ and $f_{\rm end}$ for a few different α. Note that they are larger than $f_{\rm BBN}$, as they should be.

6.5.2 Parameter space and detectability

In the present section, we put our model to the test and analyse the detectability of the generated spectrum of primordial GWs in the presence of a period of hyperkination after inflation. Since our analytical expression for the spectrum

α	$f_{\rm reh}$	$f_{\rm end}$
10^{30}	$3.9 \times 10^{-5}\,{\rm Hz}$	$4.4 \times 10^{10}\,{\rm Hz}$
10^{35}	$2.2 \times 10^{-6}\,{\rm Hz}$	$4.4 \times 10^{10}\,{\rm Hz}$
10^{40}	$1.2 \times 10^{-7}\,{\rm Hz}$	$4.4 \times 10^{10}\,{\rm Hz}$

Table 6.1: Values of the frequencies corresponding to reheating $f_{\rm reh}$ and the end of inflation $f_{\rm end}$ for different values of α, given that $H = 10^{13}\,{\rm GeV}$ and $\Omega_{\rm r}^{\rm end} = 10^{-10}$.

approximates very well its numerical counterpart, as can be seen from Fig. 6.4, we use it in order to compare with the PLICs of various detectors, namely LISA [433, 434, 435], ET [469, 470], LVK observing runs O3 and O5 [428, 429, 430, 431, 432], SKA [471], DECIGO [436, 437, 438] and BBO [439]. For each of them, we run a scan over the parameter space $\{\alpha, \Omega_{\rm r}^{\rm end}, H\}$. The successful parameter space can be found in Fig. 6.7.

Before we describe how the parameter space scan is performed, we comment on some bounds that need to be imposed. First, BBN should happen during the period of radiation domination. In other words, at (and below) the frequency associated with BBN, the spectrum needs to be in its lower plateau, *i.e.*, $f_{\rm reh} > f_{\rm BBN}$, where $f_{\rm reh}$ is given by Eq. (6.72). This imposes a bound on the maximum value α can take. Solving for α in Eq. (6.72) gives

$$\begin{aligned} \alpha &< \frac{m_{\rm P}^2}{36H^2}\left[\left(\frac{\sqrt{\Omega_{\rm r}^0(\Omega_{\rm r}^{\rm end})^3 H_0^2 H^2}}{8 f_{\rm BBN}^2} - 1\right)^2 - 1\right] \\ &\simeq \frac{m_{\rm P}^2 \Omega_{\rm r}^0 (\Omega_{\rm r}^{\rm end})^3 H_0^2}{2304 f_{\rm BBN}^4} = 6.9 \times 10^{85} (\Omega_{\rm r}^{\rm end})^3. \end{aligned} \tag{6.73}$$

Importantly, we note here that the specific value we use for $f_{\rm BBN}$ in Eq. (6.69) comes from $T_{\rm BBN} = 1\,{\rm MeV}$. However, recent studies [455, 464] have shown that the stiff era is restricted to occur at temperatures $T > 2.5\,{\rm MeV}$. This means that the value in Eq. (6.69) would become a factor of 2.5 larger, and the bound in Eq. (6.73) a factor of 0.026 smaller. However, given that the available parameter space for α spans many order of magnitude (see Fig. 6.7), this change does not affect our

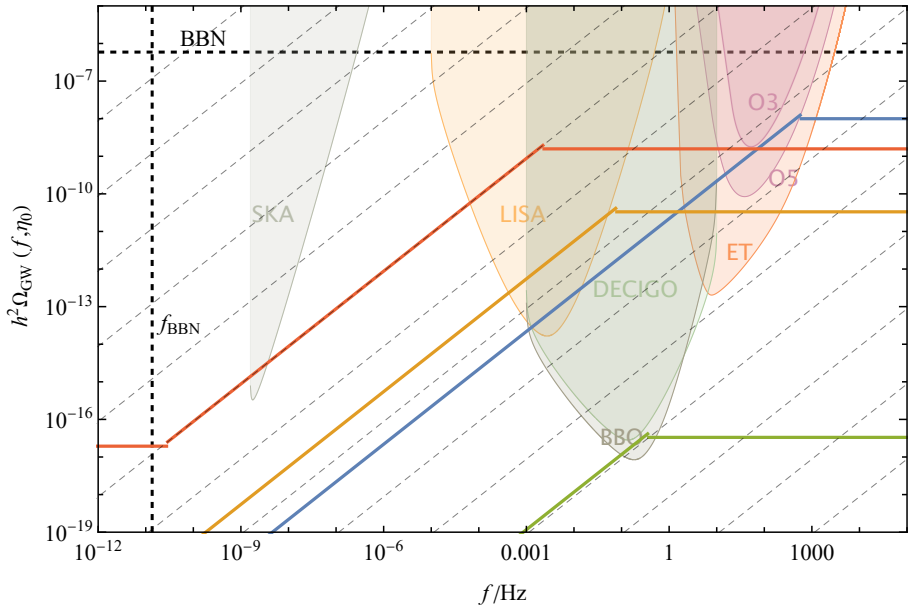

Figure 6.5: A few different spectra superimposed with the PLIC curves of the GW experiments. The parameter values $\{N, H, \Omega_{\rm r}^{\rm end}\}$ are $\{17.5,\ 4.3\times10^{11}\ \text{GeV},\ 10^{-12}\}$ for the blue curve, $\{25,\ 7.9\times10^{11}\ \text{GeV},\ 10^{-9}\}$ for the orange curve, $\{20,\ 7.9\times10^{10}\ \text{GeV},\ 10^{-5}\}$ for the green curve and $\{29.5,\ 1.7\times10^{13}\ \text{GeV}, 10^{-8}\}$ for the red curve. We also show lines parallel (dashed gray) to the kination part of the spectrum. If not for the hyperkination period the spectra would violate the BBN bound.

results appreciably. Nevertheless, the reader should keep in mind that our bound $T > 1\,\text{MeV}$ is an approximate one.

In addition, the GW energy density at BBN must be low enough not to disturb the standard results. Eqs. (6.63) and (6.64) give $\Omega_{\rm GW}^{\rm BBN} = \Omega_{\rm GW}^0/\Omega_{\rm r}^0$, allowing us to translate the bound to into the GW energy density today, yielding [295]

$$h^2\Omega_{\rm GW}^0 = \int \frac{{\rm d}f}{f} h^2\Omega_{\rm GW}(f) < 1.12\times10^{-6}\,, \tag{6.74}$$

where $h \approx 0.7$ is the dimensionless Hubble constant. In practice, however, for all detectors except LVK O5 and ET, this bound is irrelevant. Indeed, it is sufficient to impose that the hyperkination plateau be below the minimum of LVK O3, the region excluded by now by LVK, which is below the BBN bound. Note that for LVK O5 and ET there exists some parameter space where the hyperkination plateau is

between both limits. We take this into account in the scans by showing the excluded region from LVK O3 in Fig. 6.6. There, for each value of H and $\Omega_{\rm r}^{\rm end}$, we show the maximum value of α, labelled $\alpha_{\rm max}$, below which the signal is not observationally excluded.

We can also impose an upper bound on the energy scale at the end of inflation. Using the slow-roll expression for the amplitude of the scalar power spectrum, we can write the Hubble parameter at CMB scales as

$$H_{\rm CMB} = \sqrt{\frac{\rho_{\rm CMB}}{3m_{\rm P}^2}} = m_{\rm P}\sqrt{A_s\frac{\pi^2 r}{2}}\,, \tag{6.75}$$

where $A_{\rm s} = 2.1 \times 10^{-9}$ [8] and r is the tensor-to-scalar ratio. The latest constraint on r is $r < 0.036$ [9]. The energy scale at the end of inflation is always lower than at CMB scales, so Eq. (6.75) provides an upper bound on H at the end of inflation,

$$H < 4.7 \times 10^{13}\,{\rm GeV}\,. \tag{6.76}$$

Further, the plateau corresponding to radiation domination should be below the one corresponding to hyperkination, but this is not strictly guaranteed by our approximative spectrum if the kination period is short. To ensure this condition is satisfied, we impose

$$\Omega_{\rm r}^{\rm end} < \frac{8}{\pi^2} \simeq 0.81\,, \tag{6.77}$$

see Eq. (6.70).

The logic for the parameter scan is as follows. We consider a grid in the $(H, \Omega_{\rm r}^{\rm end})$ plane, with the values of H lying in the interval $[10^6, 4.7 \times 10^{13}]\,{\rm GeV}$ and those of $\Omega_{\rm r}^{\rm end}$ lying in the interval $[10^{-20}, 0.81]$, both in steps of 0.5 in logarithmic units. Then, for each point in the grid, we find the minimum value $\alpha_{\rm min}$, such that our spectrum is detectable by the specific experiment we are considering. Since the effect of increasing α (or, analogously, $N_{\rm hyp}$) is to stretch the flat region corresponding to hyperkination, if a signal is detectable for $\alpha_{\rm min}$, it will also be detectable for every $\alpha > \alpha_{\rm min}$. Note that for LVK O5 and ET, for a certain region in the $(H, \Omega_{\rm r}^{\rm end})$ plane, there is also a maximum value that α can take, see Fig. 6.6. This limitation exists

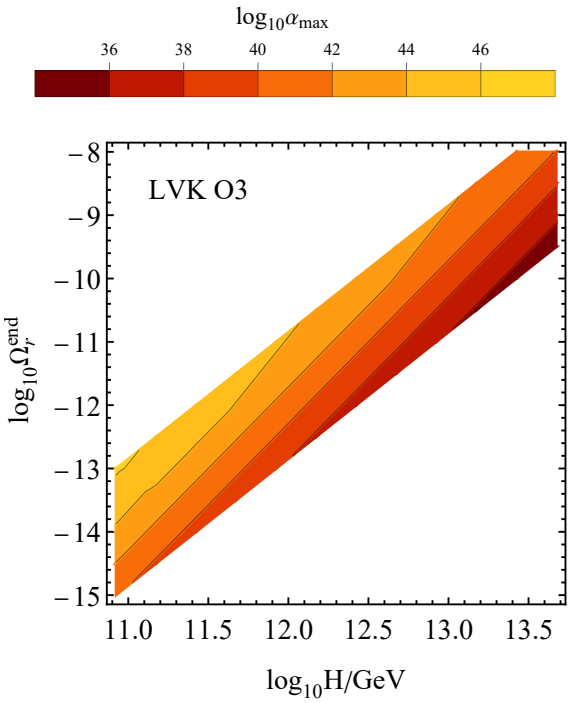

Figure 6.6: Parameter space of the theory excluded by LVK O3. For each value of H and $\Omega_{\rm r}^{\rm end}$, there is a maximum value for α, labelled $\alpha_{\rm max}$, above which the signal is observationally excluded.

only for values where the height of the hyperkination plateau is above the minimum of the LVK O3 PLIC.

In order to determine whether a signal can be detected, we compute the PLICs [472] for each experiment. Then, for each set of parameters, we find the minimum $\alpha_{\rm min}$ such that the energy density spectrum is at least as large as the PLIC under consideration. An easy way to picture this procedure is to realise that the spectra with $\alpha = \alpha_{\rm min}$ are tangent to the PLICs. Increasing α increases the length of the hyperkination plateau, so if the spectrum is tangent to a PLIC, it will be above it for some frequency range if $\alpha > \alpha_{\rm min}$.

In Fig. 6.5, we show some example spectra with a large enough SNR, superimposed with the PLICs for all considered experiments. In the same figure, we also show a grid of lines with the same slope as $\Omega_{\rm GW}^{\rm kin}(f, \eta_0)$ to showcase how in

a setup with inflation being followed by usual kination most of the signals would violate the BBN bound. Hyperkination fixes this by truncating the spectrum and introducing a new plateau at high frequencies.

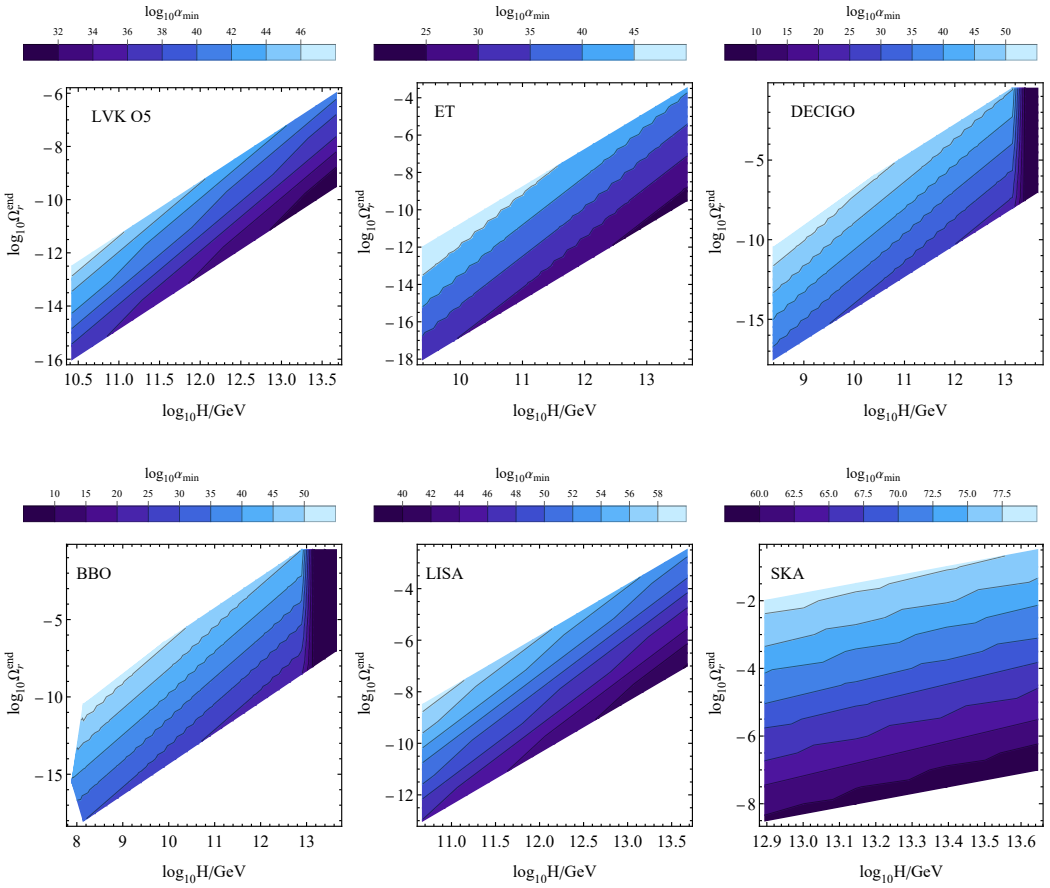

Figure 6.7: Parameter space of the theory for the minimum α such that the signal is detectable by LVK O5 (top left), ET (top middle), DECIGO (top right, BBO (bottom left), and LISA (bottom middle) and SKA (bottom right). For each value of H and $\Omega_{\rm r}^{\rm end}$, there is a minimum value for α, labelled $\alpha_{\rm min}$, above which the signal is always detectable (minus the excluded region in Fig. 6.6 for LVK O5 and ET).

We report the results of parameter space scans as contour plots in Fig. 6.7. There, for each pair $(H, \Omega_{\rm r}^{\rm end})$, we give the minimum $\alpha_{\rm min}$ such that the signal is detectable, for each experiment. We emphasize that the totality of the successful parameter space is contained in these figures. Besides the maximum value of H from

Eq. (6.76), the parameter space is bounded at small H by the BBN timing condition $f_{\rm reh} > f_{\rm BBN}$, at small $\Omega_{\rm r}^{\rm end}$ by the BBN energy density condition in Eq. (6.74) and the LVK O3 exclusion bound, and at large $\Omega_{\rm r}^{\rm end}$ by the requirement that the higher hyperkination plateau must reach the lower end of the sensitivity band for the given experiment.

We conclude that there is ample parameter space to accommodate detectability by all experiments. Indeed, as can be seen from Fig. 6.7, for a Hubble parameter $H \lesssim 10^{13}$ GeV, somewhat below the GUT scale, and a reheating efficiency in the range of $10^{-15} \lesssim \Omega_{\rm r}^{\rm end} \lesssim 10^{-2}$, which can be easily accommodated by a variety of reheating mechanisms [100, 473, 98, 99, 289, 290, 291], we can always find a detectable signal. We emphasize that the size of the parameter space is large, and there is no need for fine-tuning to obtain a detectable signal. Indeed, in Fig. 6.7 we report the minimum value α has to take in order for the signal to be detectable. However, *any* value of α larger than $\alpha_{\rm min}$ also leads to a detectable signal.

The value of $\alpha_{\rm min}$ is quite large for most experiments. This can be understood from Eq. (6.19). Indeed, we can find a lower bound on $\alpha_{\rm min}$ by taking the limit $N_{\rm hyp} \ll 1$. It gives

$$\alpha\rho_{\rm end} \simeq \frac{2m_{\rm P}^4}{3} N_{\rm hyp}. \tag{6.78}$$

Using a GUT energy scale $\rho_{\rm end} \sim 10^{-10} m_{\rm P}^4$, considering an almost non-existent period of hyperkination with $N_{\rm hyp} = 0.1$, we obtain a rough lower bound $\alpha_{\rm min} \gtrsim 10^{10}$. As soon as we have a larger $N_{\rm hyp}$, $\alpha_{\rm min}$ grows exponentially with it. This is in line with our findings in Chapter 5, where we study quintessential inflation with an action of the form in Eq. (5.1). There, we find $\alpha \sim 10^{10}$ for successful quintessential inflation, without considerable hyperkination.

6.6 Discussion

We have investigated the spectrum of primordial GWs generated by cosmic inflation in a model where after inflation but before reheating we have a period when the

Universe is dominated by the kinetic energy density of the inflaton scalar field ϕ, when the field is characterised by both the usual quadratic kinetic term and also by a higher-order quartic kinetic term. This is natural in theories of quadratic $R+\alpha R^2$ gravity in the Palatini formalism, where in the Einstein frame the quartic kinetic term is proportional to α, the coefficient of quadratic gravity. However, we can equally well envisage a k-inflation scenario where the kinetic term of the scalar field includes a term $\propto \alpha X^2$, where $X = \frac{1}{2}\dot{\phi}^2$.

This kinetically dominated period is divided into two parts. In the first part, the inflaton kinetic energy density is dominated by the higher-order kinetic term; a period which we call hyperkination. In the second part, the higher-order kinetic term becomes negligible and the inflaton kinetic energy density is dominated by the usual quadratic term; a period called kination. We have shown that, while kination is a stiff phase with barotropic parameter $w = p/\rho = 1$, as is well known, hyperkination is not; the barotropic parameter during hyperkination is that of radiation $w = 1/3$. As a result, the modes of inflation-generated primordial GWs which re-enter the horizon during hyperkination form a flat spectrum, in the same way as the modes which re-enter the horizon after reheating, in the usual radiation era. However, during usual kination, the GW spectrum is not flat but the GW density parameter per logarithmic frequency interval is $\Omega_{\rm GW}(f) \propto f$. This means that, for modes re-entering the horizon after inflation and before reheating, the GW signal is boosted. This boost corresponds to a truncated peak in the GW spectrum; truncated because the spectrum corresponding to hyperkination is flat but it can be of much larger amplitude than that corresponding to the eventual radiation era. Consequently, the period of kinetic domination (kination + hyperkination) can be made to last longer and the boosted spectrum to extend to lower frequencies without the danger of the production of excessive primordial GWs. In particular, the truncated spectrum can avoid the upper bound imposed by the requirement that Big Bang Nucleosynthesis (BBN) remains undisturbed. Thus, primordial GWs in all observable frequencies can be enhanced without a problem.

We have analytically and numerically studied thoroughly the inflationary production and the subsequent evolution of GW modes and obtained the resulting GW spectrum, linking it with the model parameters. The characteristic shape of the spectrum will be testable in the near future by forthcoming observations, such as advanced LIGO-Virgo-KAGRA, LISA, DECIGO, BBO and ET, as depicted in Fig. 6.5. If observed, such a spectrum can provide insight into the underlying theory, such as the energy scale of inflation, the reheating efficiency and the coefficient α. The latter is directly related to the duration of the hyperkination phase. Indeed, when hyperkination lasts $N_{\rm hyp}$, then Eq. (6.19) suggests

$$\alpha = \frac{m_{\rm P}^4}{3\rho_{\rm end}} \exp(4N_{\rm hyp}) \,, \tag{6.79}$$

where $\rho_{\rm end} = 3H^2 m_{\rm P}^2$ is the energy density at the end of inflation, and H is the corresponding Hubble scale. Typically, inflation is at the scale of grand unification, which implies $H^2 \sim 10^{-10}\, m_{\rm P}^2$. In this case, the above suggests that $e^{N_{\rm hyp}} \sim 10^{-3}\alpha^{1/4}$, which means that

$$N_{\rm hyp} \simeq 10 \Rightarrow \alpha \sim 10^{26}. \tag{6.80}$$

Note that, in the usual Starobinsky R^2 inflation we have $\alpha = 1.1 \times 10^9$. Such large values of alpha are non-perturbative, but this is no more a problem in our setup than it is in Starobinsky gravity.

Important information can also be deduced by the amplitude of the truncated peak corresponding to hyperkination. Indeed, Eq. (6.66) suggests that the value of the GW spectrum on the hyperkination plateau is given by

$$\Omega_{\rm GW}^{\rm hyp} = \frac{1}{12\pi^2} \frac{\Omega_r^0}{\Omega_r^{\rm end}} \left(\frac{H}{m_{\rm P}}\right)^2 \,, \tag{6.81}$$

where $\Omega_r^0 \simeq 10^{-4}$ is the density parameter of radiation at present and $\Omega_r^{\rm end}$ is the density parameter of radiation at the end of inflation, also called reheating efficiency, because the larger it is the sooner reheating takes place. As discussed, in order not to destabilise BBN, we need $\Omega_{\rm GW}^{\rm hyp} < 10^{-6}$. Thus, we obtain a lower bound on the reheating efficiency as $\Omega_r^{\rm end} > (H/m_{\rm P})^2$. Typically for inflation we have $H^2 \sim 10^{-10} m_{\rm P}^2$, which implies $\Omega_r^{\rm end} > 10^{-10}$.

In an effort to stay generic, we have not considered a specific mechanism for producing the radiation which eventually reheats the Universe. We note however, that a number of such mechanisms exist, such as instant preheating [100, 473], curvaton reheating [290, 291] or Ricci reheating [98, 99, 289] to name but some. It is even possible to avoid introducing additional degrees of freedom and consider that reheating occurs due to the dissipating properties of the inflaton field itself, as discussed in Ref. [272], where such processes become negligible after inflation.

Additional important information can be obtained by the observation of the frequency of the knee in the GW spectrum, shown in Figs. 6.4 and 6.5, which is given by $f_{\rm kin}$ in Eq. (6.71). Combining this with Eq. (6.81), in the large $N_{\rm hyp}$ limit, we obtain

$$\frac{f_{\rm kin}}{(\Omega_{\rm GW}^{\rm hyp})^{1/4}} = \frac{2}{\pi^{3/2}}\sqrt{\frac{2}{3}}\rho_0^{1/4}\,\alpha^{-1/4}\sqrt{\frac{m_{\rm P}}{H}}\,, \tag{6.82}$$

Where $\rho_0 = 3H_0^2 m_{\rm P}^2$ is the energy density of the Universe at present. Putting the numbers in the above, we find

$$\left(\frac{f_{\rm kin}}{\rm Hz}\right)\left(\frac{\Omega_{\rm GW}^{\rm hyp}}{10^{-6}}\right)^{-1/4} \sim 10^{12}\,\alpha^{-1/4}\sqrt{\frac{m_{\rm P}}{10^3\,H}}\,. \tag{6.83}$$

Observations might provide the values of the left-hand-side of the above, which means that α could be estimated provided H is known (e.g. $H^2 \sim 10^{-10} m_{\rm P}^2$ for inflation at the grand unified energy scale).

In Fig. 6.7 we display our findings with respect to observability by different missions, such as LVK 05, ET, BBO, LISA DECIGO and SKA. There, we show the minimum value α has to take in order for the spectrum to be detectable. Above this value, which we label $\alpha_{\rm min}$, the spectrum is always detectable. We see that observability requires that the reheating efficiency is smaller the lower the inflation energy scale is (the lower H is). Also, the values of $\alpha_{\rm min}$ are larger for large inflationary energy scales. For LVK 05 and LISA we find that observability requires $\alpha_{\rm min} \sim 10^{30-60}$, while for ET, BBO and DECIGO the numbers are smaller $\alpha_{\rm min} \sim 10^{10-50}$. For the reheating efficiency, we find that observability requires that the density parameter of radiation at the end of inflation is $\Omega_{\rm GW}^{\rm end} \gtrsim 10^{-16}$, a value

which may increase up to unity or so in the case of ET, BBO or DECIGO. Such a high reheating efficiency implies that the kinetic regime is very small or even non-existent (prompt reheating). This is possible because, the ET, BBO and DECIGO might be able to detect very faint signals at frequencies higher than LISA, which means that they could even marginally observe the flat GW spectrum generated by the usual radiation era (no kinetic epoch). This is why there is a region (for ET, BBO and DECIGO) when H is large ($H \sim 10^{13}\,\mathrm{GeV}$) where suddenly α can be very small (or even zero). The parameter space for this is very small though.

We conclude that, with our mechanism, the observability of primordial GWs is much enhanced compared to traditional models. We obtained concrete predictions involving H, α and the reheating efficiency in the case the characteristic form of the GW spectrum—a truncated peak—is indeed observed. Observation of the primordial GW signal would not only confirm another prediction of cosmic inflation but would also be a tantalising hint towards the quantum nature of gravity, which is behind the assumption of the Bunch-Davies vacuum in Eq. (6.32). Forthcoming GW observations may reveal new and surprising details about the physics of inflation and fundamental physics in general. Our work serves to explore such a possibility.

Chapter 7

Non-oscillating Early Dark Energy and Quintessence from α-attractors

This chapter is based on the original research article published in Astroparticle Physics [4] and in the conference paper published in Proceedings of Science [5] by the author, in collaboration with Lucy Brissenden and Konstantinos Dimopoulos.

7.1 Introduction

In the last few decades cosmological observations of the early and late Universe have converged into a broad understanding of the history of our Universe from the very first seconds of its existence until today. Thus, cosmology has developed a standard model called the concordance model, or in short ΛCDM.

However, the latest data might imply that the celebrated ΛCDM model is not that robust after all. In particular, there is a 8% discrepancy, at a confidence level of 5σ, between the locally measured and cosmologically inferred values for the expansion rate today H_0. This Hubble tension (see Sec. 2.2.3 for a full discussion on this topic) has undermined our confidence in ΛCDM and as such it is investigated

intensely at present.

In this chapter we study a toy model of unified EDE and DE, which can simultaneously raise the inferred value of the Hubble constant H_0 coming from early-time data and explain the current accelerated expansion with no more tuning that in ΛCDM. We introduce a scalar field φ in the context of α-attractors, which is frozen at early times and unfreezes around matter-radiation equality, briefly behaving as a subdominant dark energy component to then undergo free-fall, redshifting away faster than radiation. At late times φ behaves as quintessence. In contrast to most other works in the literature, the field does not exhibit oscillatory behaviour (see however Refs. [180, 179, 474, 475] for earlier attempts, the first two also in the context of α-attractors).

Models of EDE are subject to significant constraints; the primary consideration being that EDE must be subdominant at all times and should redshift away faster than radiation, *i.e.*, $\rho \propto a^{-n}$ with $n > 4$ [159], in order for it to be negligible at the time of last scattering. So far, in previous works, this has been achieved via a variety of mechanisms, such as first or second-order phase transitions [173, 178], although these might have undesirable side-effects such as the generation of inhomogeneities from bubble collisions or topological defects. Other popular models typically feature oscillatory behaviour [179, 130, 161, 159, 173, 174, 175, 176, 162, 177, 178] to achieve the required energy scaling. In this case, as with the original proposal in Ref. [161], after unfreezing, the EDE field oscillates around its vacuum expectation value in a potential minimum which is taken to be of order higher than quartic. As a result, on average, the scaling of its energy density with the scale factor reads $\rho \propto a^{-m}$, with $4 < m < 6$. In contrast, in our model, the EDE scalar field experiences a period of kinetic domination, such that its density decreases as $\rho \propto a^{-6}$, exactly rather than approximately.

Our model unifies EDE with late DE (see Refs. [180, 475] for earlier attempts) in the context of α-attractors[1] continuously interpolate between those of chaotic

[1]In the context of inflation, the predictions of models featuring the construction of $\alpha-$attractors

inflation [94] and those of Starobinsky [11] and Higgs inflation [390]. [476, 477, 478, 479, 465, 480, 481, 482, 483]. α-attractors appear naturally in supergravity. Introducing curvature to the internal field-space manifold can give rise to a non-trivial Kähler metric, which results in kinetic poles for some of the scalar fields of the theory. The free parameter α is inversely proportional to said curvature. As for the word "attractor", it is used to refer to the fact that the inflationary predictions are largely insensitive of the specific characteristics of the potential under consideration. Such an attractor behaviour is attained for sufficiently large curvature (small α) in the internal field-space manifold.

In practical terms, the scalar field has a non-canonical kinetic term, featuring two poles, which the field cannot transverse. To aid our intuition, the field can be canonically normalised via a field redefinition, such that the finite poles for the non-canonical field are transposed to infinity for the canonical one. As a result, the scalar potential is "stretched" near the poles, resulting in two plateau regions, which are useful for modelling inflation [484, 485, 486, 487, 488, 489], or quintessence [260], or both, in the context of quintessential inflation [260, 259, 258].

Before we start describing our model, we bring the attention of the reader to the fact that EDE may have a significant drawback in that not only it does not address the σ_8 tension (associated with matter clustering), but might exacerbate it [142, 490, 491, 492]. However, recent theoretical progress seems to indicate that it may be possible to alleviate both the σ_8 and the Hubble tension simultaneously, via axion models of coupled EDE and dark matter [493, 494, 495, 496, 497]. It is conceivable that an α-attractor model such as ours could feature a similar interaction term.

This chapter is organised as follows. In Sec. 7.2 we introduce the model, in the context of α-attractors, and analytically study the asymptotic behaviour of the scalar field around the origin and infinity. In Sec. 7.3 we detail how we perform the numerical simulation of the system. In Sec. 7.4 we report the results from the numerics, namely the viable parameter space and the field behaviour. Sec.

7.5 deals with the theoretical motivation behind the initial conditions of the field and we conclude in Sec. 7.6. In Appendix D we consider the posibility of the EDE/quintessence field also being the inflaton.

7.2 The Model

Following the standard recipe, we introduce two poles at $\varphi = \pm\sqrt{6\alpha}\, m_P$ by considering the Lagrangian

$$\mathcal{L} = \frac{-\frac{1}{2}(\partial\varphi)^2}{(1-\frac{\varphi^2}{6\alpha\, m_{\rm P}^2})^2} - U(\varphi)\,, \tag{7.1}$$

where φ is the non-canonical scalar field and we use the short-hand notation $(\partial\varphi)^2 \equiv g^{\mu\nu}\partial_\mu\varphi\,\partial_\nu\varphi$. We then redefine the non-canonical field in terms of the canonical scalar field ϕ as

$$\mathrm{d}\phi = \frac{\mathrm{d}\varphi}{1-\frac{\varphi^2}{6\alpha m_{\rm P}^2}} \Rightarrow \quad \varphi = m_{\rm P}\sqrt{6\alpha}\,\tanh\left(\frac{\phi}{\sqrt{6\alpha}\, m_{\rm P}}\right). \tag{7.2}$$

It is obvious that the poles $\varphi = \pm\sqrt{6\alpha}\, m_{\rm P}$ are transposed to infinity.

In terms of the canonical field, the Lagrangian now reads

$$\mathcal{L} = -\frac{1}{2}(\partial\phi)^2 - V(\phi), \tag{7.3}$$

where

$$V(\phi) = U\left(m_{\rm P}\sqrt{6\alpha}\,\tanh\left(\frac{\phi}{\sqrt{6\alpha}\, m_{\rm P}}\right)\right). \tag{7.4}$$

We consider a potential of the form

$$U(\varphi) = V_X \exp\!\big(-\lambda e^{\kappa\varphi/m_{\rm P}}\big), \tag{7.5}$$

where

$$V_\Lambda \equiv \exp\!\Big(-\lambda e^{\kappa\sqrt{6\alpha}}\Big) V_X\,, \tag{7.6}$$

and α, κ, λ are dimensionless model parameters, V_X is a constant energy density scale and φ is the non-canonical scalar field. In the above, V_Λ is the vacuum density

at present[2]. In terms of the canonical field, the potential reads

$$V(\phi) = \exp\Big(\lambda e^{\kappa\sqrt{6\alpha}}\Big) V_\Lambda \exp\Big[-\lambda e^{\kappa\sqrt{6\alpha}\tanh\left(\phi/\sqrt{6\alpha}\, m_{\rm P}\right)}\Big] \,. \tag{7.7}$$

As usual, the Klein-Gordon equation of motion for the homogeneous canonical field is

$$\ddot{\phi} + 3H\dot{\phi} + V'(\phi) = 0 \,, \tag{7.8}$$

where the dot and prime denote derivatives with respect to the cosmic time and the scalar field respectively, and we assumed that the field was homogenised by inflation, when the latter overcame the horizon problem.

7.2.1 Asymptotic behaviour of the scalar potential

We are interested in two limits for the potential in Eq. (7.7): $\phi \to 0$ ($\varphi \to 0$) and $\phi \to +\infty$ ($\varphi \to +\sqrt{6\alpha}\, m_P$). The first limit corresponds to matter-radiation equality. In this limit, the potential is

$$V_{\rm eq} \simeq \exp\Big[\lambda(e^{\kappa\sqrt{6\alpha}} - 1)\Big] V_\Lambda \exp(-\kappa\lambda\, \phi_{\rm eq}/m_{\rm P}) \,, \tag{7.9}$$

where the subscript 'eq' denotes the time of matter-radiation equality when the field unfreezes. It is assumed that the field was originally frozen there. We discuss and justify this assumption in Sec. 7.5.

After unfreezing, it is considered that the field has not varied much, for the above approximation to hold, *i.e.*,

$$0 \lesssim \phi_{\rm eq} \ll \sqrt{6\alpha} m_{\rm P} \,. \tag{7.10}$$

This is a reasonable assumption given that the field begins frozen at the origin shortly before matter-radiation equality, unfreezing at some point during this time [3].

[2] In the parameter scans of the model, we scan over V_X rather than over V_Λ.

[3] There is no suggestion in the EDE literature [179, 130, 161, 159, 173, 174, 175, 176, 162, 177, 178] that the field has to unfreeze at any particular time, as long as it does not grow to larger than the allowed fraction and its energy density is essentially negligible by the time of decoupling.

At large ϕ (*i.e.* $\phi \to \infty$), the non-canonical field is near the kinetic pole ($\varphi \to +\sqrt{6\alpha}\, m_{\rm P}$). Then the potential in this limit is

$$V_0 \simeq V_\Lambda \left[1 + 2\kappa\lambda e^{\kappa\sqrt{6\alpha}}\sqrt{6\alpha}\, \exp\left(-\frac{2\phi_0}{\sqrt{6\alpha}\, m_{\rm P}}\right)\right], \tag{7.11}$$

which, even for sub-Planckian total field excursion in ϕ, should be a good approximation for sufficiently small α. The subscript '0' denotes the present time[4].

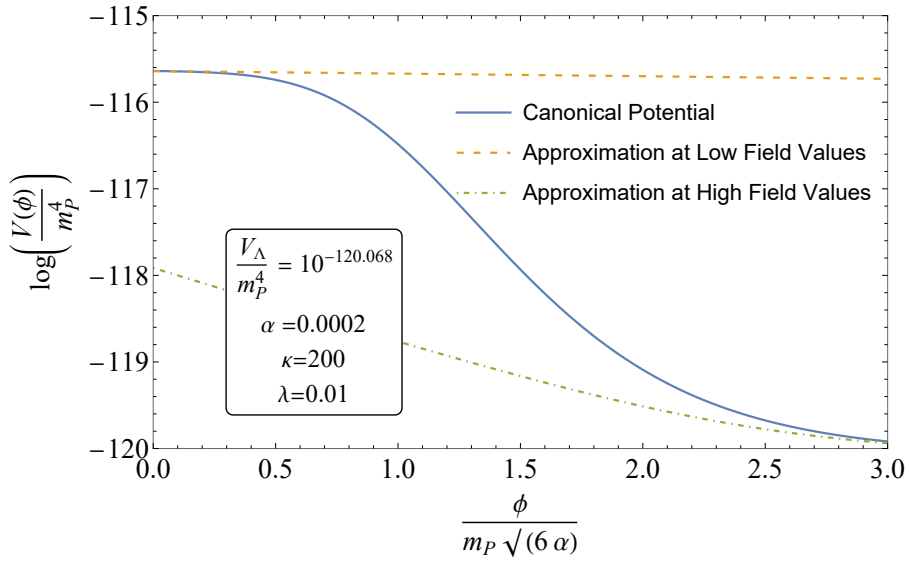

Figure 7.1: Graph of the canonical potential and its two approximations for small and large field values, given in Eqs. (7.9), (7.11) respectively. These approximations are useful because they are simple exponential potentials with well-known attractors. It can be readily seen that, after leaving the origin, the field jumps off a potential plateau and is free-falling as a result.

The above approximations describe well the scalar potential near equality and the present time, as shown in Fig. 7.1. As we explain below, in between these regions, the scalar field free-falls and becomes oblivious of the scalar potential as the term $V'(\phi)$ in its equation of motion (7.8) becomes negligible.

[4]Note that, as the field becomes sufficiently large, the potential approaches the positive constant V_Λ, which corresponds to non-zero vacuum density with $w = -1$, as in ΛCDM. Thus, our model outperforms pure quintessence (with $-1 < w < -0.95$ [8]), which can push H_0 to lower instead of higher values [498, 499].

7.2.2 Expected Field Behaviour

Here we explain the rationale behind the mechanism envisaged. We make a number of crude approximations, which enable us to follow the evolution of the scalar field, but which need to be carefully examined numerically. We do so in the next section.

First, we consider that originally the field is frozen at zero (for reasons explained in Section 7.5). Its energy density is such that it remains frozen there until equality, when it thaws following the appropriate exponential attractor, since $V_{\rm eq}$ in Eq. (7.9) is approximately exponential [213]. Assuming that this is the subdominant attractor requires that the strength of the exponential is [113, 27]

$$Z \equiv \kappa\lambda > \sqrt{3}\,. \tag{7.12}$$

The subdominant exponential attractor dictates that the energy density of the rolling scalar field mimics the dominant background energy density. Thus, the density parameter of the field is constant, given by the value [213, 113, 27]

$$\Omega_\phi^{\rm eq} \simeq \frac{3}{Z^2} = \frac{3}{(\kappa\lambda)^2} < 1 \tag{7.13}$$

This provides an estimate of the moment when the originally frozen scalar field, unfreezes and begins rolling down its potential. Unfreezing happens when Ω_ϕ (which is growing while the field is frozen, because the background density decreases with the expansion of the Universe) obtains the above value.

However, after unfreezing, the field soon experiences the full exp(exp) steeper than exponential potential so, it does not follow the subdominant attractor any more but it free-falls, *i.e.*, its energy density is dominated by its kinetic component, such that its density scales as $\rho_\phi \simeq \frac{1}{2}\dot{\phi}^2 \propto a^{-6}$, until it refreezes at a larger value ϕ_F. This value is estimated as follows.

In free-fall, the slope term in the equation of motion (7.8) of the field is negligible, so that the equation is reduced to $\ddot{\phi} + 3H\dot{\phi} \simeq 0$, where $H = 2/3t$ after equality. The solution is

$$\phi(t) = \phi_{\rm eq} + \frac{C}{t_{\rm eq}}\left(1 - \frac{t_{\rm eq}}{t}\right)\,, \tag{7.14}$$

where C is an integration constant. From the above, it is straightforward to find that $\dot{\phi} = Ct^{-2}$. Thus, the density parameter at equality is

$$\Omega_\phi^{\rm eq} = \left.\frac{\rho_\phi}{\rho}\right|_{\rm eq} = \frac{\frac{1}{2}C^2 t_{\rm eq}^{-4}}{\frac{4}{3}(\frac{m_P}{t_{\rm eq}})^2} = \frac{3}{8}\frac{C^2}{(m_P t_{\rm eq})^2} \Rightarrow C = \sqrt{\tfrac{8}{3}\Omega_\phi^{\rm eq}}\, m_P t_{\rm eq} = \frac{\sqrt{8}}{\kappa\lambda}\, m_P\, t_{\rm eq}\,, \quad (7.15)$$

where we used Eq. (7.13), $\rho_\phi \simeq \frac{1}{2}\dot{\phi}^2$ and that $\rho = 1/6\pi G t^2 = \frac{4}{3}(m_P/t)^2$. Thus, the field freezes at the value

$$\phi_0 = \phi_{\rm eq} + C/t_{\rm eq} = \phi_{\rm eq} + \frac{\sqrt{8}}{\kappa\lambda}\, m_P\,, \quad (7.16)$$

where we considered that $t_{\rm eq} \ll t_{\rm freeze} < t_0$.

Using that $t_{\rm eq} \sim 10^4\,$y and $t_0 \sim 10^{10}\,$y, we can estimate

$$\frac{V_{\rm eq}}{V_0} \simeq \frac{\Omega_\phi^{\rm eq}\rho_{\rm eq}}{0.7\,\rho_0} \simeq \frac{30}{7(\kappa\lambda)^2}\left(\frac{t_0}{t_{\rm eq}}\right)^2 \simeq \frac{3}{7(\kappa\lambda)^2}\times 10^{13}\,. \quad (7.17)$$

Now, from Eqs. (7.9), (7.11) we find

$$\frac{V_{\rm eq}}{V_0} \simeq \frac{e^{\lambda(e^{\kappa\sqrt{6\alpha}}-1)}\exp(-\kappa\lambda\,\phi_{\rm eq}/m_P)}{1+2\kappa\lambda\, e^{\kappa\sqrt{6\alpha}}\sqrt{6\alpha}\exp\big(-2\phi_0/\sqrt{6\alpha}\,m_P\big)}\,. \quad (7.18)$$

In view of Eqs. (7.10), (7.16), the above can be written as

$$\frac{V_{\rm eq}}{V_0} \simeq \frac{e^{\lambda(e^{\kappa\sqrt{6\alpha}}-1)}}{1+2\kappa\lambda\, e^{\kappa\sqrt{6\alpha}}\sqrt{6\alpha}\, e^{-2\sqrt{8}/\kappa\lambda\sqrt{6\alpha}}}\,. \quad (7.19)$$

Taking $\Omega_\phi^{\rm eq} \simeq 0.1$ as required by EDE, Eq. (7.13) suggests

$$\kappa\lambda \simeq \sqrt{30}\,. \quad (7.20)$$

Combining this with Eq. (7.17) we obtain

$$e^{\frac{\sqrt{30}}{\kappa}(e^{\kappa\sqrt{6\alpha}}-1)} \sim 10^{12}/7\,, \quad (7.21)$$

where we have ignored the second term in the denominator of the right-hand-side of Eq. (7.19).

From the above we see that, κ is large when α is small. Taking, as an example, $\alpha = 0.01$ we obtain $\kappa \simeq 18$ and $\lambda \simeq 0.30$ (from Eq. (7.20)). With these values, the

second term in the denominator of the right-hand-side of Eq. (7.19), which was ignored above, amounts to the value 3.2. This forces a correction to the ratio $V_{\rm eq}/V_0$ of order unity, which means that the order-of-magnitude estimate in Eq. (7.21) is not affected.

Using the selected values, Eq. (7.16) suggests that the total excursion of the field is

$$\Delta\phi = \phi_0 - \phi_{\rm eq} = \frac{\sqrt{8}}{\kappa\lambda}\, m_P \simeq 0.5\, m_P \ , \tag{7.22}$$

i.e., it is sub-Planckian. In the approximation of Eq. (7.9), we see that the argument of the exponential becomes $\kappa\lambda\Delta\phi/m_P \simeq 2.7 > 1$, where we used Eq. (7.20). This means that the exponential approximation breaks down and the exp(exp) potential is felt as considered, as depicted also in Fig. 7.1.

For small α, the eventual exponential potential in Eq. (7.11) is steep, which suggests that field rushes towards the minimum at infinity. However, the barotropic parameter is $w \approx -1$ because the potential is dominated by the constant V_Λ.

7.2.3 Tuning requirements

Our model addresses in a single shot two cosmological problems: firstly, the Hubble tension between inferences of H_0 using early and late-time data; and secondly, the reason for the late-time accelerated expansion of the Universe; late DE. However, its parameters, namely α, λ, κ and V_Λ, are subject to some tuning.

As we have seen κ and λ seem to take natural values, not too far from order unity. Regarding α we only need that it is small enough to lead to rapid decrease of the exponential contribution in the scalar potential in Eq. (7.11), leaving the constant V_Λ to dominate at present. We show in the next section that $\alpha \sim 10^{-4}$ is sufficient for this task. This leaves V_Λ itself.

The required tuning of this parameter is given by $V_\Lambda = \left(\frac{H_0^{\rm Planck}}{H_0^{\rm SH0ES}}\right)^2 V_\Lambda^{\rm Planck}$, where $V_\Lambda^{\rm Planck} = \Omega_\Lambda \rho_0$. Since $\left(\frac{H_0^{\rm Planck}}{H_0^{\rm SH0ES}}\right)^2 \simeq (\frac{67.44}{73.04})^2 = 0.8525$ we see that the required fine-tuning of our V_Λ is not different from the fine-tuning introduced in ΛCDM. However,

in contrast to ΛCDM, our proposal addresses two cosmological problems; not only late DE but also the Hubble tension.

7.3 Numerical Simulation

In order to numerically solve the background dynamics of the system, it is enough to solve for the scale factor $a(t)$, the field $\phi(t)$ and the background perfect fluid densities $\rho_{\rm m}(t)$ and $\rho_{\rm r}(t)$ (of matter and radiation respectively), as every other quantity depends on these. They are governed by the Friedmann equation, the Klein-Gordon equation and the continuity equations respectively. Of course, the Klein-Gordon equation is a second order ordinary differential equation, while the continuity equations are first order so that we need the initial value and velocity of ϕ and just the initial value of $\rho_{\rm m}$ and $\rho_{\rm r}$ as initial conditions. As described above, the field starts frozen and unfreezes around matter-radiation equality. Effectively, this means using $\phi_{\rm ini} = 0$ and $\dot{\phi}_{\rm ini} = 0$ as initial conditions, while the initial radiation and matter energy densities are chosen to satisfy the bounds obtained by Planck [8] at matter-radiation equality, *i.e.*, scaled back from $\rho_{\rm m}(t_{\rm eq}) = \rho_{\rm r}(t_{\rm eq}) = 1.27\times10^{-110} m_{\rm P}^4$, at some arbitrary redshift $z_{\rm ini} = 10^4$.

For convenience, we rewrite the equations in terms of the logarithmic energy densities $\tilde{\rho}_m(t) = \ln(\rho_m(t)/m_{\rm P}^4)$ and $\tilde{\rho}_r(t) = \ln(\rho_r(t)/m_{\rm P}^4)$. Plugging the first Friedmann equation in the Klein-Gordon equation, gives

$$\ddot{\phi}(t) + \frac{\sqrt{3\rho(t)}}{m_{\rm P}}\,\dot{\phi}(t) + \frac{dV}{d\phi} = 0, \tag{7.23}$$

$$\dot{\tilde{\rho}}_m(t) + \frac{\sqrt{3\rho(t)}}{m_{\rm P}} = 0, \tag{7.24}$$

$$\dot{\tilde{\rho}}_r(t) + \frac{4}{3}\frac{\sqrt{3\rho(t)}}{m_{\rm P}} = 0, \tag{7.25}$$

where $3m_{\rm P}^2 H^2(t) = \rho(t) = \rho_\phi(t) + [\exp(\tilde{\rho}_m(t)) + \exp(\tilde{\rho}_r(t))]m_{\rm P}^4$ and $\rho_\phi(t) = K(\phi(t)) + V(\phi(t))$ where $K(\phi(t)) = \frac{1}{2}\dot{\phi}^2(t)$ and $V(\phi(t))$ is given by Eq. (7.7).

As mentioned in Section 7.5, we assume the field to be initially frozen at an ESP, such that it could have been the inflaton or a spectator field at earlier times. The time of unfreezing is then controlled only by the parameters of the potential.

The simulation is terminated when the density parameter of the field becomes equal to the density parameter of dark energy today $\Omega_\Lambda = 0.6889$ [8].

Parameter	**Description**	**Constraint**
$\Omega_\phi^{\rm eq}$	Structure formation unimpeded while EDE actually has an effect	$0.015 \leq \Omega_\phi^{\rm eq} < 0.107$ [175]
$\Omega_\phi^{\rm ls}$	EDE undetectable in the CMB	$\Omega_\phi^{\rm ls} < 0.015$ [159]
$\Omega_\phi^{\rm eq}$ and $\Omega_\phi^{\rm ls}$	Consistency check	$\Omega_\phi^{\rm eq} > \Omega_\phi^{\rm ls}$
Ω_ϕ^0	Observational	$0.6833 \leq \Omega_\phi^0 \leq 0.6945$ [8]
w_ϕ^0	Observational	$-1 \leq w_\phi^0 \leq -0.95$ [8]
w_ϕ^a	Observational	$-0.55 \leq w_\phi^a \leq 0.03$ [8]
H_0 [km/s/Mpc]	Observational	$72.00 \leq H_0 \leq 74.08$ [136]
$\Delta\phi$	Sub-Planckian field excursion	$\phi_0 - \phi_{\rm eq} < m_{\rm P}$

Table 7.1: Table describing and justifying constraints used to identify the viable parameter space. In the above, $w_\phi^a = -\left.\frac{{\rm d}w_\phi}{{\rm d}a}\right|_0$, *cf.* Eq. (2.208).

7.4 Results and analysis

7.4.1 Parameter Space

We perform a scan of the parameter space of the theory, at the background level, imposing the conditions in Table 7.1. We report our findings in Fig. 7.2, Fig. 7.3[5]. We find that our model is succesful for $\kappa \sim 10^2$ and $\lambda \sim 10^{-3} - 10^{-2}$, which are rather reasonable values. In particular, the value of κ suggests that the mass-scale which suppresses the non-canonical field φ in the original potential in Eq. (7.5) is near the scale of grand unification $\sim 10^{-2}\, m_{\rm P}$. Regarding the curvature of field space we find $\alpha \sim 10^{-4}$, which again is not unreasonable.

The viable parameter space suggests that $\kappa\lambda > \sqrt{3}$, which contradicts our assumption in Eq. (7.12). This implies that, unlike the analytics in Sec. 7.2.2, the field does not adopt the subdominant exponential scaling attractor but the slow-roll exponential attractor, which leads to domination [213, 27]. As the field thaws and starts following this attractor, the approximation in Eq. (7.9) breaks down as the field experiences the full exp(exp) potential, which is steeper than the exponential (see Fig. 7.1). Consequently, instead of becoming dominant the field free-falls. This contradiction with our discussion in Sec. 7.2.2 is not very important. The existence of the scaling attractor provided an easy analytic estimate for the moment when the field unfreezes. It turns out that, because the scaling attractor has been substituted by the slow-roll attractor, the field unfreezes because its potential energy density becomes comparable to the total energy density, going straight into free-fall. It is much harder to analytically estimate when exactly this takes place, but the eventual result (free-fall) is the same.

[5]The apparent structure found in Fig. 7.3 is spurious in origin. In the left panel of the figure we show the valid points in the $\lambda - \alpha$ plane for a *range* of values in κ (and analogously for the right panel). However, would we show a different color for each value of κ, we would find simple curves in the $\lambda - \alpha$ plane. In other words, the apparent structure only has to do with how the grid of points for the scan was chosen.

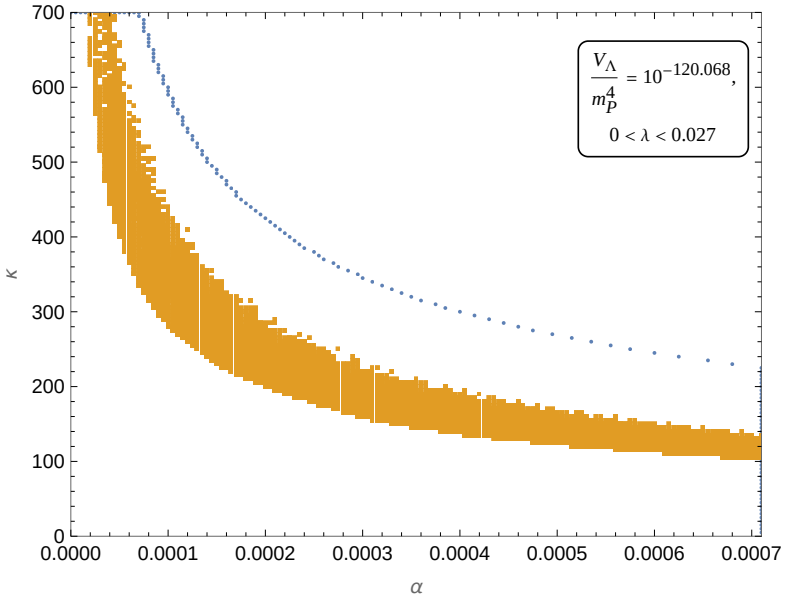

Figure 7.2: Parameter space slice in the $\kappa - \alpha$ plane with $0 < \lambda < 0.027$ and $V_\Lambda = 10^{-120.068} m_{\rm P}^4$. The blue dotted line is the boundary of the region that produces non-inflationary results (see below), while the orange region is constituted by the successful points, *i.e.*, those for which the constraints detailed in Table 7.1 are satisfied. Note that the region bounded in blue is not equal to the range of the scan, which is $0 \leq \kappa \leq 700$ and $0 \leq \alpha \leq 0.00071$. This is because points with potential larger than a certain starting value result in the field beginning the simulation dominant, which means that the Universe goes into inflation which cannot terminate and will never lead to successful EDE. These points are very close to the viable parameter space for these two parameters and therefore must be thrown away.

We obtain that the matter-radiation equality redshift is $z_{\rm eq} \simeq 4000$, larger than the Planck value $z_{\rm eq} = 3387 \pm 21$ [8]. It should be however noted that, in our simplified background analysis, we use the Planck matter density parameter $\Omega_{\rm m.0} = 0.3111 \pm 0.0056$ with the SH0ES value for the Hubble constant $H_0 = 73.04 \pm 1.04\,{\rm km/s/Mpc}$, which is bound to give a value for $\omega_{\rm m} = \Omega_{\rm m,0} h^2$ incompatible with Planck. A simple back-of-the-envelope calculation shows that there is a factor of $\left(\frac{h_{\rm SH0ES}}{h_{\rm Planck}}\right)^2 = \left(\frac{0.73}{0.67}\right)^2 = 1.187$ difference, which leads to a new $z_{\rm eq}^{\rm updated} + 1 = (1.18)^{1/3}(z_{\rm eq}+1)$, *i.e.*, resulting in $z_{\rm eq}^{\rm updated} \simeq 3500$. This pushes $z_{\rm eq}$ to higher values,

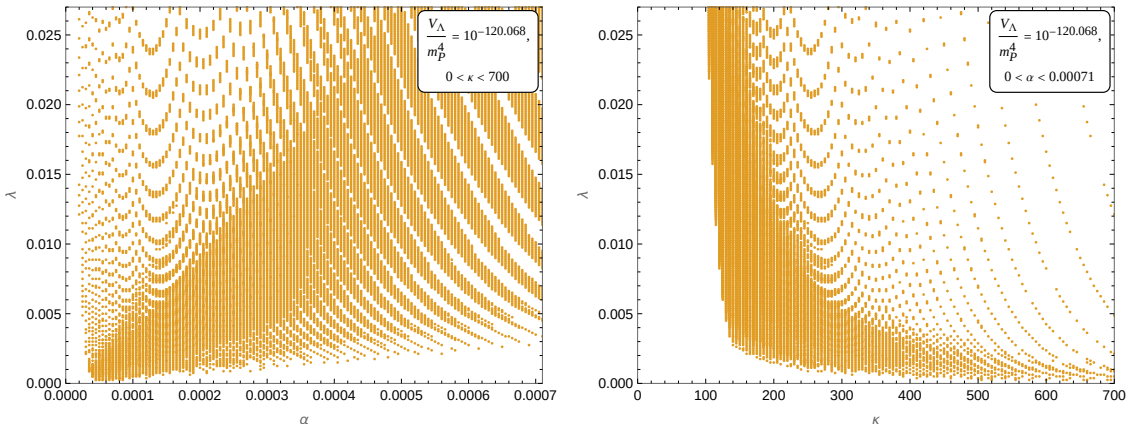

Figure 7.3: Parameter space slice in the $\lambda - \alpha$ plane with $0 < \kappa < 700$ (left) and in the $\lambda - \kappa$ plane with $0 < \alpha < 0.00071$ (right), both with $V_\Lambda = 10^{-120.068} m_{\rm P}^4$. The orange region is constituted by the successful points, *i.e.*, those for which the constraints detailed in Table 7.1 are satisfied.

closer to our findings. We emphasize, however, that a full fit to the CMB data is required in order to obtain the actual value for $z_{\rm eq}$ derived from our model. In contrast, the redshift of last scattering is where we would expect it at $z_{\rm ls} \simeq 1087$. Theoretical constraints suggest $z_{\rm ls} \simeq 1090$ [500], and the observations of the Planck satellite suggest $z_{\rm ls} = 1089.80 \pm 0.21$ [8]. We note here that the best-fit values for the cosmological parameters from ΛCDM are expected to somewhat change when incorporating EDE. In this way, the constraints in Table 7.1 should be considered as approximate only.

7.4.2 Field Behaviour

The field behaves as expected, with the mild modification of the attractor solution at unfreezing (slow-roll instead of scaling), which leads to free-fall. The evolution is depicted in Fig. 7.4, Fig. 7.5 for the example point $\{\alpha, \kappa, \lambda\} = \{0.0005, 145, 0.008125\}$, and V_Λ fixed to the SH0ES cosmological constant [136]. The observables obtained in this case (*i.e.* the values of H_0, w_0 and w_a) are shown in Table 7.2. The behaviour of the Hubble parameter is a function of redshift as can

be seen in the left panel of Fig. 7.4.

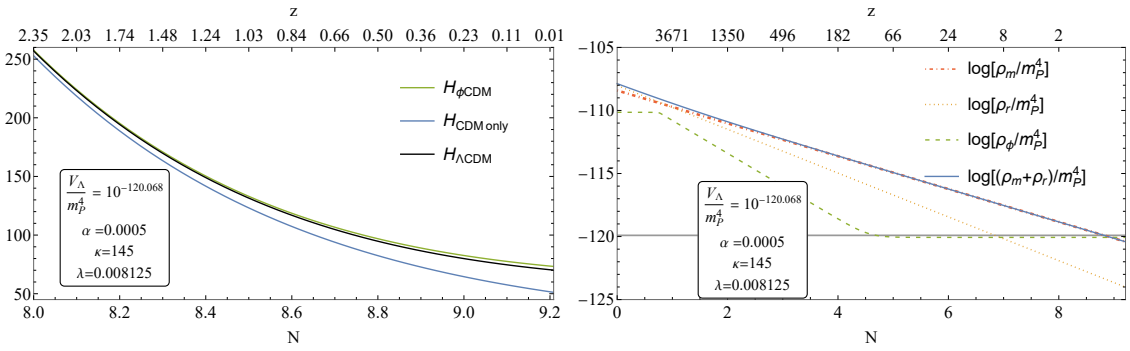

Figure 7.4: Left: The Hubble parameter (in units of km s^{-1}Mpc^{-1}) of a universe with an EDE/quintessence field (green), a ΛCDM universe (black), and one with only matter and radiation (blue), as a function of redshift (top) and e-folds (bottom) elapsed since the beginning of the simulation. The presence of the field leads to a higher value of H_0 than in the ΛCDM scenario. Right: The logarithmic densities of matter (dot-dashed red), radiation (dotted orange), the sum of both (solid blue) and the scalar field (dashed green), as a function of redshift (top) and e-folds (bottom) elapsed since the beginning of the simulation, for $\alpha = 0.0005$, $\kappa = 145$, $\lambda = 0.008125$, and $V_\Lambda = 10^{-120.068} m_{\rm P}^4$. The horizontal solid line represents the SH0ES energy density of the Universe at present. The EDE scalar field becomes momentarily subdominant near equality, then redshifting away faster than radiation to become negligible at decoupling.

As shown in Table 7.1, the maximum allowed value of the EDE density parameter at equality is just over 0.1. However, it is possible that this is too lenient a constraint because unlike the models for which this constraint was developed, our model has a true free-fall period, which means it redshifts away *exactly* as a^{-6} rather than below this rate as in oscillatory behaviour (see the right panels of Fig. 7.4, Fig. 7.5)[6]. Note that for oscillating EDE in a potential $V \propto \phi^{2n}$, as the original EDE [162], there is a limit $n < 3$ ($n < 5$) for matter (radiation) domination. This is because

[6]A more accurate constraint of ~ 0.086 for non-oscillatory models is provided in Ref. [474], which does not significantly narrow our allowed parameter space.

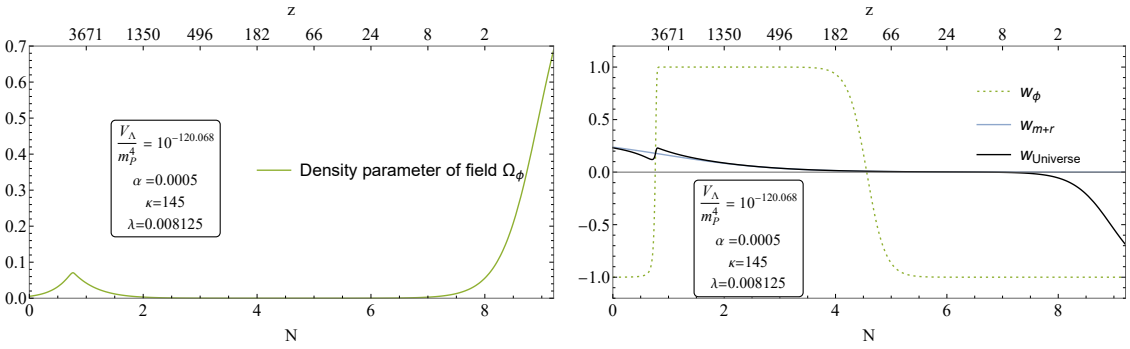

Figure 7.5: Left: The density parameter of the scalar field, for $\alpha = 0.0005$, $\kappa = 145$, $\lambda = 0.008125$, and $V_\Lambda = 10^{-120.068} m_{\rm P}^4$, as a function of redshift (top) and e-folds (bottom) elapsed since the beginning of the simulation. The density parameter experiences a bump with $f_{\rm EDE} = \Omega_\phi(z_{\rm eq}) \lesssim 0.1$, before the EDE redshifting away and refreezing to become dark energy today. Right: Barotropic parameter of the scalar field (dotted green), of the background perfect fluid (solid blue) and of the sum of both components (solid black), for $\alpha = 0.0005$, $\kappa = 145$, $\lambda = 0.008125$, and $V_\Lambda = 10^{-120.068} m_{\rm P}^4$. It is apparent that the scalar field becomes immediately kinetically dominated ($w_\phi = 1$) after thawing, remaining in freefall until it refreezes again.

for $n > 3$ ($n > 5$) there exists an scaling attractor $\phi \propto t^{1/(1-n)}$, which means that oscillations are impeded [217, 212]. Recently, a similar result was found in Ref. [164], where it is shown that the data favours $2 \lesssim n \lesssim 3.4$ at the 68% C.L. Since EDE typically unfreezes around matter-radiation equality, this implies that the density of oscillating EDE cannot decrease faster than $\rho_\phi \propto a^{-9/2}$, *i.e.*, not as fast as true free-fall, where $\rho_\phi \propto a^{-6}$ as we obtain.

At present, the exponential contribution to the potential density in Eq. (7.11) is largely subdominant to V_Λ, so the contribution of the scalar field to the total density budget is almost constant, as in ΛCDM. Its barotropic parameter is, therefore, $w_\phi \approx -1$ (see the right panel of Fig. 7.5). Technically, it is not exactly -1 but its running is negligible, with the viable parameter space for w_a fitting easily within the constraint in Eq. (2.210) by some ten orders of magnitude (see Table 7.2).

Constraint	Example Value
$0.015 \leq \Omega_\phi^{\rm eq} < 0.107$	0.05178
$\Omega_\phi^{\rm ls} < 0.015$	0.001722
$\Omega_\phi^{\rm eq} > \Omega_\phi^{\rm ls}$	YES
$0.6833 \leq \Omega_\phi^0 \leq 0.6945$	0.6889
$-1 \leq w_\phi^0 \leq -0.95$	-1.000
$-0.55 \leq w_\phi^a \equiv -\left.\frac{{\rm d}w_\phi}{{\rm d}a}\right\|_0 \leq 0.03$	-4.850×10^{-11}
$72.00 \leq \frac{H_0}{\rm km\ s^{-1}\,Mpc^{-1}} \leq 74.08$	**73.27**
$\kappa\lambda$	1.178
$(\phi_0 - \phi_{\rm eq})/m_{\rm P} < 1$	0.4274

Table 7.2: Table giving the constraints and their corresponding values for an example point, $\alpha = 0.0005,\ \kappa = 145,\ \lambda = 0.008125$, and V_Λ tuned to the SH0ES cosmological constant, in the viable parameter space. The Hubble constant obtained in this example is $H_0 = 73.27\,{\rm km/s\ Mpc}$.

7.5 Initial Conditions

Our model accounts for both EDE and late-time dark energy in a non-oscillatory manner (in contrast to Ref. [179]). The field is frozen at early times, thawing just before matter-radiation equality when its density grows to nearly 0.1 of the total

value (see left panel of Fig. 7.5), as set by constraints in Ref. [175]. A steep exp(exp) potential then forces the field into free-fall, causing its energy density to dilute away as $\rho_\phi \propto a^{-6}$. After this, the field hits the asymptote of the exponential decay and refreezes, becoming dominant at present (see the right panel of Fig. 7.4).

Thus, we achieve DE-like behaviour at the present day by ensuring that the field refreezes after its period of free-fall, therefore remaining at a constant energy density equal to the value of the potential density at that point. Although this constant potential density is initially negligible, the expansion of the Universe causes the density of matter to decrease. Because the field refreezes at a potential density that is comparable to the density of matter at present, the field starts to become dominant at the present day. Once it begins to dominate the Universe, the field thaws again, but the density of the Universe is dominated by a constant contribution V_Λ, as with ΛCDM.

The obvious question is why our scalar field finds itself frozen at the origin in the first place. One compelling explanation is the following.

We assume that the origin is an enhanced symmetry point (ESP) such that, at very early times, an interaction of φ with some other scalar field χ traps the rolling of φ at zero. The idea follows the scenario explored in Ref. [501]. In this scenario, the scalar potential includes the interaction

$$\Delta V = \frac{1}{2} g^2 \varphi^2 \chi^2 \,, \tag{7.26}$$

where the coupling $g < 1$ parametrises the strength of the interaction. Note that here φ is the non-canonical scalar field, appearing in the Lagrangian in Eq. (7.1), related to its canonical version ϕ via Eq. (7.2). It is also featured in our potential, when it is first introduced in Eq. (7.5).

We assume that initially φ is rolling down its steep potential[7]. Then, the interaction in Eq. (7.26) provides a modulated effective mass-squared $m_{\rm eff}^2 = g^2\varphi^2$ to the scalar field χ. When φ crosses the origin, this effective mass becomes

[7]Far away from the origin, the scalar potential $V(\varphi)$ does not have to be of the form in Eq. (7.5). In fact, it is conceivable that φ might play the role of the inflaton field too (see Appendix D.1).

momentarily zero. If the variation of the φ field (*i.e.* the speed $|\dot{\varphi}|$ in field space) is large enough, then there is a window around the origin when $|\dot{m}_{\rm eff}| \gg m_{\rm eff}^2$ (because, $|\dot{\varphi}| \gg \varphi^2 \simeq 0$). This violates adiabaticity and leads to copious production of χ-particles [501][8].

As the field moves past the ESP, the produced χ particles become heavy, which takes more energy from the φ field, producing an effective potential incline in the direction the φ field is moving. Indeed, the particle production generates an additional linear potential $\sim g|\varphi|n_\chi$ [501], where n_χ is the number density of the produced χ-particles. This number density is constant because the duration of the effect is much smaller than a Hubble time, so that we can ignore dilution from the Universe expansion. The rolling φ field climbs up the linear potential until its kinetic energy density is depleted. Then the field momentarily stops and afterwards reverses its motion (variation) back to the origin. When crossing the origin again, there is another bout of χ-particle production, which increases n_χ and makes the linear potential steeper to climb. This time, φ variation halts at a value closer to the origin. Then, the field reverses its motion and rushes through the origin again. Another outburst of χ-particle production steepens the linear potential further. The process continues until the φ-field is trapped at the origin [27, 501].

The trapping of a rolling scalar field at an ESP can take place only if the χ-particles do not decay before trapping occurs. If they did, the n_χ would decrease and the potential $g|\varphi|n_\chi$ would not be able to halt the motion (variation) of the φ-field. The end result of this process is that all the kinetic energy density of the rolling φ has been given to the χ-particles. Now, since φ is trapped at the origin, the effective mass of the χ-particles is zero, which means that they are relativistic matter, with density scaling as $\rho_\chi \propto a^{-4}$. As far as φ is concerned, it is trapped at the origin and its density is only $\rho_\varphi = V(\varphi = 0) = e^{-\lambda}V_X = \text{constant}$ (*cf.* Eq. (7.5)).

After some time, it may be assumed that the χ-particles do eventually decay

[8]Near the origin, when $\varphi \simeq 0$, the φ-field is approximately canonically normalised, as suggested by Eq. (7.2), so the considerations of Ref. [501] are readily applicable.

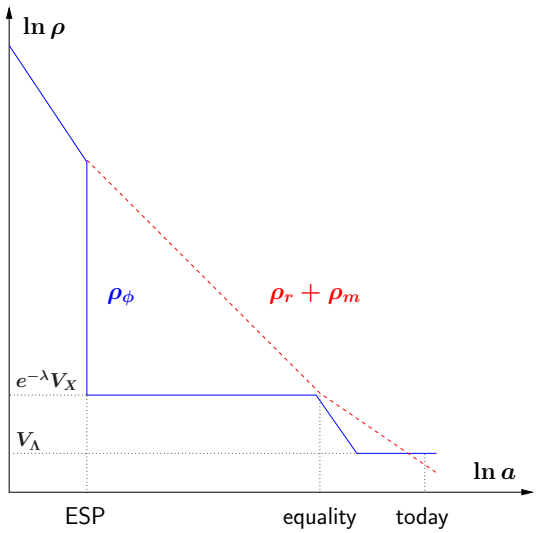

Figure 7.6: Schematic log-log plot depicting the evolution of the density of the scalar field ρ_ϕ (solid blue line) and the density of radiation and matter $\rho_r + \rho_m$ (dashed red line) in the case when the decay of the kinetic energy density of the trapped scalar field generates the thermal bath of the hot Big Bang (as in Ref. [16]). Originally the ϕ-field is rushing towards the minimum of the potential, dominated by its kinetic density, so that $\rho_\phi \propto a^{-6}$ (free-fall). When it crosses the enhanced symmetry point (ESP) its interaction to the χ-field (*cf.* Eq. (7.26)) traps the rolling ϕ-field at the ESP while all its kinetic energy is given to χ-particles, which soon decay into the radiation and matter of the hot Big Bang (the decay is assumed to be quick, just after trapping). Afterwards, the ϕ-field stays frozen, with energy density $V(\phi = 0) = e^{-\lambda} V_X$ (*cf.* Eq. (7.5)) until much later, when its potential density is comparable to the background. Then it unfreezes before dominating, acting as EDE at the time near matter-radiation equality, and subsequently free-falls to its value ϕ_0, with potential density approximately $V_\Lambda = $ constant. The field stays there until the present when it dominates the Universe and becomes late dark energy.

into the standard model particles, which comprise the thermal bath of the hot Big Bang. The confining potential, which is proportional to n_χ, disappears but, we expect the φ-field to remain frozen at the origin because the scalar potential $V(\varphi)$

in Eq. (7.5) is flat enough there. As we have discussed, the φ-field unfreezes again in matter-radiation equality. The above scenario is depicted in Fig. 7.6

For simplicity, we have considered that, apart from the obvious violation of adiabacity at the ESP, the χ direction is otherwise approximately flat and the χ-field has a negligible bare mass compared to the φ field. It would be more realistic to consider a non-zero bare mass for the χ-particles, which when they become non-relativistic (much later than the trapping of φ) can safely decay to the thermal bath of the hot Big Bang, reheating thereby the Universe, *e.g.* in a manner not dissimilar to Ref. [16].

The above scenario is one possible explanation of the initial condition considered and not directly relevant to the scope of this chapter - we simply assume that the field begins frozen at the origin. Other possibilities to explain our initial condition exist, for example considering a thermal correction of the form $\delta V \propto T^2\varphi^2$, which would make the origin an effective minimum of the potential at high temperatures and drive the φ-field there.

7.6 Discussion

In conclusion, we have proposed a toy model that unifies EDE and DE via a scalar field in the context of α-attractors. We have studied the background dynamics in detail, finding that the value of the Hubble parameter, coming from early-time data, can be raised while simultaneously explaining the current accelerated expansion, with no more fine tuning than ΛCDM.

Our work differs from Ref. [179], in that the field is not oscillating; instead after equality, it free-falls with energy density decreasing as $\rho \propto a^{-6}$, faster than most EDE proposals and the fastest possible[9]. Although, from our background

[9]Causality implies that the barotropic parameter w of a perfect fluid cannot be larger than unity because the speed of sound of the fluid $c_s^2 = w$ cannot be superluminal. This implies $w \leq 1$ and so, the density of an independent perfect fluid $\rho \propto a^{-3(1+w)}$ cannot decrease faster than a^{-6}. However, a homogeneous scalar field can be represented as a perfect fluid with $w = \frac{\rho_{\rm kin}-V}{\rho_{\rm kin}+V}$, where

analysis, we find a larger value of $z_{\rm eq}$ than found by Planck, it should be realised that Planck assumes a ΛCDM scenario to derive this quantity and hence it may not be fully applicable to other models, particularly one with a significant scalar field contribution at that time as in our case. Of course, a full fit to the CMB data is needed in order to obtain the actual $z_{\rm eq}$ derived from our model.

In our proposed scenario, the scalar field lies originally frozen at the origin, until it thaws near the time of equal matter-radiation densities, when it becomes EDE. Afterwards it free-falls until it refreezes at a lower potential energy density value, which provides the vacuum density of ΛCDM. We showed that the total excursion of the field in configuration space is sub-Planckian, which implies that our potential is stable under radiative corrections.

One explanation of our initial conditions is that the origin is an ESP. Our scalar field is originally kinetically dominated until it is trapped at the ESP when crossing it[10]. As we discuss in D.1, the scalar field could even be the inflaton, which after inflation rolls down its runaway potential until it becomes trapped at the ESP.

Our potential in Eq. (7.5) really serves to demonstrate that a model unifying EDE with ΛCDM can be achieved with a suitably steep runaway potential. With the parameters of our model assuming rather natural values, thereby not introducing fine-tuning additional to that of ΛCDM, we show that this is indeed possible with a simple design.

The challenge lies in constructing a concrete theoretical framework for such a potential. Furthermore, although the background analysis is promising, a full fit to the CMB data is lacking. We plan on running a Markov Chain Monte Carlo (MCMC) doing this in a future work. This is of paramount importance since it would show what values (if any) from our *a priori* viable parameter space lead to a

$\rho_{\rm kin}$ is the kinetic energy density of the scalar field and V the potential. It seems that $w > 1$ could indeed happen when the field transverses an AdS minimum of V, such that $V < 0$. As a result, the density of such scalar field could decrease faster than a^{-6}. The scenario of such EDE has been considered in Refs. [180, 502].

[10] A thermal correction to the scalar potential can have a similar effect.

best fit to the data.

Chapter 8

Conclusions

Inflation not only solves the horizon and flatness problems of the Hot Big Bang but also provides an elegant mechanism that accounts for the initial conditions of the primordial density perturbations that seed all structure in the Universe. The predicted statistical properties of these fluctuations for the simplest models, namely a quasi-scale invariant spectrum, well described by a Gaussian distribution with adiabatic initial conditions, are largely model-independent. The available observational evidence firmly supports this picture and so the inflationary paradigm has become a cornerstone of the concordance model of cosmology. However, there exists a plethora of models that agree with observations and there is currently no way to discriminate between them, until observations are improved. On the other hand, ever-improving observations have already ruled out many different classes of models, and this trend will likely continue as observational bounds keep being pushed. This is the case for some of the, arguably, simplest and best theoretically motivated potentials, such as chaotic and power-law inflation. Chapters 4 and 5 provide a simple and natural way of bringing them back in agreement with observational constraints, in the context of modified gravity.

One might argue that general relativity is one of the most successful physical theories ever constructed, surviving experimental tests for a century and even providing predictions, such as the existence of black holes and gravitational waves

(GWs), which have been experimentally confirmed in spectacular fashion. So why should we consider modifications of the theory? Perhaps the simplest answer is because we can. Exploring the limits of a theory is always worthwhile and, even if somehow they are excluded by experiments, theories of modified gravity have insights to be gained regarding the theory of gravitation. Further, even if general relativity is so successful at the scales it has been tested at, most of the density of the Universe corresponds to unknown dark substances. It may be that at the relevant scales of dark matter and dark energy the Einstein-Hilbert action is not a valid description. Finally, from a more fundamental perspective, we know that general relativity is not the end of the story, as it in principle should have a quantum description. Quantum corrections to the gravitational action include higher order terms of the Ricci scalar as well as non-minimal couplings between the fields of the theory and gravity.

In Chapter 4 we consider arguably the simplest model of inflation with arguably the simplest modification of gravity, namely chaotic inflation with $V \sim \phi^n$ and a Starobinski term αR^2 added to the Einstein-Hilbert action. Working in the Palatini formalism, we calculate the inflationary observables analytically. We find that the amplitude and tilt of the scalar power spectrum are unaffected by the addition of the Starobinski term, while the tensor-to-scalar ratio becomes inversely proportional to the coupling constant α. As long as $\alpha \gtrsim 10^8$, we are able to bring the hitherto discarded potentials $V = m^2\phi^2/2$ and $V = \lambda\phi^4/4!$ back within the 1σ and 2σ Planck constraints, respectively.

In Chapter 5 we consider a scalar field governed by an exponential potential and with a non-minimal coupling to gravity, as well as the same Starobinski term as in Chapter 4. Working in the Palatini formalism, we solve numerically the full non-linear dynamics in the Jordan frame, being able to bring back the hitherto discarded exponential potential within the 1σ Planck constraints. We find ample parameter space with natural parameter values, with no more fine-tuning than in regular Starobinski inflation.

All in all, Chapters 4 and 5 provide a valuable contribution to inflationary model-building, showing how a minimal and theoretically motivated modification of gravity can resurrect models otherwise discarded by the data. However, this is not the full extent of their contribution, as the aim is also to account for the dark energy observations, in the context of quintessential inflation.

In ΛCDM, dark energy is described by introducing a cosmological constant, *i.e.*, a source of negative pressure that does not dilute with the expansion of the Universe. This cosmological constant has two possible contributions, a classical one from the Einstein equations and a quantum one coming from the energy density of the vacuum. Although it accounts for the observed current accelerated expansion, it requires an incredible amount of fine-tuning. Indeed, both contributions should cancel out with a precision of 60 significant digits. One way out of this fine-tuning problem is to assume both contributions exactly cancel out, due to some unknown symmetry, and to describe dark energy via some other mechanism. This is the motivation behind quintessence, where dark energy is described by a dynamical degree of freedom, namely a scalar field. However, it is in general challenging to endow quintessence with attractor properties, and the fine-tuning problem of ΛCDM just changes shape into one of the initial conditions of quintessence. Quintessential inflation tackles this issue by identifying the inflaton with the quintessence field. In this way, the initial conditions of quintessence are fixed by the inflationary attractor.

In Chapter 4 we augment the chaotic inflation potential with an inverse-power-law potential $V \sim \phi^{-m}$ at large positive field values for the quintessence regime. It is well known that utilising the attractor regime of this potential leads to a barotropic parameter of dark energy incompatible with observations. However, it is still a viable model in the freezing-thawing regime, although the initial conditions then need to be explained. Of course, since now the quintessence field is identified with the inflaton, they are given by the inflationary attractor. We find that the contribution from the modified gravity setup is negligible for the evolution of quintessence, and achieve successful dark energy with fairly natural parameter values, thereby improving the

extreme fine-tuning of ΛCDM. We also find that the model passes solar system tests of modified gravity.

In Chapter 5 we utilise a single-branch exponential potential for both inflation and dark energy. It is notoriously difficult to endow exponential quintessence with attractor properties. Indeed, once the field enters the subdominant attractor regime, with its energy density imitating that of the background, it can never come to dominate (unless the setup is augmented, often introducing an amount of fine-tuning comparable to ΛCDM). In our case, the running of the non-minimal coupling between the field and gravity generates a minimum in the potential at large field values. At late times, the field ends up freezing at the minimum, thereby behaving as dark energy. However, the dynamics of quintessence during the matter dominated are affected by the modified gravity setup. Indeed, the coupling between the Einstein frame field and the matter action, which is zero during the radiation dominated regime, obtains an important contribution during the matter dominated era coming from the non-minimal coupling between the field and gravity (a coupling that did not feature in the action of Chapter 4). The leading effect of this coupling is an energy transfer between the field and the background, amounting to a rise in the effective barotropic parameter of the Universe, above $w = 0$. After solving the full dynamics numerically and running a parameter scan of the theory, we find that this effect narrows the viable parameter space, although not dramatically. We again find natural parameter values, in a very minimal setup which is able to account for both inflation and dark energy, with significantly less fine-tuning than in ΛCDM.

In Chapters 4 and 5 we consider different reheating mechanisms. In the former, we consider gravitational reheating, following the minimalist philosophy of the model and studying how the reheating temperature affects the number of inflationary e-folds. As for the latter, we consider Ricci reheating, where a scalar field other than the inflaton is also non-minimally coupled to gravity. During inflation, the field is trapped at the minimum of its effective potential, but the change in sign of the Ricci scalar after the end of inflation makes it oscillate around the newly formed

minimum, thereby decaying into the particles of the standard model. We ensure that reheating is efficient enough so as not to overproduce GWs.

Any viable potential for quintessential inflation must bridge an inflationary region with energy density of order $\rho \sim 10^{-10} m_{\rm P}^4$ and a quintessence region with energy density of order $\rho \sim 10^{-120} m_{\rm P}^4$, *i.e.*, the potential must bridge regions with a difference of around 110 order of magnitude in energy density. This is typically achieved with a new region of $V(\phi)$ with very large slope, in between the inflationary plateau and the quintessential tail. As the field approaches it, its kinetic energy density grows and dominates. The field becomes oblivious to the potential, engaging in free-fall during a period called kination. Among the different observational consequences, perhaps the most important one is the generation of a peak in the density spectrum of GWs for the modes that re-enter the horizon during this period. In more physical terms, since the density of GWs scales as $\rho \propto a^{-4}$ when sub-horizon and the background density scales as $\rho \propto a^{-6}$ during kination, the contribution of GWs to the total density budget grows until radiation becomes the dominant component. Therefore, if kination lasts too long, there may be enough GWs to disturb to delicate process of BBN. This is a generic issue with quintessential inflation models and one needs to ensure that reheating is efficient enough.

In Chapter 6 we address the issue of overproduction of GWs during kination by considering the same modified gravity setup as in Chapter 5. In the Einstein frame, other than the coupling between the field and the matter action (see above), the modified gravity setup also leads to the appearance of a quartic kinetic term for the field. In Chapters 4 and 5 we ignore this term, as it is negligible for the region in parameter space under consideration. In Chapter 6 we consider another limit, with α very large, after undergoing a post-inflationary sudden change in value, and study the post-inflationary evolution in the kinetic domination regime, *i.e.*, in the regime where the field becomes oblivious to the potential. We find a new period of cosmic expansion, which we call hyperkination, during which the background density, still dominated by the field, scales as radiation. This period takes place prior to regular

kination, and we find that the latter is an attractor; the field always ends up engaging in regular free-fall during kination. We calculate the density spectrum of GWs both analytically and numerically and find that the spectrum for modes that re-enter the horizon during hyperkination is flat, as for radiation, effectively truncating the kination peak. This allows us to bring the spectrum within observable frequencies without violating the BBN bound. We run a parameter space scan, looking for the required parameter values such that the gravitational wave signal is observable by upcoming gravitational wave experiments, such as LISA or ET, and find ample parameter space. It should be emphasized that our analysis is completely model-independent. This is because, during both hyperkination and kination, the field is kinetically dominated and therefore oblivious to the potential.

The spectrum we find has a distinctive shape. If it was detected, it would provide valuable insights into the background theory. Indeed, it would strongly suggest the existence of higher-order kinetic terms in the action. Furthermore, the position of the "knee" could yield the value of the coupling constant α, were the energy scale of inflation known.

The value of the density of the Universe today measured by Planck is not only at odds with the value expected from theoretical considerations, as we comment above, but also with local measurements, in what is called the Hubble tension. Although the latter is much less dramatic than the former, its statistical significance has led the cosmology community to take it more and more seriously, both from an observational and a model-building point of view. From a theoretical standpoint, the proposals that perhaps are best suited to address the problem are those that are able to reduce the comoving sound horizon at the time of decoupling. Among those, early dark energy (EDE) is the one that has received more attention, making it the leading candidate. Of course, if observational evidence in favour of EDE was to grow, one of the more pressing issues would be to embed it in a more complete theoretical framework.

In Chapter 7 we propose a toy model of unified EDE and quintessence. There,

a scalar field is initially frozen at an enhanced symmetry point. At a redshift close to matter-radiation equality, it thaws and briefly behaves as EDE, to then quickly free-fall with density $\rho \propto a^{-6}$ and re-freeze at a later time. Finally, when the energy density of the background becomes comparable to that of the field, it unfreezes again and accounts for dark energy. The free-fall, a distinctive behaviour different from most EDE models where the field oscillates around the minimum of its potential, is achieved via a potential which we take to be of the form $V \sim \exp(-\exp(\phi))$. Such a choice is phenomenological; our purpose is to show that a steep enough potential can lead to the desired behaviour. Of course, finding a potential better grounded from a theoretical standpoint is the logical next step for future work.

The research presented in this thesis leaves room for exciting new avenues. For example, the modified gravity setup used in Chapters 4-6 could help ameliorate the Hubble tension. Indeed, we found that the coupling between the matter action and the quintessence field depends on the trace of the background fluid energy-momentum tensor. In this way, the coupling disappears for a background fluid with $w = 1/3$ but is turned on for $w = 0$. This is reminiscent of Ref. [168], where the same coupling in the matter action is found and a scalar field receives an energy injection from a neutrino field around matter-radiation equality to act as EDE. In the same spirit, the inflaton could briefly act as EDE around matter-radiation equality, a behaviour coming solely from the modified gravity setup, to then become quintessence at late times. I believe this is a very attractive idea since the Hubble tension could be resolved without the introduction of any new degree of freedom.

One other possible way to address the issue with kination generating a spike in the spectrum of GWs large enough to disturb BBN would be to couple the inflaton field to a non-Abelian gauge field, via a Chern-Simmons term. Indeed, the coupling with a gauge field is expected to act as extra friction for the field [503], thereby possibly reducing the barotropic parameter of the Universe and therefore also the slope of the peak in the GW spectrum. The need for the gauge field to be non-Abelian is slightly more technical, having to do with the suppression of the large

scale anisotropy that one would obtain if simply working with abelian gauge fields [504]. Exploring the effects of one such coupling on a stiff period of the history of the Universe after the end of inflation could help obtain information about reheating from the observation of the stochastic GW background, an exciting prospect with the launch in the near future of ground and space-based observatories such as the ET or DECIGO, or the relatively futuristic BBO.

Finally, from a more open-ended perspective, I believe it would be interesting to study the generation of scalar-induced GWs in the context of Palatini modified gravity. Indeed, as discussed above, when departing from the Einstein-Hilbert action, the metric and Palatini formalisms of general relativity do not agree with each other. In particular, the appearance of a quartic kinetic term may affect the generation of large scalar perturbations, possibly leading to the formation of PBHs, as well as the generation of GWs from second-order scalar perturbations. If detected, this could provide valuable insights regarding the different formalisms of the theory of gravity.

Appendix A

Detailed Calculations

A.1 Gauge Transformations of Perturbations

Let us study the transformation properties of perturbations under the general gauge transformation

$$x^\mu \mapsto \tilde{x}^\mu = x^\mu + \xi^\mu(t, \mathbf{x}), \tag{A.1}$$

where ξ^μ is assumed to be small and can thus be treated as a perturbation. Thus,

$$\frac{\partial \tilde{x}^\mu}{\partial x^\nu} = \begin{pmatrix} 1 + (\xi^0)' & \partial_i \xi^0 \\ (\xi^i)' & \delta^i_j + \partial_j \xi^i \end{pmatrix}, \quad \frac{\partial x^\mu}{\partial \tilde{x}^\nu} = \begin{pmatrix} 1 - (\xi^0)' & -\partial_i \xi^0 \\ -(\xi^i)' & \delta^i_j - \partial_j \xi^i \end{pmatrix}, \tag{A.2}$$

where a prime denotes a derivative with respect to conformal time.

Working to linear order, we expand all quantities as

$$\chi(\eta, \mathbf{x}) = \bar{\chi}(\eta) + \delta\chi(\eta, \mathbf{x}), \tag{A.3}$$

where $\chi(\eta, \mathbf{x})$ stands for any cosmological field, like the metric $g_{\mu\nu}$ or the matter fields in the energy-momentum tensor $T_{\mu\nu}$, such as the inflaton ϕ or the background density ρ and pressure p. Note that in Eq. (A.3) we have split χ into a homogeneous background part $\bar{\chi}$, which only depends on cosmic time, and a small perturbation $\delta\chi$. Since the latter satisfies $\delta\chi \ll \bar{\chi}$, the perturbed Einstein and continuity equations, $\delta G_{\mu\nu} = \delta T_{\mu\nu}/m_{\rm P}^2$ and $\nabla_\mu \delta T^{\mu\nu} = 0$, approximate well the full non-linear solution.

Another advantage of working to linear order is that the Einstein equations do not mix scalar, vector and tensorial perturbations [32]. It is therefore convenient to use the scalar-vector-tensor (SVT) decomposition for perturbations [51]. For a 3-vector B_i this simply means

$$B_i = \partial_i B + \hat{B}_i, \tag{A.4}$$

where B is a scalar and $\hat{B}_i$ is a divergenceless 3-vector, *i.e.*, $\partial_i \hat{B}^i = 0$. For example, the spatial part of the gauge transformation in Eq. (A.1) would be decomposed as

$$\xi_i = \partial_i \xi + \hat{\xi}_i, \tag{A.5}$$

where ξ is a scalar and $\partial_i \hat{\xi}^i = 0$.

For a $(0,2)$ symmetric tensor E_{ij} we have

$$E_{ij} = C\delta_{ij} + \partial_{\langle i}\partial_{i\rangle} E + \partial_{(i}\hat{E}_{j)} + h_{ij}, \tag{A.6}$$

where C and E are scalars, $\hat{E}_i$ is a divergenceless 3-vector, *i.e.*, $\partial_i \hat{E}^i = 0$ and h_{ij} is a traceless and divergenceless $(0,2)$ symmetric tensor, *i.e.*, $\partial_i h^{ij} = 0$ and $h^i{}_i = 0$. We have also defined

$$\partial_{\langle i}\partial_{i\rangle} E \equiv \left(\partial_i\partial_j - \frac{1}{3}\delta_{ij}\nabla^2\right) E, \tag{A.7}$$

$$\partial_{(i}\hat{E}_{j)} \equiv \frac{1}{2}\left(\partial_i \hat{E}_j + \partial_j \hat{E}_i\right). \tag{A.8}$$

Note that Eq. (A.7) is the traceless contribution from the scalar perturbations.

The most general FRW metric perturbed to first order reads [49, 50]

$$\begin{aligned} \mathrm{d}s^2 &= (\bar{g}_{\mu\nu} + \delta g_{\mu\nu})\,\mathrm{d}x^\mu \mathrm{d}x^\nu \\ &= a^2(\eta)\left[-(1+2A)\mathrm{d}\eta^2 + 2B_i \mathrm{d}\eta \mathrm{d}x^i + (\delta_{ij} + 2E_{ij})\,\mathrm{d}x^i \mathrm{d}x^j\right], \end{aligned} \tag{A.9}$$

where the factors of 2 have been chosen for convenience. Note that with the SVT decomposition, the 10 d.o.f. of the metric have been decomposed into 4 scalars (A, B, C and E), two divergenceless 3-vectors ($\hat{B}_i$ and $\hat{E}_i$) and one divergenceless and traceless symmetric $(0,2)$ tensor (h_{ij}).

In order find how the metric perturbations transform under Eq. (A.1) we take into account that the spacetime interval is invariant

$$\mathrm{d}s^2 = g_{\mu\nu}\mathrm{d}x^\mu \mathrm{d}x^\nu = \tilde{g}_{\mu\nu}\mathrm{d}\tilde{x}^\mu \mathrm{d}\tilde{x}^\nu = \tilde{g}_{\alpha\beta}\frac{\partial \tilde{x}^\alpha}{\partial x^\mu}\frac{\partial \tilde{x}^\beta}{\partial x^\nu}\mathrm{d}x^\mu \mathrm{d}x^\nu, \tag{A.10}$$

where we have relabelled indices. Thus, the equation relating the metric in the old coordinates x^μ to the metric in the new coordinates $\tilde{x}^\mu$ reads

$$g_{\mu\nu}(x) = \tilde{g}_{\alpha\beta}(\tilde{x})\frac{\partial \tilde{x}^\alpha}{\partial x^\mu}\frac{\partial \tilde{x}^\beta}{\partial x^\nu}. \tag{A.11}$$

Using Eq. (A.2) it is straightforward to find that the scalar perturbations transform as

$$A \mapsto \tilde{A} = A - (\xi^0)' - \mathcal{H}\xi^0, \tag{A.12}$$

$$B \mapsto \tilde{B} = B + \xi^0 - \xi', \tag{A.13}$$

$$C \mapsto \tilde{C} = C - \mathcal{H}\xi^0 - \frac{1}{3}\nabla^2\xi, \tag{A.14}$$

$$E \mapsto \tilde{E} = E - \xi, \tag{A.15}$$

where ξ is the scalar part in Eq. (A.5). The vector perturbations transform as

$$\hat{B}_i \mapsto \hat{\tilde{B}}_i = \hat{B}_i - (\hat{\xi}_i)' \tag{A.16}$$

$$\hat{E}_i \mapsto \hat{\tilde{E}}_i = \hat{E}_i - \hat{\xi}_i, \tag{A.17}$$

where $\hat{\xi}_i$ is the divergenceless vector part in Eq. (A.5). Finally, the tensor perturbations are gauge invariant

$$h_{ij} \mapsto \hat{h}_{ij} = h_{ij}. \tag{A.18}$$

Note that we can use the freedom to choose the gauge functions ξ^0 and ξ in order to set two of the four scalar perturbations to zero. There are different possible choices, but perhaps two of the most useful ones are the Newtonian gauge, with $B = E = 0$, and the spatially flat gauge, with $C = E = 0$.

We now deal with the perturbations of the energy-momentum tensor. They can be written as

$$T^0{}_0 = -(\bar{\rho} + \delta\rho), \tag{A.19}$$

$$T^{i}_{\ 0} = -(\bar{\rho} + \bar{p})v_i \equiv q_i, \tag{A.20}$$

$$T^{i}_{\ j} = (\bar{p} + \delta p)\delta^{i}_{j} + \Pi^{i}_{\ j}, \tag{A.21}$$

where v^i is the bulk velocity (notice it is a perturbation) and we have defined the momentum density q_i and anisotropic stress $\Pi^{i}_{\ j}$, which is traceless $\Pi^{i}_{\ i} = 0$. Since the different contributions to the energy-momentum tensor are additive, the total perturbations share the same property. For example, the total momentum density is $q_i = \sum_{(a)} q_i^{(a)}$, where (a) labels the different contributing species. Note that that the velocities v_i do not add, only the momentum densities do.

In order to find how the matter perturbations transform we use the same producedure as for the metric. Indeed, under coordinate transformations, the energy-momentum tensor transforms as

$$T^{\mu}_{\ \nu}(x) = \frac{\partial x^{\mu}}{\partial \tilde{x}^{\alpha}} \frac{\partial \tilde{x}^{\beta}}{\partial x^{\nu}} \tilde{T}^{\alpha}_{\ \beta}(\tilde{x}) \tag{A.22}$$

Using Eq. (A.2) again, we obtain

$$\delta\rho \mapsto \delta\tilde{\rho} = \delta\rho - \bar{\rho}'\xi^0, \tag{A.23}$$

$$\delta p \mapsto \delta\tilde{p} = \delta p - \bar{p}'\xi^0, \tag{A.24}$$

$$q_i \mapsto \tilde{q}_i = q_i + (\bar{\rho} + \bar{p})\partial_0\xi_i, \tag{A.25}$$

$$\Pi^{i}_{\ j} \mapsto \tilde{\Pi}^{i}_{\ j} = \Pi^{i}_{\ j}. \tag{A.26}$$

A.2 The Second Order Action for Tensor Perturbations

We decompose the metric into a background part $\bar{g}_{\mu\nu}(\eta) = a^2(\eta)\eta_{\mu\nu}$ plus a small perturbation $\delta g_{\mu\nu}(\eta, \mathbf{x}) = a^2(\eta)h_{\mu\nu}$ as

$$g_{\mu\nu}(\eta, \mathbf{x}) = \bar{g}_{\mu\nu}(\eta) + \delta g_{\mu\nu}(\eta, \mathbf{x}) = a^2(\eta)\left(\eta_{\mu\nu} + h_{\mu\nu}\right), \tag{A.27}$$

where $h_{\mu 0} = \partial_i h^{ij} = h^i{}_i = 0$. Its inverse reads

$$g^{\mu\nu} = a^{-2}(\eta)\left(\eta^{\mu\nu} - h^{\mu\nu}\right). \tag{A.28}$$

Note that writing $g_{\mu\nu}$ in this way, $h_{\mu\nu}$ corresponds to a linear metric perturbation in Minkowski. Thus, since Minkowski and FRW are conformally related, we can straightforwardly obtain the scalar curvature of the perturbed FRW metric from the perturbed Minkowski one. Indeed, given two metrics $g_{\mu\nu}$ and $\tilde{g}_{\mu\nu}$ related to each other via a conformal transformation $g_{\mu\nu} \to \tilde{g}_{\mu\nu} = \Omega^2 g_{\mu\nu}$, the corresponding Ricci scalars are related via

$$R \mapsto \tilde{R} = \frac{1}{\Omega^2}\left[R - 6\nabla_\sigma\nabla^\sigma \ln\Omega - 6\nabla_\sigma \ln\Omega \nabla^\sigma \ln\Omega\right], \tag{A.29}$$

In our case $\Omega = a$, thus

$$\begin{aligned} R^{\mathrm{FRW}} &= \frac{1}{a^2(\eta)}\left[R^{\mathrm{MK}} + 6\partial_\eta^2(\ln a) + 6\left(\frac{a'}{a}\right)^2 + 6(\eta^{\alpha\beta} - h^{\alpha\beta})\Gamma^0_{\alpha\beta}\partial_\eta \ln a\right] \\ &= \frac{R^{\mathrm{MK}}}{a^2(\eta)} + \frac{6}{a^2}\left(\mathcal{H}^2 + \mathcal{H}'\right) - 3\frac{\mathcal{H}}{a^2}h^{ij}h'_{ij}, \end{aligned} \tag{A.30}$$

where R^{FRW} and R^{MK} are the Ricci scalars in perturbed FRW and Minkowski, respectively, and $\Gamma^0_{\alpha\beta}$ are the Christoffel symbols of the perturbed Minkowski metric $\eta_{\mu\nu} + h_{\mu\nu}$. In the last step, we have used that

$$\Gamma^0_{\alpha\beta} = \frac{1}{2}(\eta^{0\lambda} - h^{0\lambda})(\partial_\alpha h_{\lambda\beta} + \partial_\beta h_{\lambda\alpha} - \partial_\lambda h_{\alpha\beta}) = -\frac{1}{2}\eta^{0\lambda}\partial_\lambda h_{\alpha\beta}, \tag{A.31}$$

since $h_{\mu\nu}$ is purely spatial. Furthermore,

$$(\eta^{\alpha\beta} - h^{\alpha\beta})\Gamma^0_{\alpha\beta} = -\frac{1}{2}(\eta^{\alpha\beta} - h^{\alpha\beta})\eta^{0\lambda}\partial_\lambda h_{\alpha\beta} = -\frac{1}{2}h^{ij}h'_{ij}, \tag{A.32}$$

where we have also used that $h_{\mu\nu}$ is traceless.

We now sketch the calculation of the scalar curvature for the perturbed Minkowski metric. In order to obtain the linearized action we proceed as usual, first by computing the Riemann tensor

$$R^\rho{}_{\mu\sigma\nu} = \partial_\sigma\Gamma^\rho_{\nu\mu} - \partial_\nu\Gamma^\rho_{\sigma\mu} + \Gamma^\rho_{\sigma\lambda}\Gamma^\lambda_{\nu\mu} - \Gamma^\rho_{\nu\lambda}\Gamma^\lambda_{\rho\mu}, \tag{A.33}$$

to then obtain the scalar curvature $R = (\eta^{\mu\nu} - h^{\mu\nu})\, R_{\mu\nu}$ from the Ricci tensor $R_{\mu\nu} = R^{\rho}{}_{\mu\rho\nu}$. To first order in $h_{\mu\nu}$ the Christoffel symbols read

$$\Gamma^{\rho}_{\mu\nu} = \frac{1}{2}\eta^{\rho\lambda}\left(\partial_\mu h_{\nu\lambda} + \partial_\nu h_{\mu\lambda} + \partial_\lambda h_{\mu\nu}\right), \tag{A.34}$$

and only the $\partial\Gamma$ terms of the Riemann tensor contribute, since the Γ^2 are second order in $h_{\mu\nu}$. After some algebra, it is not difficult to find that the scalar curvature to first order in $h_{\mu\nu}$ reads

$$R^{(1)} = \partial_\mu\partial_\nu h^{\mu\nu} - \Box h = 0. \tag{A.35}$$

To second order in $h_{\mu\nu}$ we have in principle three contributions, since

$$R = (\eta^{\mu\nu} - h^{\mu\nu})R_{\mu\nu} = \eta^{\mu\nu}R^{(2)}_{\mu\nu} - h^{\mu\nu}R^{(1)}_{\mu\nu}. \tag{A.36}$$

The first are the Γ^2 terms with the Christoffel symbols given by Eq. (A.34). This gives the contribution

$$\begin{aligned}
\eta^{\mu\nu} \quad & \left(\Gamma^{(1)\rho}_{\rho\lambda}\Gamma^{(1)\lambda}_{\nu\mu} - \Gamma^{(1)\rho}_{\nu\lambda}\Gamma^{(1)\lambda}_{\rho\mu}\right) = \frac{1}{4}\eta^{\mu\nu}(\partial_\mu h_{\sigma\nu}\partial^\sigma h + \partial_\nu h_{\sigma\mu}\partial^\sigma h - \partial_\sigma h_{\mu\nu}\partial^\sigma h \\
+ \quad & 2\partial^\sigma h_\nu{}^\lambda\partial_\sigma h_{\lambda\mu} - 2\partial^\lambda h^\sigma{}_\nu\partial_\sigma h_{\lambda\mu} - \partial_\mu h_{\lambda\sigma}\partial_\nu h^{\lambda\sigma}) \\
= \quad & \frac{1}{4}(2\partial_\lambda h_\sigma{}^\lambda\partial^\sigma h - \partial_\sigma h\partial^\sigma h + \partial_\sigma h_{\mu\nu}\partial^\sigma h^{\mu\nu} - 2\partial^\lambda h^\sigma{}_\mu\partial_\sigma h_\lambda{}^\mu)
\end{aligned} \tag{A.37}$$

The second are the $\partial\Gamma$ terms with the second order Christoffel symbols

$$\Gamma^{\rho}_{\mu\nu} = -\frac{1}{2}h^{\rho\lambda}\left(\partial_\mu h_{\nu\lambda} + \partial_\nu h_{\mu\lambda} + \partial_\lambda h_{\mu\nu}\right). \tag{A.38}$$

This gives the contribution

$$\begin{aligned}
\eta^{\mu\nu} \quad & \left(\partial_\rho{}^{(2)}\Gamma^{\rho}_{\mu\nu} - \partial_\nu{}^{(2)}\Gamma^{\rho}_{\rho\mu}\right) = \frac{1}{2}\eta^{\mu\nu}h^{\rho\lambda}\left(\partial_\rho\partial_\lambda h_{\mu\nu} + \partial_\nu\partial_\mu h_{\lambda\rho} - \partial_\rho\partial_\mu h_{\lambda\nu} - \partial_\nu\partial_\lambda h_{\rho\mu}\right) \\
+ \quad & \frac{1}{2}\eta^{\mu\nu}\left(\partial_\rho h^{\rho\lambda}\partial_\lambda h_{\mu\nu} + \partial_\nu h^{\rho\lambda}\partial_\mu h_{\lambda\rho} - \partial_\rho h^{\rho\lambda}\partial_\nu h_{\lambda\mu} - \partial_\rho h^{\rho\lambda}\partial_\mu h_{\lambda\nu}\right) \\
= \quad & \frac{1}{2}h^{\rho\lambda}\left(\partial_\rho\partial_\lambda h + \Box h_{\lambda\rho} - \partial_\rho\partial_\sigma h_\lambda{}^\sigma - \partial_\sigma\partial_\lambda h_\rho{}^\sigma\right) \\
+ \quad & \frac{1}{2}\left(\partial_\rho h^{\rho\lambda}\partial_\lambda h + \partial_\mu h^{\rho\lambda}\partial^\mu h_{\lambda\rho} - 2\partial_\rho h^{\rho\lambda}\partial_\sigma h_\lambda{}^\sigma\right)
\end{aligned} \tag{A.39}$$

The third come from

$$-h^{\mu\nu}R^{(1)}_{\mu\nu} = -\frac{1}{2}h^{\mu\nu}\left(\partial_\sigma\partial_\nu h^\sigma{}_\mu + \partial_\sigma\partial_\mu h^\sigma{}_\nu - \partial_\mu\partial_\nu h - \Box h_{\mu\nu}\right), \tag{A.40}$$

where $R^{(1)}_{\mu\nu}$ is the Ricci tensor to first order in $h_{\mu\nu}$.

Using that $\partial_\mu h^{\mu\nu} = h^\mu{}_\mu = 0$ and summing the three contributions in Eqs. (A.37), (A.39) and (A.40) gives the second-order scalar curvature for the perturbed Minkowski metric

$$R^{(2)} = \frac{3}{4}\partial_\mu h_{\rho\sigma}\partial^\mu h^{\rho\sigma} - \frac{1}{2}\partial_\mu h_{\nu\beta}\partial^\nu h^{\mu\beta} + h^{\mu\nu}\Box h_{\mu\nu} \tag{A.41}$$

Finally, combining Eqs. (A.35) and (A.41) with Eq. (A.30) we obtain the scalar curvature for the perturbed FRW metric to all order up to two.

$$\begin{aligned} {}^{(0)}R^{\rm FRW} &= \frac{6}{a^2}\left(\mathcal{H}^2 + \mathcal{H}'\right) \\ {}^{(1)}R^{\rm FRW} &= 0 \\ {}^{(2)}R^{\rm FRW} &= \frac{1}{a^2}\left[\frac{3}{4}\partial_\mu h_{\rho\sigma}\partial^\mu h^{\rho\sigma} - \frac{1}{2}\partial_\mu h_{\nu\beta}\partial^\nu h^{\mu\beta} + h^{\mu\nu}\Box h_{\mu\nu} - 3\mathcal{H}h^{ij}h'_{ij}\right] \end{aligned} \tag{A.42}$$

In order to obtain the action to second order in h_{ij} we still have to perturb the determinant of the metric. We start by writing

$$\begin{aligned} -g &= -\det\big(a^2(\eta_{\mu\nu} + h_{\mu\nu})\big) = -\det\big(a^2\eta_{\mu\sigma}\big)\det\big(\delta^\sigma{}_\nu + \eta^{\sigma\gamma}h_{\gamma\nu}\big) \\ &= a^8\det\big(\delta^\sigma{}_\nu + \eta^{\sigma\gamma}h_{\gamma\nu}\big). \end{aligned} \tag{A.43}$$

Now we use the series expansion of the determinant which, schematically, reads

$$\det(1+\epsilon A) = 1 + \epsilon\,\mathrm{Tr}\,A + \frac{\epsilon^2}{2}\left[(\mathrm{Tr}\,A)^2 - \mathrm{Tr}\big(A^2\big)\right], \tag{A.44}$$

where ϵ simply keeps track of each order in the expansion. In our case $A = \eta^{\sigma\gamma}h_{\gamma\nu} = h^\sigma{}_\nu$. Thus, only the zeroth and second order in the expansion of the determinant have surviving terms. From Eq. (A.43), we have

$$\begin{aligned} {}^{(0)}(-g) &= a^8 \\ {}^{(1)}(-g) &= 0 \\ {}^{(2)}(-g) &= -\frac{a^8}{2}\,\mathrm{Tr}\big(h^\sigma{}_\nu h^\nu{}_\rho\big) = -\frac{a^8}{2}h_{\mu\nu}h^{\mu\nu} \end{aligned} \tag{A.45}$$

Therefore, the full expansion of $\sqrt{-g}$, up to second order in $h_{\mu\nu}$, reads

$$\sqrt{-g} = \sqrt{a^8 - \frac{a^8}{2}h_{\mu\nu}h^{\mu\nu}} = a^4\sqrt{1 - \frac{1}{2}h_{\mu\nu}h^{\mu\nu}} = a^4 - \frac{a^4}{4}h_{\mu\nu}h^{\mu\nu}, \tag{A.46}$$

or, order by order,

$$\begin{aligned} {}^{(0)}\sqrt{-g} &= a^4 \\ {}^{(1)}\sqrt{-g} &= 0 \\ {}^{(2)}\sqrt{-g} &= -\frac{a^4}{4}h_{\mu\nu}h^{\mu\nu}. \end{aligned} \tag{A.47}$$

We are getting closer to our final result. The Einstein-Hilbert part of the action, to second order, reads

$$\begin{aligned} {}^{(2)}(\sqrt{-g}R) = {}^{(0)}\sqrt{-g}{}^{(2)}R + {}^{(2)}\sqrt{-g}{}^{(0)}R = -\frac{3a^2}{2}h_{\mu\nu}h^{\mu\nu}\left(\mathcal{H}^2+\mathcal{H}'\right) \\ +a^2\left[\frac{3}{4}\partial_\mu h_{\rho\sigma}\partial^\mu h^{\rho\sigma} - \frac{1}{2}\partial_\mu h_{\nu\beta}\partial^\nu h^{\mu\beta} + h^{\mu\nu}\Box h_{\mu\nu} - 3\mathcal{H}h^{ij}h'_{ij}\right]. \end{aligned} \tag{A.48}$$

By using $h_{0\mu}=0$, this expression can be further simplified to obtain

$$\begin{aligned} \delta^{(2)}S = -\frac{3m_{\rm P}^2}{4}\int \mathrm{d}^3x\mathrm{d}\eta\, a^2\left(\mathcal{H}^2+\mathcal{H}'\right)h_{\mu\nu}h^{\mu\nu} \\ +\frac{m_{\rm P}^2}{2}\int \mathrm{d}^3x\mathrm{d}\eta\, a^2\Big[-\frac{3}{4}(h_{ij})'(h^{ij})' + \frac{3}{4}\partial_k h_{ij}\partial^k h^{ij} - \frac{1}{2}\partial_k h_{ij}\partial^i h^{kj} \\ -h^{ij}h''_{ij} + h^{ij}\partial_k\partial^k h_{ij} - 3\mathcal{H}h^{ij}h'_{ij}\Big]. \end{aligned} \tag{A.49}$$

Noting that the prefactor in the integrand depends only on time, we can integrate by parts the spatial derivatives without picking up an extra term. This kills the third term and the fifth can be combined with the second to give

$$\begin{aligned} S &= -\frac{3m_{\rm P}^2}{4}\int \mathrm{d}^3x\mathrm{d}\eta\, a^2\left(\mathcal{H}^2+\mathcal{H}'\right)h_{\mu\nu}h^{\mu\nu} \\ &+ \frac{m_{\rm P}^2}{2}\int \mathrm{d}^3x\mathrm{d}\eta\, a^2\left(-\frac{3}{4}(h_{ij})'(h^{ij})' - \frac{1}{4}\partial_k h_{ij}\partial^k h^{ij} - h^{ij}h''_{ij} - 3\mathcal{H}h^{ij}h'_{ij}\right). \end{aligned} \tag{A.50}$$

Now, integrating by parts the third term gives

$$\begin{aligned} S &= -\frac{3m_{\rm P}^2}{4}\int \mathrm{d}^3x\mathrm{d}\eta\, a^2\left(\mathcal{H}^2+\mathcal{H}'\right)h_{\mu\nu}h^{\mu\nu} \\ &+ \frac{m_{\rm P}^2}{2}\int \mathrm{d}^3x\mathrm{d}\eta\, a^2\left(\frac{1}{4}(h_{ij})'(h^{ij})' - \frac{1}{4}\partial_k h_{ij}\partial^k h^{ij} - \mathcal{H}h^{ij}h'_{ij}\right). \end{aligned} \tag{A.51}$$

Finally, integrating by parts the last term, we arrive at

$$S = \frac{m_{\rm P}^2}{8}\int \mathrm{d}^3x\mathrm{d}\eta\, a^2\left((h_{ij})'(h^{ij})' - \partial_k h_{ij}\partial^k h^{ij}\right) - \frac{m_{\rm P}^4}{4}\int \mathrm{d}^3x\mathrm{d}\eta\, a^2(2\mathcal{H}'+\mathcal{H}^2)h^{ij}h'_{ij}. \tag{A.52}$$

The last contribution comes from the matter action. We do this for the Palatini Lagrangian in Eq. (5.15), but the the proof is general. As before, we have two terms (remember ${}^{(1)}\sqrt{-g}=0$)

$$ {}^{(2)}(\sqrt{-g}\mathcal{L}_\phi) = {}^{(0)}\sqrt{-g}{}^{(2)}\mathcal{L}_\phi + {}^{(2)}\sqrt{-g}{}^{(0)}\mathcal{L}_\phi, \tag{A.53}$$

where

$$\mathcal{L}_\phi = -\frac{1}{2}g^{\mu\nu}\partial_\mu\phi\partial_\nu\phi + \frac{\alpha}{4}f(\phi)(g^{\mu\nu}\partial_\mu\phi\partial_\nu\phi)(g^{\alpha\beta}\partial_\alpha\phi\partial_\beta\phi) - \bar{V}. \tag{A.54}$$

The zeroth-order Lagrangian is simply

$${}^{(0)}\mathcal{L}_\phi = -\frac{1}{2}\bar{g}^{\mu\nu}\partial_\mu\phi\partial_\nu\phi + \frac{\alpha}{4}f(\phi)(\bar{g}^{\mu\nu}\partial_\mu\phi\partial_\nu\phi)(\bar{g}^{\alpha\beta}\partial_\alpha\phi\partial_\beta\phi) - \bar{V}, \tag{A.55}$$

while to second order, using the inverse metric (A.28), we have

$${}^{(2)}\mathcal{L}_\phi = -\frac{a^{-4}}{2}h^{\mu\sigma}h_\sigma{}^\nu\partial_\mu\phi\partial_\nu\phi + \frac{\alpha a^{-4}}{4}f(\phi)\left(h^{\mu\nu}\partial_\mu\phi\partial_\nu\phi\right)\left(h^{\alpha\beta}\partial_\alpha\phi\partial_\beta\phi\right) = 0, \tag{A.56}$$

where we have used that $\phi=\phi(t)$ and $h^{0\mu}=0$. This means that the second-order matter action reads

$$\begin{aligned} {}^{(2)}(\sqrt{-g}\mathcal{L}_\phi) &= {}^{(2)}\sqrt{-g}{}^{(0)}\mathcal{L}_\phi = -\frac{a^4}{4}h_{\mu\nu}h^{\mu\nu}\left(\frac{1}{2a^2}\phi'^2 + \frac{\alpha f(\phi)}{4a^4}\phi'^4 - \bar{V}\right) \\ &= -\frac{a^4}{4}h_{\mu\nu}h^{\mu\nu}p_\phi, \end{aligned} \tag{A.57}$$

where we have used the second line in Eq. (5.34).

Solving for p_ϕ in the Friedmann equations and plugging it back in Eq. (A.57) finally gives

$$S_m = \int \mathrm{d}^3x\mathrm{d}\eta\,{}^{(2)}(\sqrt{-g}\mathcal{L}_\phi) = \frac{m_{\rm P}^2}{4}\int \mathrm{d}^3x\mathrm{d}\eta\, a^2\left(2\mathcal{H}' + \mathcal{H}^2\right)h_{\mu\nu}h^{\mu\nu}, \tag{A.58}$$

which exactly cancels the second integral in Eq. (A.52).

Putting everything together, the action to second order in the tensor perturbations finally reads

$$S = -\frac{m_{\rm P}^2}{8}\int \mathrm{d}^4x\sqrt{-\bar{g}}\bar{g}^{\alpha\beta}\partial_\alpha h^{\mu\nu}\partial_\beta h_{\mu\nu} \tag{A.59}$$

$$= \frac{m_{\rm P}^2}{8}\int \mathrm{d}\eta\mathrm{d}^3x a^2\left[(h'_{ij})^2 - \partial_m h_{ij}\partial^m h^{ij}\right]. \tag{A.60}$$

A.3 The Gravitational Wave Density Spectrum During Kination

We give here some details regarding the calculation of the GW density spectrum during a period of kination, followed by a period of radiation domination.

The first step is to obtain the scale factor by solving the first Friedmann equation. It reads

$$a = \begin{cases} \left[-\dfrac{1}{(1-\epsilon_H)H_{\rm end}\eta}\right]^{1/(1-\epsilon_H)}, & \eta \leq \eta_{\rm end}\,, \\ \sqrt{2H_{\rm end}\eta + 3}\,, & \eta_{\rm end} \leq \eta \leq \eta_{\rm reh}\,, \\ \dfrac{H_{\rm end}(\eta+\eta_{\rm reh})+3}{\sqrt{2H_{\rm end}\eta_{\rm reh}+3}}\,, & \eta_{\rm reh} \leq \eta\,, \end{cases} \tag{A.61}$$

where $H_{\rm end}$ and $\eta_{\rm end} < 0$ are the Hubble parameter and conformal time at the end of inflation, respectively, and $\eta_{\rm reh}$ is the time of reheating. We have assumed that the first Hubble slow-roll parameter ϵ_H is constant during inflation and normalised the scale factor as $a(\eta_{\rm end}) = 1$. We also approximate

$$\eta_{\rm end} = -\frac{1}{(1-\epsilon_H)H_{\rm end}} \simeq -\frac{1}{H_{\rm end}} \equiv -\frac{1}{H}, \tag{A.62}$$

where, to avoid clutter, and slightly abusing notation, we have defined $H \equiv H_{\rm end}$. Note that in the pure de Sitter case, with $\epsilon_H = 0$, the Hubble parameter is constant and equal to H.

The next step is to solve the equation

$$(f_k^s)'' + \left(k^2 - \frac{a''}{a}\right) f_k^s = 0, \tag{A.63}$$

where f_k^s are the GW mode functions and, from Eq. (A.61),

$$\frac{a''}{a} = \begin{cases} \dfrac{2+3\epsilon}{\eta^2}\,, & \eta \leq \eta_{\rm end}, \\ -\dfrac{1}{4z^2}\,, & \eta_{\rm end} \leq \eta \leq \eta_{\rm reh}, \\ 0\,, & \eta_{\rm reh} \leq \eta, \end{cases} \tag{A.64}$$

where

$$z \equiv \eta + \frac{3}{2H}\,. \tag{A.65}$$

We solved Eq. (A.63) for constant slow-parameters (and to first order) during inflation in Sec. 2.1.3 (see Eq. (2.146) and below). Following an analogous procedure for kination and radiation domination, we find

$$f_k^s(\eta) = \begin{cases} \sqrt{\dfrac{\pi}{4k}}\sqrt{-k\eta}\,e^{i\frac{\pi}{4}(2\mu+1)}H_\mu^{(1)}(-k\eta)\,, & \eta \le \eta_{\rm end}\,, \\ \sqrt{\dfrac{\pi}{4k}}\sqrt{kz}\left[\alpha_+(k)e^{-i\pi/4}H_0^{(2)}(kz) + \alpha_-(k)e^{i\pi/4}H_0^{(1)}(kz)\right]\,, & \eta_{\rm end} \le \eta \le \eta_{\rm reh}\,, \\ \dfrac{1}{\sqrt{2k}}\left[\beta_+(k)e^{-ik\eta} + \beta_-(k)e^{ik\eta}\right]\,, & \eta_{\rm reh} \le \eta\,, \end{cases} \tag{A.66}$$

where

$$\mu = \frac{3}{2} + \epsilon_H. \tag{A.67}$$

In order to fix the coefficients $\alpha_\pm$ and $\beta_\pm$, we impose continuity of the mode functions and their derivatives at each transition

$$\lim_{\eta\to\eta_{\rm end}^-} f_k^s(\eta) = \lim_{\eta\to\eta_{\rm end}^+} f_k^s(\eta) \quad \text{and} \quad \lim_{\eta\to\eta_{\rm end}^-} f_k^{s'}(\eta) = \lim_{\eta\to\eta_{\rm end}^+} f_k^{s'}(\eta), \tag{A.68}$$

and likewise at $\eta_{\rm reh}$. Defining the new variable

$$x_{\rm end} \equiv \frac{k}{H}, \tag{A.69}$$

we have

$$k\eta_{\rm end} = -x_{\rm end} \quad \text{and} \quad kz_{\rm end} = \frac{x_{\rm end}}{2}. \tag{A.70}$$

The continuity of the mode functions at the end of inflation reads

$$\sqrt{2}e^{i\frac{\pi}{4}(2\mu+1)}H_\mu^{(1)}(x_{\rm end}) = \alpha_+ e^{-i\pi/4}H_0^{(2)}(\frac{x_{\rm end}}{2}) + \alpha_- e^{i\pi/4}H_0^{(1)}(\frac{x_{\rm end}}{2}), \tag{A.71}$$

while the continuity of their derivatives reads

$$e^{i\frac{\pi}{4}(2\mu+1)}\left[\left(\frac{1}{2}+\mu\right)\frac{H_\mu^{(1)}(x_{\rm end})}{\sqrt{x_{\rm end}}} - \sqrt{x_{\rm end}}H_{\mu+1}^{(1)}(x_{\rm end})\right] = \sqrt{\frac{x_{\rm end}}{2}}\Bigg[\alpha_+ e^{-i\pi/4}H_1^{(2)}(\frac{x_{\rm end}}{2}) + \alpha_- e^{i\pi/4}H_1^{(1)}(\frac{x_{\rm end}}{2})\Bigg] - \frac{1}{\sqrt{2x_{\rm end}}}\left[\alpha_+ e^{-i\pi/4}H_0^{(2)}(\frac{x_{\rm end}}{2}) + \alpha_- e^{i\pi/4}H_0^{(1)}(\frac{x_{\rm end}}{2})\right], \tag{A.72}$$

where we have omitted the k dependence of $\alpha_\pm$ to avoid clutter. The second continuity condition can be simplified by plugging Eq. (A.71) in Eq. (A.72) to obtain

$$\begin{aligned} & e^{i\frac{\pi}{4}(2\mu+1)}\sqrt{\frac{2}{x_{\rm end}}}\left[\left(\frac{3}{2}+\mu\right)\frac{H_\mu^{(1)}(x_{\rm end})}{\sqrt{x_{\rm end}}}-\sqrt{x_{\rm end}}H_{\mu+1}^{(1)}(x_{\rm end})\right] \\ & = \alpha_+ e^{-i\pi/4}H_1^{(2)}(\frac{x_{\rm end}}{2})+\alpha_- e^{i\pi/4}H_1^{(1)}(\frac{x_{\rm end}}{2}). \end{aligned} \tag{A.73}$$

In order to obtain α_- (α_+) we multiply Eq. (A.71) by $H_1^{(2)}(\frac{x_{\rm end}}{2})$ ($H_1^{(1)}(\frac{x_{\rm end}}{2})$) and Eq. (A.73) by $H_0^{(2)}(\frac{x_{\rm end}}{2})$ ($H_0^{(1)}(\frac{x_{\rm end}}{2})$) and substract one from the other. The result reads

$$\begin{aligned} \alpha_- &= -\frac{\pi e^{i\pi(\mu+1)/2}}{4\sqrt{2}}\Bigg\{x_{\rm end}H_\mu^{(1)}(x_{\rm end})H_1^{(2)}(\frac{x_{\rm end}}{2})-H_0^{(2)}(\frac{x_{\rm end}}{2})\Bigg[\left(\frac{3}{2}+\mu\right)H_\mu^{(1)}(x_{\rm end}) \\ &- x_{\rm end}H_{\mu+1}^{(1)}(x_{\rm end})\Bigg]\Bigg\}, \end{aligned} \tag{A.74}$$

$$\begin{aligned} \alpha_+ &= \frac{i\pi e^{i\pi(\mu+1)/2}}{4\sqrt{2}}\Bigg\{x_{\rm end}H_\mu^{(1)}(x_{\rm end})H_1^{(1)}(\frac{x_{\rm end}}{2})-H_0^{(1)}(\frac{x_{\rm end}}{2})\Bigg[\left(\frac{3}{2}+\mu\right)H_\mu^{(1)}(x_{\rm end}) \\ &- x_{\rm end}H_{\mu+1}^{(1)}(x_{\rm end})\Bigg]\Bigg\} \end{aligned} \tag{A.75}$$

In the super-horizon limit, *i.e.*, in the limit where $x_{\rm end}\ll 1$, they read

$$\alpha_- = 2^{\mu-3/2}e^{i\pi(\mu+1)/2}\Gamma(\mu)\left[-\frac{2}{\pi}-i\left(\frac{3}{2}-\mu\right)\left(\frac{1}{2}-\frac{i}{\pi}\ln\frac{x_{\rm end}}{2}\right)\right]x_{\rm end}^{-\mu}, \tag{A.76}$$

$$\alpha_+ = i2^{\mu-3/2}e^{i\pi(\mu+1)/2}\Gamma(\mu)\left[-\frac{2}{\pi}+i\left(\frac{3}{2}-\mu\right)\left(\frac{1}{2}+\frac{i}{\pi}\ln\frac{x_{\rm end}}{2}\right)\right]x_{\rm end}^{-\mu}. \tag{A.77}$$

Defining the new variable

$$x_{\rm reh} = k\eta_{\rm reh}\simeq kz_{\rm reh}, \tag{A.78}$$

where in the last step we have taken into account that $\eta_{\rm reh}\gg\eta_{\rm end}$, the continuity of the mode functions at reheating reads

$$\sqrt{\frac{\pi x_{\rm reh}}{2}}\left[\alpha_+e^{-i\pi/4}H_0^{(2)}(x_{\rm reh})+\alpha_-e^{i\pi/4}H_0^{(1)}(x_{\rm reh})\right]=\beta_+e^{-ix_{\rm reh}}+\beta_-e^{ix_{\rm reh}}, \tag{A.79}$$

while the continuity of their derivatives reads

$$i\sqrt{\frac{\pi}{2}}\Bigg\{\frac{1}{2\sqrt{x_{\rm reh}}}\left[\alpha_+ e^{-i\pi/4}H_0^{(2)}(x_{\rm reh})+\alpha_- e^{i\pi/4}H_0^{(1)}(x_{\rm reh})\right]$$
$$-\sqrt{x_{\rm reh}}\left[\alpha_+ e^{-i\pi/4}H_1^{(2)}(x_{\rm reh})+\alpha_- e^{i\pi/4}H_1^{(1)}(x_{\rm reh})\right]\Bigg\}=\beta_+ e^{-ix_{\rm reh}}-\beta_- e^{ix_{\rm reh}}. \quad \text{(A.80)}$$

Subtracting (summing) Eq. (A.80) from Eq. (A.79) we find

$$\begin{aligned}\beta_\pm &= \sqrt{\frac{\pi}{2}}\frac{e^{\pm ix_{\rm reh}}}{2}\Bigg\{\sqrt{x_{\rm reh}}\left[\alpha_+ e^{-i\pi/4}H_0^{(2)}(x_{\rm reh})+\alpha_- e^{i\pi/4}H_0^{(1)}(x_{\rm reh})\right]\\ &\pm \frac{i}{2\sqrt{x_{\rm reh}}}\left[\alpha_+ e^{-i\pi/4}H_0^{(2)}(x_{\rm reh})+\alpha_- e^{i\pi/4}H_0^{(1)}(x_{\rm reh})\right]\\ &\mp i\sqrt{x_{\rm reh}}\left[\alpha_+ e^{-i\pi/4}H_1^{(2)}(x_{\rm reh})+\alpha_- e^{i\pi/4}H_1^{(1)}(x_{\rm reh})\right]\Bigg\} \qquad \text{(A.81)}\end{aligned}$$

In the super-horizon limit, *i.e.*, in the limit where $x_{\rm reh}\ll 1$, they read

$$\begin{aligned}\beta_\pm &= \pm\sqrt{\frac{\pi}{2}}\frac{1}{2\sqrt{x_{\rm reh}}}\left[\frac{i}{2}\left(\alpha_+ e^{-i\pi/4}+\alpha_- e^{i\pi/4}\right)+\frac{1}{\pi}\left(2+\ln x_{\rm reh}\right)\left(\alpha_+ e^{-i\pi/4}-\alpha_- e^{i\pi/4}\right)\right]\\ &= \pm\frac{e^{i\pi(2\mu+1)/4}2^{\mu-3}\Gamma(\mu)}{\sqrt{\pi}\sqrt{x_{\rm reh}}x_{\rm end}^{\mu}}\left(\mu-\frac{3}{2}\right)\left[\ln\frac{\eta_{\rm reh}}{\eta_{\rm end}}+2+\ln 2+\frac{2}{\left(\mu-\frac{3}{2}\right)}\right], \qquad \text{(A.82)}\end{aligned}$$

where we have used the relations

$$\frac{\alpha_+ e^{-i\pi/4}-\alpha_- e^{i\pi/4}}{e^{i\pi/4}2^{\mu-3/2}e^{i\pi(\mu+1)/2}\Gamma(\mu)x_{\rm end}^{-\mu}} = i\left(\frac{3}{2}-\mu\right), \qquad \text{(A.83)}$$

$$\frac{\alpha_+ e^{-i\pi/4}+\alpha_- e^{i\pi/4}}{e^{i\pi/4}2^{\mu-3/2}e^{i\pi(\mu+1)/2}\Gamma(\mu)x_{\rm end}^{-\mu}} = -\frac{4}{\pi}-\frac{2}{\pi}\left(\frac{3}{2}-\mu\right)\ln\frac{x_{\rm end}}{2}. \qquad \text{(A.84)}$$

In the scale-invariant case, with $\epsilon_H=0$ and $\mu=3/2$, the coefficients read

$$\alpha_- = -i\alpha_+ = -\frac{e^{i5\pi/4}}{\sqrt{\pi}x_{\rm end}^{3/2}}, \qquad \text{(A.85)}$$

$$\beta_\pm = \mp\frac{1}{2^{3/2}\sqrt{x_{\rm reh}}x_{\rm end}^{3/2}}. \qquad \text{(A.86)}$$

The coefficients in Eqs. (A.85)-(A.86) can be further simplified. The time of reheating $\eta_{\rm reh}$ can be obtained by remembering that during kination the background density scales as $\rho\propto a^{-6}$ while the radiation density escales as $\rho\propto a^{-4}$. Therefore,

the density parameter of radiation scales as $\Omega_{\rm r} \propto a^2$. Noting that at reheating radiation is the dominant component we have

$$1 \simeq \Omega_{\rm r}^{\rm reh} = \Omega_{\rm r}^{\rm end} \left(\frac{a_{\rm reh}}{a_{\rm end}}\right)^2 = \Omega_{\rm r}^{\rm end} \left(2H\eta_{\rm reh} + 3\right) \simeq 2\Omega_{\rm r}^{\rm end} H\eta_{\rm reh}, \tag{A.87}$$

where we used Eq. (A.61) and the normalization $a(\eta_{\rm end}) = 1$. Thus, also using Eqs. (A.69) and (A.78), we find

$$|\alpha_-|^2 = \frac{H^3}{\pi k^3} \quad \text{and} \quad |\beta_-|^2 = \frac{H^4 \Omega_{\rm r}^{\rm end}}{4k^4}. \tag{A.88}$$

Appendix B

Appendix of Chapter 5

B.1 Solving for the Hubble parameter

In this appendix, we solve the Jordan frame Hubble parameter H in (5.20) explicitly in terms of φ, $\dot{\varphi}$, and the fluid energy density ρ. We begin by using (5.18), (5.23), and (5.25) to decompose the time derivative of f_R as

$$\partial_0 f_R = A + HB\,, \tag{B.1}$$

where

$$A = \frac{2\varphi\dot{\varphi}\tilde{\xi}}{m_{\rm P}^2} + \frac{2\alpha\dot{\varphi}\left(3V'(\varphi) - \tilde{\xi}\varphi R\right)}{m_{\rm P}^4\left(1+\frac{\xi\varphi^2}{m_{\rm P}^2}\right)} + \frac{2\alpha\varphi\dot{\varphi}\tilde{\xi}}{m_{\rm P}^6\left(1+\frac{\xi\varphi^2}{m_{\rm P}^2}\right)^2}T \tag{B.2}$$

and

$$B = \frac{3\alpha}{m_{\rm P}^4}\left[\frac{2\dot{\varphi}^2 - \rho(1+w)(1-3w)}{1+\frac{\xi\varphi^2}{m_{\rm P}^2}}\right], \tag{B.3}$$

where $\tilde{\xi}$ and T are given by Eqs. (5.26) and (5.19) respectively. Note that by using Eq. (5.17), the expression for A can be simplified further to obtain

$$A = \frac{2\varphi\dot{\varphi}\tilde{\xi}}{m_{\rm P}^2}\left(1 + \frac{2\alpha T}{m_{\rm P}^4\left(1+\frac{\xi\varphi^2}{m_{\rm P}^2}\right)^2}\right) + \frac{6\alpha\dot{\varphi}V'}{m_{\rm P}^4\left(1+\frac{\xi\varphi^2}{m_{\rm P}^2}\right)}. \tag{B.4}$$

With these, Eq. (5.20) can be recast as

$$H^2\left(3F_R+3B+\frac{3}{4F_R}B^2\right)+H\left(3A+\frac{3}{2F_R}AB\right)+\frac{3}{4F_R}A^2-\frac{T_{00}}{m_{\rm P}^2}-\frac{\alpha}{4m_{\rm P}^2}R^2=0 \quad \text{(B.5)}$$

and solved for H as

$$H=-\frac{A}{B+2f_R}+\frac{\sqrt{3f_R(4T_{00}+\alpha R^2)}}{3(B+2f_R)}\,, \quad \text{(B.6)}$$

with R, F_R, and T_{00} from Eqs. (5.17), (5.18) and (5.22), respectively. Demanding H to be real sets the requirement $f_R \geq 0$ (note that T_{00} and R^2 are always positive). From Eq. (5.18), this reads

$$\left(1+\frac{\xi\varphi^2}{m_{\rm P}^2}\right)^2 > \frac{\alpha T}{m_{\rm P}^4}=\frac{\alpha}{m_{\rm P}^4}\big(\dot\varphi^2-4V(\varphi)-\rho(1-3w)\big)\,. \quad \text{(B.7)}$$

During inflation, the background matter energy density $\rho = 0$, and the condition is always satisfied when the potential dominates the kinetic term, $4V(\varphi) > \dot\varphi^2$, in particular during slow-roll. It is also easy to satisfy later on, when $\rho > 0$ becomes important and α contributions become irrelevant.

B.2 A bound on the bare mass-squared of the spectator field

Let us estimate the upper bound of $|m^2|$, the mass squared of the spectator field ψ from (5.50), such that it remains negligible at least until reheating. Firstly, let us obtain an upper bound of the value of $\langle\psi^2\rangle$ at the end of inflation. Imposing the requirement that $\bar\rho_\psi^{\rm end} < \bar\rho_r^{\rm end}$, as found by Ref. [289], and using that $\bar\rho_\psi^{\rm end} = \frac{1}{4}\lambda\langle\psi^2\rangle^2$, we find

$$\langle\psi^2\rangle_{\rm end} < 6\sqrt{2}\,(\hat\xi/\sqrt{\lambda})\,\bar H_{\rm end}^2\,. \quad \text{(B.8)}$$

where we considered Eq. (5.51). Considering that the typical value of the amplitude of the oscillating condensate at a given location is of the order $|\psi| \sim \sqrt{\langle\psi^2\rangle}$, we can estimate how it evolves after the end of inflation. Indeed, because

$\frac{1}{4}\lambda|\psi|^4 = \bar{\rho}_\psi \propto \bar{a}^{-4}$, we have $|\psi| \propto \bar{a}^{-1}$. Thus, we obtain

$$|\psi|_{\rm reh} = \frac{\bar{a}_{\rm end}}{\bar{a}_{\rm reh}}|\psi|_{\rm end} \Rightarrow |\psi|_{\rm reh} < 6\left(\frac{2}{\lambda}\right)^{1/4} \hat{\xi}^{3/2}\,\frac{\bar{H}_{\rm end}^2}{m_P}\,, \tag{B.9}$$

where we used Eqs. (5.53) and (B.8).

The quadratic term in Eq. (5.50) takes over from the quartic term at a critical value $\psi_{\rm x}^2$ when $\frac{1}{2}m^2\psi_{\rm x}^2 = \frac{1}{4}\lambda\psi_{\rm x}^4$, which suggests

$$\psi_{\rm x}^2 = 2m^2/\lambda\,. \tag{B.10}$$

To make sure that this does not happen until reheating, we simply require $\psi_{\rm x}^2 \leq |\psi|_{\rm reh}^2$ ($|\psi|$ is reducing in time). Then the bound in Eq. (B.9) results in the bound

$$m^2 < m_{\rm max}^2 \equiv 18\sqrt{2\lambda}\,\hat{\xi}^3\,\frac{\bar{H}_{\rm end}^4}{m_P^2}\,. \tag{B.11}$$

The above is too strict because, if $\bar{\rho}_\psi \ll \bar{\rho}_r$ after the end of inflation, then $\bar{\rho}_\psi$ can remain subdominant until reheating even if the quadratic term in $V(\psi)$ takes over before reheating. So the above bound is sufficient but not, strictly speaking, necessary. Its numerical value may be estimated using the range obtained in Eq. (5.57). Taking $\lambda \sim 1$, we find

$$10^2\ {\rm GeV} \lesssim m_{\rm max} < 10^{15}\ {\rm GeV}. \tag{B.12}$$

The lower bound in the above might be unrealistic because such a particle could have been already observed in the LHC. But we see that the mass range extends well above the TeV scale so there is no real conflict with the observational data.

B.3 Energy density of gravitational radiation at the end of inflation

The energy density of GWs is [505]

$$\rho_{\rm GW}(\tau,\mathbf{x}) = \frac{\langle h'_{ij}(\tau,\mathbf{x})h'_{ij}(\tau,\mathbf{x})\rangle}{32\pi G a^2}\,, \tag{B.13}$$

where the prime denotes derivatives with respect to conformal time τ, h_{ij} are the spatial components of the metric perturbation and we consider superhorizon scales. We consider the Einstein frame and omit the overbar for simplicity. Switching to momentum space, we can define the density parameter of GWs per logarithmic momentum interval

$$\Omega_{\rm GW}(\tau,k) \equiv \frac{1}{\rho_c}\frac{{\rm d}\rho_{\rm GW}(\tau,k)}{{\rm d}\ln k}\,, \tag{B.14}$$

where $\rho_c = 3H^2 m_P^2$. GWs generated by inflation obtain a predominantly scale-invariant superhorizon spectrum given by [425]

$$\Delta_h^2(k) = \frac{2}{\pi^2}\left(\frac{H_{\rm end}}{m_P}\right)^2\left(\frac{k}{k_*}\right)^{n_t} \simeq \frac{2}{\pi^2}\left(\frac{H_{\rm end}}{m_P}\right)^2\,, \tag{B.15}$$

where $|n_t| \ll 1$ ia the tensor spectral index, the star denotes the pivot scale and

$$\langle h_{ij}(\tau,\mathbf{x}) h_{ij}(\tau,\mathbf{x})\rangle = \int \frac{{\rm d}k}{k}\Delta_h^2(k)(\tau,k)\,. \tag{B.16}$$

Then, the final expression of the stochastic GW background from inflation is [423]

$$\Omega_{\rm GW}(\tau,k) = \left(\frac{a_k}{a(\tau)}\right)^4\left(\frac{H_k}{H(\tau)}\right)^2\frac{\Delta_h^2(k)}{24}\,, \tag{B.17}$$

for arbitraty evolution $a(\tau)$, where $a_k H_k = k$ corresponds to horizon re-entry of scale k. Evaluating the above at the end of inflation and integrating over all superhorizon modes we obtain

$$\Omega_{\rm GW}^{\rm end} \simeq \frac{1}{12\pi^2}\left(\frac{H_{\rm end}}{m_P}\right)^2\,, \tag{B.18}$$

where we considered that the integral is dominated by the highest k (i.e. $k_{\rm end}$). Using that $\rho_{\rm GW} = \Omega_{\rm GW}\rho_c$, we find

$$\rho_{\rm GW} \simeq \frac{1}{4\pi^2}H_{\rm end}^4, \tag{B.19}$$

which agrees nicely with the estimate in Ref. [97].

Appendix C

Appendix of Chapter 6

C.1 A toy model for a drastic change of α at the end of inflation

The coefficient α parametrising quadratic gravity can experiece a drastic change at the end of inflation if it is a function of a degree of freedom which changes rapidly at that time. For example, if inflation takes place at the energy of grand unification, as is typically the case, then this degree of freedom could be the Higgs field χ of a Grand Unified Theory (GUT). If the breaking of grand unification takes place via spontaneous symmetry breaking, then the expectation value of χ changes from zero to $M \sim 10^{16}\,\mathrm{GeV}$.

A toy model example of the inflaton potential, which leads to the GUT phase transition but still retains the runaway nature assumed in this work is

$$V(\varphi,\chi) = \frac{1}{4}\lambda(\chi^2 - M^2)^2 + \begin{cases} \frac{1}{2}(m^2 + g^2\chi^2)(\varphi^2 + \mu^2) & ,\ \varphi < 0 \\ \frac{1}{2}(m^2 + g^2\chi^2)\,\frac{\mu^6}{\varphi^4+\mu^4} & ,\ \varphi \geq 0 \end{cases} , \tag{C.1}$$

where m and μ are mass scales with $0 < \mu \ll m < M$ and $\lambda, g \lesssim \mathcal{O}(1)$. By taking $\lambda = 0 = g$, we recover the $(n,q) = (2,4)$ case of the quintessential inflation potential in an $R + \alpha R^2$ Palatini modified gravity theory, which was investigated in Ref. [1]. This potential, in turn, is a minor modification of the original quintessential inflation

potential in Ref. [15]. Switching λ and g on, and considering the limit $|\varphi| \gg \mu$ with $\varphi < 0$, we obtain the original hybrid inflation potential [96].

Let us first consider standard gravity without an R^2 term. In the beginning, $\varphi \ll -\mu$. Then the effective mass-squared of the GUT Higgs field χ is positive, which sends χ to zero. The scalar potential then becomes

$$V = \frac{1}{2}m^2\varphi^2 + \frac{1}{4}\lambda M^4 \,. \tag{C.2}$$

When the constant term dominates, we have an inflationary plateau. The effective mass-squared of the GUT Higgs field is $m^2_{\text{eff}\chi} = g^2\varphi^2 - \lambda M^2$. Thus, $m^2_{\text{eff}\chi}$ is positive as long as $|\varphi| > |\varphi_c|$, where $\varphi_c \equiv -(\sqrt{\lambda}/g)M$, where for simplicity we assume $|\varphi_c| \gg \mu$. Inflation ends when $\varphi = \varphi_c$, which triggers a phase transition that sends the GUT Higgs field towards its vacuum expectation value (VEV) $\chi = M$, in which case $m^2_{\text{eff}\chi} = 2\lambda M^2$. At this time, the effective mass-squared of the inflaton field becomes $m^2_{\text{eff}\varphi} = g^2M^2 > 0$, when the inflaton is still negative $\varphi_c < \varphi < 0$. This propels the inflaton to the origin.

When φ becomes positive, it free-falls in its steep runaway potential. In the limit $\varphi \gg \mu$, the potential is

$$V = \frac{\frac{1}{2}g^2M^2\mu^6}{\varphi^4} \,, \tag{C.3}$$

where we assumed $gM > m$. The above inverse quartic potential can indeed work not as tracker quintessece, as in the original quintessential inflation model [15], but as a freezing-thawing quintessence, which unfreezes at present provided the mass-scale $(\frac{1}{2}g^2M^2\mu^6)^{1/8}$ is of the correct magnitude to satisfy the coincidence requirement. Inflation, however, as described above would not work. Indeed, the original hybrid inflation model of Ref. [96], which is characterised by the inflationary potential in Eq. (C.2), produces a blue spectral index for the scalar curvature perturbation.

As shown in Ref. [1], things change when we embed the above model in $R+\alpha R^2$ Palatini modified gravity. We assume that λ is small enough, such that the potential in Eq. (C.2) during inflation is $V \simeq \frac{1}{2}m^2\varphi^2$. Then, the inflationary plateau is due to the quadratic gravity term, which flattens the potential and creates the

inflationary plateau with $U_{\rm inf} \simeq m_{\rm P}^4/4\alpha$ as discussed in Sec. 6.2.1. As mentioned, the scenario with $\lambda = 0 = g$ was investigated in Ref. [1], which found that successful quintessential inflation in achieved if $m \sim 10^{13}\,\text{GeV}$ and $(\frac{1}{2}g^2M^2\mu^6)^{1/8} \sim 10\,\text{GeV}$, which means $\mu \sim g^{-1/3}10^{-4}\,\text{GeV}$. The assumption $g > m/M \sim 10^{-3}$ suggests that $\mu \lesssim \mathcal{O}(\text{MeV})$.

In Ref. [1] it was shown that for successful quintessential inflation with this model we need $\alpha \sim 10^8$, so that $U_{\rm inf}^{1/4} \sim 10^{16}\,\text{GeV}$. The canonical inflaton field rolls down the Palatini inflationary plateau $U_{\rm inf}$ until it triggers the GUT phase transition and sends the GUT Higgs field to its VEV. Then, the potential V is reduced drastically so that the system exits the Palatini plateau and $U \simeq V$.

The change of the expectation value of the GUT Higgs field χ at the phase transition not only terminates inflation but may also affect the value of α provided the latter depends on χ. Indeed, suppose that

$$\alpha = \alpha(\chi) = \alpha_0\, e^{\kappa\chi/M}\,, \tag{C.4}$$

where $\kappa = \mathcal{O}(10)$ is a coefficient and $\alpha_0 \sim 10^8$. Before the phase transition, $\chi = 0$ and $\alpha = \alpha_0 \sim 10^8$. After the phase transition, $\chi = M \sim 10^{16}\,\text{GeV}$ and $\kappa\chi/M \lesssim 10^2$. As a consequence, α becomes huge. Indeed, for the range $\kappa = 5 - 166$ we find $\alpha \sim 10^{10\text{–}80}$, which comfortably includes the values considered in Fig. 6.7. Note that α should not depend on the inflaton field, $\alpha \neq \alpha(\varphi)$, because the latter changes substantially during kination and hyperkination, while α is taken to be constant.

Finally, it must be pointed out that the period of hyperkination in the post-inflationary history would modify the treatment of Ref. [1] somewhat. As a result, the value of μ for successful coincidence might change, but this is beyond the scope of the present work.

C.2 Numerical solutions

To check our analytical results, we solve numerically the time evolution of the background composed of the field and radiation and the GW mode functions. The

full set of equations reads

$$\begin{aligned}
&\left(1+3\alpha\frac{\dot\phi^2}{m_{\rm P}^4}\right)\ddot\phi+3\left(1+\alpha\frac{\dot\phi^2}{m_{\rm P}^4}\right)H\dot\phi=0\,,\\
&\dot\rho_f=-3H\rho_f(1+w_f)\,,\quad 3H^2m_{\rm P}^2=\rho_\phi+\rho_f\,,\\
&\rho_\phi=\frac{1}{2}\left[1+\frac{3}{2}\alpha\frac{\dot\phi^2}{m_{\rm P}^4}\right]\dot\phi^2\,,\ h_k^{s\prime\prime}+2\frac{a'}{a}h_k^{s\prime}+k^2h_k^s=0.
\end{aligned}\tag{C.5}$$

Many of the variables vary by orders of magnitude during cosmic evolution. To make numerics easier, we define new, rescaled variables x, y, and Z, a new time variable s, and a constant s_0 through

$$\begin{aligned}
&\dot\phi=m_{\rm P}^2\alpha^{-1/2}e^{-s_0-s+x}\,,\quad \rho_f=m_{\rm P}^4\alpha^{-1}e^{-2s_0-2s+y}\,,\\
&H=m_{\rm P}\alpha^{-1/2}Ze^{-s_0-s}\,,\quad s_0=-\ln\left(2\sqrt{\alpha}H_0/m_{\rm P}\right),\\
&{\rm d}t=m_{\rm P}^{-1}\sqrt{\alpha}e^{s_0+s}{\rm d}s\,,
\end{aligned}\tag{C.6}$$

where H_0 is the initial Hubble parameter. Definitions in Eq. (C.6) are chosen to ensure the new numerical quantities remain of order one throughout the computation. The equations of motion become

$$\begin{aligned}
\mathring{x}\ &=\ 1-\frac{3Z(1+e^{-2s_0-2s+2x})}{1+3e^{-2s_0-2s+2x}}\,,\ \mathring{y}=2-3Z(1+w_f)\,,\\
&3Z^2=\frac{1}{2}\left(1+\frac{3}{2}e^{-2s_0-2s+2x}\right)e^{2x}+e^y\,,\\
&\mathring{\mathring{h}}_k+(3Z-1)\mathring{h}_k+\frac{k^2}{m_{\rm P}^2a^2}\alpha e^{2s+2s_0}h_k=0\,,
\end{aligned}\tag{C.7}$$

where a circle over a variable indicates a derivative with respect to the new time variable s.

The initial conditions for the field velocity and fluid energy density are set as described in the text, engineered to match a desired end-of-inflation Hubble parameter $H_{\rm end}$, duration of hyperkination $N_{\rm hyp}$, and initial radiation energy density fraction $\Omega_{\rm r}^{\rm end}$. We then follow their evolution from the end of inflation until the BBN temperature is reached, see Fig. 6.2. The GW modes are evolved from their frozen super-Hubble state in Eq. (6.62) starting somewhat before they re-enter the Hubble

radius, until somewhat after the re-entry, after which they are taken to behave as radiation. To get the mode energy density, we use the first equation in Eq. (6.34)—as explained in the text, the error related to regularization is negligible for all relevant modes. Iterated over a number of modes, this produces the spectra in Fig. 6.4.

C.3 Mode function matching

In this appendix, we report the more technical results concerning the mode function matching at the transition between the different cosmological eras. We start with the transition from inflation to hyperkination, which takes place at $\eta_{\rm end}$. During the hyperkination, the Mukhanov Sasaki equation reads (see Eqs. (6.31) and (6.51))

$$v_k^{s\prime\prime} + k^2 v_k^s = 0\,. \tag{C.8}$$

The solution is simply a superposition of plane waves,

$$v_k^s(\eta) = \frac{1}{\sqrt{2k}}\left(\alpha_+ e^{-ik\eta} + \alpha_- e^{ik\eta}\right)\,. \tag{C.9}$$

Matching this to the standard slow-roll result (see the first line of Eq. (6.55)) at $\eta_{\rm end}$ gives

$$e^{i\frac{\pi}{4}(1+2\nu)}\sqrt{\frac{\pi}{2}}\sqrt{x_{\rm end}}H_\nu^{(1)}(x_{\rm end}) = \alpha_+ e^{ik|\eta_{\rm end}|} + \alpha_- e^{-ik|\eta_{\rm end}|}\,, \tag{C.10}$$

where $x_{\rm end} \equiv k|\eta_{\rm end}|$ and we dropped the subindex I from ν. Matching the derivatives gives

$$\begin{aligned} i\sqrt{\frac{\pi}{2}}e^{i\frac{\pi}{4}(1+2\nu)}\Big[\frac{1}{\sqrt{x_{\rm end}}}\Big(\frac{1}{2}+\nu\Big)H_\nu^{(1)}(x_{\rm end}) \;&-\; \sqrt{x_{\rm end}}H_{\nu+1}^{(1)}(x_{\rm end})\Big] = \\ &-\; \alpha_+ e^{ik|\eta_{\rm end}|} + \alpha_- e^{-ik|\eta_{\rm end}|}\,. \end{aligned} \tag{C.11}$$

Summing (subtracting) both expressions, we obtain

$$\alpha_\mp = \frac{e^{i\frac{\pi}{4}(1+2\nu)\pm ix_{\rm end}}}{2}\sqrt{\frac{\pi}{2}}\Big[H_\nu^{(1)}(x_{\rm end})\Big(\sqrt{x_{\rm end}} \pm \frac{i}{\sqrt{x_{\rm end}}}(\nu+\frac{1}{2})\Big) \mp i\sqrt{x_{\rm end}}H_{\nu+1}^{(1)}(x_{\rm end})\Big]\,. \tag{C.12}$$

We now take the super-Hubble (small argument) limit $x_{\rm end} \ll 1$. Noting that the leading contributions come from the terms proportional to $H_\nu^{(1)}(x_{\rm end})/\sqrt{x_{\rm end}}$ and

$H^{(1)}_{\nu+1}(x_{\rm end})\sqrt{x_{\rm end}}$, it reads

$$\alpha_{\mp} = \pm\frac{2^{\nu-1}e^{i\frac{\pi}{4}(1+2\nu)}}{\sqrt{2\pi}}\left(\frac{1}{2}-\nu\right)\Gamma(\nu)\frac{1}{(k|\eta_{\rm end}|)^{\nu+\frac{1}{2}}}\,. \tag{C.13}$$

Using $\nu = 3/2+\epsilon$, this expression can be further simplified to

$$\alpha_{\mp} = \pm\frac{2^{\epsilon-1}e^{i\pi\epsilon/2}\Gamma(3/2+\epsilon)}{\Gamma(3/2)}\left(\frac{H}{k}\right)^{2+\epsilon}\,. \tag{C.14}$$

For pure de Sitter, with $\epsilon \to 0$, we obtain

$$\alpha_{\mp} = \pm\frac{H^2}{2k^2}\,. \tag{C.15}$$

We continue with the transition from hyperkination to kination, which takes place at $\eta_{\rm kin}$. During kination, the Mukhanov–Sasaki equation takes the form

$$v_k^{s\prime\prime} + \left[k^2 - \frac{1}{4\left[\eta - \frac{\eta_{\rm kin}}{2} + \frac{1}{H}\right]^2}\right]v_k^s = 0\,. \tag{C.16}$$

Making the change of variables $y \equiv k\,(\eta - \eta_{\rm kin}/2 + 1/H)$ (where $y = kz$ in the notation of Eq. (6.52)) and redefining the mode functions as $g = \sqrt{y}v$, this equation can be recast as a Bessel equation with $\nu = 0$ (see Eq. (6.53)). Thus, the solution reads

$$v_k^s(\eta) = \sqrt{\frac{\pi}{4k}}\sqrt{y}\left[e^{-i\pi/4}\beta_+(k)H_0^{(2)}(y) + e^{i\pi/4}\beta_-(k)H_0^{(1)}(y)\right], \tag{C.17}$$

where the overall constant and phase has been chosen such that the mode functions have a simple sub-Hubble ($y \gg 1$) limit, as discussed below Eq. (6.55). We match this equation (and its derivative) with Eq. (C.9) (and its derivative) at time $\eta_{\rm kin}$, *i.e.*, at

$$y_{\rm kin} \equiv y(\eta_{\rm kin}) = \frac{k}{2}\left(\eta_{\rm kin} + \frac{2}{H}\right) \simeq \frac{k\eta_{\rm kin}}{2}\,, \tag{C.18}$$

where we have taken into account that $\eta_{\rm kin} \gg \eta_{\rm end}$. To avoid clutter we also define $r \equiv e^{i\pi/4}\sqrt{\pi/2}$. Equating the mode functions gives

$$\alpha_+ e^{-ik\eta_{\rm kin}} + \alpha_- e^{ik\eta_{\rm kin}} = \sqrt{y_{\rm kin}}\left[r^*\beta_+ H_0^{(2)}(y_{\rm kin}) + r\beta_- H_0^{(1)}(y_{\rm kin})\right], \tag{C.19}$$

while doing so for the derivatives gives

$$\begin{aligned} i\left(-\alpha_+ e^{-ik\eta_{\rm kin}} + \alpha_- e^{ik\eta_{\rm kin}}\right) &= \frac{1}{2\sqrt{y_{\rm kin}}}\left[r^*\beta_+ H_0^{(2)}(y_{\rm kin}) + r\beta_- H_0^{(1)}(y_{\rm kin})\right] \\ &+\sqrt{y_{\rm kin}}\left[r^*\beta_+ \frac{{\rm d}H_0^{(2)}}{{\rm d}y}(y_{\rm kin}) + r\beta_- \frac{{\rm d}H_0^{(1)}}{{\rm d}y}(y_{\rm kin})\right]. \end{aligned} \tag{C.20}$$

Now, using Eq. (C.19) in Eq. (C.20) allows us to rewrite the latter as

$$\begin{aligned} &\left[\alpha_+\left(-i - \frac{1}{2y_{\rm kin}}\right)e^{-ik\eta_{\rm kin}} + \alpha_-\left(i - \frac{1}{2y_{\rm kin}}\right)e^{ik\eta_{\rm kin}}\right] \\ &= \sqrt{y_{\rm kin}}\left[r^*\beta_+ \frac{{\rm d}H_0^{(2)}}{{\rm d}y}(y_{\rm kin}) + r\beta_- \frac{{\rm d}H_0^{(1)}}{{\rm d}y}(y_{\rm kin})\right]. \end{aligned} \tag{C.21}$$

In order to obtain β_- (β_+), we multiply Eq. (C.21) by $H_0^{(2)}(y_{\rm kin})$ ($H_0^{(1)}(y_{\rm kin})$) and Eq. (C.19) by ${\rm d}H_0^{(2)}/{\rm d}y$ (${\rm d}H_0^{(1)}/{\rm d}y$), subtract the latter from the former and use the Wronskian of the Hankel functions. The results read

$$\begin{aligned} \beta_- = e^{-i\pi/4}\frac{\sqrt{\pi y_{\rm kin}}}{i2\sqrt{2}}\Bigg\{ & H_0^{(2)}(y_{\rm kin})\Big[\alpha_+\left(-i - \frac{1}{2y_{\rm kin}}\right)e^{-ik\eta_{\rm kin}} + \alpha_-\left(i - \frac{1}{2y_{\rm kin}}\right)e^{ik\eta_{\rm kin}}\Big] \\ & + H_1^{(2)}(y_{\rm kin})\left(\alpha_+ e^{-ik\eta_{\rm kin}} + \alpha_- e^{ik\eta_{\rm kin}}\right)\Bigg\} \end{aligned} \tag{C.22}$$

and

$$\begin{aligned} \beta_+ = -e^{i\pi/4}\frac{\sqrt{\pi y_{\rm kin}}}{i2\sqrt{2}}\Bigg\{ & H_0^{(1)}(y_{\rm kin})\Big[\alpha_+\left(-i - \frac{1}{2y_{\rm kin}}\right)e^{-ik\eta_{\rm kin}} \\ & + \alpha_-\left(i - \frac{1}{2y_{\rm kin}}\right)e^{ik\eta_{\rm kin}}\Big] + H_1^{(1)}(y_{\rm kin})\Big(\alpha_+ e^{-ik\eta_{\rm kin}} + \alpha_- e^{ik\eta_{\rm kin}}\Big)\Bigg\}. \end{aligned} \tag{C.23}$$

Noting that $\alpha_+ = -\alpha_-$, these expressions can be rewritten as

$$\begin{aligned} \beta_- = e^{-i\pi/4}\sqrt{\frac{\pi y_{\rm kin}}{2}}\alpha_-\Bigg\{ & H_0^{(2)}(y_{\rm kin})\Big[\cos\left(k\eta_{\rm kin}\right) \\ & - \frac{1}{2y_{\rm kin}}\sin\left(k\eta_{\rm kin}\right)\Big] + H_1^{(2)}(y_{\rm kin})\sin\left(k\eta_{\rm kin}\right)\Bigg\} \end{aligned} \tag{C.24}$$

and

$$\begin{aligned} \beta_+ = -e^{i\pi/4}\sqrt{\frac{\pi y_{\rm kin}}{2}}\alpha_-\Bigg\{ & H_0^{(1)}(y_{\rm kin})\Big[\cos\left(k\eta_{\rm kin}\right) \\ & - \frac{1}{2y_{\rm kin}}\sin\left(k\eta_{\rm kin}\right)\Big] + H_1^{(1)}(y_{\rm kin})\sin\left(k\eta_{\rm kin}\right)\Bigg\}. \end{aligned} \tag{C.25}$$

We can now take the super-Hubble limit $k\eta_{\rm kin} \ll 1$. Using $k\eta_{\rm kin} = 2y_{\rm kin}$, the term in brackets multiplying $H_0^{(1,2)}(y_{\rm kin})$ cancels out, and we obtain the result

$$\beta_\pm = 2ie^{\pm i\pi/4}\alpha_- \sqrt{\frac{k\eta_{\rm kin}}{\pi}}\,, \tag{C.26}$$

where α_- is given by Eq. (C.14). Note that

$$\beta_+ = i\beta_-\,. \tag{C.27}$$

For pure de Sitter, we have the simplified expression

$$\beta_\pm = ie^{\pm i\pi/4}\left(\frac{H}{k}\right)^2 \sqrt{\frac{k\eta_{\rm kin}}{\pi}}\,. \tag{C.28}$$

Finally, we consider the transition from kination to the radiation-dominated era at $\eta_{\rm reh}$. During the latter, the Mukhanov–Sasaki equation is identical to the one corresponding to hyperkination,

$$v_k^{s\prime\prime} + k^2 v_k^s = 0\,, \tag{C.29}$$

the solution to which reads

$$v_k^s(\eta) = \frac{1}{\sqrt{2k}}\left(\gamma_+ e^{-ik\eta} + \gamma_- e^{ik\eta}\right)\,. \tag{C.30}$$

The matching conditions at $\eta_{\rm reh}$ now read

$$\sqrt{y_{\rm reh}}\left[r^*\beta_+ H_0^{(2)}(y_{\rm reh}) + r\beta_- H_0^{(1)}(y_{\rm reh})\right] = \left(\gamma_+ e^{-ik\eta_{\rm reh}} + \gamma_- e^{ik\eta_{\rm reh}}\right) \tag{C.31}$$

and

$$\begin{aligned}&\frac{1}{2\sqrt{y_{\rm reh}}}\left[r^*\beta_+ H_0^{(2)}(y_{\rm reh}) + r\beta_- H_0^{(1)}(y_{\rm reh})\right]\\ &+\sqrt{y_{\rm reh}}\left[r^*\beta_+ \frac{{\rm d}H_0^{(2)}}{{\rm d}y}(y_{\rm reh}) + r\beta_- \frac{{\rm d}H_0^{(1)}}{{\rm d}y}(y_{\rm reh})\right] = i\left(-\gamma_+ e^{-ik\eta_{\rm reh}} + \gamma_- e^{ik\eta_{\rm reh}}\right)\,,\end{aligned} \tag{C.32}$$

where

$$y_{\rm reh} = k\left(\eta_{\rm reh} - \frac{\eta_{\rm kin}}{2} + \frac{1}{H}\right) \simeq k\eta_{\rm reh}\,, \tag{C.33}$$

where we have taken into account that $\eta_{\rm reh} \gg \eta_{\rm kin} \gg \eta_{\rm end}$. Summing (subtracting) both expressions gives

$$\begin{aligned}\gamma_{\pm} = \frac{e^{\pm ik\eta_{\rm reh}}}{2}\Bigg\{ & r^{*}\beta_{+}\Big[H_{0}^{(2)}(y_{\rm reh})\left(\sqrt{y_{\rm reh}} \pm i\frac{1}{2\sqrt{y_{\rm reh}}}\right) \mp i\sqrt{y_{\rm reh}}H_{1}^{(2)}(y_{\rm reh})\Big] \\ & + r\beta_{-}\Big[H_{0}^{(1)}(y_{\rm reh})\left(\sqrt{y_{\rm reh}} \pm i\frac{1}{2\sqrt{y_{\rm reh}}}\right) \mp i\sqrt{y_{\rm reh}}H_{1}^{(1)}(y_{\rm reh})\Big]\Bigg\}\,.\end{aligned} \tag{C.34}$$

We use Eq. (C.27) and take the super-Hubble limit $k\eta_{\rm reh} \ll 1$ to obtain

$$\gamma_{\pm} = \pm\frac{r\beta_{-}}{2}\frac{i}{\sqrt{y_{\rm reh}}}\,, \tag{C.35}$$

where β_{-} is given by Eq. (C.26). For pure de Sitter, we have the simplified expression

$$\gamma_{\pm} = \mp\frac{H^{2}}{2k^{2}}\sqrt{\frac{\eta_{\rm kin}}{2\eta_{\rm reh}}}\,. \tag{C.36}$$

Appendix D

Appendix of Chapter 7

D.1 Quintessential Inflation

Is it possible that our scalar field can not only be early and late dark energy, but also be the inflaton field, responsible for accelerated expansion in the early Universe?

The α-attractors construction leads to two flat regions in the scalar potential of the canonical field, as the kinetic poles of the non-canonical field are displaced to infinity. This idea has been employed in the construction of quintessential inflation models in Refs. [260, 259, 258], where the low-energy plateau was the quintessential tail, responsible for quintessence and the high-energy plateau was responsible for inflation.

However, if we inspect the potential in Eq. (7.5) at the poles $\varphi = \pm\sqrt{6\alpha}\, m_{\rm P}$, we find that the potential for the positive pole is $V(\varphi_+) = V_\Lambda$ as expected, while for the negative pole we have $V(\varphi_-) = V_\Lambda \exp\big[2\lambda \sinh\big(\kappa\sqrt{6\alpha}\big)\big]$. For the values of the parameters obtained ($\kappa \sim 10^2$, $\lambda \sim 10^{-3}$ and $\alpha \sim 10^{-4}$) it is easy to check that $V(\varphi_-)$ is unsuitable for the inflationary plateau. Thus, our model needs to be modified to lead to quintessential inflation.

The first modification is a shift in field space such that our new field is

$$\tilde{\varphi} = \varphi + \Phi\,, \tag{D.1}$$

where Φ is a constant. The α-attractors construction applies now on the new field $\tilde{\varphi}$ for which the Lagrangian density is given by the expression in Eq. (7.1) with the substitution $\varphi \to \tilde{\varphi}$. The poles of our new field lie at $\tilde{\varphi}_{\pm} = \pm\sqrt{6\tilde{\alpha}}\, m_{\rm P}$, where $\tilde{\alpha}$ is the new α-attractors parameter.

We want all our results to remain unaffected, which means that, for the positive pole, Eq. (D.1) suggests

$$\varphi_+ = \sqrt{6\alpha}\, m_{\rm P} = \tilde{\varphi}_+ - \Phi = \sqrt{6\tilde{\alpha}}\, m_{\rm P} - \Phi \;\Rightarrow\; \tilde{\alpha} = \frac{1}{6}\left(\frac{\Phi}{m_{\rm P}} + \sqrt{6\alpha}\right)^2 . \tag{D.2}$$

The above, however, is not enough. It turns out we need to modify the scalar potential as well. This modification must be such that near the positive pole the scalar potential reduces to the one in Eq. (7.5). A simple proposal is

$$V(\tilde{\varphi}) = V_X \exp\{-2\lambda \sinh[\kappa(\tilde{\varphi} - \Phi)/m_{\rm P}]\}\,, \tag{D.3}$$

which indeed reduces to Eq. (7.5) when $\kappa(\tilde{\varphi} - \Phi) = \kappa\varphi > m_{\rm P}$. Note that $\kappa\sqrt{6\alpha} > 1$ is implied from the requirement that near the positive pole we have $\kappa\sqrt{6\alpha}\, m_{\rm P} = \kappa\varphi_+ > m_{\rm P}$.

The ESP discussed in Sec. 7.5 is now located at $\tilde{\varphi} = \Phi$, such that Eq. (7.26) is now $\Delta V = \frac{1}{2} g^2 (\tilde{\varphi} - \Phi)^2 \chi^{21}$.

We are interested in investigating the inflationary plateau. This is generated for the canonical field near the negative pole $\tilde{\varphi}_- = -\sqrt{6\tilde{\alpha}}\, m_{\rm P}$, where the scalar potential of the canonical field "flattens out" [465].

Assuming that $\Phi > \sqrt{6\alpha}\, m_{\rm P}$, we have that $\tilde{\varphi}_- - \Phi = -2\Phi - \sqrt{6\alpha}\, m_{\rm P} \simeq -2\Phi$, where we used Eq. (D.2). Hence, for the potential energy density of the inflationary plateau we obtain

[1]Near the ESP the potential does not approximate Eq. (7.5). However, we assume that, after unfreezing, the field rolls away fast from the ESP, such that soon the exp(exp) form of the potential becomes valid and the evolution is the one discussed in the main text of our paper.

$$
\begin{aligned}
V_{\rm inf} = V(\tilde{\varphi}_-) &\simeq V_X \exp[-2\lambda \sinh(-2\kappa\Phi/m_{\rm P})] \\
&\simeq \exp\Big(\lambda\, e^{\kappa\sqrt{6\alpha}}\Big) V_\Lambda \exp[\lambda \exp(2\kappa\Phi/m_{\rm P})] \\
&= \exp\Big[\lambda(e^{\kappa\sqrt{6\alpha}} + e^{2\kappa\Phi/m_{\rm P}})\Big] V_\Lambda \simeq V_\Lambda \exp\big(\lambda\, e^{2\kappa\Phi/m_{\rm P}}\big)\,, \quad \text{(D.4)}
\end{aligned}
$$

where we used Eq. (7.5) and that in $-2\sinh(-x) \simeq e^x$, when $x \gg 1$.

With α-attractors, the inflationary predictions are $n_s = 1 - 2/N$ and $r = 12\tilde{\alpha}/N^2$ [465], where n_s is the spectral index of the scalar curvature perturbation and r is the ratio of the spectrum of the tensor curvature perturbation to the spectrum of the scalar curvature perturbation, with N being the number of inflationary efolds remaining after the cosmological scales exit the horizon. Typically, $N = 60 - 65$ for quintessential inflation, which means that $n_s = 0.967 - 0.969$, in excellent agreement with the observations [10][2]. For the tensor-to-scalar ratio the observations provide the bound $r < 0.036$ [9], which suggests $\tilde{\alpha} < 0.003\, N^2 = 10.8 - 12.7$.

The COBE constraint requires $V_{\rm inf} \sim 10^{-10}\, m_{\rm P}^4$. Using that $V_\Lambda \sim 10^{-120}\, m_{\rm P}^4$, Eq. (D.4) suggests that $\kappa\Phi/m_{\rm P} = \frac{1}{2}\ln(110 \ln 10/\lambda)$. Hence. the conditions $\Phi > \sqrt{6\alpha}\, m_{\rm P}$ and $\kappa\sqrt{6\alpha} > 1$ suggest

$$
1 < \kappa\sqrt{6\alpha} < \kappa\Phi/m_{\rm P} = \frac{1}{2}\ln(110 \ln 10/\lambda)\,. \quad \text{(D.5)}
$$

Our findings in Section 7.4 are marginally in agreement with the above requirements. For example, taking $\alpha = 0.0006$ and $\kappa = 100$ we find $\kappa\sqrt{6\alpha} = 6$ and then Eq. (D.5) suggests $\lambda < 1.556 \times 10^{-3}$. We also find $\Phi/m_{\rm P} > \sqrt{6\alpha} = 0.06$, which is rather reasonable. Then, Eq. (D.2) implies $\tilde{\alpha} > 12\alpha = 7.2 \times 10^{-3}$, which comfortably satisfies the observational constraint on r. In fact, taking $N \simeq 60$, we find $r = 12\tilde{\alpha}/N^2 > \alpha/25 = 2.4 \times 10^{-5}$.

The above should be taken with a pinch of salt because the approximations employed are rather crude. However, they seem to suggest that our augmented

[2]It should be however noted that recent results [506, 507, 508, 509] suggest that, in the presence of EDE, the data seems to favour larger values of n_s, closer to unity. This would somewhat undermine the use of α-attractors.

model in Eq. (D.3) may lead to successful quintessential inflation while also resolving the Hubble tension, with no more fine-tuning than that of ΛCDM[3]. A full numerical investigation is needed to confirm this.

[3]Unifying inflation, EDE and late DE in $f(R)$ modified gravity has been investigated in Refs. [510, 511].

Bibliography

[1] K. Dimopoulos and S. Sánchez López, *Quintessential inflation in Palatini $f(R)$ gravity*, *Phys. Rev. D* **103** (2021), no. 4 043533, [arXiv:2012.06831].

[2] K. Dimopoulos, A. Karam, S. Sánchez López, and E. Tomberg, *Modelling Quintessential Inflation in Palatini-Modified Gravity*, *Galaxies* **10** (2022), no. 2 57, [arXiv:2203.05424].

[3] K. Dimopoulos, A. Karam, S. Sánchez López, and E. Tomberg, *Palatini R^2 quintessential inflation*, *JCAP* **10** (2022) 076, [arXiv:2206.14117].

[4] L. Brissenden, K. Dimopoulos, and S. Sánchez López, *Non-oscillating early dark energy and quintessence from α-attractors*, *Astropart. Phys.* **157** (2024) 102925, [arXiv:2301.03572].

[5] K. Dimopoulos, L. Brissenden, and S. Sánchez López, *Explaining the Hubble tension and dark energy from α-attractors*, *PoS* **CORFU2022** (2023) 247, [arXiv:2303.15523].

[6] S. Sánchez López, K. Dimopoulos, A. Karam, and E. Tomberg, *Observable gravitational waves from hyperkination in Palatini gravity and beyond*, *Eur. Phys. J. C* **83** (2023), no. 12 1152, [arXiv:2305.01399].

[7] D. N. Spergel and M. Zaldarriaga, *CMB polarization as a direct test of inflation*, *Phys. Rev. Lett.* **79** (1997) 2180–2183, [astro-ph/9705182].

[8] **Planck** Collaboration, N. Aghanim et al., *Planck 2018 results. VI. Cosmological parameters*, *Astron. Astrophys.* **641** (2020) A6, [arXiv:1807.06209]. [Erratum: Astron.Astrophys. 652, C4 (2021)].

[9] **BICEP, Keck** Collaboration, P. A. R. Ade et al., *Improved Constraints on Primordial Gravitational Waves using Planck, WMAP, and BICEP/Keck Observations through the 2018 Observing Season*, *Phys. Rev. Lett.* **127** (2021), no. 15 151301, [arXiv:2110.00483].

[10] **Planck** Collaboration, Y. Akrami et al., *Planck 2018 results. X. Constraints on inflation*, *Astron. Astrophys.* **641** (2020) A10, [arXiv:1807.06211].

[11] A. A. Starobinsky, *A New Type of Isotropic Cosmological Models Without Singularity*, *Phys. Lett. B* **91** (1980) 99–102.

[12] E. Abdalla et al., *Cosmology intertwined: A review of the particle physics, astrophysics, and cosmology associated with the cosmological tensions and anomalies*, *JHEAp* **34** (2022) 49–211, [arXiv:2203.06142].

[13] E. Di Valentino, O. Mena, S. Pan, L. Visinelli, W. Yang, A. Melchiorri, D. F. Mota, A. G. Riess, and J. Silk, *In the realm of the Hubble tension—a review of solutions*, *Class. Quant. Grav.* **38** (2021), no. 15 153001, [arXiv:2103.01183].

[14] L. Perivolaropoulos and F. Skara, *Challenges for ΛCDM: An update*, *New Astron. Rev.* **95** (2022) 101659, [arXiv:2105.05208].

[15] P. J. E. Peebles and A. Vilenkin, *Quintessential inflation*, *Phys. Rev. D* **59** (1999) 063505, [astro-ph/9810509].

[16] K. Dimopoulos, M. Karčiauskas, and C. Owen, *Quintessential inflation with a trap and axionic dark matter*, *Phys. Rev. D* **100** (2019), no. 8 083530, [arXiv:1907.04676].

[17] A. Einstein, *Einheitliche Feldtheorie von Gravitation und Elektrizität*, *Sitzungber.Preuss.Akad.Wiss.* **22** (1925) 414–419.

[18] M. Ferraris, M. Francaviglia, and C. Reina, *Variational formulation of general relativity from 1915 to 1925 "Palatini's method" discovered by Einstein in 1925*, *General Relativity and Gravitation* **14** (mar, 1982) 243–254.

[19] A. Palatini, *Deduzione invariantiva delle equazioni gravitazionali dal principio di hamilton*, *Rendiconti del Circolo Matematico di Palermo (1884-1940)* **43** (Dec, 1919) 203–212.

[20] R. Brout, F. Englert, and E. Gunzig, *The Creation of the Universe as a Quantum Phenomenon*, *Annals Phys.* **115** (1978) 78.

[21] D. Kazanas, *Dynamics of the Universe and Spontaneous Symmetry Breaking*, *Astrophys. J. Lett.* **241** (1980) L59–L63.

[22] K. Sato, *First Order Phase Transition of a Vacuum and Expansion of the Universe*, *Mon. Not. Roy. Astron. Soc.* **195** (1981) 467–479.

[23] L. Z. Fang, *Entropy Generation in the Early Universe by Dissipative Processes Near the Higgs' Phase Transitions*, *Phys. Lett. B* **95** (1980) 154–156.

[24] A. H. Guth, *The Inflationary Universe: A Possible Solution to the Horizon and Flatness Problems*, *Phys. Rev. D* **23** (1981) 347–356.

[25] A. D. Linde, *A New Inflationary Universe Scenario: A Possible Solution of the Horizon, Flatness, Homogeneity, Isotropy and Primordial Monopole Problems*, *Phys. Lett. B* **108** (1982) 389–393.

[26] A. Albrecht and P. J. Steinhardt, *Cosmology for Grand Unified Theories with Radiatively Induced Symmetry Breaking*, *Phys. Rev. Lett.* **48** (1982) 1220–1223.

[27] K. Dimopoulos, *Introduction to Cosmic Inflation and Dark Energy*. CRC Press, 5, 2022.

[28] W. H. Kinney, *Tasi lectures on inflation*, 2009.

[29] L. Senatore, *Lectures on Inflation*, in *Theoretical Advanced Study Institute in Elementary Particle Physics: New Frontiers in Fields and Strings*, pp. 447–543, 2017. arXiv:1609.00716.

[30] D. H. Lyth and A. Riotto, *Particle physics models of inflation and the cosmological density perturbation*, *Phys. Rept.* **314** (1999) 1–146, [hep-ph/9807278].

[31] C. H. Lineweaver, *Inflation and the cosmic microwave background*, in *16th Canberra International Physics Summer School: The New Cosmology*, 5, 2003. astro-ph/0305179.

[32] D. Baumann, *Inflation*, in *Theoretical Advanced Study Institute in Elementary Particle Physics: Physics of the Large and the Small*, pp. 523–686, 2011. arXiv:0907.5424.

[33] D. Baumann and L. McAllister, *Inflation and String Theory*. Cambridge Monographs on Mathematical Physics. Cambridge University Press, 5, 2015.

[34] D. Baumann, *Primordial Cosmology*, *PoS* **TASI2017** (2018) 009, [arXiv:1807.03098].

[35] D. Baumann, *Cosmology*. Cambridge University Press, 7, 2022.

[36] A. R. Liddle and S. M. Leach, *How long before the end of inflation were observable perturbations produced?*, *Phys. Rev. D* **68** (2003) 103503, [astro-ph/0305263].

[37] S. Dodelson and L. Hui, *A Horizon ratio bound for inflationary fluctuations*, *Phys. Rev. Lett.* **91** (2003) 131301, [astro-ph/0305113].

[38] A. R. Liddle, P. Parsons, and J. D. Barrow, *Formalizing the slow roll approximation in inflation*, *Phys. Rev. D* **50** (1994) 7222–7232, [astro-ph/9408015].

[39] D. H. Lyth and A. R. Liddle, *The primordial density perturbation: Cosmology, inflation and the origin of structure*. 2009.

[40] C.-P. Ma and E. Bertschinger, *Cosmological perturbation theory in the synchronous and conformal Newtonian gauges*, *Astrophys. J.* **455** (1995) 7–25, [astro-ph/9506072].

[41] V. F. Mukhanov, H. A. Feldman, and R. H. Brandenberger, *Theory of cosmological perturbations. Part 1. Classical perturbations. Part 2. Quantum theory of perturbations. Part 3. Extensions*, *Phys. Rept.* **215** (1992) 203–333.

[42] K. A. Malik and D. Wands, *Cosmological perturbations*, *Phys. Rept.* **475** (2009) 1–51, [arXiv:0809.4944].

[43] A. A. Starobinsky, *Spectrum of relict gravitational radiation and the early state of the universe*, *JETP Lett.* **30** (1979) 682–685.

[44] V. F. Mukhanov and G. V. Chibisov, *Quantum Fluctuations and a Nonsingular Universe*, *JETP Lett.* **33** (1981) 532–535.

[45] S. W. Hawking, *The Development of Irregularities in a Single Bubble Inflationary Universe*, *Phys. Lett. B* **115** (1982) 295.

[46] A. H. Guth and S. Y. Pi, *Fluctuations in the New Inflationary Universe*, *Phys. Rev. Lett.* **49** (1982) 1110–1113.

[47] A. A. Starobinsky, *Dynamics of Phase Transition in the New Inflationary Universe Scenario and Generation of Perturbations*, *Phys. Lett. B* **117** (1982) 175–178.

[48] A. D. Linde, *Scalar Field Fluctuations in Expanding Universe and the New Inflationary Universe Scenario*, *Phys. Lett. B* **116** (1982) 335–339.

[49] J. M. Bardeen, *Gauge-invariant cosmological perturbations*, *Phys. Rev. D* **22** (Oct, 1980) 1882–1905.

[50] H. Kodama and M. Sasaki, *Cosmological Perturbation Theory*, *Prog. Theor. Phys. Suppl.* **78** (1984) 1–166.

[51] E. Lifshitz, *Republication of: On the gravitational stability of the expanding universe*, *J. Phys. (USSR)* **10** (1946), no. 2 116.

[52] R. Saito and J. Yokoyama, *Gravitational-wave constraints on the abundance of primordial black holes*, *Progress of Theoretical Physics* **123** (may, 2010) 867–886.

[53] J. Garcia-Bellido, M. Peloso, and C. Unal, *Gravitational waves at interferometer scales and primordial black holes in axion inflation*, *JCAP* **12** (2016) 031, [arXiv:1610.03763].

[54] R.-g. Cai, S. Pi, and M. Sasaki, *Gravitational Waves Induced by non-Gaussian Scalar Perturbations*, *Phys. Rev. Lett.* **122** (2019), no. 20 201101, [arXiv:1810.11000].

[55] N. Bartolo, V. De Luca, G. Franciolini, M. Peloso, D. Racco, and A. Riotto, *Testing primordial black holes as dark matter with LISA*, *Phys. Rev. D* **99** (2019), no. 10 103521, [arXiv:1810.12224].

[56] N. Bartolo, V. De Luca, G. Franciolini, A. Lewis, M. Peloso, and A. Riotto, *Primordial Black Hole Dark Matter: LISA Serendipity*, *Phys. Rev. Lett.* **122** (2019), no. 21 211301, [arXiv:1810.12218].

[57] C. Unal, *Imprints of Primordial Non-Gaussianity on Gravitational Wave Spectrum*, *Phys. Rev. D* **99** (2019), no. 4 041301, [arXiv:1811.09151].

[58] S. Wang, T. Terada, and K. Kohri, *Prospective constraints on the primordial black hole abundance from the stochastic gravitational-wave backgrounds produced by coalescing events and curvature perturbations*, *Phys. Rev. D* **99** (2019), no. 10 103531, [arXiv:1903.05924]. [Erratum: Phys.Rev.D 101, 069901 (2020)].

[59] R.-G. Cai, S. Pi, S.-J. Wang, and X.-Y. Yang, *Pulsar Timing Array Constraints on the Induced Gravitational Waves*, *JCAP* **10** (2019) 059, [arXiv:1907.06372].

[60] V. De Luca, G. Franciolini, A. Kehagias, and A. Riotto, *On the Gauge Invariance of Cosmological Gravitational Waves*, *JCAP* **03** (2020) 014, [arXiv:1911.09689].

[61] K. Inomata and T. Terada, *Gauge Independence of Induced Gravitational Waves*, *Phys. Rev. D* **101** (2020), no. 2 023523, [arXiv:1912.00785].

[62] C. Yuan, Z.-C. Chen, and Q.-G. Huang, *Scalar induced gravitational waves in different gauges*, *Phys. Rev. D* **101** (2020), no. 6 063018, [arXiv:1912.00885].

[63] S. Pi and M. Sasaki, *Gravitational Waves Induced by Scalar Perturbations with a Lognormal Peak*, *JCAP* **09** (2020) 037, [arXiv:2005.12306].

[64] C. Yuan and Q.-G. Huang, *Gravitational waves induced by the local-type non-Gaussian curvature perturbations*, *Phys. Lett. B* **821** (2021) 136606, [arXiv:2007.10686].

[65] **LISA Cosmology Working Group** Collaboration, N. Bartolo et al., *Probing anisotropies of the Stochastic Gravitational Wave Background with LISA*, *JCAP* **11** (2022) 009, [arXiv:2201.08782].

[66] N. Bartolo, D. Bertacca, V. De Luca, G. Franciolini, S. Matarrese, M. Peloso, A. Ricciardone, A. Riotto, and G. Tasinato, *Gravitational wave anisotropies from primordial black holes*, *JCAP* **02** (2020) 028, [arXiv:1909.12619].

[67] E. Dimastrogiovanni, M. Fasiello, A. Malhotra, and G. Tasinato, *Enhancing gravitational wave anisotropies with peaked scalar sources*, *JCAP* **01** (2023) 018, [arXiv:2205.05644].

[68] G. Orlando, *Probing parity-odd bispectra with anisotropies of GW V modes*, *JCAP* **12** (2022) 019, [arXiv:2206.14173].

[69] E. Dimastrogiovanni, M. Fasiello, A. Malhotra, P. D. Meerburg, and G. Orlando, *Testing the early universe with anisotropies of the gravitational wave background*, *JCAP* **02** (2022), no. 02 040, [arXiv:2109.03077].

[70] V. Acquaviva, N. Bartolo, S. Matarrese, and A. Riotto, *Second order cosmological perturbations from inflation*, *Nucl. Phys. B* **667** (2003) 119–148, [astro-ph/0209156].

[71] S. Matarrese, S. Mollerach, and M. Bruni, *Second order perturbations of the Einstein-de Sitter universe*, *Phys. Rev. D* **58** (1998) 043504, [astro-ph/9707278].

[72] K. N. Ananda, C. Clarkson, and D. Wands, *The Cosmological gravitational wave background from primordial density perturbations*, *Phys. Rev. D* **75** (2007) 123518, [gr-qc/0612013].

[73] D. Baumann, P. J. Steinhardt, K. Takahashi, and K. Ichiki, *Gravitational Wave Spectrum Induced by Primordial Scalar Perturbations*, *Phys. Rev. D* **76** (2007) 084019, [hep-th/0703290].

[74] G. Domènech, *Scalar Induced Gravitational Waves Review*, *Universe* **7** (2021), no. 11 398, [arXiv:2109.01398].

[75] J. M. Bardeen, P. J. Steinhardt, and M. S. Turner, *Spontaneous Creation of Almost Scale - Free Density Perturbations in an Inflationary Universe*, *Phys. Rev. D* **28** (1983) 679.

[76] S. Weinberg, *Adiabatic modes in cosmology*, *Phys. Rev. D* **67** (2003) 123504, [astro-ph/0302326].

[77] R. L. Arnowitt, S. Deser, and C. W. Misner, *The Dynamics of general relativity*, *Gen. Rel. Grav.* **40** (2008) 1997–2027, [gr-qc/0405109].

[78] M. Bojowald, *Canonical Gravity and ApplicationsCosmology, Black Holes, and Quantum Gravity*. Cambridge University Press, 12, 2010.

[79] J. M. Maldacena, *Non-Gaussian features of primordial fluctuations in single field inflationary models*, *JHEP* **05** (2003) 013, [astro-ph/0210603].

[80] V. F. Mukhanov, *Quantum Theory of Gauge Invariant Cosmological Perturbations*, *Sov. Phys. JETP* **67** (1988) 1297–1302.

[81] M. Sasaki, *Large Scale Quantum Fluctuations in the Inflationary Universe*, *Prog. Theor. Phys.* **76** (1986) 1036.

[82] N. D. Birrell and P. C. W. Davies, *Quantum Fields in Curved Space*. Cambridge Monographs on Mathematical Physics. Cambridge Univ. Press, Cambridge, UK, 2, 1984.

[83] D. Wands, K. A. Malik, D. H. Lyth, and A. R. Liddle, *A New approach to the evolution of cosmological perturbations on large scales*, *Phys. Rev. D* **62** (2000) 043527, [astro-ph/0003278].

[84] **Planck** Collaboration, Y. Akrami et al., *Planck 2018 results. IX. Constraints on primordial non-Gaussianity*, *Astron. Astrophys.* **641** (2020) A9, [arXiv:1905.05697].

[85] A. Riotto, *Inflation and the theory of cosmological perturbations*, *ICTP Lect. Notes Ser.* **14** (2003) 317–413, [hep-ph/0210162].

[86] D. H. Lyth, *What would we learn by detecting a gravitational wave signal in the cosmic microwave background anisotropy?*, *Phys. Rev. Lett.* **78** (1997) 1861–1863, [hep-ph/9606387].

[87] R. H. Brandenberger and C. Vafa, *Superstrings in the Early Universe*, *Nucl. Phys. B* **316** (1989) 391–410.

[88] R. H. Brandenberger, *String Gas Cosmology*, 8, 2008. arXiv:0808.0746.

[89] **Planck** Collaboration, P. A. R. Ade et al., *Planck 2013 results. XVI. Cosmological parameters*, *Astron. Astrophys.* **571** (2014) A16, [arXiv:1303.5076].

[90] J. Martin, C. Ringeval, R. Trotta, and V. Vennin, *The Best Inflationary Models After Planck*, *JCAP* **03** (2014) 039, [arXiv:1312.3529].

[91] S. Dodelson, *Coherent phase argument for inflation*, *AIP Conf. Proc.* **689** (2003), no. 1 184–196, [hep-ph/0309057].

[92] M. Bucher, K. Moodley, and N. Turok, *The General primordial cosmic perturbation*, *Phys. Rev. D* **62** (2000) 083508, [astro-ph/9904231].

[93] M. Bucher, K. Moodley, and N. Turok, *Characterizing the primordial cosmic perturbations using map and Planck*, *Phys. Rev. D* **66** (2002) 023528, [astro-ph/0007360].

[94] A. D. Linde, *Chaotic Inflation*, *Phys. Lett. B* **129** (1983) 177–181.

[95] F. Lucchin and S. Matarrese, *Power Law Inflation*, *Phys. Rev. D* **32** (1985) 1316.

[96] A. D. Linde, *Hybrid inflation*, *Phys. Rev. D* **49** (1994) 748–754, [astro-ph/9307002].

[97] L. H. Ford, *Gravitational Particle Creation and Inflation*, *Phys. Rev. D* **35** (1987) 2955.

[98] K. Dimopoulos and T. Markkanen, *Non-minimal gravitational reheating during kination*, *JCAP* **06** (2018) 021, [arXiv:1803.07399].

[99] T. Opferkuch, P. Schwaller, and B. A. Stefanek, *Ricci Reheating*, *JCAP* **07** (2019) 016, [arXiv:1905.06823].

[100] G. N. Felder, L. Kofman, and A. D. Linde, *Instant preheating*, *Phys. Rev. D* **59** (1999) 123523, [hep-ph/9812289].

[101] B. A. Bassett, S. Tsujikawa, and D. Wands, *Inflation dynamics and reheating*, *Rev. Mod. Phys.* **78** (2006) 537–589, [astro-ph/0507632].

[102] R. Allahverdi, R. Brandenberger, F.-Y. Cyr-Racine, and A. Mazumdar, *Reheating in Inflationary Cosmology: Theory and Applications*, *Ann. Rev. Nucl. Part. Sci.* **60** (2010) 27–51, [arXiv:1001.2600].

[103] A. V. Frolov, *Non-linear Dynamics and Primordial Curvature Perturbations from Preheating*, *Class. Quant. Grav.* **27** (2010) 124006, [arXiv:1004.3559].

[104] M. A. Amin, M. P. Hertzberg, D. I. Kaiser, and J. Karouby, *Nonperturbative Dynamics Of Reheating After Inflation: A Review*, *Int. J. Mod. Phys. D* **24** (2014) 1530003, [arXiv:1410.3808].

[105] J. Haro, *Different reheating mechanisms in quintessence inflation*, *Phys. Rev. D* **99** (2019), no. 4 043510, [arXiv:1807.07367].

[106] M. S. Turner, *Coherent Scalar Field Oscillations in an Expanding Universe*, *Phys. Rev. D* **28** (1983) 1243.

[107] P. Peter and J.-P. Uzan, *Primordial Cosmology*. Oxford Graduate Texts. Oxford University Press, 2, 2013.

[108] L. Kofman, A. D. Linde, and A. A. Starobinsky, *Towards the theory of reheating after inflation*, *Phys. Rev. D* **56** (1997) 3258–3295, [hep-ph/9704452].

[109] S. W. Hawking, *Particle Creation by Black Holes*, *Commun. Math. Phys.* **43** (1975) 199–220. [Erratum: Commun.Math.Phys. 46, 206 (1976)].

[110] **Supernova Search Team** Collaboration, A. G. Riess et al., *Observational evidence from supernovae for an accelerating universe and a cosmological constant*, *Astron. J.* **116** (1998) 1009–1038, [astro-ph/9805201].

[111] **Supernova Cosmology Project** Collaboration, S. Perlmutter et al., *Measurements of* Ω *and* Λ *from 42 high redshift supernovae*, *Astrophys. J.* **517** (1999) 565–586, [astro-ph/9812133].

[112] M. S. Turner, *Dark matter and dark energy in the universe*, *ASP Conf. Ser.* **165** (1999) 431, [astro-ph/9811454].

[113] E. J. Copeland, M. Sami, and S. Tsujikawa, *Dynamics of dark energy*, *Int. J. Mod. Phys. D* **15** (2006) 1753–1936, [hep-th/0603057].

[114] M. Chevallier and D. Polarski, *Accelerating universes with scaling dark matter*, *Int. J. Mod. Phys. D* **10** (2001) 213–224, [gr-qc/0009008].

[115] E. V. Linder, *Exploring the expansion history of the universe*, *Phys. Rev. Lett.* **90** (2003) 091301, [astro-ph/0208512].

[116] **EUCLID** Collaboration, R. Laureijs et al., *Euclid Definition Study Report*, arXiv:1110.3193.

[117] S. M. Carroll, *The Cosmological constant*, *Living Rev. Rel.* **4** (2001) 1, [astro-ph/0004075].

[118] V. Sahni and A. A. Starobinsky, *The Case for a positive cosmological Lambda term*, *Int. J. Mod. Phys. D* **9** (2000) 373–444, [astro-ph/9904398].

[119] V. Sahni, *Dark matter and dark energy*, *Lect. Notes Phys.* **653** (2004) 141–180, [astro-ph/0403324].

[120] P. J. E. Peebles and B. Ratra, *The Cosmological Constant and Dark Energy*, *Rev. Mod. Phys.* **75** (2003) 559–606, [astro-ph/0207347].

[121] E. Hubble, *A relation between distance and radial velocity among extra-galactic nebulae*, *Proc. Nat. Acad. Sci.* **15** (1929) 168–173.

[122] G. Gamow, *My Worldline*. Viking Press, 4, 1970.

[123] S. Weinberg, *The Cosmological Constant Problem*, *Rev. Mod. Phys.* **61** (1989) 1–23.

[124] J. Sola Peracaula, *The cosmological constant problem and running vacuum in the expanding universe*, *Phil. Trans. Roy. Soc. Lond. A* **380** (2022) 20210182, [arXiv:2203.13757].

[125] H. B. G. Casimir, *On the attraction between two perfectly conducting plates*, *Indag. Math.* **10** (1948), no. 4 261–263.

[126] W. L. Freedman, *Cosmology at a Crossroads*, *Nature Astron.* **1** (2017) 0121, [arXiv:1706.02739].

[127] M. Kamionkowski and A. G. Riess, *The Hubble Tension and Early Dark Energy*, *Ann. Rev. Nucl. Part. Sci.* **73** (2023) 153–180, [arXiv:2211.04492].

[128] J. L. Bernal, L. Verde, and A. G. Riess, *The trouble with H_0*, *JCAP* **10** (2016) 019, [arXiv:1607.05617].

[129] L. Verde, T. Treu, and A. G. Riess, *Tensions between the Early and the Late Universe*, *Nature Astron.* **3** (7, 2019) 891, [arXiv:1907.10625].

[130] L. Knox and M. Millea, *Hubble constant hunter's guide*, *Phys. Rev. D* **101** (2020), no. 4 043533, [arXiv:1908.03663].

[131] P. Shah, P. Lemos, and O. Lahav, *A buyer's guide to the Hubble constant*, *Astron. Astrophys. Rev.* **29** (2021), no. 1 9, [arXiv:2109.01161].

[132] G. Efstathiou, *To H0 or not to H0?*, *Mon. Not. Roy. Astron. Soc.* **505** (2021), no. 3 3866–3872, [arXiv:2103.08723].

[133] V. Poulin, T. L. Smith, and T. Karwal, *The Ups and Downs of Early Dark Energy solutions to the Hubble tension: A review of models, hints and constraints circa 2023*, *Phys. Dark Univ.* **42** (2023) 101348, [arXiv:2302.09032].

[134] N. Schöneberg, G. Franco Abellán, A. Pérez Sánchez, S. J. Witte, V. Poulin, and J. Lesgourgues, *The H0 Olympics: A fair ranking of proposed models*, *Phys. Rept.* **984** (2022) 1–55, [arXiv:2107.10291].

[135] R. F. Christy, *Pulsation theory*, *Ann. Rev. Astron. Astrophys.* **4** (1966) 353–392.

[136] A. G. Riess et al., *A Comprehensive Measurement of the Local Value of the Hubble Constant with 1 km/s/Mpc Uncertainty from the Hubble Space Telescope and the SH0ES Team*, *Astrophys. J. Lett.* **934** (2022), no. 1 L7, [arXiv:2112.04510].

[137] D. Brout et al., *The Pantheon+ Analysis: Cosmological Constraints*, *Astrophys. J.* **938** (2022), no. 2 110, [arXiv:2202.04077].

[138] S. Dodelson and M. S. Turner, *Nonequilibrium neutrino statistical mechanics in the expanding universe*, *Phys. Rev. D* **46** (Oct, 1992) 3372–3387.

[139] M. G. Dainotti, B. De Simone, T. Schiavone, G. Montani, E. Rinaldi, and G. Lambiase, *On the Hubble constant tension in the SNe Ia Pantheon sample*, *Astrophys. J.* **912** (2021), no. 2 150, [arXiv:2103.02117].

[140] M. G. Dainotti, B. De Simone, T. Schiavone, G. Montani, E. Rinaldi, G. Lambiase, M. Bogdan, and S. Ugale, *On the Evolution of the Hubble*

Constant with the SNe Ia Pantheon Sample and Baryon Acoustic Oscillations: A Feasibility Study for GRB-Cosmology in 2030, *Galaxies* **10** (2022), no. 1 24, [arXiv:2201.09848].

[141] E. Mörtsell and S. Dhawan, *Does the Hubble constant tension call for new physics?*, *JCAP* **09** (2018) 025, [arXiv:1801.07260].

[142] H. G. Escudero, J.-L. Kuo, R. E. Keeley, and K. N. Abazajian, *Early or phantom dark energy, self-interacting, extra, or massive neutrinos, primordial magnetic fields, or a curved universe: An exploration of possible solutions to the H0 and $\sigma 8$ problems*, *Phys. Rev. D* **106** (2022), no. 10 103517, [arXiv:2208.14435].

[143] V. Poulin, K. K. Boddy, S. Bird, and M. Kamionkowski, *Implications of an extended dark energy cosmology with massive neutrinos for cosmological tensions*, *Phys. Rev. D* **97** (2018), no. 12 123504, [arXiv:1803.02474].

[144] R. R. Caldwell, *A Phantom menace?*, *Phys. Lett. B* **545** (2002) 23–29, [astro-ph/9908168].

[145] E. Di Valentino, A. Mukherjee, and A. A. Sen, *Dark Energy with Phantom Crossing and the H_0 Tension*, *Entropy* **23** (2021), no. 4 404, [arXiv:2005.12587].

[146] E. Di Valentino, A. Melchiorri, and J. Silk, *Reconciling Planck with the local value of H_0 in extended parameter space*, *Phys. Lett. B* **761** (2016) 242–246, [arXiv:1606.00634].

[147] E. Di Valentino, A. Melchiorri, E. V. Linder, and J. Silk, *Constraining Dark Energy Dynamics in Extended Parameter Space*, *Phys. Rev. D* **96** (2017), no. 2 023523, [arXiv:1704.00762].

[148] R. E. Keeley and A. Shafieloo, *Ruling Out New Physics at Low Redshift as a Solution to the H0 Tension*, *Phys. Rev. Lett.* **131** (2023), no. 11 111002, [arXiv:2206.08440].

[149] E. Di Valentino, E. V. Linder, and A. Melchiorri, *Vacuum phase transition solves the H_0 tension*, *Phys. Rev. D* **97** (2018), no. 4 043528, [arXiv:1710.02153].

[150] N. Khosravi, S. Baghram, N. Afshordi, and N. Altamirano, *H_0 tension as a hint for a transition in gravitational theory*, *Phys. Rev. D* **99** (2019), no. 10 103526, [arXiv:1710.09366].

[151] A. Banihashemi, N. Khosravi, and A. H. Shirazi, *Ginzburg-Landau Theory of Dark Energy: A Framework to Study Both Temporal and Spatial Cosmological Tensions Simultaneously*, *Phys. Rev. D* **99** (2019), no. 8 083509, [arXiv:1810.11007].

[152] A. Banihashemi, N. Khosravi, and A. H. Shirazi, *Phase transition in the dark sector as a proposal to lessen cosmological tensions*, *Phys. Rev. D* **101** (2020), no. 12 123521, [arXiv:1808.02472].

[153] S. Kumar and R. C. Nunes, *Probing the interaction between dark matter and dark energy in the presence of massive neutrinos*, *Phys. Rev. D* **94** (2016), no. 12 123511, [arXiv:1608.02454].

[154] E. Di Valentino, A. Melchiorri, and O. Mena, *Can interacting dark energy solve the H_0 tension?*, *Phys. Rev. D* **96** (2017), no. 4 043503, [arXiv:1704.08342].

[155] R.-G. Cai, Z.-K. Guo, S.-J. Wang, W.-W. Yu, and Y. Zhou, *No-go guide for the Hubble tension: Late-time solutions*, *Phys. Rev. D* **105** (2022), no. 2 L021301, [arXiv:2107.13286].

[156] R.-G. Cai, Z.-K. Guo, S.-J. Wang, W.-W. Yu, and Y. Zhou, *No-go guide for late-time solutions to the Hubble tension: Matter perturbations*, *Phys. Rev. D* **106** (2022), no. 6 063519, [arXiv:2202.12214].

[157] C. Wetterich, *Phenomenological parameterization of quintessence*, *Phys. Lett. B* **594** (2004) 17–22, [astro-ph/0403289].

[158] M. Doran and G. Robbers, *Early dark energy cosmologies*, *JCAP* **06** (2006) 026, [astro-ph/0601544].

[159] V. Pettorino, L. Amendola, and C. Wetterich, *How early is early dark energy?*, *Phys. Rev. D* **87** (2013) 083009, [arXiv:1301.5279].

[160] E. Calabrese, D. Huterer, E. V. Linder, A. Melchiorri, and L. Pagano, *Limits on Dark Radiation, Early Dark Energy, and Relativistic Degrees of Freedom*, *Phys. Rev. D* **83** (2011) 123504, [arXiv:1103.4132].

[161] T. Karwal and M. Kamionkowski, *Dark energy at early times, the Hubble parameter, and the string axiverse*, *Phys. Rev. D* **94** (2016), no. 10 103523, [arXiv:1608.01309].

[162] V. Poulin, T. L. Smith, T. Karwal, and M. Kamionkowski, *Early Dark Energy Can Resolve The Hubble Tension*, *Phys. Rev. Lett.* **122** (2019), no. 22 221301, [arXiv:1811.04083].

[163] V. I. Sabla and R. R. Caldwell, *No H_0 assistance from assisted quintessence*, *Phys. Rev. D* **103** (2021), no. 10 103506, [arXiv:2103.04999].

[164] T. L. Smith, V. Poulin, and M. A. Amin, *Oscillating scalar fields and the Hubble tension: a resolution with novel signatures*, *Phys. Rev. D* **101** (2020), no. 6 063523, [arXiv:1908.06995].

[165] K. Murai, F. Naokawa, T. Namikawa, and E. Komatsu, *Isotropic cosmic birefringence from early dark energy*, *Phys. Rev. D* **107** (2023), no. 4 L041302, [arXiv:2209.07804].

[166] L. M. Capparelli, R. R. Caldwell, and A. Melchiorri, *Cosmic birefringence test of the Hubble tension*, *Phys. Rev. D* **101** (2020), no. 12 123529, [arXiv:1909.04621].

[167] K. V. Berghaus and T. Karwal, *Thermal friction as a solution to the Hubble and large-scale structure tensions*, *Phys. Rev. D* **107** (2023), no. 10 103515, [arXiv:2204.09133].

[168] J. Sakstein and M. Trodden, *Early Dark Energy from Massive Neutrinos as a Natural Resolution of the Hubble Tension*, *Phys. Rev. Lett.* **124** (2020), no. 16 161301, [arXiv:1911.11760].

[169] T. Karwal, M. Raveri, B. Jain, J. Khoury, and M. Trodden, *Chameleon early dark energy and the Hubble tension*, *Phys. Rev. D* **105** (2022), no. 6 063535, [arXiv:2106.13290].

[170] V. I. Sabla and R. R. Caldwell, *Microphysics of early dark energy*, *Phys. Rev. D* **106** (2022), no. 6 063526, [arXiv:2202.08291].

[171] E. McDonough and M. Scalisi, *Towards Early Dark Energy in string theory*, *JHEP* **10** (2023) 118, [arXiv:2209.00011].

[172] V. Poulin, T. L. Smith, D. Grin, T. Karwal, and M. Kamionkowski, *Cosmological implications of ultralight axionlike fields*, *Phys. Rev. D* **98** (2018), no. 8 083525, [arXiv:1806.10608].

[173] F. Niedermann and M. S. Sloth, *Resolving the Hubble tension with new early dark energy*, *Phys. Rev. D* **102** (2020), no. 6 063527, [arXiv:2006.06686].

[174] J. C. Hill, E. McDonough, M. W. Toomey, and S. Alexander, *Early dark energy does not restore cosmological concordance*, *Phys. Rev. D* **102** (2020), no. 4 043507, [arXiv:2003.07355].

[175] T. L. Smith, V. Poulin, J. L. Bernal, K. K. Boddy, M. Kamionkowski, and R. Murgia, *Early dark energy is not excluded by current large-scale structure data*, *Phys. Rev. D* **103** (2021), no. 12 123542, [arXiv:2009.10740].

[176] S. Nojiri, S. D. Odintsov, D. Saez-Chillon Gomez, and G. S. Sharov, *Modeling and testing the equation of state for (Early) dark energy*, *Phys. Dark Univ.* **32** (2021) 100837, [arXiv:2103.05304].

[177] K. Freese and M. W. Winkler, *Chain early dark energy: A Proposal for solving the Hubble tension and explaining today's dark energy*, *Phys. Rev. D* **104** (2021), no. 8 083533, [arXiv:2102.13655].

[178] P. Agrawal, F.-Y. Cyr-Racine, D. Pinner, and L. Randall, *Rock 'n' Roll Solutions to the Hubble Tension*, arXiv:1904.01016.

[179] M. Braglia, W. T. Emond, F. Finelli, A. E. Gumrukcuoglu, and K. Koyama, *Unified framework for early dark energy from α-attractors*, *Phys. Rev. D* **102** (2020), no. 8 083513, [arXiv:2005.14053].

[180] G. Ye and Y.-S. Piao, *T_0 censorship of early dark energy and AdS vacua*, *Phys. Rev. D* **102** (2020), no. 8 083523, [arXiv:2008.10832].

[181] B. S. Haridasu, H. Khoraminezhad, and M. Viel, *Scrutinizing Early Dark Energy models through CMB lensing*, arXiv:2212.09136.

[182] K. V. Berghaus and T. Karwal, *Thermal Friction as a Solution to the Hubble Tension*, *Phys. Rev. D* **101** (2020), no. 8 083537, [arXiv:1911.06281].

[183] H. Moshafi, H. Firouzjahi, and A. Talebian, *Multiple Transitions in Vacuum Dark Energy and H_0 Tension*, *Astrophys. J.* **940** (2022), no. 2 121, [arXiv:2208.05583].

[184] E. Guendelman, R. Herrera, and D. Benisty, *Unifying inflation with early and late dark energy with multiple fields: Spontaneously broken scale*

invariant two measures theory, *Phys. Rev. D* **105** (2022), no. 12 124035, [arXiv:2201.06470].

[185] O. Seto and Y. Toda, *Comparing early dark energy and extra radiation solutions to the Hubble tension with BBN*, *Phys. Rev. D* **103** (2021), no. 12 123501, [arXiv:2101.03740].

[186] S. Vagnozzi, *New physics in light of the H_0 tension: An alternative view*, *Phys. Rev. D* **102** (2020), no. 2 023518, [arXiv:1907.07569].

[187] A. Reeves, L. Herold, S. Vagnozzi, B. D. Sherwin, and E. G. M. Ferreira, *Restoring cosmological concordance with early dark energy and massive neutrinos?*, *Mon. Not. Roy. Astron. Soc.* **520** (2023), no. 3 3688–3695, [arXiv:2207.01501].

[188] H. Mohseni Sadjadi and V. Anari, *Early dark energy and the screening mechanism*, *Eur. Phys. J. Plus* **138** (2023), no. 1 84, [arXiv:2205.15693].

[189] G. Franco Abellán, M. Braglia, M. Ballardini, F. Finelli, and V. Poulin, *Probing early modification of gravity with Planck, ACT and SPT*, *JCAP* **12** (2023) 017, [arXiv:2308.12345].

[190] A. Gómez-Valent, Z. Zheng, L. Amendola, C. Wetterich, and V. Pettorino, *Coupled and uncoupled early dark energy, massive neutrinos, and the cosmological tensions*, *Phys. Rev. D* **106** (2022), no. 10 103522, [arXiv:2207.14487].

[191] T. L. Smith and V. Poulin, *Current small-scale CMB constraints to axion-like early dark energy*, arXiv:2309.03265.

[192] J. Khoury and A. Weltman, *Chameleon fields: Awaiting surprises for tests of gravity in space*, *Phys. Rev. Lett.* **93** (2004) 171104, [astro-ph/0309300].

[193] P. Brax, C. van de Bruck, A.-C. Davis, J. Khoury, and A. Weltman, *Detecting dark energy in orbit: The cosmological chameleon*, *Phys. Rev. D* **70** (2004) 123518, [astro-ph/0408415].

[194] T. Chiba, T. Okabe, and M. Yamaguchi, *Kinetically driven quintessence*, *Phys. Rev. D* **62** (2000) 023511, [astro-ph/9912463].

[195] C. Armendariz-Picon, V. F. Mukhanov, and P. J. Steinhardt, *A Dynamical solution to the problem of a small cosmological constant and late time cosmic acceleration*, *Phys. Rev. Lett.* **85** (2000) 4438–4441, [astro-ph/0004134].

[196] C. Armendariz-Picon, V. F. Mukhanov, and P. J. Steinhardt, *Essentials of k essence*, *Phys. Rev. D* **63** (2001) 103510, [astro-ph/0006373].

[197] S. Capozziello, S. Carloni, and A. Troisi, *Quintessence without scalar fields*, *Recent Res. Dev. Astron. Astrophys.* **1** (2003) 625, [astro-ph/0303041].

[198] S. M. Carroll, V. Duvvuri, M. Trodden, and M. S. Turner, *Is cosmic speed - up due to new gravitational physics?*, *Phys. Rev. D* **70** (2004) 043528, [astro-ph/0306438].

[199] S. Nojiri and S. D. Odintsov, *Introduction to modified gravity and gravitational alternative for dark energy*, *eConf* **C0602061** (2006) 06, [hep-th/0601213].

[200] A. Y. Kamenshchik, U. Moschella, and V. Pasquier, *An Alternative to quintessence*, *Phys. Lett. B* **511** (2001) 265–268, [gr-qc/0103004].

[201] N. Bilic, G. B. Tupper, and R. D. Viollier, *Unification of dark matter and dark energy: The Inhomogeneous Chaplygin gas*, *Phys. Lett. B* **535** (2002) 17–21, [astro-ph/0111325].

[202] M. C. Bento, O. Bertolami, and A. A. Sen, *Generalized Chaplygin gas, accelerated expansion and dark energy matter unification*, *Phys. Rev. D* **66** (2002) 043507, [gr-qc/0202064].

[203] T. Padmanabhan, *Accelerated expansion of the universe driven by tachyonic matter*, *Phys. Rev. D* **66** (2002) 021301, [hep-th/0204150].

[204] T. Padmanabhan and T. R. Choudhury, *Can the clustered dark matter and the smooth dark energy arise from the same scalar field?*, *Phys. Rev. D* **66** (2002) 081301, [hep-th/0205055].

[205] P. J. Steinhardt and N. Turok, *Why the cosmological constant is small and positive*, *Science* **312** (2006) 1180–1182, [astro-ph/0605173].

[206] N. Arkani-Hamed, P. Creminelli, S. Mukohyama, and M. Zaldarriaga, *Ghost inflation*, *JCAP* **04** (2004) 001, [hep-th/0312100].

[207] F. Piazza and S. Tsujikawa, *Dilatonic ghost condensate as dark energy*, *JCAP* **07** (2004) 004, [hep-th/0405054].

[208] C. Wetterich, *Cosmology and the Fate of Dilatation Symmetry*, *Nucl. Phys. B* **302** (1988) 668–696, [arXiv:1711.03844].

[209] B. Ratra and P. J. E. Peebles, *Cosmological Consequences of a Rolling Homogeneous Scalar Field*, *Phys. Rev. D* **37** (1988) 3406.

[210] R. R. Caldwell, R. Dave, and P. J. Steinhardt, *Cosmological imprint of an energy component with general equation of state*, *Phys. Rev. Lett.* **80** (1998) 1582–1585, [astro-ph/9708069].

[211] E. V. Linder, *The Dynamics of Quintessence, The Quintessence of Dynamics*, *Gen. Rel. Grav.* **40** (2008) 329–356, [arXiv:0704.2064].

[212] A. R. Liddle and R. J. Scherrer, *A Classification of scalar field potentials with cosmological scaling solutions*, *Phys. Rev. D* **59** (1999) 023509, [astro-ph/9809272].

[213] E. J. Copeland, A. R. Liddle, and D. Wands, *Exponential potentials and cosmological scaling solutions*, *Phys. Rev. D* **57** (1998) 4686–4690, [gr-qc/9711068].

[214] D. Wands, E. J. Copeland, and A. R. Liddle, *Exponential potentials, scaling solutions and inflation*, in *16th Texas Symposium on Relativistic Astrophysics and 3rd Particles, Strings, and Cosmology Symposium*, pp. 0647–652, 3, 1993.

[215] T. Barreiro, E. J. Copeland, and N. J. Nunes, *Quintessence arising from exponential potentials*, *Phys. Rev. D* **61** (2000) 127301, [astro-ph/9910214].

[216] I. Zlatev, L.-M. Wang, and P. J. Steinhardt, *Quintessence, cosmic coincidence, and the cosmological constant*, *Phys. Rev. Lett.* **82** (1999) 896–899, [astro-ph/9807002].

[217] B. Ratra and P. J. E. Peebles, *Cosmological consequences of a rolling homogeneous scalar field*, *Phys. Rev. D* **37** (Jun, 1988) 3406–3427.

[218] R. D. Peccei, J. Sola, and C. Wetterich, *Adjusting the Cosmological Constant Dynamically: Cosmons and a New Force Weaker Than Gravity*, *Phys. Lett. B* **195** (1987) 183–190.

[219] C. Wetterich, *The Cosmon model for an asymptotically vanishing time dependent cosmological 'constant'*, *Astron. Astrophys.* **301** (1995) 321–328, [hep-th/9408025].

[220] M. Peloso and F. Rosati, *On the construction of quintessential inflation models*, *JHEP* **12** (1999) 026, [hep-ph/9908271].

[221] M. Giovannini, *Spikes in the relic graviton background from quintessential inflation*, *Class. Quant. Grav.* **16** (1999) 2905–2913, [hep-ph/9903263].

[222] A. B. Kaganovich, *Field theory model giving rise to 'quintessential inflation' without the cosmological constant and other fine tuning problems*, *Phys. Rev. D* **63** (2001) 025022, [hep-th/0007144].

[223] G. Huey and J. E. Lidsey, *Inflation, brane worlds and quintessence*, *Phys. Lett. B* **514** (2001) 217–225, [astro-ph/0104006].

[224] A. S. Majumdar, *From brane assisted inflation to quintessence through a single scalar field*, *Phys. Rev. D* **64** (2001) 083503, [astro-ph/0105518].

[225] K. Dimopoulos and J. W. F. Valle, *Modeling quintessential inflation*, *Astropart. Phys.* **18** (2002) 287–306, [astro-ph/0111417].

[226] R. Rosenfeld and J. A. Frieman, *A Simple model for quintessential inflation*, *JCAP* **09** (2005) 003, [astro-ph/0504191].

[227] R. Rosenfeld and J. A. Frieman, *Cosmic microwave background and large-scale structure constraints on a simple quintessential inflation model*, *Phys. Rev. D* **75** (2007) 043513, [astro-ph/0611241].

[228] A. H. Campos, H. C. Reis, and R. Rosenfeld, *Preheating in quintessential inflation*, *Phys. Lett. B* **575** (2003) 151–156, [hep-ph/0210152].

[229] K. Dimopoulos, *The Curvaton hypothesis and the eta-problem of quintessential inflation, with and without branes*, *Phys. Rev. D* **68** (2003) 123506, [astro-ph/0212264].

[230] E. Masso and G. Zsembinszki, *Unified model for inflation and dark energy with planck-scale pseudo-goldstone bosons*, *JCAP* **02** (2006) 012, [astro-ph/0602166].

[231] P. Di Bari, S. F. King, C. Luhn, A. Merle, and A. Schmidt-May, *Radiative Inflation and Dark Energy*, *Phys. Rev. D* **84** (2011) 083524, [arXiv:1010.5729].

[232] P. Di Bari, S. F. King, C. Luhn, A. Merle, and A. Schmidt-May, *Radiative Inflation and Dark Energy RIDEs Again after BICEP2*, *JCAP* **08** (2014) 040, [arXiv:1404.0009].

[233] M. W. Hossain, R. Myrzakulov, M. Sami, and E. N. Saridakis, *Variable gravity: A suitable framework for quintessential inflation*, *Phys. Rev. D* **90** (2014), no. 2 023512, [arXiv:1402.6661].

[234] S. C. C. Ng, N. J. Nunes, and F. Rosati, *Applications of scalar attractor solutions to cosmology*, *Phys. Rev. D* **64** (2001) 083510, [astro-ph/0107321].

[235] K. Dimopoulos, *Towards a model of quintessential inflation*, *Nucl. Phys. B Proc. Suppl.* **95** (2001) 70–73, [astro-ph/0012298].

[236] N. J. Nunes and E. J. Copeland, *Tracking quintessential inflation from brane worlds*, *Phys. Rev. D* **66** (2002) 043524, [astro-ph/0204115].

[237] M. Giovannini, *Low scale quintessential inflation*, *Phys. Rev. D* **67** (2003) 123512, [hep-ph/0301264].

[238] M. Sami and V. Sahni, *Quintessential inflation on the brane and the relic gravity wave background*, *Phys. Rev. D* **70** (2004) 083513, [hep-th/0402086].

[239] C. Pallis, *Quintessential kination and cold dark matter abundance*, *JCAP* **10** (2005) 015, [hep-ph/0503080].

[240] C. Pallis, *Kination-dominated reheating and cold dark matter abundance*, *Nucl. Phys. B* **751** (2006) 129–159, [hep-ph/0510234].

[241] P. Brax and J. Martin, *Coupling quintessence to inflation in supergravity*, *Phys. Rev. D* **71** (2005) 063530, [astro-ph/0502069].

[242] V. H. Cardenas, *Tachyonic quintessential inflation*, *Phys. Rev. D* **73** (2006) 103512, [gr-qc/0603013].

[243] J. C. Bueno Sanchez and K. Dimopoulos, *Trapped quintessential inflation in the context of flux compactifications*, *JCAP* **10** (2007) 002, [hep-th/0606223].

[244] J. C. Bueno Sanchez and K. Dimopoulos, *Trapped Quintessential Inflation*, *Phys. Lett. B* **642** (2006) 294–301, [hep-th/0605258]. [Erratum: Phys.Lett.B 647, 526 (2007)].

[245] M. E. Gomez, S. Lola, C. Pallis, and J. Rodriguez-Quintero, *Quintessential Kination and Thermal Production of Gravitinos and Axinos*, *JCAP* **01** (2009) 027, [arXiv:0809.1859].

[246] M. Bastero-Gil, A. Berera, B. M. Jackson, and A. Taylor, *Hybrid Quintessential Inflation*, *Phys. Lett. B* **678** (2009) 157–163, [arXiv:0905.2937].

[247] T. Chiba, A. De Felice, and S. Tsujikawa, *Observational constraints on quintessence: thawing, tracker, and scaling models*, *Phys. Rev. D* **87** (2013), no. 8 083505, [arXiv:1210.3859].

[248] M. W. Hossain, R. Myrzakulov, M. Sami, and E. N. Saridakis, *Class of quintessential inflation models with parameter space consistent with BICEP2*, *Phys. Rev. D* **89** (2014), no. 12 123513, [arXiv:1404.1445].

[249] M. W. Hossain, R. Myrzakulov, M. Sami, and E. N. Saridakis, *Evading Lyth bound in models of quintessential inflation*, *Phys. Lett. B* **737** (2014) 191–195, [arXiv:1405.7491].

[250] C.-Q. Geng, M. W. Hossain, R. Myrzakulov, M. Sami, and E. N. Saridakis, *Quintessential inflation with canonical and noncanonical scalar fields and Planck 2015 results*, *Phys. Rev. D* **92** (2015), no. 2 023522, [arXiv:1502.03597].

[251] J. Haro and S. Pan, *Bulk viscous quintessential inflation*, *Int. J. Mod. Phys. D* **27** (2018), no. 05 1850052, [arXiv:1512.03033].

[252] J. de Haro, *On the viability of quintessential inflation models from observational data*, *Gen. Rel. Grav.* **49** (2017), no. 1 6, [arXiv:1602.07138].

[253] E. Guendelman, E. Nissimov, and S. Pacheva, *Quintessential Inflation, Unified Dark Energy and Dark Matter, and Higgs Mechanism*, *Bulg. J. Phys.* **44** (2017), no. 1 015–030, [arXiv:1609.06915].

[254] A. Agarwal, R. Myrzakulov, M. Sami, and N. K. Singh, *Quintessential inflation in a thawing realization*, *Phys. Lett. B* **770** (2017) 200–208, [arXiv:1708.00156].

[255] S. Ahmad, R. Myrzakulov, and M. Sami, *Relic gravitational waves from Quintessential Inflation*, *Phys. Rev. D* **96** (2017), no. 6 063515, [arXiv:1705.02133].

[256] C.-Q. Geng, C.-C. Lee, M. Sami, E. N. Saridakis, and A. A. Starobinsky, *Observational constraints on successful model of quintessential Inflation*, *JCAP* **06** (2017) 011, [arXiv:1705.01329].

[257] J. Rubio and C. Wetterich, *Emergent scale symmetry: Connecting inflation and dark energy*, *Phys. Rev. D* **96** (2017), no. 6 063509, [arXiv:1705.00552].

[258] K. Dimopoulos and C. Owen, *Quintessential Inflation with α-attractors*, *JCAP* **06** (2017) 027, [arXiv:1703.00305].

[259] K. Dimopoulos, L. Donaldson Wood, and C. Owen, *Instant preheating in quintessential inflation with α-attractors*, *Phys. Rev. D* **97** (2018), no. 6 063525, [arXiv:1712.01760].

[260] Y. Akrami, R. Kallosh, A. Linde, and V. Vardanyan, *Dark energy, α-attractors, and large-scale structure surveys*, *JCAP* **06** (2018) 041, [arXiv:1712.09693].

[261] D. Bettoni and J. Rubio, *Quintessential Affleck-Dine baryogenesis with non-minimal couplings*, *Phys. Lett. B* **784** (2018) 122–129, [arXiv:1805.02669].

[262] K. Dimopoulos and T. Markkanen, *Dark energy as a remnant of inflation and electroweak symmetry breaking*, *JHEP* **01** (2019) 029, [arXiv:1807.04359].

[263] J.-B. Durrive, J. Ooba, K. Ichiki, and N. Sugiyama, *Updated observational constraints on quintessence dark energy models*, *Phys. Rev. D* **97** (2018), no. 4 043503, [arXiv:1801.09446].

[264] D. Bettoni, G. Domènech, and J. Rubio, *Gravitational waves from global cosmic strings in quintessential inflation*, *JCAP* **02** (2019) 034, [arXiv:1810.11117].

[265] J. Haro, W. Yang, and S. Pan, *Reheating in quintessential inflation via gravitational production of heavy massive particles: A detailed analysis*, *JCAP* **01** (2019) 023, [arXiv:1811.07371].

[266] C. Wetterich, *Quantum scale symmetry*, arXiv:1901.04741.

[267] I. Dalianis and G. Tringas, *Primordial black hole remnants as dark matter produced in thermal, matter, and runaway-quintessence postinflationary scenarios*, *Phys. Rev. D* **100** (2019), no. 8 083512, [arXiv:1905.01741].

[268] S. Hashiba and J. Yokoyama, *Dark matter and baryon-number generation in quintessential inflation via hierarchical right-handed neutrinos*, *Phys. Lett. B* **798** (2019) 135024, [arXiv:1905.12423].

[269] S. Ahmad, A. De Felice, N. Jaman, S. Kuroyanagi, and M. Sami, *Baryogenesis in the paradigm of quintessential inflation*, *Phys. Rev. D* **100** (2019), no. 10 103525, [arXiv:1908.03742].

[270] K. Kleidis and V. K. Oikonomou, *A Study of an Einstein Gauss-Bonnet Quintessential Inflationary Model*, *Nucl. Phys. B* **948** (2019) 114765, [arXiv:1909.05318].

[271] D. Bettoni and J. Rubio, *Hubble-induced phase transitions: Walls are not forever*, *JCAP* **01** (2020) 002, [arXiv:1911.03484].

[272] K. Dimopoulos and L. Donaldson-Wood, *Warm quintessential inflation*, *Phys. Lett. B* **796** (2019) 26–31, [arXiv:1906.09648].

[273] D. Benisty, E. I. Guendelman, E. Nissimov, and S. Pacheva, *Quintessential Inflation with Dynamical Higgs Generation as an Affine Gravity*, *Symmetry* **12** (2020) 734, [arXiv:2003.04723].

[274] J. H. Cases and L. Aresté Saló, *The Spectrum of Gravitational Waves, Their Overproduction in Quintessential Inflation and Its Influence in the Reheating Temperature*, *Universe* **6** (2020), no. 6 87, [arXiv:2004.11843].

[275] D. Benisty and E. I. Guendelman, *Quintessential Inflation from Lorentzian Slow Roll*, *Eur. Phys. J. C* **80** (2020), no. 6 577, [arXiv:2006.04129].

[276] A. Arbey and J. F. Coupechoux, *Unifying dark matter, dark energy and inflation with a fuzzy dark fluid*, *JCAP* **01** (2021) 033, [arXiv:2007.05376].

[277] M. R. Gangopadhyay, S. Myrzakul, M. Sami, and M. K. Sharma, *A paradigm of warm quintessential inflation and production of relic gravity waves*, 11, 2020. arXiv:2011.09155.

[278] M. Es-haghi and A. Sheykhi, *Two fields quintessential Higgs Inflation*, arXiv:2012.08035.

[279] L. Aresté Saló, D. Benisty, E. I. Guendelman, and J. d. Haro, *Quintessential inflation and cosmological seesaw mechanism: reheating and observational constraints*, *JCAP* **07** (2021) 007, [arXiv:2102.09514].

[280] L. Aresté Saló, D. Benisty, E. I. Guendelman, and J. de Haro, *α-attractors in quintessential inflation motivated by supergravity*, *Phys. Rev. D* **103** (2021), no. 12 123535, [arXiv:2103.07892].

[281] L. A. Saló and J. de Haro, *Gravitational particle production of superheavy massive particles in quintessential inflation: A numerical analysis*, *Phys. Rev. D* **104** (2021), no. 8 083544, [arXiv:2108.10795].

[282] M. Karčiauskas, S. Rusak, and A. Saez, *Quintessential inflation and nonlinear effects of the tachyonic trap mechanism*, *Phys. Rev. D* **105** (2022), no. 4 043535, [arXiv:2112.11536].

[283] D. Bettoni and J. Rubio, *Quintessential inflation: A tale of emergent and broken symmetries*, arXiv:2112.11948.

[284] N. Jaman and M. Sami, *What Is Needed of a Scalar Field If It Is to Unify Inflation and Late Time Acceleration?*, *Galaxies* **10** (2022), no. 2 51, [arXiv:2202.06194].

[285] J. de Haro and L. A. Saló, *A Review of Quintessential Inflation*, *Galaxies* **9** (2021), no. 4 73, [arXiv:2108.11144].

[286] M. Joyce and T. Prokopec, *Turning around the sphaleron bound: Electroweak baryogenesis in an alternative postinflationary cosmology*, *Phys. Rev. D* **57** (1998) 6022–6049, [hep-ph/9709320].

[287] B. Spokoiny, *Deflationary universe scenario*, *Phys. Lett. B* **315** (1993) 40–45, [gr-qc/9306008].

[288] M. Joyce, *Electroweak Baryogenesis and the Expansion Rate of the Universe*, *Phys. Rev. D* **55** (1997) 1875–1878, [hep-ph/9606223].

[289] D. Bettoni, A. Lopez-Eiguren, and J. Rubio, *Hubble-induced phase transitions on the lattice with applications to Ricci reheating*, *JCAP* **01** (2022), no. 01 002, [arXiv:2107.09671].

[290] B. Feng and M.-z. Li, *Curvaton reheating in nonoscillatory inflationary models*, *Phys. Lett. B* **564** (2003) 169–174, [hep-ph/0212213].

[291] J. Bueno Sanchez and K. Dimopoulos, *Curvaton reheating allows TeV Hubble scale in NO inflation*, *JCAP* **11** (2007) 007, [arXiv:0707.3967].

[292] V. Sahni, *The Energy Density of Relic Gravity Waves From Inflation*, *Phys. Rev. D* **42** (1990) 453–463.

[293] M. Giovannini, *Production and detection of relic gravitons in quintessential inflationary models*, *Phys. Rev. D* **60** (1999) 123511, [astro-ph/9903004].

[294] V. Sahni, M. Sami, and T. Souradeep, *Relic gravity waves from brane world inflation*, *Phys. Rev. D* **65** (2002) 023518, [gr-qc/0105121].

[295] R. H. Cyburt, B. D. Fields, K. A. Olive, and E. Skillman, *New BBN limits on physics beyond the standard model from ^4He*, *Astropart. Phys.* **23** (2005) 313–323, [astro-ph/0408033].

[296] T. P. Sotiriou and V. Faraoni, *f(R) Theories Of Gravity*, *Rev. Mod. Phys.* **82** (2010) 451–497, [arXiv:0805.1726].

[297] A. De Felice and S. Tsujikawa, *f(R) theories*, *Living Rev. Rel.* **13** (2010) 3, [arXiv:1002.4928].

[298] G. J. Olmo, *Palatini Approach to Modified Gravity: f(R) Theories and Beyond*, *Int. J. Mod. Phys. D* **20** (2011) 413–462, [arXiv:1101.3864].

[299] S. Capozziello and M. Francaviglia, *Extended Theories of Gravity and their Cosmological and Astrophysical Applications*, *Gen. Rel. Grav.* **40** (2008) 357–420, [arXiv:0706.1146].

[300] H. A. Buchdahl, *Non-linear Lagrangians and cosmological theory*, *Mon. Not. Roy. Astron. Soc.* **150** (1970) 1.

[301] F. Bauer and D. A. Demir, *Inflation with Non-Minimal Coupling: Metric versus Palatini Formulations*, *Phys. Lett.* **B665** (2008) 222–226, [arXiv:0803.2664].

[302] F. Bauer, *Filtering out the cosmological constant in the Palatini formalism of modified gravity*, *Gen. Rel. Grav.* **43** (2011) 1733–1757, [arXiv:1007.2546].

[303] N. Tamanini and C. R. Contaldi, *Inflationary Perturbations in Palatini Generalised Gravity*, *Phys. Rev. D* **83** (2011) 044018, [arXiv:1010.0689].

[304] F. Bauer and D. A. Demir, *Higgs-Palatini Inflation and Unitarity*, *Phys. Lett. B* **698** (2011) 425–429, [arXiv:1012.2900].

[305] S. Rasanen and P. Wahlman, *Higgs inflation with loop corrections in the Palatini formulation*, *JCAP* **11** (2017) 047, [arXiv:1709.07853].

[306] T. Tenkanen, *Resurrecting Quadratic Inflation with a non-minimal coupling to gravity*, *JCAP* **12** (2017) 001, [arXiv:1710.02758].

[307] A. Racioppi, *Coleman-Weinberg linear inflation: metric vs. Palatini formulation*, *JCAP* **12** (2017) 041, [arXiv:1710.04853].

[308] T. Markkanen, T. Tenkanen, V. Vaskonen, and H. Veermäe, *Quantum corrections to quartic inflation with a non-minimal coupling: metric vs. Palatini*, *JCAP* **03** (2018) 029, [arXiv:1712.04874].

[309] L. Järv, A. Racioppi, and T. Tenkanen, *Palatini side of inflationary attractors*, *Phys. Rev. D* **97** (2018), no. 8 083513, [arXiv:1712.08471].

[310] C. Fu, P. Wu, and H. Yu, *Inflationary dynamics and preheating of the nonminimally coupled inflaton field in the metric and Palatini formalisms*, *Phys. Rev. D* **96** (2017), no. 10 103542, [arXiv:1801.04089].

[311] A. Racioppi, *New universal attractor in nonminimally coupled gravity: Linear inflation*, *Phys. Rev. D* **97** (2018), no. 12 123514, [arXiv:1801.08810].

[312] P. Carrilho, D. Mulryne, J. Ronayne, and T. Tenkanen, *Attractor Behaviour in Multifield Inflation*, *JCAP* **06** (2018) 032, [arXiv:1804.10489].

[313] A. Kozak and A. Borowiec, *Palatini frames in scalar–tensor theories of gravity*, *Eur. Phys. J. C* **79** (2019), no. 4 335, [arXiv:1808.05598].

[314] S. Rasanen and E. Tomberg, *Planck scale black hole dark matter from Higgs inflation*, *JCAP* **01** (2019) 038, [arXiv:1810.12608].

[315] S. Rasanen, *Higgs inflation in the Palatini formulation with kinetic terms for the metric*, *Open J. Astrophys.* **2** (2019), no. 1 1, [arXiv:1811.09514].

[316] J. P. B. Almeida, N. Bernal, J. Rubio, and T. Tenkanen, *Hidden Inflaton Dark Matter*, *JCAP* **03** (2019) 012, [arXiv:1811.09640].

[317] K. Shimada, K. Aoki, and K.-i. Maeda, *Metric-affine Gravity and Inflation*, *Phys. Rev. D* **99** (2019), no. 10 104020, [arXiv:1812.03420].

[318] T. Takahashi and T. Tenkanen, *Towards distinguishing variants of non-minimal inflation*, *JCAP* **04** (2019) 035, [arXiv:1812.08492].

[319] R. Jinno, K. Kaneta, K.-y. Oda, and S. C. Park, *Hillclimbing inflation in metric and Palatini formulations*, *Phys. Lett. B* **791** (2019) 396–402, [arXiv:1812.11077].

[320] J. Rubio and E. S. Tomberg, *Preheating in Palatini Higgs inflation*, *JCAP* **1904** (2019), no. 04 021, [arXiv:1902.10148].

[321] N. Bostan, *Non-minimally coupled quartic inflation with Coleman-Weinberg one-loop corrections in the Palatini formulation*, *Phys. Lett. B* **811** (2020) 135954, [arXiv:1907.13235].

[322] N. Bostan, *Quadratic, Higgs and hilltop potentials in the Palatini gravity*, *Commun. Theor. Phys.* **72** (2020) 085401, [arXiv:1908.09674].

[323] T. Tenkanen and L. Visinelli, *Axion dark matter from Higgs inflation with an intermediate H_**, *JCAP* **08** (2019) 033, [arXiv:1906.11837].

[324] A. Racioppi, *Non-Minimal (Self-)Running Inflation: Metric vs. Palatini Formulation*, arXiv:1912.10038.

[325] T. Tenkanen, *Tracing the high energy theory of gravity: an introduction to Palatini inflation*, *Gen. Rel. Grav.* **52** (2020), no. 4 33, [arXiv:2001.10135].

[326] M. Shaposhnikov, A. Shkerin, and S. Zell, *Quantum Effects in Palatini Higgs Inflation*, *JCAP* **07** (2020) 064, [arXiv:2002.07105].

[327] A. Borowiec and A. Kozak, *New class of hybrid metric-Palatini scalar-tensor theories of gravity*, *JCAP* **07** (2020) 003, [arXiv:2003.02741].

[328] L. Järv, A. Karam, A. Kozak, A. Lykkas, A. Racioppi, and M. Saal, *Equivalence of inflationary models between the metric and Palatini formulation of scalar-tensor theories*, *Phys. Rev. D* **102** (2020), no. 4 044029, [arXiv:2005.14571].

[329] A. Karam, M. Raidal, and E. Tomberg, *Gravitational dark matter production in Palatini preheating*, arXiv:2007.03484.

[330] J. McDonald, *Does Palatini Higgs Inflation Conserve Unitarity?*, arXiv:2007.04111.

[331] M. Långvik, J.-M. Ojanperä, S. Raatikainen, and S. Rasanen, *Higgs inflation with the Holst and the Nieh-Yan term*, arXiv:2007.12595.

[332] M. Shaposhnikov, A. Shkerin, I. Timiryasov, and S. Zell, *Higgs inflation in Einstein-Cartan gravity*, arXiv:2007.14978.

[333] M. Shaposhnikov, A. Shkerin, I. Timiryasov, and S. Zell, *Einstein-Cartan gravity, matter, and scale-invariant generalization*, *JHEP* **10** (2020) 177, [arXiv:2007.16158].

[334] I. D. Gialamas, A. Karam, A. Lykkas, and T. D. Pappas, *Palatini-Higgs inflation with nonminimal derivative coupling*, *Phys. Rev. D* **102** (2020), no. 6 063522, [arXiv:2008.06371].

[335] Y. Mikura, Y. Tada, and S. Yokoyama, *Conformal inflation in the metric-affine geometry*, *EPL* **132** (2020), no. 3 39001, [arXiv:2008.00628].

[336] S. Verner, *Quintessential Inflation in Palatini Gravity*, arXiv:2010.11201.

[337] V.-M. Enckell, S. Nurmi, S. Rasanen, and E. Tomberg, *Critical point Higgs inflation in the Palatini formulation*, arXiv:2012.03660.

[338] Y. Reyimuaji and X. Zhang, *Natural inflation with a nonminimal coupling to gravity*, *JCAP* **03** (2021) 059, [arXiv:2012.14248].

[339] A. Karam, S. Karamitsos, and M. Saal, *β-function reconstruction of Palatini inflationary attractors*, *JCAP* **10** (2021) 068, [arXiv:2103.01182].

[340] Y. Mikura, Y. Tada, and S. Yokoyama, *Minimal k-inflation in light of the conformal metric-affine geometry*, arXiv:2103.13045.

[341] M. Kubota, K.-Y. Oda, K. Shimada, and M. Yamaguchi, *Cosmological Perturbations in Palatini Formalism*, *JCAP* **03** (2021) 006, [arXiv:2010.07867].

[342] D. Sáez-Chillón Gómez, *3+1 decomposition in modified gravities within the Palatini formalism and some applications*, arXiv:2103.16319.

[343] Y. Mikura and Y. Tada, *On UV-completion of Palatini-Higgs inflation*, *JCAP* **05** (2022), no. 05 035, [arXiv:2110.03925].

[344] F. Bombacigno and G. Montani, *Big bounce cosmology for Palatini R^2 gravity with a Nieh–Yan term*, *Eur. Phys. J. C* **79** (2019), no. 5 405, [arXiv:1809.07563].

[345] V.-M. Enckell, K. Enqvist, S. Rasanen, and L.-P. Wahlman, *Inflation with R^2 term in the Palatini formalism*, *JCAP* **02** (2019) 022, [arXiv:1810.05536].

[346] I. Antoniadis, A. Karam, A. Lykkas, and K. Tamvakis, *Palatini inflation in models with an R^2 term*, *JCAP* **11** (2018) 028, [arXiv:1810.10418].

[347] I. Antoniadis, A. Karam, A. Lykkas, T. Pappas, and K. Tamvakis, *Rescuing Quartic and Natural Inflation in the Palatini Formalism*, *JCAP* **03** (2019) 005, [arXiv:1812.00847].

[348] T. Tenkanen, *Minimal Higgs inflation with an R^2 term in Palatini gravity*, *Phys. Rev. D* **99** (2019), no. 6 063528, [arXiv:1901.01794].

[349] A. Edery and Y. Nakayama, *Palatini formulation of pure R^2 gravity yields Einstein gravity with no massless scalar*, *Phys. Rev. D* **99** (2019), no. 12 124018, [arXiv:1902.07876].

[350] M. Giovannini, *Post-inflationary phases stiffer than radiation and Palatini formulation*, *Class. Quant. Grav.* **36** (2019), no. 23 235017, [arXiv:1905.06182].

[351] T. Tenkanen, *Trans-Planckian censorship, inflation, and dark matter*, *Phys. Rev. D* **101** (2020), no. 6 063517, [arXiv:1910.00521].

[352] I. D. Gialamas and A. Lahanas, *Reheating in R^2 Palatini inflationary models*, *Phys. Rev. D* **101** (2020), no. 8 084007, [arXiv:1911.11513].

[353] T. Tenkanen and E. Tomberg, *Initial conditions for plateau inflation: a case study*, *JCAP* **04** (2020) 050, [arXiv:2002.02420].

[354] A. Lloyd-Stubbs and J. McDonald, *Sub-Planckian ϕ^2 inflation in the Palatini formulation of gravity with an R^2 term*, *Phys. Rev. D* **101** (2020), no. 12 123515, [arXiv:2002.08324].

[355] I. Antoniadis, A. Lykkas, and K. Tamvakis, *Constant-roll in the Palatini-R^2 models*, *JCAP* **04** (2020), no. 04 033, [arXiv:2002.12681].

[356] D. Ghilencea, *Palatini quadratic gravity: spontaneous breaking of gauged scale symmetry and inflation*, arXiv:2003.08516.

[357] N. Das and S. Panda, *Inflation and Reheating in f(R,h) theory formulated in the Palatini formalism*, arXiv:2005.14054.

[358] I. D. Gialamas, A. Karam, and A. Racioppi, *Dynamically induced Planck scale and inflation in the Palatini formulation*, *JCAP* **11** (2020) 014, [arXiv:2006.09124].

[359] D. Ghilencea, *Gauging scale symmetry and inflation: Weyl versus Palatini gravity*, arXiv:2007.14733.

[360] S. Bekov, K. Myrzakulov, R. Myrzakulov, and D. S.-C. Gómez, *General slow-roll inflation in $f(R)$ gravity under the Palatini approach*, *Symmetry* **12** (2020), no. 12 1958, [arXiv:2010.12360].

[361] D. S.-C. Gómez, *Variational principle and boundary terms in gravity à la Palatini*, *Phys. Lett. B* **814** (2021) 136103, [arXiv:2011.11568].

[362] A. Karam, E. Tomberg, and H. Veermäe, *Tachyonic preheating in Palatini R 2 inflation*, *JCAP* **06** (2021) 023, [arXiv:2102.02712].

[363] J. Annala and S. Rasanen, *Inflation with R ($\alpha\beta$) terms in the Palatini formulation*, *JCAP* **09** (2021) 032, [arXiv:2106.12422].

[364] A. Lykkas and K. Tamvakis, *Extended interactions in the Palatini-R^2 inflation*, *JCAP* **08** (2021), no. 043 [arXiv:2103.10136].

[365] I. D. Gialamas, A. Karam, T. D. Pappas, and V. C. Spanos, *Scale-invariant quadratic gravity and inflation in the Palatini formalism*, *Phys. Rev. D* **104** (2021), no. 2 023521, [arXiv:2104.04550].

[366] M. AlHallak, A. AlRakik, N. Chamoun, and M. S. El-Daher, *Palatini f(R) Gravity and Variants of k-/Constant Roll/Warm Inflation within Variation of Strong Coupling Scenario*, *Universe* **8** (2022), no. 2 126, [arXiv:2111.05075].

[367] C. Dioguardi, A. Racioppi, and E. Tomberg, *Slow-roll inflation in Palatini $F(R)$ gravity*, arXiv:2112.12149.

[368] X.-H. Meng and P. Wang, *R**2 corrections to the cosmological dynamics of inflation in the Palatini formulation*, *Class. Quant. Grav.* **21** (2004) 2029–2036, [gr-qc/0402011].

[369] X.-H. Meng and P. Wang, *Palatini formulation of modified gravity with squared scalar curvature*, *Gen. Rel. Grav.* **36** (2004) 2673, [astro-ph/0308284].

[370] T. P. Sotiriou and S. Liberati, *The Metric-affine formalism of f(R) gravity*, *J. Phys. Conf. Ser.* **68** (2007) 012022, [gr-qc/0611040].

[371] T. P. Sotiriou and S. Liberati, *Metric-affine f(R) theories of gravity*, *Annals Phys.* **322** (2007) 935–966, [gr-qc/0604006].

[372] C. W. Misner, K. S. Thorne, and J. A. Wheeler, *Gravitation*. W. H. Freeman, San Francisco, 1973.

[373] G. W. Gibbons and S. W. Hawking, *Action Integrals and Partition Functions in Quantum Gravity*, *Phys. Rev. D* **15** (1977) 2752–2756.

[374] J. W. York, Jr., *Role of conformal three geometry in the dynamics of gravitation*, *Phys. Rev. Lett.* **28** (1972) 1082–1085.

[375] T. P. Sotiriou, *Modified Actions for Gravity: Theory and Phenomenology*. PhD thesis, SISSA, Trieste, 2007. arXiv:0710.4438.

[376] T. Koivisto, *Covariant conservation of energy momentum in modified gravities*, *Class. Quant. Grav.* **23** (2006) 4289–4296, [gr-qc/0505128].

[377] T. P. Sotiriou, *f(R) gravity and scalar-tensor theory*, *Class. Quant. Grav.* **23** (2006) 5117–5128, [gr-qc/0604028].

[378] E. E. Flanagan, *The Conformal frame freedom in theories of gravitation*, *Class. Quant. Grav.* **21** (2004) 3817, [gr-qc/0403063].

[379] T. Chiba, *1/R gravity and scalar - tensor gravity*, *Phys. Lett. B* **575** (2003) 1–3, [astro-ph/0307338].

[380] D. Wands, *Extended gravity theories and the Einstein-Hilbert action*, *Class. Quant. Grav.* **11** (1994) 269–280, [gr-qc/9307034].

[381] J. D. Barrow and S. Cotsakis, *Inflation and the Conformal Structure of Higher Order Gravity Theories*, *Phys. Lett. B* **214** (1988) 515–518.

[382] P. Teyssandier and P. Tourrenc, *The Cauchy problem for the R+R**2 theories of gravity without torsion*, *J. Math. Phys.* **24** (1983) 2793.

[383] G. J. Olmo, *Limit to general relativity in f(R) theories of gravity*, *Phys. Rev. D* **75** (2007) 023511, [gr-qc/0612047].

[384] J. O'Hanlon, *Intermediate-range gravity - a generally covariant model*, *Phys. Rev. Lett.* **29** (1972) 137–138.

[385] S. M. Carroll, *Spacetime and Geometry: An Introduction to General Relativity*. Cambridge University Press, 7, 2019.

[386] H. Burton and R. B. Mann, *Palatini variational principle for an extended Einstein-Hilbert action*, *Phys. Rev. D* **57** (1998) 4754–4759, [gr-qc/9711003].

[387] Q. Exirifard and M. Sheikh-Jabbari, *Lovelock gravity at the crossroads of Palatini and metric formulations*, *Phys. Lett. B* **661** (2008) 158–161, [arXiv:0705.1879].

[388] L. Querella, *Variational principles and cosmological models in higher order gravity*, other thesis, 12, 1998.

[389] B. Shahid-Saless, *First Order Formalism Treatment of R + R**2 Gravity*, *Phys. Rev. D* **35** (1987) 467–470.

[390] F. L. Bezrukov and M. Shaposhnikov, *The Standard Model Higgs boson as the inflaton*, *Phys. Lett. B* **659** (2008) 703–706, [arXiv:0710.3755].

[391] L. Amendola, R. Gannouji, D. Polarski, and S. Tsujikawa, *Conditions for the cosmological viability of f(R) dark energy models*, *Phys. Rev. D* **75** (2007) 083504, [gr-qc/0612180].

[392] I. Sawicki and W. Hu, *Stability of Cosmological Solution in f(R) Models of Gravity*, *Phys. Rev. D* **75** (2007) 127502, [astro-ph/0702278].

[393] **LIGO Scientific, Virgo, Fermi-GBM, INTEGRAL** Collaboration, B. Abbott et al., *Gravitational Waves and Gamma-rays from a Binary Neutron Star Merger: GW170817 and GRB 170817A*, *Astrophys. J. Lett.* **848** (2017), no. 2 L13, [arXiv:1710.05834].

[394] C. van de Bruck, K. Dimopoulos, C. Longden, and C. Owen, *Gauss-Bonnet-coupled Quintessential Inflation*, 7, 2017. arXiv:1707.06839.

[395] J. J. Terente Díaz, K. Dimopoulos, M. Karčiauskas, and A. Racioppi, *Gauss-Bonnet Dark Energy and the speed of gravitational waves*, *JCAP* **10** (2023) 031, [arXiv:2307.06163].

[396] J. J. Terente Díaz, K. Dimopoulos, M. Karčiauskas, and A. Racioppi, *Quintessence in the Weyl-Gauss-Bonnet Model*, arXiv:2310.08128.

[397] S. Nojiri, S. Odintsov, and V. Oikonomou, *Modified Gravity Theories on a Nutshell: Inflation, Bounce and Late-time Evolution*, *Phys. Rept.* **692** (2017) 1–104, [arXiv:1705.11098].

[398] C. Hoyle, D. Kapner, B. R. Heckel, E. Adelberger, J. Gundlach, U. Schmidt, and H. Swanson, *Sub-millimeter tests of the gravitational inverse-square law*, *Phys. Rev. D* **70** (2004) 042004, [hep-ph/0405262].

[399] G. Magnano and L. M. Sokolowski, *On physical equivalence between nonlinear gravity theories and a general relativistic selfgravitating scalar field*, *Phys. Rev. D* **50** (1994) 5039–5059, [gr-qc/9312008].

[400] D. H. Lyth, *What would we learn by detecting a gravitational wave signal in the cosmic microwave background anisotropy?*, *Phys. Rev. Lett.* **78** (1997) 1861–1863, [hep-ph/9606387].

[401] D. H. Lyth and D. Wands, *Generating the curvature perturbation without an inflaton*, *Phys. Lett. B* **524** (2002) 5–14, [hep-ph/0110002].

[402] J. a. G. Rosa and L. B. Ventura, *Warm Little Inflaton becomes Dark Energy*, *Phys. Lett. B* **798** (2019) 134984, [arXiv:1906.11835].

[403] E. Chun, S. Scopel, and I. Zaballa, *Gravitational reheating in quintessential inflation*, *JCAP* **07** (2009) 022, [arXiv:0904.0675].

[404] J. de Haro, S. Pan, and L. Aresté Saló, *Understanding gravitational particle production in quintessential inflation*, *JCAP* **06** (2019) 056, [arXiv:1903.01181].

[405] T. P. Sotiriou, *Unification of inflation and cosmic acceleration in the Palatini formalism*, *Phys. Rev. D* **73** (2006) 063515, [gr-qc/0509029].

[406] D. N. Vollick, *1/R Curvature corrections as the source of the cosmological acceleration*, *Phys. Rev. D* **68** (2003) 063510, [astro-ph/0306630].

[407] G. J. Olmo, *Violation of the Equivalence Principle in Modified Theories of Gravity*, *Phys. Rev. Lett.* **98** (2007) 061101, [gr-qc/0612002].

[408] G. J. Olmo, *The Gravity Lagrangian according to solar system experiments*, *Phys. Rev. Lett.* **95** (2005) 261102, [gr-qc/0505101].

[409] G. J. Olmo, *Hydrogen atom in Palatini theories of gravity*, *Phys. Rev. D* **77** (2008) 084021, [arXiv:0802.4038].

[410] B. Li, D. F. Mota, and D. J. Shaw, *Microscopic and Macroscopic Behaviors of Palatini Modified Gravity Theories*, *Phys. Rev. D* **78** (2008) 064018, [arXiv:0805.3428].

[411] L. Gorlich, S. Kachru, P. K. Tripathy, and S. P. Trivedi, *Gaugino condensation and nonperturbative superpotentials in flux compactifications*, *JHEP* **12** (2004) 074, [hep-th/0407130].

[412] M. Haack, D. Krefl, D. Lust, A. Van Proeyen, and M. Zagermann, *Gaugino Condensates and D-terms from D7-branes*, *JHEP* **01** (2007) 078, [hep-th/0609211].

[413] Z. Lalak, G. G. Ross, and S. Sarkar, *Racetrack inflation and assisted moduli stabilisation*, *Nucl. Phys. B* **766** (2007) 1–20, [hep-th/0503178].

[414] I. Dalianis and G. P. Kodaxis, *Reheating in Runaway Inflation Models via the Evaporation of Mini Primordial Black Holes*, *Galaxies* **10** (2022), no. 1 31, [arXiv:2112.15576].

[415] E. J. Copeland, S. Pascoli, and A. Rajantie, *Dynamics of tachyonic preheating after hybrid inflation*, *Phys. Rev. D* **65** (2002) 103517, [hep-ph/0202031].

[416] P. G. Ferreira and M. Joyce, *Structure formation with a selftuning scalar field*, *Phys. Rev. Lett.* **79** (1997) 4740–4743, [astro-ph/9707286].

[417] A. Karam, T. Pappas, and K. Tamvakis, *Frame-dependence of higher-order inflationary observables in scalar-tensor theories*, *Phys. Rev. D* **96** (2017), no. 6 064036, [arXiv:1707.00984].

[418] A. Racioppi and M. Vasar, *On the number of e-folds in the Jordan and Einstein frames*, *Eur. Phys. J. Plus* **137** (2022), no. 5 637, [arXiv:2111.09677].

[419] R. Thomas et al., *The extended epoch of galaxy formation: Age dating of ˜3600 galaxies with 2 < z < 6.5 in the VIMOS Ultra-Deep Survey*, *Astron. Astrophys.* **602** (2017) A35, [arXiv:1602.01841].

[420] **Euclid** Collaboration, S. Ilić et al., *Euclid preparation - XV. Forecasting cosmological constraints for the Euclid and CMB joint analysis*, *Astron. Astrophys.* **657** (2022) A91, [arXiv:2106.08346].

[421] M. S. Turner, *Detectability of inflation produced gravitational waves*, *Phys. Rev. D* **55** (1997) R435–R439, [astro-ph/9607066].

[422] T. L. Smith, M. Kamionkowski, and A. Cooray, *Direct detection of the inflationary gravitational wave background*, *Phys. Rev. D* **73** (2006) 023504, [astro-ph/0506422].

[423] L. A. Boyle and P. J. Steinhardt, *Probing the early universe with inflationary gravitational waves*, *Phys. Rev. D* **77** (2008) 063504, [astro-ph/0512014].

[424] M. C. Guzzetti, N. Bartolo, M. Liguori, and S. Matarrese, *Gravitational waves from inflation*, *Riv. Nuovo Cim.* **39** (2016), no. 9 399–495, [arXiv:1605.01615].

[425] C. Caprini and D. G. Figueroa, *Cosmological Backgrounds of Gravitational Waves*, *Class. Quant. Grav.* **35** (2018), no. 16 163001, [arXiv:1801.04268].

[426] **LIGO Scientific, Virgo** Collaboration, B. P. Abbott et al., *Observation of Gravitational Waves from a Binary Black Hole Merger*, *Phys. Rev. Lett.* **116** (2016), no. 6 061102, [arXiv:1602.03837].

[427] **LIGO Scientific, Virgo** Collaboration, B. P. Abbott et al., *GW151226: Observation of Gravitational Waves from a 22-Solar-Mass Binary Black Hole Coalescence*, *Phys. Rev. Lett.* **116** (2016), no. 24 241103, [arXiv:1606.04855].

[428] **LIGO Scientific** Collaboration, G. M. Harry, *Advanced LIGO: The next generation of gravitational wave detectors*, *Class. Quant. Grav.* **27** (2010) 084006.

[429] **VIRGO** Collaboration, F. Acernese et al., *Advanced Virgo: a second-generation interferometric gravitational wave detector*, *Class. Quant. Grav.* **32** (2015), no. 2 024001, [arXiv:1408.3978].

[430] **LIGO Scientific** Collaboration, J. Aasi et al., *Advanced LIGO*, *Class. Quant. Grav.* **32** (2015) 074001, [arXiv:1411.4547].

[431] **LIGO Scientific, Virgo** Collaboration, R. Abbott et al., *Open data from the first and second observing runs of Advanced LIGO and Advanced Virgo*, *SoftwareX* **13** (2021) 100658, [arXiv:1912.11716].

[432] **KAGRA** Collaboration, T. Akutsu et al., *Overview of KAGRA: Detector design and construction history*, *PTEP* **2021** (2021), no. 5 05A101, [arXiv:2005.05574].

[433] N. Bartolo et al., *Science with the space-based interferometer LISA. IV: Probing inflation with gravitational waves*, *JCAP* **12** (2016) 026, [arXiv:1610.06481].

[434] C. Caprini, D. G. Figueroa, R. Flauger, G. Nardini, M. Peloso, M. Pieroni, A. Ricciardone, and G. Tasinato, *Reconstructing the spectral shape of a stochastic gravitational wave background with LISA*, *JCAP* **11** (2019) 017, [arXiv:1906.09244].

[435] **LISA Cosmology Working Group** Collaboration, P. Auclair et al., *Cosmology with the Laser Interferometer Space Antenna*, arXiv:2204.05434.

[436] S. Kawamura et al., *The Japanese space gravitational wave antenna DECIGO*, *Class. Quant. Grav.* **23** (2006) S125–S132.

[437] S. Kawamura et al., *The Japanese space gravitational wave antenna: DECIGO*, *Class. Quant. Grav.* **28** (2011) 094011.

[438] S. Kawamura et al., *Current status of space gravitational wave antenna DECIGO and B-DECIGO*, *PTEP* **2021** (2021), no. 5 05A105, [arXiv:2006.13545].

[439] G. M. Harry, P. Fritschel, D. A. Shaddock, W. Folkner, and E. S. Phinney, *Laser interferometry for the big bang observer*, *Class. Quant. Grav.* **23** (2006) 4887–4894. [Erratum: Class.Quant.Grav. 23, 7361 (2006)].

[440] J. Ellis, D. V. Nanopoulos, K. A. Olive, and S. Verner, *Non-Oscillatory No-Scale Inflation*, *JCAP* **03** (2021) 052, [arXiv:2008.09099].

[441] N. Bose and A. S. Majumdar, *A k-essence Model Of Inflation, Dark Matter and Dark Energy*, *Phys. Rev. D* **79** (2009) 103517, [arXiv:0812.4131].

[442] M. Wali Hossain, R. Myrzakulov, M. Sami, and E. N. Saridakis, *Unification of inflation and dark energy à la quintessential inflation*, *Int. J. Mod. Phys. D* **24** (2015), no. 05 1530014, [arXiv:1410.6100].

[443] R. T. Co, L. J. Hall, and K. Harigaya, *Axion Kinetic Misalignment Mechanism*, *Phys. Rev. Lett.* **124** (2020), no. 25 251802, [arXiv:1910.14152].

[444] R. T. Co, L. J. Hall, K. Harigaya, K. A. Olive, and S. Verner, *Axion Kinetic Misalignment and Parametric Resonance from Inflation*, *JCAP* **08** (2020) 036, [arXiv:2004.00629].

[445] V. K. Oikonomou, *Kinetic axion F(R) gravity inflation*, *Phys. Rev. D* **106** (2022), no. 4 044041, [arXiv:2208.05544].

[446] A. Riazuelo and J.-P. Uzan, *Quintessence and gravitational waves*, *Phys. Rev. D* **62** (2000) 083506, [astro-ph/0004156].

[447] H. Tashiro, T. Chiba, and M. Sasaki, *Reheating after quintessential inflation and gravitational waves*, *Class. Quant. Grav.* **21** (2004) 1761–1772, [gr-qc/0307068].

[448] M. Artymowski, O. Czerwinska, Z. Lalak, and M. Lewicki, *Gravitational wave signals and cosmological consequences of gravitational reheating*, *JCAP* **04** (2018) 046, [arXiv:1711.08473].

[449] D. G. Figueroa and E. H. Tanin, *Inconsistency of an inflationary sector coupled only to Einstein gravity*, *JCAP* **10** (2019) 050, [arXiv:1811.04093].

[450] V. K. Oikonomou, *Effects of the axion through the Higgs portal on primordial gravitational waves during the electroweak breaking*, *Phys. Rev. D* **107** (2023), no. 6 064071, [arXiv:2303.05889].

[451] V. K. Oikonomou, *Amplification of the Primordial Gravitational Waves Energy Spectrum by a Kinetic Scalar in $F(R)$ Gravity*, *Astropart. Phys.* **144** (2023) 102777, [arXiv:2209.09781].

[452] V. K. Oikonomou, *Flat energy spectrum of primordial gravitational waves versus peaks and the NANOGrav 2023 observation*, *Phys. Rev. D* **108** (2023), no. 4 043516, [arXiv:2306.17351].

[453] D. Langlois, R. Maartens, and D. Wands, *Gravitational waves from inflation on the brane*, *Phys. Lett. B* **489** (2000) 259–267, [hep-th/0006007].

[454] Y. Gouttenoire, G. Servant, and P. Simakachorn, *Kination cosmology from scalar fields and gravitational-wave signatures*, arXiv:2111.01150.

[455] R. T. Co, D. Dunsky, N. Fernandez, A. Ghalsasi, L. J. Hall, K. Harigaya, and J. Shelton, *Gravitational wave and CMB probes of axion kination*, *JHEP* **09** (2022) 116, [arXiv:2108.09299].

[456] Y. Gouttenoire, G. Servant, and P. Simakachorn, *Revealing the Primordial Irreducible Inflationary Gravitational-Wave Background with a Spinning Peccei-Quinn Axion*, arXiv:2108.10328.

[457] D. G. Figueroa and E. H. Tanin, *Ability of LIGO and LISA to probe the equation of state of the early Universe*, *JCAP* **08** (2019) 011, [arXiv:1905.11960].

[458] K. Dimopoulos, *Waterfall stiff period can generate observable primordial gravitational waves*, *JCAP* **10** (2022) 027, [arXiv:2206.02264].

[459] K. Dimopoulos and L. Brissenden, *in preparation*, .

[460] I. Antoniadis, A. Guillen, and K. Tamvakis, *Late time acceleration in Palatini gravity*, *JHEP* **11** (2022) 144, [arXiv:2207.13732].

[461] I. D. Gialamas, A. Karam, T. D. Pappas, and E. Tomberg, *Implications of Palatini gravity for inflation and beyond*, arXiv:2303.14148.

[462] I. D. Gialamas and K. Tamvakis, *Inflation in metric-affine quadratic gravity*, *JCAP* **03** (2023) 042, [arXiv:2212.09896].

[463] C. Armendariz-Picon, T. Damour, and V. F. Mukhanov, *k - inflation*, *Phys. Lett. B* **458** (1999) 209–218, [hep-th/9904075].

[464] V. K. Oikonomou, *A Stiff Pre-CMB Era with a Mildly Blue-tilted Tensor Inflationary Era can Explain the 2023 NANOGrav Signal*, arXiv:2309.04850.

[465] R. Kallosh, A. Linde, and D. Roest, *Superconformal Inflationary α-Attractors*, *JHEP* **11** (2013) 198, [arXiv:1311.0472].

[466] J. Garriga and V. F. Mukhanov, *Perturbations in k-inflation*, *Phys. Lett. B* **458** (1999) 219–225, [hep-th/9904176].

[467] D. H. Lyth, K. A. Malik, and M. Sasaki, *A General proof of the conservation of the curvature perturbation*, *JCAP* **05** (2005) 004, [astro-ph/0411220].

[468] Y. Watanabe and E. Komatsu, *Improved Calculation of the Primordial Gravitational Wave Spectrum in the Standard Model*, *Phys. Rev. D* **73** (2006) 123515, [astro-ph/0604176].

[469] M. Punturo et al., *The Einstein Telescope: A third-generation gravitational wave observatory*, *Class. Quant. Grav.* **27** (2010) 194002.

[470] S. Hild et al., *Sensitivity Studies for Third-Generation Gravitational Wave Observatories*, *Class. Quant. Grav.* **28** (2011) 094013, [arXiv:1012.0908].

[471] G. Janssen et al., *Gravitational wave astronomy with the SKA*, *PoS* **AASKA14** (2015) 037, [arXiv:1501.00127].

[472] E. Thrane and J. D. Romano, *Sensitivity curves for searches for gravitational-wave backgrounds*, *Phys. Rev. D* **88** (2013), no. 12 124032, [arXiv:1310.5300].

[473] G. N. Felder, L. Kofman, and A. D. Linde, *Inflation and preheating in NO models*, *Phys. Rev. D* **60** (1999) 103505, [hep-ph/9903350].

[474] M.-X. Lin, G. Benevento, W. Hu, and M. Raveri, *Acoustic Dark Energy: Potential Conversion of the Hubble Tension*, *Phys. Rev. D* **100** (2019), no. 6 063542, [arXiv:1905.12618].

[475] A. Adil, A. Albrecht, and L. Knox, *Quintessential cosmological tensions*, *Phys. Rev. D* **107** (2023), no. 6 063521, [arXiv:2207.10235].

[476] R. Kallosh and A. Linde, *Universality Class in Conformal Inflation*, *JCAP* **07** (2013) 002, [arXiv:1306.5220].

[477] A. Linde, D.-G. Wang, Y. Welling, Y. Yamada, and A. Achúcarro, *Hypernatural inflation*, *JCAP* **07** (2018) 035, [arXiv:1803.09911].

[478] R. Kallosh and A. Linde, *Planck, LHC, and α-attractors*, *Phys. Rev. D* **91** (2015) 083528, [arXiv:1502.07733].

[479] S. Cecotti and R. Kallosh, *Cosmological Attractor Models and Higher Curvature Supergravity*, *JHEP* **05** (2014) 114, [arXiv:1403.2932].

[480] S. Ferrara, R. Kallosh, A. Linde, and M. Porrati, *Minimal Supergravity Models of Inflation*, *Phys. Rev. D* **88** (2013), no. 8 085038, [arXiv:1307.7696].

[481] S. Ferrara, P. Fré, and A. S. Sorin, *On the Topology of the Inflaton Field in Minimal Supergravity Models*, *JHEP* **04** (2014) 095, [arXiv:1311.5059].

[482] S. Ferrara, P. Fre, and A. S. Sorin, *On the Gauged Kähler Isometry in Minimal Supergravity Models of Inflation*, *Fortsch. Phys.* **62** (2014) 277–349, [arXiv:1401.1201].

[483] R. Kallosh, A. Linde, and D. Roest, *Large field inflation and double α-attractors*, *JHEP* **08** (2014) 052, [arXiv:1405.3646].

[484] A. Alho and C. Uggla, *Inflationary α-attractor cosmology: A global dynamical systems perspective*, *Phys. Rev. D* **95** (2017), no. 8 083517, [arXiv:1702.00306].

[485] S. D. Odintsov and V. K. Oikonomou, *Inflationary α-attractors from $F(R)$ gravity*, *Phys. Rev. D* **94** (2016), no. 12 124026, [arXiv:1612.01126].

[486] M. Braglia, A. Linde, R. Kallosh, and F. Finelli, *Hybrid α-attractors, primordial black holes and gravitational wave backgrounds*, arXiv:2211.14262.

[487] R. Kallosh and A. Linde, *Hybrid cosmological attractors*, *Phys. Rev. D* **106** (2022), no. 2 023522, [arXiv:2204.02425].

[488] A. Achúcarro, R. Kallosh, A. Linde, D.-G. Wang, and Y. Welling, *Universality of multi-field α-attractors*, *JCAP* **04** (2018) 028, [arXiv:1711.09478].

[489] O. Iarygina, E. I. Sfakianakis, D.-G. Wang, and A. Achúcarro, *Multi-field inflation and preheating in asymmetric α-attractors*, arXiv:2005.00528.

[490] R. de Sá, M. Benetti, and L. L. Graef, *An empirical investigation into cosmological tensions*, *Eur. Phys. J. Plus* **137** (2022), no. 10 1129, [arXiv:2209.11476].

[491] S. Vagnozzi, *Consistency tests of ΛCDM from the early integrated Sachs-Wolfe effect: Implications for early-time new physics and the Hubble tension*, *Phys. Rev. D* **104** (2021), no. 6 063524, [arXiv:2105.10425].

[492] R. C. Nunes and S. Vagnozzi, *Arbitrating the S8 discrepancy with growth rate measurements from redshift-space distortions*, *Mon. Not. Roy. Astron. Soc.* **505** (2021), no. 4 5427–5437, [arXiv:2106.01208].

[493] G. Liu, Z. Zhou, Y. Mu, and L. Xu, *Alleviating cosmological tensions with a coupled scalar fields model*, *Phys. Rev. D* **108** (2023), no. 8 083523, [arXiv:2307.07228].

[494] G. Liu, Z. Zhou, Y. Mu, and L. Xu, *Kinetically Coupled Scalar Fields Model and Cosmological Tensions*, arXiv:2308.07069.

[495] M. Lucca, *Multi-interacting dark energy and its cosmological implications*, *Phys. Rev. D* **104** (2021), no. 8 083510, [arXiv:2106.15196].

[496] J. Beltrán Jiménez, D. Bettoni, D. Figueruelo, F. A. Teppa Pannia, and S. Tsujikawa, *Probing elastic interactions in the dark sector and the role of S8*, *Phys. Rev. D* **104** (2021), no. 10 103503, [arXiv:2106.11222].

[497] T. Patil, Ruchika, and S. Panda, *Coupled Quintessence scalar field model in light of observational datasets*, arXiv:2307.03740.

[498] A. Banerjee, H. Cai, L. Heisenberg, E. O. Colgáin, M. M. Sheikh-Jabbari, and T. Yang, *Hubble sinks in the low-redshift swampland*, *Phys. Rev. D* **103** (2021), no. 8 L081305, [arXiv:2006.00244].

[499] B.-H. Lee, W. Lee, E. O. Colgáin, M. M. Sheikh-Jabbari, and S. Thakur, *Is local H_0 at odds with dark energy EFT?*, *JCAP* **04** (2022), no. 04 004, [arXiv:2202.03906].

[500] D. Wands, O. F. Piattella, and L. Casarini, *Physics of the Cosmic Microwave Background Radiation*, *Astrophys. Space Sci. Proc.* **45** (2016) 3–39, [arXiv:1504.06335].

[501] L. Kofman, A. D. Linde, X. Liu, A. Maloney, L. McAllister, and E. Silverstein, *Beauty is attractive: Moduli trapping at enhanced symmetry points*, *JHEP* **05** (2004) 030, [hep-th/0403001].

[502] G. Ye and Y.-S. Piao, *Is the Hubble tension a hint of AdS phase around recombination?*, *Phys. Rev. D* **101** (2020), no. 8 083507, [arXiv:2001.02451].

[503] Y. Cui and E. I. Sfakianakis, *Detectable gravitational wave signals from inflationary preheating,*, *Phys. Lett. B* **840** (2023) 137825, [arXiv:2112.00762].

[504] A. Maleknejad and M. M. Sheikh-Jabbari, *Gauge-flation: Inflation From Non-Abelian Gauge Fields,*, *Phys. Lett. B* **723** (2013) 224–228, [arXiv:1102.1513].

[505] J. F. Dufaux, A. Bergman, G. N. Felder, L. Kofman, and J.-P. Uzan, *Theory and Numerics of Gravitational Waves from Preheating after Inflation*, *Phys. Rev. D* **76** (2007) 123517, [arXiv:0707.0875].

[506] G. Ye, B. Hu, and Y.-S. Piao, *Implication of the Hubble tension for the primordial Universe in light of recent cosmological data*, *Phys. Rev. D* **104** (2021), no. 6 063510, [arXiv:2103.09729].

[507] J.-Q. Jiang and Y.-S. Piao, *Toward early dark energy and ns=1 with Planck, ACT, and SPT observations*, *Phys. Rev. D* **105** (2022), no. 10 103514, [arXiv:2202.13379].

[508] G. Ye, J.-Q. Jiang, and Y.-S. Piao, *Toward inflation with ns=1 in light of the Hubble tension and implications for primordial gravitational waves*, *Phys. Rev. D* **106** (2022), no. 10 103528, [arXiv:2205.02478].

[509] J.-Q. Jiang, G. Ye, and Y.-S. Piao, *Return of Harrison-Zeldovich spectrum in light of recent cosmological tensions*, arXiv:2210.06125.

[510] S. Nojiri, S. D. Odintsov, and V. K. Oikonomou, *Unifying Inflation with Early and Late-time Dark Energy in $F(R)$ Gravity*, *Phys. Dark Univ.* **29** (2020) 100602, [arXiv:1912.13128].

[511] V. K. Oikonomou, *Unifying inflation with early and late dark energy epochs in axion $F(R)$ gravity*, *Phys. Rev. D* **103** (2021), no. 4 044036, [arXiv:2012.00586].